

Final Research Performance Report

Federal Agency and Organization: DOE EERE – Geothermal Technologies Program

Recipient Organization: ATLAS Geosciences Inc
DUNS Number: 078451191
Recipient Address: 3372 Skyline View Dr
Reno, NV 89509

Award Number: DE-EE0006725

Project Title: Geothermal Potential of the Cascade and Aleutian Arcs, with Ranking of Individual Volcanic Centers for their Potential to Host Electricity-Grade Reservoirs

Project Period: 10/1/14 – 10/31/15
Principal Investigator: Lisa Shevenell
President
lisas@atlasgeoinc.com
775-240-7323

Report Submitted by: Lisa Shevenell
Date of Report Submission: October 16, 2015
Reporting Period: September 1, 2014 through October 15, 2015
Report Frequency: Final Report

Project Partners: Cumming Geoscience (William Cumming) – cost share partner
GEODE (Glenn Melosh) – cost share partner
University of Nevada, Reno (Nick Hinz) – cost share partner
Western Washington University (Pete Stelling) – cost share partner

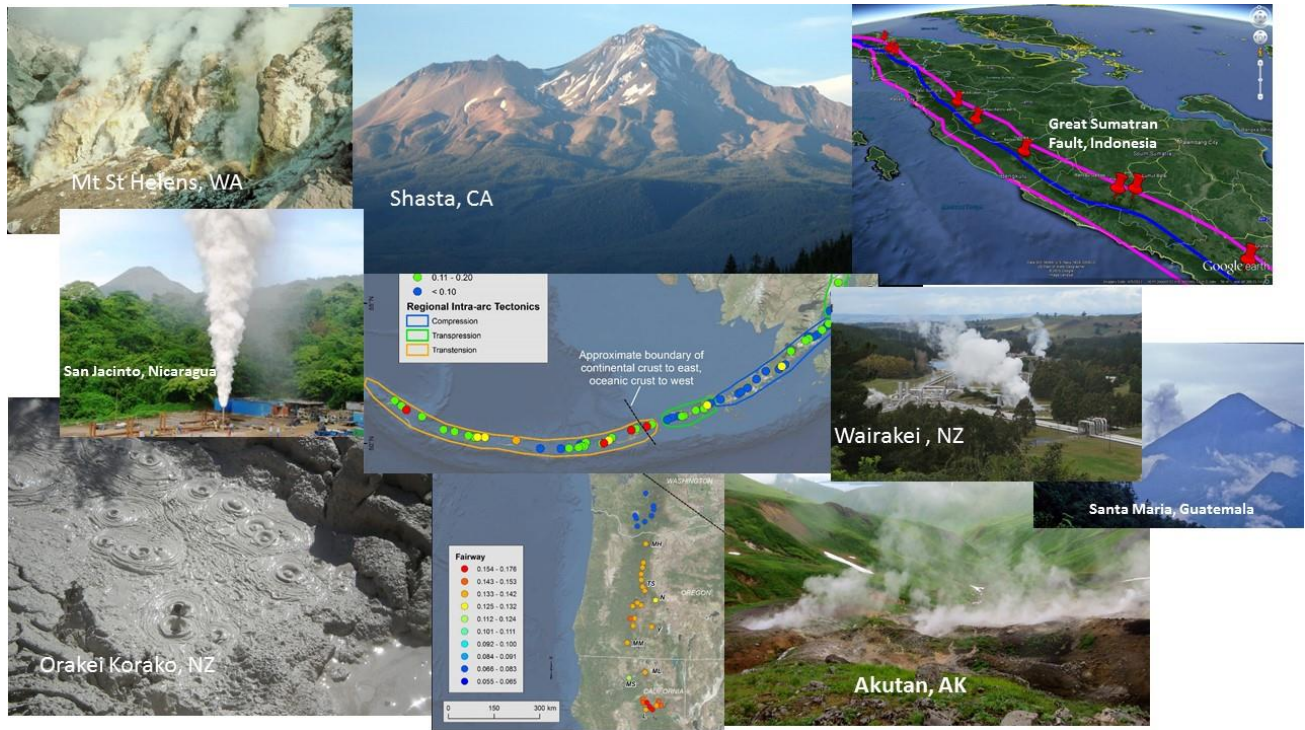
DOE Project Team: DOE Contracting Officer – Laura Merrick
DOE Project Officer – Eric Hass
Project Monitor – Laura Garchar



Signature _____ Date 10/16/15

***The Prime Recipient certifies that the information provided in this report is accurate and complete as of the date shown. Any errors or omissions discovered/identified at a later date will be duly reported to the funding agency.**

Geothermal Potential of the Cascade and Aleutian Arcs, with Ranking of Individual Volcanic Centers for their Potential to Host Electricity-Grade Reservoirs



Lisa Shevenell, Mark Coolbaugh, Nick Hinz, Pete Stelling, Glenn Melosh, William Cumming

A Global Perspective of Volcanic Arc Geothermal Play Fairway Analysis

Using knowledge from abroad to target US prospects

October 16, 2015

EXECUTIVE SUMMARY

This project brings a global perspective to volcanic arc geothermal play fairway analysis by developing statistics for the occurrence of geothermal reservoirs and their geoscience context worldwide in order to rank U.S. prospects. The focus of the work was to develop play fairways for the Cascade and Aleutian arcs to rank the individual volcanic centers in these arcs by their potential to host electricity grade geothermal systems. The Fairway models were developed by describing key geologic factors expected to be indicative of productive geothermal systems in a global training set, which includes 74 volcanic centers world-wide with current power production. To our knowledge, this is the most robust geothermal benchmark training set for magmatic systems to date that will be made public.

All work discussed in this report was conducted within the 12 month period of Phase I of this project. These activities included data collection, evaluation, correlations and weightings, fairway and favorability modeling and mapping, prediction of blind systems, and uncertainty analysis to estimate errors associated with model predictions.

The project consisted of a large data compilation and collection effort using existing digital databases and data entry from hundreds of published sources. Data plots and summaries were constructed to evaluate trends, correlations and assign both data-driven and expert-driven weighting factors to individual data types. These weighting factors were included in the numerical modeling of the probability of encountering a productive geothermal system at each of the 100 volcanic centers in the Cascade and Aleutian volcanic arcs. Other data types that may be important were not available in this project. A worldwide geothermal well database was identified but was not available within the budget of the current project. Inclusion of well deliverabilities and lithologies in this database have the potential to improve this fairway analysis. Similarly, a lack of available fumarole gas geothermometry limited predictive capabilities in some areas, and increased sharing of that data would help improve model accuracies.

The project team modeled play fairways, geothermal favorabilities, and associated errors/uncertainties, and combined them to produce fairway and favorability models. The favorability model was used to modify play fairway results by incorporating direct evidence from springs, wells and surface manifestations. The models provide probabilities of occurrence of power-grade geothermal systems using relationships among structure, tectonics, volcanology, fluid geochemistry and surface manifestations. The model results include a ranking of all 100 sites and a determination of which sites are most prospective, and which are best suited for more detailed direct data collection based on geopolitical criteria. All results are presented in table and map format, noting development constraints associated with each volcanic center based on land classification and transmission issues.

Among many tested relationships, five main correlations between geothermal production and geological parameters have been identified and/or clarified during the study. These are:

- 1) production potential is positively correlated with extensional and transtensional environments and less well correlated with more compressive environments, based on both world-wide and local assessments of stress and strain;
- 2) production potential increases where the relative plate motion angle of obliqueness (and/or arc-parallel velocity of the under-riding plate) is relatively high;
- 3) production is greater in systems hosted by Pleistocene calderas relative to Holocene calderas or non-caldera-hosted systems;
- 4) favorable predictors of geothermal potential include high Quaternary fault scarp densities and high slip rates on faults, and;
- 5) extensional structural settings favor electrical production, including pull-aparts, step-overs, accommodation zones, and displacement transfer zones.

These relationships are used to define a comprehensive list of structural play fairway types.

Several criteria were tested but not used in the analysis in the Cascades or Aleutians because of a lack of correlation with geothermal production. These included criteria widely expected to be correlated with production, including the volume of volcanic rock in each center, the presence and number of domes and other flank vents, eruptive chemistry and the recency of eruptive activity. These criteria turned out to not have a significant correlation. Correlated and uncorrelated criteria in this study will provide guidance for geothermal exploration efforts worldwide.

The project has clearly defined relative favorabilities along the Cascade and Aleutian arcs. The best fairway potential in the Cascades lies near its southern end where extensional processes related to Basin and Range extension overlap the heat corridor of the Cascade arc. In the Aleutians, the geothermal fairway improves noticeably west of the transition from continental to oceanic crust near Akutan and Makushin; such an improvement in favorabilities is related to more complex structural settings that may in turn be related to more complex deformational processes associated with changes in crustal rheologies.

Four sites in the Cascades (Lassen, Newberry, Olallie Butte, and Shasta) show probabilities of >25% based on favorability model results, with Lassen and parts of Shasta being unavailable for development based on land use designations. Six of the centers in the Aleutians (Akutan, Makushin, Recheschnoi, Little Sitkin, Korovin, and Adagdak) have probabilities >25%, with all nominally available for development based on land status considerations. Although these and many other Aleutian volcanic centers could be developable based on technical considerations, most will likely not be developed unless/until market and/or population dynamics change (except for at Akutan, which is currently being evaluated in other projects, Makushin, and possibly Korovin, each of which have small population bases and industries to support a power market). Most of the other Aleutians volcanic centers are remote with no population or access to transmission.

Average scores in the fairway model for the Cascades and Aleutians are similar to the average scores calculated for producing volcanic arc centers outside the U.S. However, geothermal power plants and thermal manifestations indicative of potential for geothermal production are more common in the arcs outside the U.S. Since 2 or possibly 3 volcanic centers in the Cascades (Lassen, Medicine Lake, and possibly Meager) could produce electrical energy under more favorable market circumstances, and if 2-3 systems in the Aleutians are likely power-capable (e.g., Akutan, Makushin) but haven't been developed because of remoteness and/or cost, then approximately 5% of the volcanic centers in both the Cascades and Aleutians could be considered developable based on known data. This is less than the world arc average of 10% of centers that are either producing electricity or have been shown to be power-capable. The discrepancy between the fairway scores in the U.S. and the relative lack of direct evidence of hydrothermal activity in the U.S. arcs suggests that either there are more blind systems or that important conceptual issues are not constrained in the current analysis. Because of poor data availability, geothermal indicators such as the presence of host rock favorable for reservoir or clay cap development could not be considered in the Phase 1 play fairway modeling or favorability assessments. However, basic surface geological mapping supported by remote sensing is low cost and can help constrain these parameters. Until stronger indications of potential become available, geophysical surveys remain high risk.

In addition to using the play fairway model to independently identify and rank volcanic centers in the Cascades that had been already assessed based on their hydrothermal manifestations, the modeling of geothermal potential identified several volcanic centers that could host blind geothermal systems, i.e., those with relatively high play fairway modeling scores, but lower favorability scores due to minimal direct evidence having been collected at the sites. The team proposes additional work to better characterize these poorly explored volcanic centers with high play fairway scores located in southern Oregon and northern California.

The proposed focus of future work in the second stage of this project in this geographic region is based on high play fairway rankings and their location in and adjacent to California, which has a new renewable energy portfolio standard (SB-350 enacted 10/7/15) of 50%, which will require significant development of renewable energy in the coming years that geothermal development in the southern Cascades can help address. Geothermal development at the identified high ranking volcanic centers in the southern Cascades can make a significant contribution to achieving the most aggressive renewable portfolio standard in the US.

Table of Contents

EXECUTIVE SUMMARY	3
1.0 INTRODUCTION	10
1.1 BACKGROUND	10
1.2 PURPOSE	11
1.3 OBJECTIVES	12
2.0 METHODS.....	12
2.1 VOLCANIC ARCS.....	15
2.2 SELECTION OF VOLCANIC CENTERS.....	16
2.3 COMPILATION OF POWER PLANTS	17
2.4 DATA COLLECTION.....	18
2.5 PLAY TYPES	19
2.6 DEGREE OF EXPLORATION AND BLIND GEOTHERMAL SYSTEMS.....	20
3.0 DATA COLLECTION.....	22
3.1 CRUSTAL STRAIN, PLATE MOTION, AND CRUSTAL THICKNESS - REGIONAL	23
Sources of Data.....	23
Processing Data	23
3.2 POWER DENSITIES - REGIONAL.....	23
Sources of Data.....	23
3.3 TECTONIC DATA - REGIONAL	24
<i>Sources of Data.....</i>	<i>24</i>
Processing Data	24
Quality of Data and Error Potential	24
3.4 HEAT FLOW - REGIONAL.....	25
Source of Data	25
3.5 GEOCHEMICAL DATA - LOCAL	25
Sources of Data.....	25
Processing of Geochemical Data.....	27
3.6 SURFACE MANIFESTATIONS - LOCAL	28
Sources of Data.....	28
Processing Data	29

Summary.....	29
3.7 SUMMARY OF GEOCHEMICAL AND SURFACE MANIFESTATION DATA.....	30
3.8 STRUCTURAL DATA	31
Sources of Data.....	31
Processing Data	31
Quality of Data and Error Potential	35
3.9 VOLCANIC DATA - LOCAL.....	35
Data Collection and Sources	35
Processing of Rock Geochemistry Data	38
3.10 DATA COMPILATION SUMMARY	38
Sources of Information.....	38
Compiled Data Types.....	40
4.0 DATA EXPLORATION.....	42
4.1 GEOCHEMICAL AND SURFACE MANIFESTATION DATA.....	42
Temperatures	42
Fumaroles	45
Correlations	45
4.2 STRUCTURAL-TECTONIC DATA.....	49
Tectonic Setting	49
Quaternary Fault Slip Rate	53
Quaternary Fault Scarp Concentration.....	56
Structural Setting.....	60
Dilation Potential	63
Geodetic Data	64
4.3 VOLCANIC DATA EXPLORATION.....	65
Physical Geographic parameters	65
Important non-correlations of physical characteristics	66
Statistically significant correlations of physical characteristics.....	70
4.4 WORLD STRAIN, PLATE MOTION, AND POWER DENSITY DATA	73
4.5 STATISTICAL ANALYSIS	78
Regression Results.....	78
Regression Discussion	79

5.0 TRENDS AND WEIGHTING FACTORS	80
5.1 STRUCTURAL AND TECTONIC DATA.....	80
5.2 GEOCHEMICAL AND SURFACE MANIFESTATION DATA.....	82
6.0 MODEL FORMULATION	84
6.1 PRINCIPAL HIERARCHAL TIERS	84
6.2 FAIRWAY MODEL.....	86
Permeability	87
Scaling to Probability Space and Creation of the Predictive Fairway.....	87
Errors.....	88
6.3 DEGREE-OF-EXPLORATION	92
Sub-surface Degree-of-Exploration	92
Surface Degree-of-Exploration	93
Total Degree-of-Exploration	93
Errors.....	94
6.4 DIRECT EVIDENCE AND ESTIMATION OF THE FAVORABILITY MODEL.....	94
Assignment of Incremental Probabilities	94
Scaling Negative Membership with Degree-of-Exploration	94
Conversion of Incremental Probabilities into Equivalent Weights-of-Evidence.....	95
Generation of the Favorability Index	95
Errors.....	95
7.0 RESULTS	97
7.1 PLAY FAIRWAYS.....	97
7.2 PRELIMINARY MODEL	99
7.3 FINAL MODEL.....	100
7.4 RANKING OF CASCADE VOLCANIC CENTERS.....	104
7.5 RANKING OF ALEUTIAN VOLCANIC CENTERS	107
7.6 LAND STATUS CONSIDERATIONS	110
7.7 TRANSMISSION.....	114
8.0 DISCUSSION	117
8.1 TECHNICAL	117
Potentially Blind Geothermal Systems	117
Global Benchmarks by Arc Segment – Looking for Analogues	118

8.2 ADMINISTRATIVE.....	121
9.0 CONCLUSIONS.....	123
10.0 RECOMMENDATIONS – PHASE 2	126
10.1 BACKGROUND	126
10.2 PROPOSED WORK.....	128
10.3 PLANNED ACTIVITIES.....	130
<i>Task 1: Reconnaissance Field Mapping (ATLAS, UNR, WWU, Sawyer)</i>	130
<i>Task 2: Geochemistry of fluids (ATLAS)</i>	130
<i>Task 3: Clay Caps (ATLAS)</i>	130
<i>Task 4: LiDAR Acquisition and Evaluation (UNR, Sawyer)</i>	131
<i>Task 5: Structural Geology</i>	131
<i>Task 6: Administrative (ATLAS)</i>	132
<i>Task 7: Analog Study – Trans-Mexico Volcanic Belt (ATLAS, UNR, WWU)</i>	132
10.4 PARTNERS AND ROLES	134
10.5 DRAFT BUDGET AND TIMELINE.....	135
11.0 DIGITAL DATA SUBMITTED TO GDR.....	136
Publications	137
Networks/Collaborations Fostered:	137
12.0 REFERENCES.....	138
13.0 TMT QUARTERLY REVIEW	140
13.1 Q1 Review	140
13.2 Q2 Peer Review	140
13.3 Q3 Review.....	149
14.0 DOWNSELECT CRITERIA.....	149
APPENDICES.....	152

1.0 INTRODUCTION

1.1 BACKGROUND

Much of the world's geothermal production comes from young eruptive centers in active volcanic arcs. Although the United States is the largest producer of geothermal energy in the world, and is well endowed with young volcanic centers in both the Cascades and Aleutian volcanic arcs, no production from either of those arcs is currently realized. Possible explanations for this lack of production include 1) the environmentally protected status or permitting challenges at some areas (e.g. Mt. Lassen, CA; Mt. Newberry, OR; Medicine Lake (Glass Mtn), CA), 2) the remoteness of some volcanic centers (e.g. many of the island volcanos of the Aleutian Arc), or 3) underlying physical properties of these arcs that make them relatively unfavorable settings for hosting geothermal reservoirs. Geothermal exploration wells have been drilled at some volcanic centers in these arcs (e.g., Mt. Meager, BC; Mt. Spurr, AK; Glass Mtn, CA) without commercial success. It is understood that not all arc volcanic centers in the world are created equal in terms of geothermal potential, because of local differences in structural setting, host rocks, eruption frequency and composition, and other factors. This project evaluates to what extent the lack of development of the Cascades and Aleutian Arcs is influenced by such underlying physical and chemical favorability.

No recent studies have been undertaken to systematically and regionally assess the underlying physiochemical favorability for geothermal production in the Cascade and Aleutian Arcs. Earlier studies in the 1980s (e.g., summarized by Motyka, et al., 1993 for the Aleutians) are excellent descriptions of known geothermal areas of the arc, but are not quantitative in their evaluation of geothermal potential, nor did they define potential from the perspective of hierarchal tiers in an occurrence model or play fairway analysis.

The current work quantitatively evaluates the geothermal potential in the context of play fairway analysis in the Cascade and Aleutian Arcs based on a comparison of key physiochemical parameters present at producing young arc volcanic centers around the world. Although the focus in fairway analysis is on factors that affect the physical favorability for hosting a reservoir, like the suitability of the structural setting for creating open space permeability, more direct evidence for the existence of commercial reservoirs, like fumaroles and hot springs, are also considered. The parameters considered are necessarily those that are available without conducting detailed field assessments so, although suitability of formation types for hosting reservoirs might be decisive in assessing resource probability, this information was not available on a sufficiently broad scale to include in the analysis. The available parameters are statistically evaluated within the context of hierarchal tiers in a play fairway analysis to define favorability at young volcanic centers throughout both the Aleutian and Cascade volcanic arcs. It is anticipated that multiple occurrence models may best define the range of potential geothermal plays.

A similar study was conducted in the Great Basin by Coolbaugh et al. (2005) that helped develop the application of statistical methodology to geothermal assessment using weights-of-evidence and logistic regression statistics, which pioneered the integration of degree-of-exploration into those models (Coolbaugh et al., 2007). These models were further developed and adjusted in this study to apply to the US volcanic arc settings with benchmark sites from around the world used to evaluate the US sites.

The scope of this project was broad, since it involved the collection and comparative consideration of favorability properties at a significant number of the world's producing geothermal systems from arc settings around the world. The large amount of data compilation, integration, and processing over a short period of time presented logistical and organizational challenges to the team. Availability of some data types considered for compilation in the proposal and early stages of the project proved to be more limited than hoped, making their inclusion problematic. Important parameters related to favorability that could not be integrated due to limited availability included evidence for clay cap disruption (such as exposure of high temperature reservoir alteration by glacial erosion) and evidence for formation properties unsuitable for hosting a reservoir, such as clay-rich metamorphic rocks outcropping beneath a veneer of recent volcanic rocks. Nevertheless several key parameters provided useful indicators.

Working in favor of the project was the increasing availability of world-wide databases and visualization systems; key examples of which were Google Earth, as well as the Smithsonian volcano database. During the project, relatively high-resolution global maps of crustal thickness (USGS) and strain rate (UNR Nevada Geodetic Laboratory) became available. In the case of strain rate data, this information includes discrimination of the type of strain (compressional, dilatational, shear) as well as magnitude, and the strain model has also been used to resolve the rate of plate convergence and obliqueness (i.e. plate convergence vector) for all plate boundaries. Important relationships between regional plate boundary interactions, local structure, and geothermal power plants were documented, clarified, and quantified with this study to identify play fairway types and ranking of geothermal potential of volcanic centers.

1.2 PURPOSE

The initial hypothesis of this work is that a statistical analysis of various data types from productive arc systems world-wide can be used to quantifiably rank the geothermal potential of arc volcanic systems in the Cascade and Aleutian arcs of the US. This statistical framework allows for estimation of uncertainties associated with the rankings to better assess which areas require additional data collection to fully evaluate geothermal potential of the system.

The primary goal of this research is to look beyond issues of permitting and accessibility to quantify the underlying geothermal favorability and rank the geothermal potential of the young volcanic centers of the Cascade and Aleutian Arcs. The results of this effort helps to focus future exploration efforts into the most prospective, underdeveloped areas of the US: Cascade and Aleutian Arcs. If initial success can be gained in one or more areas, it would encourage expanded

exploration in the remaining portions of the arcs. This study interprets geothermal potential in the context of play fairway analysis, in which key hierarchical tiers are assembled in a statistical framework to quantify geothermal potential and optimize future exploration through the definition of “play fairways”. An additional benefit of the study is the quantification of the production potential of different geothermal plays within the arcs in the US and elsewhere. The project consists of a statistical evaluation of arc geothermal systems around the world, incorporating to the extent possible past geothermal exploration success stories to better understand which physiochemical conditions are most favorable for geothermal production and the magnitude of that potential production. The statistical quantification of correlations between geological, geochemical, and surface signatures of geothermal systems have led to improvements and refinements in our understanding of the conditions necessary for geothermal systems to form and what size they are likely to attain.

1.3 OBJECTIVES

The primary objective of this research (Phase I) is to quantitatively rank the geothermal potential of each of the young volcanic centers of the Cascade and Aleutian Arcs. This ranking is conducted to help focus future exploration efforts into the most prospective areas. Three rankings of the volcanic centers (VC) are included:

1. Ranking #1 based on play fairway types – primarily dominated by the structural and tectonic setting of the VC as a proxy for permeability.
2. Ranking #2 using results from the play fairway with the additional of direct evidence from the VCs in the form of measured and calculated temperature and geochemical data associated with hot springs and fumaroles.
3. Ranking #3 of the VCs is based on considerations of land use, removing VC from the previous two rankings based on their locations in areas off-limits to development (e.g., wilderness, national parks, etc.).

The objective of the work is to provide a listing of VC in the Cascades and Aleutians available for development based on their relative ranking for power production potential. The results of the work should help open the door to competitive geothermal development of the Cascade and Aleutian volcanic arcs by making the results publicly available to all potential developers.

2.0 METHODS

The objective of the DOE-funded Geothermal Play Fairway Analysis is to identify play fairways across a given region and evaluate relative favorability by mapping the combined distribution of key component geologic factors. In this volcanic arc project, the key geologic factors are considered to comprise heat, permeability, fluid composition, and cap rock. The net permeability of the crust associated with each VC is the sum of the primary stratigraphic permeability and secondary permeability associated with faults and fractures that have formed through tectonism, magma buoyancy, gravitational collapse, and/or fracturing of country rock around intrusive bodies during emplacement. Many of these VCs have formed in association with active tectonic structures that predate the VCs by hundreds of thousands or millions of years and continue to co-evolve with the volcanoes, yielding a strong kinematic linkage between the regional structural framework and the structure of the magmatic system associated with each VC. The focus for

phase 1 (year 1) of this play fairway study was to develop a workflow module to singularly evaluate the tectonic-induced structural permeability and effectively integrate this key factor into the overarching play fairway analysis.

This study covers 100 VCs between the Cascades and the Aleutians. A benchmark data set was compiled that included 74 “productive” volcanoes in subduction arc settings around the world. Identical structural-tectonic data parameters were collected for both the study area and the global training set. The training data were analyzed along with the study area data to develop the final model weighting factors through a combination of expert-driven and data-driven approaches.

The first part of this project consisted primarily of a large data collection effort. Data were acquired from digital databases and published literature from the 59 Aleutian, 37 US Cascade (plus 4 Canadian) and 74 world benchmark VCs for multiple data types (geologic, geochemical, volcanologic) described in this section. All references consulted in the construction of the database appear in Appendix I. The data from the US VC are compared to power-producing Arc systems world-wide, which are used as benchmarks of known high potential geothermal systems from which to classify the US VC in relative rankings.

Data at both regional and local scales were used to predict geothermal potential at individual volcanic centers in the Cascade and Aleutian arcs, based on relationships among the data at other power-producing arc volcanic centers around the world. Both local and regional-scale data compiled and evaluated in this work are listed in Section 2.3 described in greater detail in the data-specific sections in Section 3.0 DATA COLLECTION.

The data are then incorporated into geothermal play fairway models using statistical approaches to rank the VC and estimate uncertainties in the estimates. Figure 2.0-1 depicts the flow chart of the modeling methodology used in the work, where the Fairway is first constructed and modeled with data input from structural and tectonic factors. Other relevant factors feeding into the play fairway type include heat source, fluid geochemistry and presence of clay cap. As all are in volcanic arc settings with clear, young heat sources, a default value is used throughout the model for heat source such that this factor is not weighted more or less at any particular VC. Similarly, the geochemistry and clay cap factors are weighted the same among VC, although for different reasons. With the available data, none of the Aleutian or Cascade VC possess fluid chemistries that would be prohibitive of production, and thus all are weighted the same. On the other hand, information on clay cap integrity and depth could not be obtained from sufficient numbers of VC in the time frame of this project. Thus, this factor has the same weight for all VC in the study. The primary factors dictating the play fairway types in this phase of the work are therefore characteristics associated with the structure and tectonics at the individual VC, which serve as a proxy for system permeability. The results of this phase of modeling provide the ranking #1 noted in section 1.3 Objectives.

From Figure 2.0-1, the play fairway rankings are then adjusted with direct, local evidence of geothermal favorability obtained from the individual VC. These factors are weighted by the degree of exploration, which is a measure of the extent to which an area has been explored by evaluating data completeness and type. The results of this phase of modeling provide the ranking #2 noted in section 1.3 Objectives.

Finally, considerations of land availability are incorporated into the model to provide a third ranking showing the sites with highest geothermal potential that are available for development (e.g., VC outside of wilderness and national parks). The results of this phase of modeling provide the ranking #3 noted in section 1.3 Objectives.

In constructing the model for Ranking #2, direct evidence of the existence of a geothermal system was gathered and documented in the literature for many geothermal systems in volcanic arcs. This evidence prominently includes hot springs and fumaroles, their temperatures and geothermometry, and well temperatures and corresponding fluid compositions and geothermometry. Additional evidence includes MT or other resistivity surveys of clay caps, presence of silica sinters, and other types of data. Because these data have a major impact on geothermal potential for each VC, their consideration will be important to include in any detailed site survey or any follow-up analysis to the Play Fairway model.

The model methodology and assumptions to construct all 3 ranking lists are discussed in greater detail in Section 6.0 Model Formulation.

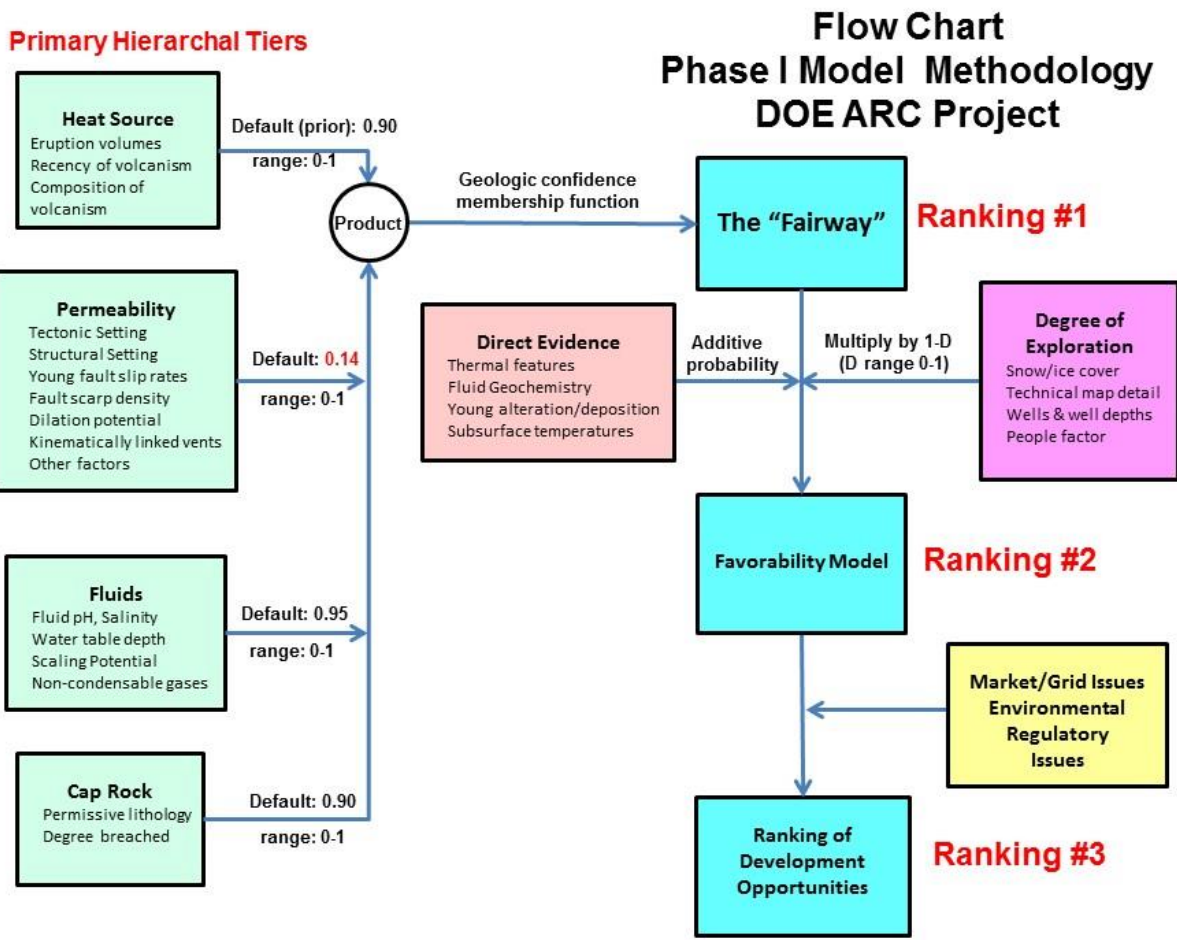


Figure 2.0-1. Flow chart showing the sequence of modeling to obtain three ranked lists of geothermal favorability of the Cascade and Aleutian VC.

2.1 VOLCANIC ARCS

The Cascade and Aleutian arcs are compared to volcanic arcs around the world that similarly involve the subduction of oceanic crust. Volcanic arcs included in the project are listed in Table 2.1-1 on the following page.

Table 2.1-1. Volcanic Arcs included in the study.

Arc-Trench System	Lower Plate	Upper Plate
Aleutians	Pacific	North American
Cascades (US and Canada)	Juan de Fuca	North American
Mexico	Cocos	North American
Central America	Cocos	Caribbean
	South	
Caribbean	American	Caribbean
South America - Columbia, Ecuador	Nazca- Antarctic	South American
South America - Peru, Bolivia, N. Chile	Nazca- Antarctic	South American
South America - S. Chile, Argentina	Nazca- Antarctic	South American
Kamchatka-Kuril Islands	Pacific	"East Siberia" (N. American)
Japan, central	Pacific	"Japan" (N. American)
Marianas	Pacific	Filipino
Japan, south-Taiwan	Filipino	Eurasian
Philippines-Taiwan	Filipino	Eurasian
Celebes-Maluku Microplates (3)	various	various
Sumatra-Java-Timor	Australian	Eurasian
Papua-Solomon Microplates (3+)	various	various
Vanuatu-Fiji-Samoa (2?)	Australian	Eurasian
Tonga	Pacific	Australian
New Zealand	Pacific	Australian
Greece	African	Aegean microplate
Italy	Adriatic	European

2.2 SELECTION OF VOLCANIC CENTERS

Not all VC were selected for inclusion into the data collection and modeling efforts. A database of “qualifying” volcanic centers played a key role in this project. Regional and local attributes were compiled for each volcanic center in volcanic arcs outside the US, along with the presence

of power plants, to build predictive indices to model geothermal potential at each of a series of volcanic centers in the Cascade and Aleutian arcs. For this purpose, a “volcanic center” is different from a “volcanic vent”, given that there may be many vents associated with one “volcanic center”. The following definitions are employed to ensure rigor and consistency in the definition of volcanic centers in each of the arcs studied in this work:

To qualify as a young volcanic center (VC), the VC must have the following characteristics:

- 1) Most recent eruption occurred less than 500,000 years ago.
- 2) Age can be inferred based on geomorphology where radiometric data are lacking
- 3) In absence of dates, presence of persistent fumaroles with temperatures within 10°C of boiling
- 4) In absence of dates, documented earthquake swarm with strongly suspected volcanic cause
- 5) In absence of dates, significant, measured, volcanic-related, deformation (InSAR, geodetic)
- 6) Comprises a composite, cone, crater, or dome complex >300 meters in height (unless a crater/caldera)
- 7) Can include more eroded subjacent sister volcanoes
- 8) Adjacent vents located at a distance of ≤ 8 km were generally grouped in to one VC.

The Smithsonian database on Holocene volcanoes provided a major source of information for volcanic centers around the world in the initial data gathering phase. Other data sets included are those maintained by the Alaska Volcano Observatory (AVO), Cascades Volcano Observatory (CVO), and the National Geothermal Data System (NGDS). All volcanic centers world-wide were evaluated with the assistance of Google Earth to estimate size, distances and to update location coordinates. Many volcanic vents were eliminated from the AVO and GVP data sets that were either submarine vents, intraplate rather than subduction, or on islands <5 km diameter.

A listing of VC included in the study appears in Appendix II. The unique identifier for each VC is listed in the first column. Vents that were grouped based on criteria #8 above are listed in the third column (Linked_Centers).

2.3 COMPILATION OF POWER PLANTS

Key to this project was the identification of all geothermal power plants in the volcanic arcs subject to this study. Given that geothermal power plants are not typically designed to have an infinite life, it was decided to include both past and presently operating geothermal power plants. Sites at which successful flow tests have been completed at economic temperatures are also included even though power plants may not yet exist for various reasons. A nominal 5-km-distance between power plants is used as a criterion for distinguishing power plant clusters that may be associated with the same geothermal system. These criteria resulted in compilation of power production information from a total of 74 VC (represented by 84 power plants) in world arc settings.

An effort was made to compile the following types of data for each power plant. Data availability and completeness varied for these parameters, although the primary data type used in this work of MW capacity was available for all benchmark VC:

- 1) Installed (or estimated) capacity (MWe)
- 2) Maximum average annual net output (maximum in the sense that it may slowly decline over years)
- 3) Fluid composition
- 6) Reservoir depth range, thickness, and horizontal extent

The compilation included data for 74 benchmark power production facilities in world arcs representing 0.7 to 795 MW facilities (average of 90.5 ± 137 MW) in the temperature range of 190-353°C (average: 266 ± 32 °C). In addition 59 Aleutian VC, none with power plants, were included where the maximum temperature (geothermometer) of a VC is 220°C. A total of 37 US Cascade VC are included in the study, none with power plants, and with a maximum measured temperature of 265°C. A listing of these power plants appears in Appendix III, whereas a summary of the available power plants is depicted in Figure 2.3-1, and a full, digital listing including MW capacities is provided through GDR.

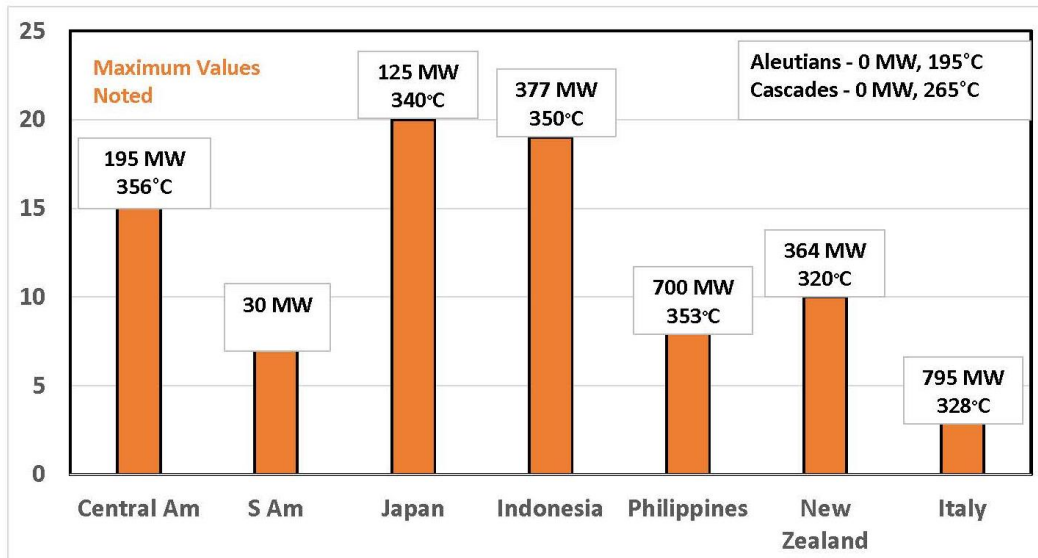


Figure 2.3-1. Summary of power plants used as benchmarks in this study showing maximum measured temperatures.

2.4 DATA COLLECTION

Data collection is more completely described in subsections of Section 3.0. A summary of acquired data appears here in Table 2.4-1.

Table 2.4-1. Summary of data types collected at world, Aleutian and Cascade arcs for inclusion in the modeling. Note the Cascades numbers do not include the 4 VC in Canada.

Data Type	Scale	World Arcs	Aleutians	Cascades	Categories
Crustal Thickness	Regional	633	59	37	1
Geodetic - Crustal Strain	Regional	633	59	37	15
Tectonic Setting	Regional	633	59	37	6
Fumarole Surface Area	Local	65	58	11	5
General (name, loc.)	Local	633	59	37	10
Geochemistry	Local	63	24	18	60
Structure	Local	78	59	37	39
Power Plants	Local	84 (74 VC)	0	0	6
Surface Expressions	Local	22	9	5	5
Volcanic Data	Local	633	59	37	135
Total Data Categories:					298

2.5 PLAY TYPES

The Play Fairway Model was built without any consideration of direct evidence of the existence of a geothermal system, thus it comprises a “fairway” within which geothermal exploration can be directed. As such, it represents a compilation of both regional and local predictors of geothermal potential.

A number of play fairway types and component hierarchal tiers have been identified. Four principal hierarchal tiers identified are (See Figure 2.0-1 above):

- 1) Source of heat
- 2) Permeability
- 3) Presence of working fluids of suitable chemistry
- 4) Containment (e.g. such as cap rock).

A potential 5th hierarchal tier could be added in amagmatic environments, or where the distance between a heat source and the reservoir is significant: 5) Permeability to allow transfer of heat from the heat source to reservoir. This fifth tier may be especially relevant in amagmatic geothermal terrains such as the Great Basin, USA, where such heat transport is commonly deep-seated and likely to operate under stress-strain conditions and permeability constraints that are different from those of the producing reservoirs. Such a distinction is less clear in magmatic heated geothermal systems typical of volcanic arcs where the heat source and reservoir commonly occur in close proximity.

Play fairway types considered include:

- 1) Liquid-dominated systems
- 2) Vapor-dominated systems (where tier 3 confinement plays a more crucial role)
- 3) Intermediate to felsic-volcanism-dominated systems
- 4) Basaltic-dominated systems (potentially requiring more frequent volcanism)
- 5) Various permeability setting plays, including, for example:

Transtensional terranes dominated by strike-slip faults and containing:

- i) pull-aparts
 - ii) displacement transfer zones
 - iii) fault intersections
- b) Extensional terranes dominated by normal faults and containing:
- i) normal fault step-overs
 - ii) accommodation zones
 - iii) fault intersections
- c) Compressive terranes dominated by reverse faults and containing:
- i) fault terminations
 - iii) fault intersections
- c) Other structural settings, including volcanic breccias, dome margins, or,
d) Primary permeabilities in carbonates, sandstones, or breccias.

These play fairway types include 1) typical volcanic-heat associated geothermal systems, 2) strike-slip pull-apart settings (e.g. Leyte), 3) back-arc and intra-arc extensional (rift-like) settings (Larderello, New Zealand, Kyushu (SE Japan)), and 4) steam-dominated systems (Larderello). Given that all of these play fairway types are considered to require the same key hierarchical tiers of physio-chemical environments, they were treated similarly in the model. Steam-dominated systems are believed to represent a time-dependent stage of the evolution of geothermal systems that at other times may be liquid-dominated. Strike-slip pull-apart settings and rift-like settings are recognized for their potential productivity, due to their inherent active, extensional strain, and they were implicitly modeled by assigning more favorable indices for those respective structural environments.

2.6 DEGREE OF EXPLORATION AND BLIND GEOTHERMAL SYSTEMS

The direct evidence collected can be considered obtained through a process of some type of exploration. Thus, if absolutely no “exploration” has been conducted, the lack of direct evidence should not be considered a negative factor. In contrast, if exploration has been significant, then the lack of positive direct evidence can be considered a negative factor. In the model, negative factors reflecting a lack of favorable temperature or surface feature data were only applied where exploration was considered to be present. More specifically, negative weights were scaled by a “degree-of-exploration” index scaled from 0 to 1.

It is challenging to assess the “degree-of-exploration”, since it is influenced by many qualitative exploration parameters and it is also heavily influenced by the ability of a geothermal system to remain blind or hidden. After initial investigations, it remained unclear how much of a role

climate and topography play a role in preventing surface thermal features from forming, such as the “rain curtain” hypothesized for the Cascade Arc. For the model presented, data on ice cap development at volcanic centers was used as a minimum estimate of “degree of exploration”, with the index being proportional to the percentage of ice cover present. Additionally, the presence/absence and depth of exploration wells is used as a degree of exploration in the model.

Data Quality/Completeness and Uncertainties: Data quality and completeness is a significant issue for the project. During compilation of arc volcanic centers, it was recognized that many volcanic arcs in remote areas (e.g. Antarctica and smaller islands of the southwest Pacific) were even less well explored than their counterparts in the Aleutians and Cascades, and hence of limited value in understanding or predicting geothermal potential. Similarly, for many remote volcanic centers, few data are available with which to assess geothermal potential. To constrain bias associated with these issues, it was decided in the case of volcanic arcs outside North America, to limit data compilations to volcanic centers with established geothermal production and/or centers with demonstrated potential to produce geothermal power (e.g., successful flow tests). These limitations complicate the ability to produce robust statistics because of a lack of demonstrated cases outside North America where volcanic centers are not believed to host economically viable geothermal systems. However, the more restricted data set provides a higher level of data quality, which in turn helps to reduce data uncertainty.

Expert-based uncertainties for structural and tectonic settings are assigned and calculated. A methodology for estimating uncertainties in geothermometer estimates has also been developed. These indices are integrated together in the final model to assist in uncertainty estimates.

The occurrence of blind geothermal systems in arc terrains was investigated as part of this project. In dry climates, the ability of a geothermal system to remain blind (without active surface manifestations) has been correlated with depth to water table, presence of shallow, cold aquifers, and presence of shallow cap rocks. Most of the arcs in this study occur in more humid climates with relatively high precipitation rates and shallower water tables, and the applicability of parameters established in dryer climates is less clear. Furthermore, team members with experience in the jungles of the southwest Pacific cast doubt on the ability of “rain curtains” to conceal or prevent the occurrence of geothermal manifestations, based on the prolific abundance of such features at many geothermal systems in these settings. At a minimum, however, the percent ocean cover and ice cover on a volcanic center clearly play important roles in determining if thermal manifestations will be visible, though these two factors also potentially adversely affect the economics of producing power.

The ability to predict blind geothermal systems was assessed during this project considering indices on a closely related variable, the “degree-of-exploration”. These indices, as well as parameters associated with “blindness”, are listed in Table 2.6-1.

Table 2.6-1. Degree of Exploration Parameters

construction of power plant
appropriately completed feasibility study
large-diameter drilling with flow tests
presence of direct use facility, type, MWt, flow rate, temperature, depth, fluid state
large-diameter drilling without flow tests
slim holes
surface manifestations data/survey with fluid geochemistry
surface manifestations data/survey
MT survey
temperature gradient wells or other shallow wells
presence of breached cap rocks
geologic mapping (alteration, lithology, structure)

Factors related to ability of geothermal system to remain concealed:

percent ocean cover
percent ice cover (depends on thickness, presence at base of volcanoes, etc.)
but not rainfall or precipitation rate?
depth to water table?
presence of shallow cold permeable aquifers
presence of shallow cap rocks

Although all factors were considered, insufficient data coverage for many data types were available from which to perform any quantitative analysis. The treatment of degree of exploration and associated uncertainties in this work is described more fully in Section 6.0

3.0 DATA COLLECTION

Parameters were identified that were considered to be important to both regional and local scale geothermal modeling. Data types useful for recognizing blind geothermal systems and/or defining degree-of-exploration were also identified. Numerous datasets were compiled and investigated for use in the Cascades-Aleutian Arc play fairway modeling to assess the power production geothermal potential of different volcanic centers associated with several play fairway types. Data were collected from a variety of sources including existing digital databases as well as entered from published literature. All VC were assigned a unique identifier such that future data sets can be linked via this number. Volcanic centers world-wide were evaluated and new data collected with the assistance of Google Earth. Some volcanoes were grouped as one center for consideration (those within 8 km of one another). Many volcanic vents were

eliminated from the AVO and GVP data sets that were either submarine vents, intraplate rather than subduction, or on islands <5 km diameter. The selections of VCs considered in this work are described in Section 2.1.

3.1 CRUSTAL STRAIN, PLATE MOTION, AND CRUSTAL THICKNESS - REGIONAL

Sources of Data

Data from a new comprehensive global geodetic strain rate and plate motion model (GSRM v. 2.1, released in Oct. 2014; Kreemer, et al., 2014) were downloaded and transformed into respective components of dilatational and shear strain as well as 2nd invariant and strain style. A world crustal thickness model created by the USGS (Laske et al., 2013), made publically available in the summer of 2014, was also downloaded.

Processing Data

The geodetic strain rate parameters were intersected in a GIS with the VC database to assign strain rate parameters to all 733 VCs in the database. Dilatational and shear strain rates, and the second invariant of strain were calculated from the principal strain axes. A strain style index was calculated using the formulation of Kreemer et al. (2014) in which the style progressively changes from 1 (dilatation) through transtension (0.5) to pure shear (0), transpression (-0.5) and compression (-1).

The relative plate motion vector of the subducting plate relative to the overriding plate was also estimated for the arc volcanic centers using the GSRM model. This was done using the equations of plate motion for each plate and the coordinates of the central point of each VC. This vector was then compared with the orientation of each arc segment (azimuth or surface trend of each volcanic arc segment) to calculate arc-perpendicular and arc-parallel velocities. The azimuth of each arc segment was measured for each volcanic center in Google Earth based on the alignment of the trench (usually in areas of thicker continental crust) or the alignment of active volcanic centers (for some oceanic arcs), depending on which method appeared most reliable. In some areas, including Panama and the Molucca Sea, Indonesia, plate motion vectors were not calculated because the GSRM model was not sufficiently accurate and/or detailed.

The world crustal thickness model was digitally intersected with the power plant and arc VC databases such that one crustal thickness value was assigned to each VC, including those without power plants, resulting in 733 data points extracted from the world crustal thickness model. Because of coarse grid spacing and locations of some VC near boundaries of grids, some values for crustal thickness were individually assigned based on professional judgement in consultation with this database.

3.2 POWER DENSITIES - REGIONAL

Sources of Data

A database of power densities of producing geothermal systems from around the world was recently compiled by Wilmarth and Stimac (2015). This database was incorporated into the VC

database for comparison with other geologic and geophysical data, including the data on global strain rates and plate motion.

3.3 TECTONIC DATA - REGIONAL

A review of existing data on the structural controls of both magmatic and amagmatic geothermal systems around the world indicates that three primary structural-tectonic characteristics are paramount for geothermal favorability: 1) type of structure and overall structural complexity, 2) extensional strain, and 3) strain rate. To assist in assessing these characteristics along volcanic arcs, we have assembled a list of geologic parameters to be populated for each VC that captures the regional tectonic parameters (section 3.3) and the local structural parameters (section 3.8). The classifications are based on recognized favorable structural settings for geothermal systems as documented in the published literature and including the team's experience with fault-controlled geothermal systems in the Great Basin, USA. These classifications provided the key components for modeling permeability and also grouping of VCs by potential play types. Other influences on permeability such as the interaction of structure and lithology were not considered in this phase.

Sources of Data

These data were collected from published geologic maps (digital and analog), digital databases including in particular the World Stress database (Heidbach et al., 2008), the USGS Quaternary fault and fold database for the continental USA (USGS, 2010), and numerous peer review papers.

Processing Data

Tectonic Setting: This was a qualitative characterization based on synergistic integration of local and regional structural data, stress data, and strain data. This category is useful for evaluating broad trends in the data sets, as well as providing favorability weighting based on regional data, especially where the local structural setting cannot be identified due to absence of data (e.g., unmapped and/or covered by snow). Categories include:

- a. Extensional
- b. Transtensional-SS (strike-slip dominant transtension)
- c. Transtensional-EXT (extension dominant transtension)
- d. Transpression
- e. Compression

Quality of Data and Error Potential

The error potential and combined relative data quality and data availability were assessed for every VC. Two scores were derived for each of the seven categories described above per each VC, each ranging from 0 to 1. Data quality and availability relate to many factors including, limited available geologic mapping, peer review papers or reports on regional tectonics, limited

seismometer distribution for assessing seismicity and tectonic stress orientations, and limited GPS geodetic stations for assessing intra-arc strain.

- A) Error potential (+/-)
- B) Quality/availability of the data

3.4 HEAT FLOW - REGIONAL

Source of Data

New regional Cascade heat flow data were acquired from Dave Blackwell and Maria Richards of SMU. Although the newly processed data set has considerable value in evaluating the local and regional geothermal potential of the Cascades, it could not be utilized in Phase I in a consistent manner as was done with the structural and direct evidence data types. In constructing the play fairways, the team relied heavily on the 74 VC global training set, and heat flow data is sparse to non-existent for the non-US areas used in this work. As such, there was nothing with which to compare Cascade heat flow information, and thus, this aspect could not be incorporated into the play fairway model construction or execution. Given the intrinsic value of this data set, it should be used in future studies collecting data for specific areas for which local, more detailed geothermal assessments are desired.

3.5 GEOCHEMICAL DATA - LOCAL

Sources of Data

Data were compiled for the Aleutian and Cascade arc VCs from files prepared for the National Geothermal Data System (NGDS) and published literature. Some of the NGDS data (AK, CA, WA) contain major and trace element (and other) data in separate tabs necessitating a complicated recombination of the data to obtain a complete analysis. In addition to required reformatting and recombination of NGDS data, in some cases, HCO_3 was not reported with other species in the same worksheet tab. For instance, Washington data that were posted were not complete, and data originators were contacted to rectify this. NGDS data were screened for those located within 20 km of a volcanic center in order to minimize hand data entry to correct for incomplete files posted for the states evaluated. Once all data were compiled, charge balances and geothermometers were calculated.

Charge balances were calculated for all analyses and all analyses with an incomplete analysis (e.g., one or only a few chemical constituents) or a charge balance >20% were omitted from the database. However, any record that contained a SiO_2 analysis was retained regardless of charge balance so that silica geothermometers could be calculated for the location. When more than one analysis was available for a location, the highest temperature and/or the one with the best balance was selected. The data were then clipped to the study area in ArcMap, reducing the records to only those located within the study area for the play fairway project (NW California, W Washington and Oregon, and Aleutian Islands). Sample sites were selected from a 20 km buffer zone around each volcanic center. The data were then sorted and all samples that were creeks, streams, lakes or rainwater were removed from the database. If no data were available for a VC in NGDS, literature searches were conducted in GRC, IGA, OSTI, Geothermics and

GeoRef, searching by both primary and secondary geothermal and VC names. Many VC still did not have any analyses or even mention of the sites in searched on-line library resources. Nevertheless, additional geochemical data from VCs were obtained from review of 115 published sources resulting in 32 partial or complete additional geochemical analyses added to the database.

After this compilation was completed, William Evans (USGS retired) provide an early release of a report on the geochemistry of springs in the Aleutians in mid-2015, from which an additional 3 sites were added to the database (Evans, 2015). Following this tabulation, the “completed” geochemical database was submitted to AVO (John Powers) to request input on any missing information from VCs in the Aleutians. No geochemical additions were available for the Aleutians according to AVO.

International - Power Plant sites only

Data for the volcanic centers (VC) in other arcs of the world were obtained almost exclusively through data entry from published sources. Name searches for geochemical data by primary and secondary volcanic center and geothermal field names were conducted in the following source databases: GRC, IGA, OSTI, Geothermics, GeoRef, CVO and AVO. Searches were conducted on both primary and secondary VC and geothermal field names. Over 200 publications were reviewed, obtained through downloads or interlibrary loans, from which data were entered and compiled, some of which contained information on multiple geothermal fields or volcanic centers. Additional geochemical data were obtained for arc VCs in South America from a digital database of published data maintained by co-author Glenn Melosh.

Raw data were compiled whenever available such that the same geothermometers could be calculated for the international as for the US sites. For all VC, both a representative well and spring (both highest T available) were included when both were located for a particular VC. However, many had no published geochemical analyses, but had notations of one or more geothermometer values in the publications. These data are included in the data set (along with associated references), as were maximum spring, well and field measured temperatures. Once the proceedings became available, the WGC 2015 conference papers were reviewed, from which additional analyses were included for five sites. When possible, preferred data to be included in the database for the international sites had a complete analysis with a charge balance <5%, and pH>5.5. This condition could not be met at all sites, and the less reliable analyses were weighted lower during the modeling phase of this work.

Once the data were reduced to the study areas (VC), the analyses were evaluated through various sorts, and additional analyses were removed from the data set. Ones that were removed at this stage typically had a good charge balance, but the balance was fortuitous and based on a limited, incomplete analysis, such as an analysis that only reported Na and Cl. Because the charge balances on these samples was misleading, the records were removed from the database.

Processing of Geochemical Data

One analysis, geothermometer, and measured temperature was compiled for both a spring and deep well (where available) for each site in an attempt to obtain geochemical and geothermometer data from springs, as well as potential or actual reservoir fluids. When multiple spring or well data were available for a particular volcanic center, one representative sample was included in the master geochemical data set such that one entry per volcanic center would be included in modeling. The highest temperature spring or well sample with the most complete analysis and best charge balance was selected when a choice of samples was available. In many cases, only one complete analysis was available for a particular VC (although most had good charge balances of <5%). Low pH samples were avoided when possible as their chemistry would lead to unreliable calculated geothermometer temperatures due to a variety of factors including leaching of soluble SiO₂ near discharge.

In many cases for all locations (World VCs as well as Cascades and Aleutian VCs), only minimal information could be gleaned from published literature such as a single temperature or geothermometer value without an accompanying full chemical analysis to evaluate. Although the quality of these data could not be directly ascertained via methods such as charge balances, the data were retained in the master data set to maximize the amount of information available for the model. For these cases without full chemical analyses, and only a notation of a geothermometer value, the value was listed in a Best Estimate column regardless of whether the geothermometer was obtained from a water or gas sample or if it was unstated by what method the source of the estimate was made. It is recognized that a “Best Estimate” for a particular VC is not necessarily a good estimate, only the best available. Those estimates without accompanying geochemical analyses are weighted low in the model due to lower reliability.

Geothermometer Calculations

Estimated subsurface temperatures were calculated using all compiled water analyses using the following geothermometers:

Geothermometer	Reference
K-Mg	Giggenbach, 1988
Na-K	Giggenbach, 1988
Na-K-Ca	Fournier and Truesdell, 1973
Na-K-Ca, Mg corrected	Fournier and Potter, 1979
Quartz	Fournier, 1981
Chalcedony	Fournier, 1981
Quartz-Adiabatic cooling	Fournier, 1981
SiO ₂ -Gigg	Giggenbach, 1992
SiO ₂ -Mariner	Mariner et al., 1983

Each geothermometer was calculated in a spreadsheet along with a column for the average of the Na-K-Ca, Mg-corrected and SiO₂-Mariner geothermometer values. The SiO₂-Mariner temperature is based on a threshold in which the quartz geothermometer is used if the Mg-

corrected Na-K-Ca temperature is $\geq 100^{\circ}\text{C}$, and the chalcedony temperature is used if this temperature is $< 100^{\circ}\text{C}$.

One “representative” geothermometer value was selected for each record based on the following criteria. If the record had multiple geothermometers in agreement ($\leq 20^{\circ}\text{C}$ variance), the approximate average of the geothermometers was selected within $\pm 5^{\circ}\text{C}$. If the record had both a SiO_2 and Na-K-Ca, Mg-corr geothermometer in agreement, the average was taken as the geothermometer for that sample (again, reporting geothermometers in 5°C increments). If the record only reported SiO_2 and no cation data, the SiO_2 -Gigg geothermometer was selected as the value for that record. When either or both the Na-K-Ca, Mg-corr and SiO_2 geothermometers were lacking or unrealistically low, the K-Mg geothermometer was selected as the sample was most likely from a lower temperature source for which this geothermometer is preferred. When SiO_2 was either lacking or unrealistically low (e.g., negative numbers), the Na-K-Ca geothermometer was recorded for the record. However, when the maturity index (MI) for a samples was > 2.5 , the Na-K-Ca geothermometer was selected in preference to the quartz, although in many cases, when $\text{MI} > 2.5$, the quartz and Na-K-Ca geothermometers were in fairly good agreement, particularly for the international sites. When the MI was < 2 , the best estimate of the sample was based on the quartz geothermometer for higher temperature systems, and chalcedony for the lower temperature systems ($< 120^{\circ}\text{C}$). As noted, low pH waters were avoided but were used in some cases when those were the only analyses available. The “best” analysis was picked in this case based on what appeared most reasonable from the various SiO_2 and Na-K-Ca geothermometer availability and MI.

3.6 SURFACE MANIFESTATIONS - LOCAL

Sources of Data

The same published sources used to collect geochemical data were also searched for notations of the presence or absence of fumaroles, sinters and travertines, and summaries compiled. Notations of surface manifestations in the Smithsonian database were also included in this compilation. Relatively few notations were located in the literature relating to the presence or absence of sinters and travertines, although these were included into the master data set where available.

Data on flank fumarole presence and temperatures from the published literature were compiled, including a few MW estimates from heat loss calculations. Most data sources did not specify fumarole temperatures or manifestation sizes. A visual search for fumaroles was then initiated in Google Earth to locate fumarole fields associated with all world volcanic centers to estimate size of the surface expression of the fumarole fields. Preliminary searches indicate data from these evaluations could be quite subjective, as well as incomplete due to the variation of image quality among areas. However, extensive international experience by co-authors Glenn Melosh and Bill Cumming, as well as Tom Powell (who volunteered his time), helped to identify many of the fumarole fields throughout the world. These experts identified locations of fumaroles in most

countries based on previous field visits to the VCs.

Processing Data

From these fumaroles located in Google Earth, a polygon was drawn around the altered areas or areas on known acid-sulfate mud pot occurrence, and the areas (in m²) of the polygons were calculated in ArcMap. When more than one fumarole area was located for a particular VC, the areas were summed to obtain a total surface area of fumarole manifestations for each VC. Figure 3.5-1 shows one example site at Salak, Indonesia where two power plants (push pins) and four fumarole (triangles with area outlines) areas are within the extent of the figure. In this case the areas for each of the four fumarole areas identified were calculated and summed to be associated with the Salak VC.



Figure 3.5-1. Google Earth image of the Salak VC area showing four fumarole areas identified and outlined by project team members.

The calculated areas were then plotted and compared to known power production and structural and tectonic characteristics of the VC.

Summary

Appendix IV lists the fumarole occurrence by area and country along with surface area of impact where available. It is unknown if or where fumaroles occur in many of the VC, as noted in the table. Note the number of VC with fumarole notations in the literature includes those where it was noted that no fumaroles are present. Most of the VC where fumaroles are definitely known not to occur are in Alaska, and noted as “None” in the appendix. This information was primarily obtained from Schaefer et al. (2014).

3.7 SUMMARY OF GEOCHEMICAL AND SURFACE MANIFESTATION DATA

Geochemical data entered and used to calculate geothermometers and best geothermometer estimates by field were selected for incorporation into a master geochemical data file and several plots and maps were made. Either spring or well chemistry (or both when available) were included for 96 (spring) and 67 (well) samples from the 174 volcanic centers, with the non-US VC only represented by those with existing power plants.

Table 3.5-1. Summary of available data from geothermal manifestations along with the percent of coverage of each data type over all VC included in this study. The total number of World VC in the table is 74, the number of VC with power plants. The number of volcanic centers containing data for the individual columns is listed. Temperatures are in °C.

	Total Number of VC	Meas Spring Temp	Spring Geother mometer	Measured Well Temp	Well Geother mometer	Fumarole	Surface Manifest ation
<i>US Volcanic Arcs</i>							
Aleutians	63	22	21	2	2	45	8
Cascades	41	18	16	7	5	11	5
<i>World Volcanic Arcs</i>							
Central America	14	8	8	12	9	8	6
Europe	2	1	1	3	2	1	1
Indonesia	20	14	15	9	7	17	6
Japan	14	8	8	10	10	4	1
New Zealand	9	2	9	6	9	2	4
Papua New Guinea	1	0	0	1	1	1	0
Philippines	9	3	4	8	7	7	1
Russia	6	4	5	3	3	3	0
South America	7	7	7	4	5	6	2
West Indies	2	1	2	2	2	1	0
Totals:	188	88	96	67	62	106	34
% Aleutian with data		35%	33%	3%	3%	71%	13%
% Cascades with data		44%	39%	17%	12%	27%	12%
% World with data		57%	70%	69%	65%	60%	25%

Surface manifestations in Table 3.5-1 include VC at which either or both sinter and travertine were noted in the literature searches. The large number of data for fumaroles in the Aleutians is a result of a specific notation of the presence or absence of fumaroles on Alaska VC by Schaefer et al. (2014). No other area includes comprehensive information on the absence of fumaroles at particular VCs. Many of the data gaps apparent in geothermometer and measured temperatures are due to the inability to locate data for a particular volcanic center in the literature. Although it is known that geochemical and temperature data exist for many of these geothermal fields, the information is currently held proprietary. The exception to this trend is seen in the Alaska data

in which the low number of well temperatures and geothermometers occurs because there are very few VCs drilled in the Aleutians. Hence, much of the “missing” data for VCs can be attributed to Alaska where geochemistry for wells is only available at two of the 59 volcanic centers, and for springs at 21 of the centers as many of the islands have not been explored to any great extent. Hence, final rankings among the Aleutian VC are more dependent on regional data sets that include all of the VC such as crustal strain, thickness, and regional tectonics, and less on measured and calculated temperatures.

Water pH was compiled along with other geochemical data and many of the producing, world VC have a low pH zone in their geothermal fields, but not within the production zone. Hence, low pH of surface manifestations do not eliminate a geothermal system from further evaluation based on corrosive considerations. As such, none of the systems in the Cascades and Aleutians have been eliminated from the study based on this consideration. Low pH zones are often indicative of a high temperature system within a VC as they are indicators of boiling. Low pH can also be an indication of magmatic contributions, which isn't necessarily an indicator of power producing systems. This situation is largely addressed in compilation of fumarole and acid-sulfate mud pot features where summit fumaroles (presumed to be magmatic) are distinguished from flank fumaroles/features (presumed to be hydrothermal).

All previously noted data are submitted as a project deliverable in spreadsheet format, with one tab of the spreadsheet allocated to description of the individual columns, and one tab showing the references consulted to obtain the data.

3.8 STRUCTURAL DATA

Sources of Data

These data were collected from published geologic maps (digital and analog), digital databases, peer review papers, geothermal conference papers, agency and industry reports, and thorough cross-checking against structures visible in available imagery available through Google Earth and ArcGIS Online.

Processing Data

Most of the structural parameters were populated from data within a 10 km radius of each VC, based on the observation that roughly 80% of the geothermal areas associated with VCs in arcs around the world are located within 10 km of a significant volcanic vent. The one exception for the 10 km radius was regional stress field data for dilation potential analysis which was assessed over a much broader area. These parameters were completed for all VCs in the Cascade and Aleutian Arcs, as well as for all “power-capable” VCs in other volcanic arcs in the world.

These data include the following six categories:

1. Structural Setting: Primary, Secondary, and Tertiary structural settings associated with each VC. This was also a qualitative characterization based on evaluation of faults within a 10 km radius of each VC. In many cases, VCs are associated with 2 or 3 major structural settings,

acting singly on separate parts of the VC or in direct overlapping and compound fashion. The type of structural setting contributes to the relative geothermal potential of a structural target area. Recent research shows that structural settings with greater complexity (e.g., accommodation zones) have greater geothermal potential to host a viable geothermal resource than those with less structural complexity (e.g., fault termination; Figure 3.8-1). The relatively more complex structural settings may correspond to greater bulk permeability, or broader areas with high permeability, which can facilitate larger commercial reservoir volumes and provided more efficient conduits for conductive heat transfer through the crust to drive the geothermal system (Faulds et al., 2013; Faulds and Hinz, 2015; Siler et al., 2015).

The structures listed below are listed in order of relative decreasing structural complexity.

- a. Accommodation zone
- b. Displacement transfer zone
- c. Pull-apart
- d. Step-over
- e. Fault intersection
- f. Fault termination
- g. Gravitational collapse normal faults
- h. Restraining bend
- i. Unknown/No Data

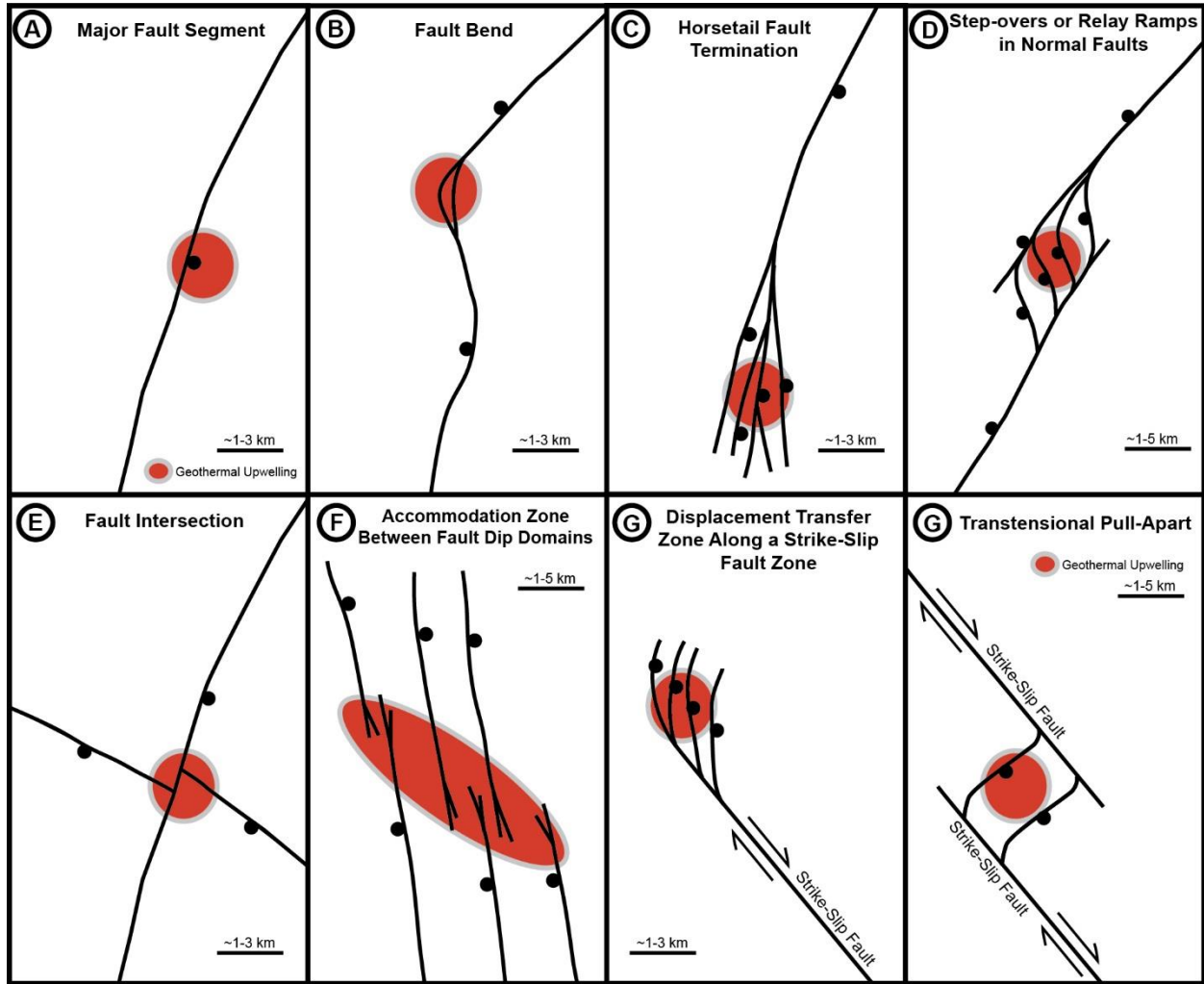


Figure 3.8-1. Examples of many of the structural settings identified in this study (modified from Faulds et al., 2015). These structures are listed with generally increasing complexity from A through G.

- 2. Quaternary Fault Slip Rate:** Slip rates of normal faults associated within a 10 km radius of each VC. Generally, higher strain rates provide greater geothermal favorability, by increasing the rate at which fractures form and open (e.g., Faulds et al., 2012). Therefore, distinguishing strain rates associated with specific faults that make up the structural settings associated with specific volcanoes is important for predicting relative favorability. This parameter focuses on the normal faults accommodating extensional strain. Locally higher rate strike-slip faults are present in some subduction arcs (e.g., Sumatra fault), however only the normal faulting slip rate component is recorded in this category for pull-aparts or displacement transfer zones along these high-rate strike-slip faults. Pure translation along a strike-slip fault does not accommodate extensional strain. This category is populated from the USGS Quaternary Fault and Fold Database (USGS, 2010 – CA, NV, WA only), paleoseismic data in reports and peer

review literature, geodetic data, image analysis, and map data were used to populate this field for other areas. Categories include:

- a. 1-3 mm/yr
 - b. 0.3-1 mm/yr
 - c. 0.1-0.3 mm/yr
 - d. <0.1 mm/yr
 - e. 0 mm/yr
 - f. Unknown/No Data
3. Relative Concentration of Quaternary Fault Scarps: This category assess the relative number of Quaternary faults associated within a 10 km radius of each VC. Faults and structures active in the Quaternary demonstrate a positive relationship with geothermal activity around the world (e.g., Bell and Ramelli, 2007). The density of Quaternary faults associated with the VCs provides a relative measure of the recency of faulting and the complexity of the structure. Recency of faulting is broadly correlative with Quaternary fault slip rates, but provides a key detail for the faults with lower slip rates that may only rupture once every 10,000 to 100,000 years. Faults with identical fault slip rates but with different recency of faulting will have different geothermal favorabilities. The relative measure of the number of Quaternary fault scarps in association with each VC provides a measure of geothermal favorability. In addition, earthquake-induced stresses show a correlation with permeability in active hydrothermal systems and with epithermal mineral deposits (Sibson, 1987, 1994; Micklethwaite, and Cox, 2004). Relative categories include:
- a. High (many)
 - b. Medium (few)
 - c. Low (one)
 - d. Zero (none)
 - e. Unknown/No Data
4. Fault Orientations: Azimuth of primary, secondary, and tertiary (when present) fault sets in a 10 km radius of each VC were recorded. Faults at higher angles to S_{Hmin} are more favorable for dilation and enhanced permeability.
5. S_{Hmin} : Azimuth of least principle horizontal stress. Stress data are compiled from published data local to each VC and/or gleaned from regional data available in the World Stress Map (Heidbach et al., 2008). The least principle horizontal stress was used along with fault orientation data to assess dilation potential. Presence of faults oriented at high angles to S_{Hmin} are more favorable for dilation and enhanced permeability than those at low angles to S_{Hmin} (Ferrill et al., 1999).
6. Dilation potential: Angular comparison of S_{Hmin} versus strike of fault(s). This is a relatively simple way (Ferrill et al., 1999) to analyze for dilation potential systematically and evenly across VCs associated with all levels of detail in data. This parameter was derived with the following calculation for normalizing from 0 to 1: $\sin(|S_{Hmin} - \text{Fault Strike}|)$.

Quality of Data and Error Potential

The error potential and combined relative data quality and data availability were assessed for each of the seven categories listed above for every VC. Two scores were derived for each of the seven categories described above per each VC, each ranging from 0 to 1. Data quality and availability relate to many factors including, latest Pleistocene glaciation removing evidence of earlier Quaternary fault activity, Holocene volcanic rocks concealing Pleistocene age Quaternary fault scarps, perennial snow cover, vegetation cover, limited available geologic mapping (many Aleutians VCs only mapped at 1:2,500,000 scale), limited seismometer distribution for assessing seismicity and tectonic stress orientations, and limited GPS geodetic stations for assessing intra-arc strain.

- C) Error potential: Assigned a +/- range relative to the internal scoring steps, standard deviation of the results in each data set, and the quality/availability of the data.
- D) Quality/availability of the data: This score was qualitatively defined based on assessing all available quantitative and qualitative data available per VC per data category.

3.9 VOLCANIC DATA - LOCAL

Data Collection and Sources

Data collected for global volcanic features included information about the physiography, eruptive history, eruptive styles and composition. Physical information collected from Google Earth was heavily augmented with the written and tabulated data from the Smithsonian database, as well as information present in the Google Earth database. For the Cascades and the Aleutian arcs, additional volcanic center locations from the Alaska Volcano Observatory (AVO) and Cascades Volcano Observatory (CVO) were included and given higher priority if the data conflicted with those present in other databases. This was more common in the Aleutians where discovery-level studies are still being conducted by AVO and the data have not yet been added to the Smithsonian database.

Physical parameters

Using Google Earth, all VC's were inventoried for a wide variety of physical parameters (Table 3.9-1). Google Earth proved to be an invaluable tool for the global investigation of volcanic features, and many of the measurements have a high degree of confidence. These include the number and footprint of all volcanic features and topology (distance and azimuth between various volcanic features). Rather than attempt to estimate the volume of volcanic features, which would introduce unnecessary error by assuming of a conical form using radius and total relief, the footprint of volcanic features (domes, stratocones, shield volcanoes and calderas) was used as a proxy for volcano size. Similarly, data collected regarding the presence and extent of ice, based on the minimum extent of iced and crevassed areas in the historical imagery, has a high confidence level.

Although Google Earth is well suited for the measurement of the physical aspects of volcanic features, other aspects of the collected data are limited. For instance, the extent of alteration present, based on discoloration of the ground surface, is strongly affected by image quality and ground cover, particularly in forest/jungle areas. Even in areas above tree line, the interpretation of altered ground is somewhat subjective, and the values recorded are regarded with less certainty. Other limitations are present when trying to correlate outside datasets with Google Earth imagery. In particular, combining Google Earth imagery with text-based external data sets (e.g., the Smithsonian database, Google Earth written descriptions) is challenging. For example, cases in which rhyolite domes are mentioned in the Smithsonian database, it is commonly not possible to distinguish which of several domes present might be rhyolitic. For cases in which the correlation between complementary datasets were easily recognizable (e.g., “A large, rhyolite flow is present on the northeast flank of the volcano”), these features were separated by chemical composition. However, these cases were rare enough that this additional discrimination was not useful.

Ages

The age of volcanic centers was estimated using the Smithsonian and Volcano Observatory databases. Initially our team intended to report the ages of volcanic features in categories of <1,000 years, 1,000-5,000 years, Holocene and Pleistocene. Data contained within the various text-based external data sets, however, were not specific enough to allow this level of age resolution for individual volcanic features. We were therefore forced to eliminate the finer-resolution age categories from our original spreadsheet, and broad age divisions of Holocene and Pleistocene were used. The Holocene vs. Pleistocene determinations were based fundamentally on Volcano Observatory and Smithsonian databases, with subsequent age determination based on morphology observed in Google Earth using glaciated and otherwise heavily eroded surfaces to indicate pre-Holocene VCs. In cases where only Pleistocene and Holocene age determinations were possible, or if no information could be determined, no numeric age was assigned. These features were therefore not included in analyses based on numeric ages (e.g., Fig. 4.3-3).

The ages and dates of the most recent eruption from each VC are based on information in the Smithsonian and Volcano Observatory databases. In most cases, the date of the last eruption was readily available. For a small number of cases the most recent eruption had to be generally classified as either Holocene or Pleistocene. The age of the most recent eruption was used to distinguish the general age of the VC. In some instances the age of volcanic features had to be logically deduced. Most notably, several calderas were identified as “inter-vent,” or located between the VC of interest and an adjacent VC. Because these calderas are absent from the Smithsonian database of Holocene volcanoes, these were interpreted to be Pleistocene in age.

Eruptive Compositions

The compositions of erupted material from each VC was compiled from two main resources. Information regarding the composition of the most recent eruption from each VC was collected from the Smithsonian database, which provided data for 51% of the VCs in the global training set, 62% of the Aleutian VCs and 91% of Cascades VCs.

In order to investigate linkages between magmatic compositions on geothermal systems we attempted to compile the compositions for all analyzed samples from each of the VCs. Very few volcanoes have a comprehensive chemical history, and many of the VCs that are part of this study have enjoyed substantial scientific investigation. In order to estimate the average eruptive composition and the chemical diversity of erupted products, we used the GeoROC database (<http://georoc.mpch-mainz.gwdg.de/georoc/>), the most complete global clearinghouse of igneous rock geochemistry. Other igneous geochemical databases (www.EarthChem.org; www.earthref.org/GERM/; Volcano Observatory databases, and others) have entries that also appear in GeoROC. In order to avoid duplication, only the GeoROC database was used. GeoROC was queried for volcanic and plutonic samples from each of the volcanic arcs present in the global training set as well as the Aleutians and Cascades. This resulted in over 94,000 whole rock geochemical analyses, of which 11,000 from >3,400 scientific publication were related to the VC's inventoried. This data set includes data for the majority of VCs in this study (80% of global training set VCs, 86% of Aleutian VCs, 62% of Cascades VCs).

Although the GeoROC database is the most complete global data set for igneous rock chemistry, it is by no means complete. The database is populated by researchers voluntarily submitting their data in the interest of public distribution. Thus, there is a reporting bias toward more heavily studied volcanoes and for more intensely studied eruptions. For example, of the 319 samples listed for Mt. St. Helens, Washington State, USA, 99 (31%) are from the 1980 eruption. In comparison, the three large dacitic Plinian eruptions from Glacier Peak volcano (also in Washington State) between 13,000 and 11,000 years ago has only a single entry in the database among them. Thus, the GeoROC database (and all other igneous geochemical clearinghouses) is skewed toward volcanoes and deposits that have piqued scientific interest. Regardless, GeoROC represents the most complete dataset for the VC's inventoried in this study, and data are available for 77% of the VCs studied.

Table 3.9-1. Volcanic features inventoried for all Cascades and Aleutian VCs and VCs present in the 74 VC global training set.

Category	Characteristics inventoried	Data Source*
Ice	Presence, extent (based on historical imagery)	G.E.
Alteration	Presence, extent (based on coloration in imagery)	G.E.
Primary Vents		
Stratocone	Number, age, footprint, most recent eruption	G.E., Smith., V.O.
Shield volcano	Number, age, footprint, most recent eruption	G.E., Smith., V.O.
caldera	Number, age, footprint, most recent eruption	G.E., Smith., V.O.
Subsidiary vents		
Cinder cones	Number, age, orientation/clustering	G.E.
Domes	Number, age, orientation/clustering	G.E.
Topology		
Tectonic	Distance, azimuth to trench; arc-trench gap	G.E.

Along arc	Distance, angle to next VC; distance from main volcanic arc	G.E.
<i>Intervent features</i>		
Non-VC Pleistocene vents	number	G.E., Smith., V.O.
Non-VC Holocene vents	number	G.E., Smith., V.O.
shield	number	G.E., Smith., V.O.
caldera	number	G.E., Smith., V.O.
Cinder cones	Isolated, field, lineament	G.E.
domes	number	G.E.
Alteration	presence	G.E.
Lava flows	presence	G.E.
Ocean cover	Presence (affects degree of exploration)	G.E.
Erupted Composition	Whole rock SiO ₂ content	GeoROC

*Data sources: G.E.=Google Earth; Smith.=Smithsonian Global Volcanism Network Database; V.O.= Alaska and/or Cascades Volcano Observatory.

Processing of Rock Geochemistry Data

The compositions obtained from GeoROC were separated into four broad categories (basalt, andesite, dacite, rhyolite) based on SiO₂ wt%. From this, the number of entries for volcanic samples of each compositional group were tabulated. A weighted average for the number of samples in each category was calculated, where basalt = 1, andesite = 2, dacite = 3, rhyolite = 4, and no data = 0, and the average composition was separated into groups (basalt=1-1.75, andesite=1.75-2.5, dacite=2.5-3.25, rhyolite=3.25-4). For example, Los Azufres Volcano, Mexico, has 31 basaltic samples, 50 andesitic samples, 11 dacitic samples and 56 rhyolitic samples, yielding a weighted average of 2.62, equivalent to an average composition of andesite. The diversity of eruptive products was also calculated by adding the number of different compositional categories that occurred. Volcanoes that erupted only basalt would receive a compositional diversity score of one. For the example above, Los Azufres received the highest possible compositional diversity score of four.

3.10 DATA COMPILATION SUMMARY

Sources of Information

The following tables summarize the data compiled for the project. Data were compiled from the following digital data sources:

Table 3.10-1. Sources of digital data used in this work.

Digital Data Sets	Database Source	Web Link
Active Volcanoes	State of Alaska AVO	www.dggs.alaska.gov/pubs/id/20181 www.avo.alaska.edu/downloads/searchbib.php
Alaska Fumaroles	Janet Schaefer	personal communication
Crustal Thickness	Laske, 2014	igppweb.ucsd.edu/~gabi/crust2.html
Heat Flow	SMU	www.smu.edu/Dedman/Academics/Programs/GeothermalLab/DataMaps
Gobal Strain Rate	Nevada Geodetic Laboratory	geodesy.unr.edu/cornekreeemer/gsr.htm
Land Use	BLM GeoCommunicator	www.geocommunicator.gov/GeoComm/site_alter_notice.htm
	Alaska	sdms.ak.blm.gov/sdms
	California	www.blm.gov/ca/gis/index.html
	Oregon/Washington	www.blm.gov/or/gis/data-details.php?id=9
Multiple data sets*	NGDS	geothermaldata.org/ repository.stategeothermaldata.org/repository/browse/ www.thinkgeoenergy.com
Power Plants	ThinkGeoEnergy	
Quaternary Vent database	State of Alaska	www.dggs.alaska.gov/pubs/id/27357
Rock Chemisry/composition	GeoRoc	georoc.mpch-mainz.gwdg.de/georoc/
Structure	World Stress Database	dc-app3-14.gfz-potsdam.de/pub/download_data/download_data.html
	AK volcanoes	pubs.usgs.gov/dds/dds-40/album.html
	Active fault database for Japan	gbank.gsj.jp/activefault/cgi-bin/search_e.cgi?search_no=e007&version_no=1&search_mode=0
	National geologic map for Japan	gbank.gsj.jp/seamless/maps.html?lang=en
	Quadrangles for Japan	gbank.gsj.jp/seamless/download/downloadIndex_e.html
	Volcanoes of Japan	gbank.gsj.jp/volcano/index_e.htm
	Continental-scale geologic maps	OFR 97-470; pubs.usgs.gov/ds/424/
	multiple countries	search.usa.gov/search?utf8=%E2%9C%93&affiliate=usgs&query=open+file+report+97-470
	Geologic Map of North America	USGS DS 424; http://search.usa.gov/search?utf8=%E2%9C%93&affiliate=usgs&query=DS+424
Volcano data	Smithsonian Global Volcanism Program	volcano.si.edu/
Volcanic Vent database	Washington state	fortress.wa.gov/dnr/geology/?Theme=wigm
Water Geochemistry	NGDS	repository.stategeothermaldata.org/repository/browse/
Wells	CA Div of Oil and Gas	www.conservation.ca.gov/dog/Pages/WellFinder.aspx

*spring/well locations, spring/well chemistry, volcanic vents, borehole lithology, borehole temperature, active faults, rock chemistry, well logs and header files, direct use and power plant sites

Additional data were compiled and hand entered from published literature. Various geothermal literature sources were searched by volcano name and geothermal field name for geologic, geochemical, geophysical, power and other information input into the data sheets to describe the physical conditions present at the individual volcanic centers. Most data categories have gaps in information as no data are currently published. The library search engines that were used to search peer reviewed articles, and published reports and conference proceedings follow.

Table 3.10-2. Library search engines used to locate publications.

Online Library Resources	
Alaska Volcano Observatory	www.avo.alaska.edu/downloads/searchbib.php
Cascades Volcano Observatory	volcanoes.usgs.gov/vsc/publications.html
GeoRef	www.engineeringvillage.com.unr.idm.oclc.org/search/quick.url?CID=quickSearch&database=2097152&acw=&utt=
Geothermics	www.sciencedirect.com.unr.idm.oclc.org/science/journal/03756505
GRC	www.geothermal.org
IGA	www.geothermal-energy.org/publications_and_services/conference_paper_database.html
OSTI	www.osti.gov/geothermal/index.jsp

Google Earth Data Compilation

Particular data compiled from volcano examination in Google Earth include the following based on examination of multiple imagery dates for each data type.

Table 3.10-3. Data compiled from Google Earth

Feature	Data Type
Fumaroles	surface area, type
Ice Presence	% ice cover, surface area
Intervent	types, numbers, relationships
Surface Alteration	surface area
Volcanic Vents	types, numbers

Compiled Data Types

A summary of the compiled data appears in the following table. The table indicates the number of volcanic centers (VC) for which data were acquired for each category. Data values could not be located for all VC for all data types. The number of fields in the constructed database(s) associated with each general category (e.g., geothermometry) is noted in the last column “Data Categories”. For instance, several geothermometers were calculated from several chemical constituents, and hence, the number of data categories represents distinct fields in the database (e.g., several Silica geothermometers, Na-K-Ca geothermometer, etc. in individual columns in a spreadsheet). Some of the interim and calculated fields were omitted in final data submission, and thus the number of data categories submitted is less than those indicated below in the final submission to GDR.

Table 3.10-4. Summary of data types collected in Phase I of this project..

Data Type	Scale	Volcanic Centers			Data
		World Arcs	Aleutian	Cascades	Categories
Crustal Thickness	Regional	633	63	37	1
Fumarole surface Area	Local	65	62	11	5
General (name, loc.)	Local	633	63	37	10
Geochemistry					
Representative Spring	Local	50	18	10	13
Representative Well	Local	58	5	2	13
MaxTemp (°C) - Spring	Local	48	24	18	1
MaxTemp (°C) - Well	Local	63	2	7	1
Geothermometry - Spring	Local	59	23	16	16
Geothermometry - Well	Local	58	5	2	16
Geodetic - Crustal Strain	Regional	633	63	37	15
Geology-Rock Type	Local	0	46	19	11
Structure	Local	72	59	37	14
Tectonic Setting	Local	78	59	37	1
Structural Setting	Local	78	59	37	6
Slip Rate	Local	31	59	37	4
Structural Azimuth	Local	78	59	37	14
Power Density	Local	41	--	--	1
Power Plants	Local	84	0	0	6
Surface Expressions	Local	53	22	35	5
Tectonic Setting	Regional	633	63	37	6
Volcanic Data					
Age	Local	71	63	37	4
Alteration	Local	73	62	36	2
Arc Characteristics	Local	75	63	37	7
Caldera Info	Local	633	63	37	12
Composition & Diversity	Local	72	63	37	8
Edifice Volume	Local	3	0	15	1
Eruption Freq	Local	628	54	26	5
Eruption Volume	Local	1	0	10	1
Historic Eruptions	Local	416	43	18	1
Holocene Eruptions	Local	416	42	18	1
Ice Cover	Local	74	62	35	3
Intervent characteristic	Local	75	63	37	31
Vent Types	Local	4	50	19	56
Volcano Type	Local	631	63	37	3
Total Data Categories:					294

4.0 DATA EXPLORATION

A preliminary analysis of interrelationships among the various data sets was completed using graphs, scatter plots, cumulative distribution curves, and statistics. A more comprehensive analysis, including the use of multivariate statistics and other statistical treatments was completed after the final data collection task in associating with the construction of the numerical play fairway models.

4.1 GEOCHEMICAL AND SURFACE MANIFESTATION DATA

Temperature and fumarole data are compared with information from the 74 benchmark sites representing power producing systems in arc environments outside of the US.

Temperatures

As with other data types compiled for this project, many plots of various data groupings were constructed to evaluate trends and data interrelationships. A summary of world maximum temperatures by region appears in Figure 4.1-1 which shows that the maximum, known temperatures of US systems are typically less than those in other areas of the world in volcanic arc environments. The highest temperatures systems in both the north and south Cascades (Meager and Newberry) are both known to be of low permeability, with Newberry being an active site for EGS studies.

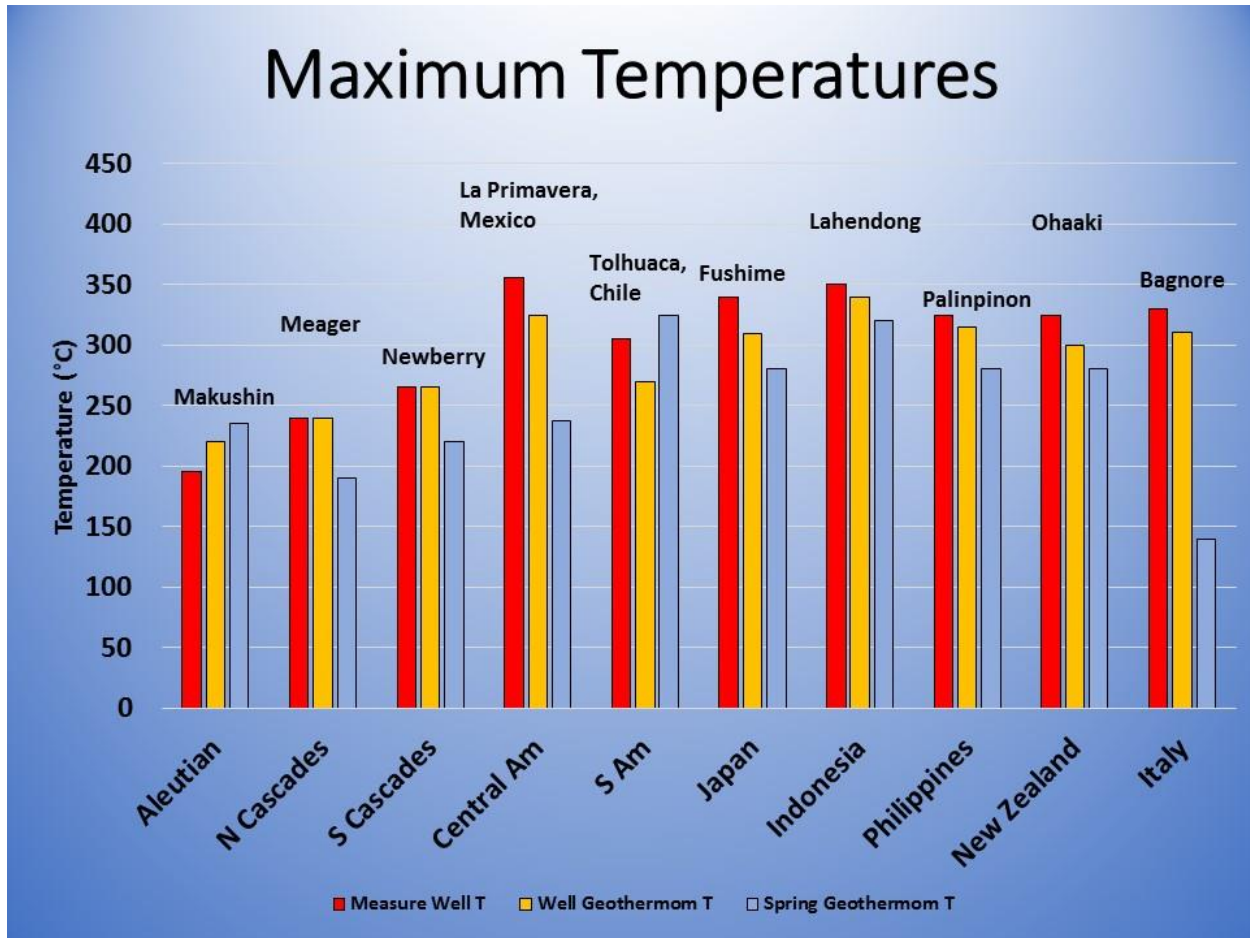


Figure 4.1-1. Summary of maximum known temperatures from geothermal systems around the world in arc settings.

Temperatures range from 190-353°C (ave: $266 \pm 32^\circ\text{C}$) for all world arc power plant systems, whereas the maximum temperatures in the Aleutians is 220°C (geothermometer estimate at Makushin) and Cascades is 265°C (measured at Newberry). Thus, maximum known temperatures in the Aleutians and Cascades are at or lower than the average global value at producing power systems.

The temperature data were further investigated to evaluate various relationships including local and regional trends. Figure 4.1-2 illustrates the best estimate of spring geothermometer temperatures versus the maximum measured well temperatures at the site. Nearly all sites worldwide have higher measured temperatures relative to those indicated by geothermometer temperatures obtained with spring chemistry. Among the outliers is the point plotted for Lassen which is the temperature of a 1400 m well located in an outflow at Terminal Geyser (13 km from the summit of Lassen), and thus not representative of reservoir conditions. The Walker "O" No. 1 Well BHT of 124°C (175°C at maximum temperature in the outflow zone) is not used in the statistical modeling as it is not believed to represent the high temperature resource at depth given the elevated temperatures indicated from spring (220°C; Na-K-Ca) and well

geothermometers (232°C; Na-K-Ca). No wells in the Lassen area tap a high temperature resource closer to the VC.

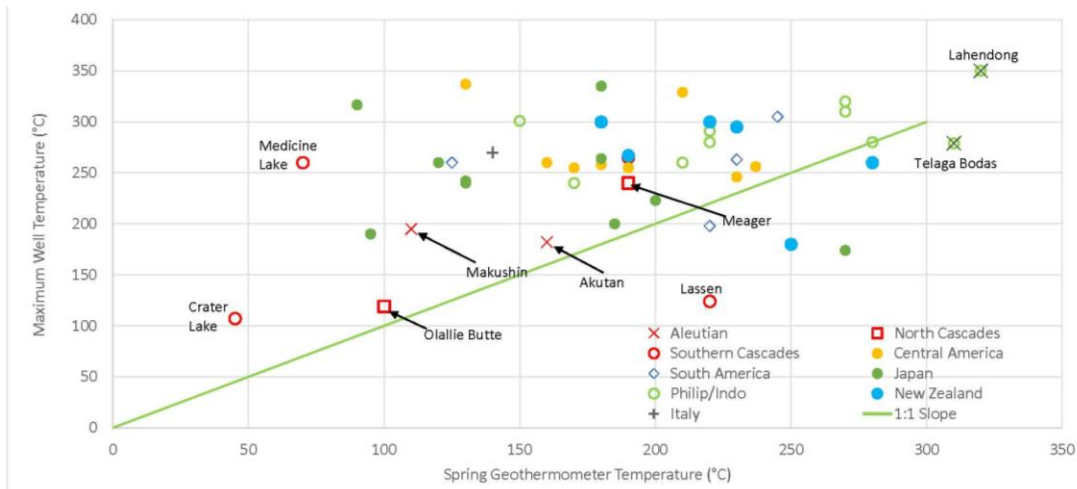


Figure 4.1-2. Plot of spring geothermometer temperatures versus maximum measured well temperatures for geothermal systems in volcanic arcs.

Medicine Lake and Crater Lake are also outliers from the general trend with the spring geothermometer temperatures available showing much lower “reservoir” temperatures than actually measured at this site. Similarly, the geothermometers calculated from wells from the same areas as geothermometers calculated from local springs are nearly always higher (Figure 4.1-3). This results because they are obtained from the high temperature resource, whereas the spring waters often undergo variations in chemistry (mixing, precipitation, dissolution, etc.) prior to sample collection, thus indicating lower than actual deep temperatures. However, the Lassen (and several other VC) samples from the representative well and spring both indicate nearly the same reservoir temperature (220-230°C).

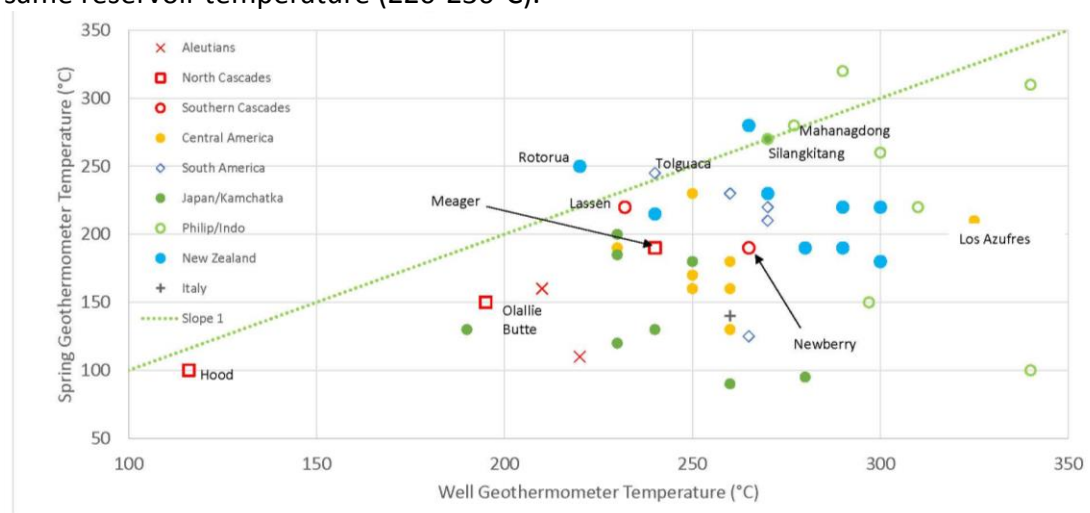


Figure 4.1-3. Plot showing geothermometer temperatures calculated from a representative spring and well from each VC.

Fumaroles

A summary of the fumarole occurrence from the acquired data shows a strong correlation between flank fumaroles and power producing systems. Table 4.1-1 shows that 70% of all world power producing systems have known flank fumaroles, with the occurrence of flank fumaroles being unknown in 30% of the benchmark systems. Nevertheless, 93% of all power produced in total MW at world arc VC are from systems with known flank fumaroles demonstrating the strong correlation of power production with flank fumarole occurrence. Thus, one factor to consider in Cascade and Aleutian exploration should include the mapping of flank fumarole occurrences. Currently it is unknown (undocumented) if there are flank fumaroles at 68% of the VC in the Cascades, and 10% of the Aleutians. 49% of the Aleutian VC are **not** reported to have flank fumaroles based on Schaefer et al. (2014). However, work in other areas shows that these features can be discovered even after fairly extensive work has been conducted in an area, and the Aleutian VC are likely not thoroughly explored to date. Hence, some of these VC may indeed have currently unknown flank fumaroles.

Table 4.1-1. Percent of VC in Aleutian, Cascade and World with known flank fumaroles. See text.

	None	Known	Unknown
Aleutians	49%	41%	10%
Cascades	22%	11%	68%
World	<1%	70%	30%
<i>Power Production - % Total MW Produced from Arc Systems</i>			
World	<1%	93%	7%

Correlations

Numerous box plots were constructed to evaluate relationships among data types and facilitate comparisons of Aleutian and Cascade VC to power producing systems in the World VC benchmark sites. Figure 4.1-4 through 4.1-6 provide an example of how the various plots were constructed for the data categories of fumarole area (rows) and well geothermometer temperatures (columns). The numbers within the box represent the average MW per benchmark system within the particular data categories. For instance, the red box with the average of 4MW/system in the upper right corner represents 3 systems producing a total of 1310 MW, with the three VC in this case being Mahagagdong and Palinpinon (Philippines) and Salak (Indonesia). In this example, only 1 system with an installed 2 MW plots in the 150-200°C geothermometer range at the

>100,000 m² fumarole area size (Mendeleev, Russia). Nevertheless, there is a general trend of higher mean MW for systems with larger flank fumarole areas at higher temperatures.

Color coding of average MW size are included as follows:

- Largest – Red
- Large – Orange
- Medium – Yellow
- Small – Green
- Smallest – Blue

The heavy box in the upper right corner outlines the systems with the higher average MW values. The numbers along the horizontal axis show average MW increases with increasing well geothermometer temperature whereas the right vertical axis shows generally increasing average MW with increasing flank fumarole areas, with the <10,000 m² row being somewhat anomalous at an average of 112 MW/system. As can be seen, the benchmark VC systems producing power are poorly represented at lower temperature (<200°C) systems.

Fumarole Area (m ²)	Mean MWe/System						Mean MW
	Unknown	100-150	150-200	200-250	250-300	>300	
>100,000 - 300,000			2		174	437	224
>30,000 - 100,000				15	264	102	123
10,000 - 30,000					80	38	81
<10,000				61	180	242	112
Y-Unk Area							0
N							0
Unknown				59	36	76	45
	0%	0%	0%	8%	42%	51%	
Mean MW	0	0	2	53	128	167	

Figure 4.1-4. Mean MW per system in the 74 world benchmark sites grouped by their respective fumarole areas (vertical) and well geothermometer temperatures (horizontal).

This plot with the same color scheme defined by the benchmark systems is repeated below in Figures 4.1-5 and 4.1-6 for the Aleutian and Cascade VCs. For the Aleutians, there is a considerable percentage of unknowns both in terms of geothermometer values and fumarole areas. However, two systems (Akutan and Makushin), while plotting outside the area of highest potential based on the world benchmark VCs, suggest power production potential on the order of 50-100 MW.

	Unknown	100-150	150-200	200-250	250-300	>300	
Fumarole Area (m ²)	Mean MWe/System						Mean MW
>100,000 - 300,000							224
>30,000 - 100,000							123
10,000 - 30,000							81
<10,000				Akutan			112
Y-Unk Area	6			Makushin			0
N	34						0
Unknown	19						45
	68%	0%	0%	0%	0%	0%	
Mean MW	0	0	2	53	128	167	

Figure 4.1-5. Summary of Aleutian VC relative to fumarole area, well geothermometer temperatures and mean MW obtained from the world benchmark VC.

The plot for the Cascade VCs also shows that none of the Cascade VC plot within the highest box for anticipated high MW per system, but the highest ranking system (Lassen) plots close to the higher average size of world VC suggesting a possible resource size on the order of 125 MW.

	Unknown	100-150	150-200	200-250	250-300	>300	
Fumarole Area (m ²)	Mean MWe/System						Mean MW
>100,000 - 300,000							224
>30,000 - 100,000				Lassen			123
10,000 - 30,000							81
<10,000							112
Y-Unk Area	2						0
N	7		1				0
Unknown	24		1		Newberry		45
	94%	0%	6%	0%	0%	0%	
Mean MW	0	0	2	53	128	167	

Figure 4.1-6. Summary of Cascade VC relative to fumarole area, well geothermometer temperatures and mean MW obtained from the world benchmark VC.

Similar, additional plots were evaluated that show essentially the same types of trends (increasing potential in the upper right of the plots). These plots include correlation of fumarole areas with tectonic setting, regional strain rate, slip rate, structural setting, Quaternary fault density, and spring geothermometry. Figures 4.1-8 and 4.1-8 show an additional example of these box plots for fumarole area versus tectonic setting, where the color coded boxes are obtained from the world VC benchmark sites with red showing those with the highest MW per system as in the previous figures. The two Aleutian systems that plot closest to the high MW/system box (orange box with fumarole areas <10,000 m²) are the Akutan and Semisopchnoi VCs suggestive of mean MW production on the order of 100-125 MW are possible.

	Unknown	Comp.	Transpress.	Transtension-SS	Transtension-EX	Extensional	
Fumarole Area (m ²)	Mean MWe/System						Mean MW
>100,000 - 300,000							224
>30,000 - 100,000							123
10,000 - 30,000							81
<10,000	1			2			112
Y-Unk Area	1	6	4	12			50
N		11	10	10			0
Unknown	3			3			45
	6%	29%	22%	43%	0%	0%	
Mean MW	22	33	116	124	149	113	

Figure 4.1-7. Summary of Aleutian VC relative to fumarole area, tectonic setting and mean MW obtained from the world benchmark VC.

As discussed in greater detail in the structural analysis sections, the systems within transtensional and extensional settings can be expected to have much larger mean MW per system (>110 MW) relative to those in compressional settings (33 MW on Fig. 4.1-7), which also account for fewer of the world VC power plants where only 15% of the power producers (9% of the power production) occur in the compressional and transpressional settings in comparison to 45% (54% of the power) in the transtensional-strike slip environments in the world settings. In comparison, 29% of the Aleutian VC occur in compressional settings, with 43% occurring in transtensional, strike-slip settings.

	Unknown	Comp.	Transpress.	Transtension-SS	Transtension-EX	Extensional	
Fumarole Area (m ²)	Mean MWe/System						Mean MW
>100,000 - 300,000							224
>30,000 - 100,000					1		123
10,000 - 30,000							81
<10,000							112
Y-Unk Area		2			1		50
N			4			4	0
Unknown			5		8	12	45
	0%	5%	24%	0%	27%	43%	
Mean MW	22	33	116	124	149	113	

Figure 4.1-8. Summary of Cascade VC relative to fumarole area, tectonic setting and mean MW obtained from the world benchmark VC.

The systems that consistently rank high from this type of analysis, although typically not within the high ranges found in producing arc systems around the world, are Lassen for the Cascades, and Akutan, Makushin and Semisopochnoi in the Aleutians. Based on these types of plots, these systems could produce 100 MW, or more at Lassen, which consistently plots into a zone of some of the highest productivity, world-class, geothermal power producing systems. Those that rank higher in some of the plots include Kaguyak, Korovin, Little Sitkin, and Seguam in the Aleutians.

However, most systems in the Cascades and Aleutians are expected to produce ≤ 50 MW at any individual VC.

4.2 STRUCTURAL-TECTONIC DATA

Structural-tectonic data were successfully collected across all of the Cascades, Aleutians, and Global Benchmark VCs. Results for each primary structural-tectonic parameter are summarized below.

Tectonic Setting

In the Aleutian arc, the angle of plate convergence between the North American and Pacific plates varies steadily from sinistral oblique convergence at the far eastern end, near-perpendicular convergence in the east central part, dextral oblique convergence for much of the western half, and a nearly pure transform motion at the far west end of the arc (e.g., Buurman et al., 2014). Oblique subduction drives translocation of the entire western half of the arc along arc-parallel strike-slip faults and arc-parallel extension accommodated by a complex system of normal and strike-slip faults (Ave Lallemand, 1996; Ave Lallemand and Oldow, 2000). As obliquity of subduction increases from east to west along the Aleutian arc, so do the magnitude of dextral shear along intra-arc dextral strike-slip faults. The Aleutian arc also straddles a passive oceanic-continental crustal boundary, with the western half subducting beneath oceanic crust forming an oceanic arc, and the eastern half subducting under continental crust forming a continental arc. This boundary between oceanic arc and the continental arc is also coincident with the transition from transtension to the west and transpression and compression to the east (Fig. 4.2-1).

The Cascade arc is undergoing clockwise rotation resulting from oblique plate convergence in combination with arc translation related to slab roll-back and back-arc extension (Wells and McCaffrey, 2014). South of the Oregon-Washington border the arc is dominated by extension and transtension as the arc overlaps with the Basin and Range province and locally with the Walker Lane at the southern end. North of the Oregon-Washington border the arc is dominated by transpression and compression and is undergoing arc-perpendicular shortening and arc-parallel extension (Fig. 4.2-2; McCaffrey et al, 2013). In contrast to the Aleutian arc, the Cascade arc is entirely a continental arc.

About half of the Aleutian VCs are extensional or transtensional and half are transpressional or compressional (Table 4.2-1, Fig. 4.2-1). About two thirds of the Cascade VCs are extensional or transtensional and one third are transpressional/compressional. Nearly 75% of the global benchmark VCs are in extensional or transtensional settings and these VCs also account for nearly 90% of the global MWe production in subduction arcs. The benchmark VCs account for about 10% of the volcanoes in subduction arcs around the world. The tectonic setting is unknown for the other 90% of the global subduction arc VCs. A brief review of global tectonic data supports that upwards of 30 to 50% of all subduction arc VCs are in transpressional or compressional

settings, however further work is needed to evaluate the other 90% of VCs that are not part of the benchmark list.

Table 4.2-1. Tectonic settings of the Aleutian, Cascade, and Global Benchmark VCs with MWe per category and average MWe/VC.

Aleutians	# of VCs	% of VCs	Total MWe	% MWe/Total	Ave MWe/VC
Extensional	--	--	--	--	--
Transtensional-EXT	--	--	--	--	--
Transtensional-SS	27	46%	--	--	--
Transpressional	14	24%	--	--	--
Compressional	18	31%	--	--	--
Unknown	--	--	--	--	--
Total	59	100%	0		
Cascades	# of VCs	% of VCs	Total MWe	% MWe/Total	Ave MWe/VC
Extensional	10	24%	--	--	--
Transtensional-EXT	16	39%	25	84%	--
Transtensional-SS	--	--	--	--	--
Transpressional	10	24%	--	--	--
Compressional	5	12%	4.8	16%	--
Unknown	--	--	--	--	--
Total	41	100%	29.8	100%	
Benchmarks	# of VC	% of VCs	Total MWe	% MWe/Total	Ave MWe/VC
Extensional	11	15%	1246	16%	113
Transtensional-EXT	10	14%	1363	18%	136
Transtensional-SS	33	45%	4099	54%	124
Transpressional	4	5%	463	6%	116
Compressional	7	9%	234	3%	33.4
Unknown	9	12%	202	3%	22
Total	74	100%	7605	100%	90.5 ± 137 MW

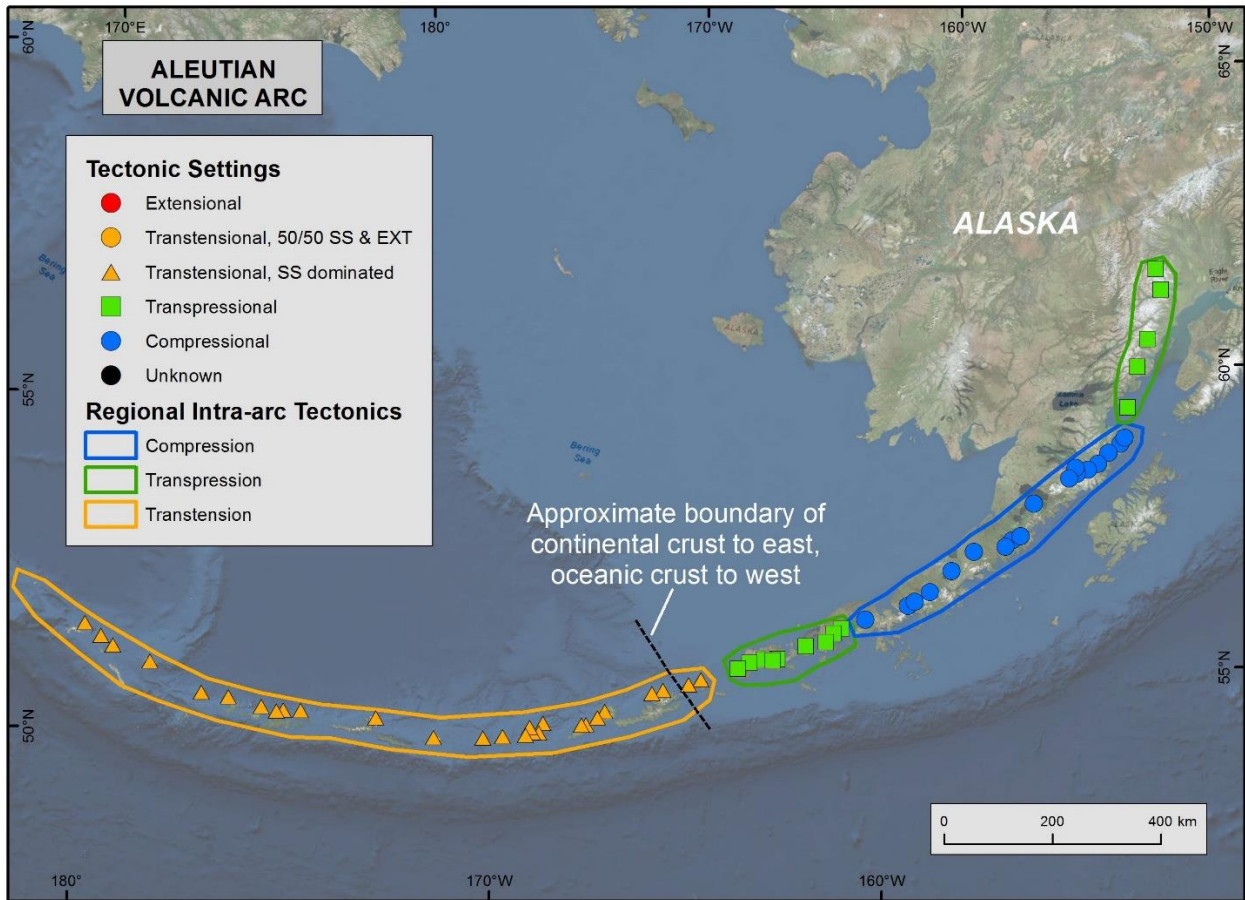


Figure 4.2-1. Tectonic settings of the VCs in the Aleutian arc.

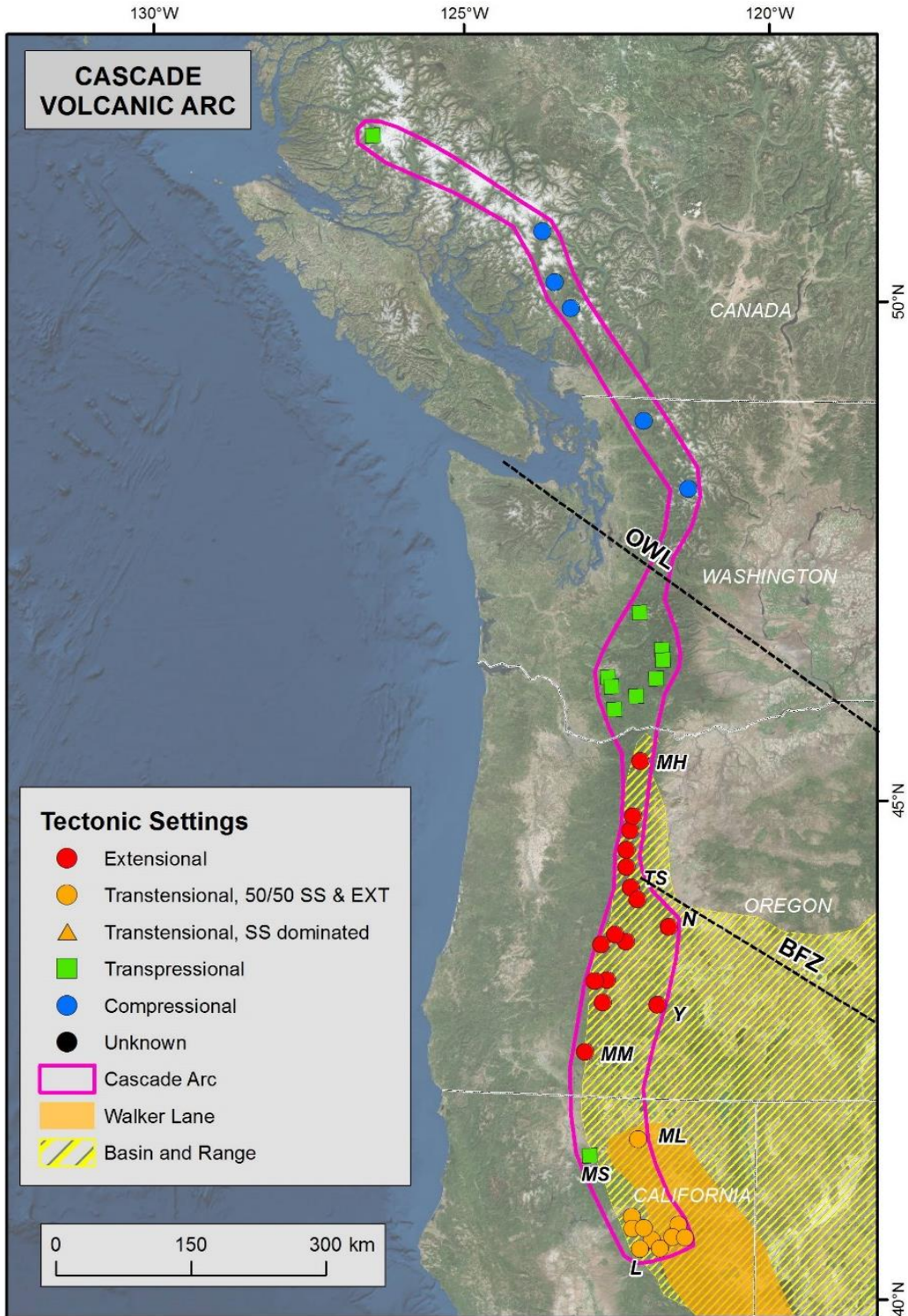


Figure 4.2-2. Tectonic settings of the VCs in the Cascade arc. BFZ, Brothers fault zone; L, Lassen; MH, Mount Hood; ML, Medicine Lake; MM, Mount McLaughlin; MS, Mount Shasta; N, Newberry; TS, Three Sisters, OWL, Olympic Wallowa Lineament; Y, Yamsay.

Quaternary Fault Slip Rate

Quaternary fault activity associated with the Aleutian VCs is greater in the western half than the eastern half, coincident with the boundary between oceanic and continental crust in the overriding plate, and coincident with region of transtension versus transpression and compression (Table 4.2-2, Fig. 4.2-3). All of the VCs with Quaternary fault slip rate data fall into three categories; <0.1 mm/yr, 0 mm/yr, or unknown. The available data is exceedingly sparse on Quaternary faults in the Aleutians and the fact that one third of VCs have unknown slip rate data is reflective of the data availability.

In the Cascades, slip rates are greatest in the south where the arc overlaps with the northern Walker Lane and faults have slip rate ranges of up to 0.3-1 or 1-3 mm/yr (Table 4.2-2, Fig. 4.2-4). In Oregon, the arc overlaps with Basin and Range extension and all volcanic centers are associated with Quaternary faults with slip rates of <0.1 mm/yr. Quaternary faults have not been identified in association with Cascade VCs in Washington or Canada.

Active Quaternary faults are associated with 67% of the global benchmark VCs and 83% of the MWe coming from the global benchmark VCs (Table 4.2-2). The average MWe for VCs associated with fault slip rates of <0.1 or 0-1-0.3 mm/yr are about 3x as great as the average MWe for VCs not known to be associated Quaternary faults. Average MWe for VCs associated with fault slip rates of 0.3 to 1.0 mm/yr are about 2x as great as average MWe for VCs with fault slip rates of 0.1 to 0.3 mm/yr. This trend continues with the upper end of the slip rate category where the average MWe for VCs associated with fault slip rates of 1.0 to 3.0 mm/yr is about 2x as great as the average MWe for VCs with fault slip rates of 0.3 to 1.0 mm/yr.

Table 4.2-2. Quaternary fault slip rates of the Aleutian, Cascade, and Global Benchmark VCs with MWe per category and average MWe/VC.

Aleutians					
mm/yr	# of VCs	% of VCs	Total MWe	% MWe of Total	Ave MWe/System
1-3	0	0%	--	--	--
0.3-1	0	0%	--	--	--
0.1-0.3	0	0%	--	--	--
<0.1	25	42%	--	--	--
0	13	22%	--	--	--
Unknown	21	36%	--	--	--
Totals	59	100%	0		
Cascades					
mm/yr	# of VCs	% of VCs	Total MWe	% MWe of Total	Ave MWe/System
1-3	3	7%	--	--	--
0.3-1	--	--	--	--	--
0.1-0.3	2	5%	25	--	--

<0.1	22	54%	--	--	--
0	10	24%	--	--	--
Unknown	4	10%	5	--	--
Totals	41	100%	30		
Benchmarks					
mm/yr	# of VC	% of VCs	Total MWe	% MWe of Total	Ave MWe/System
1-3	2	3%	853	11%	427
0.3-1	9	12%	1784	23%	198
0.1-0.3	14	19%	1346	18%	96
<0.1	25	34%	2306	30%	92
0	8	11%	229	3%	29
Unknown	16	22%	1087	14%	68
Totals	74	100%	7605	100%	90.5 ± 137 MW

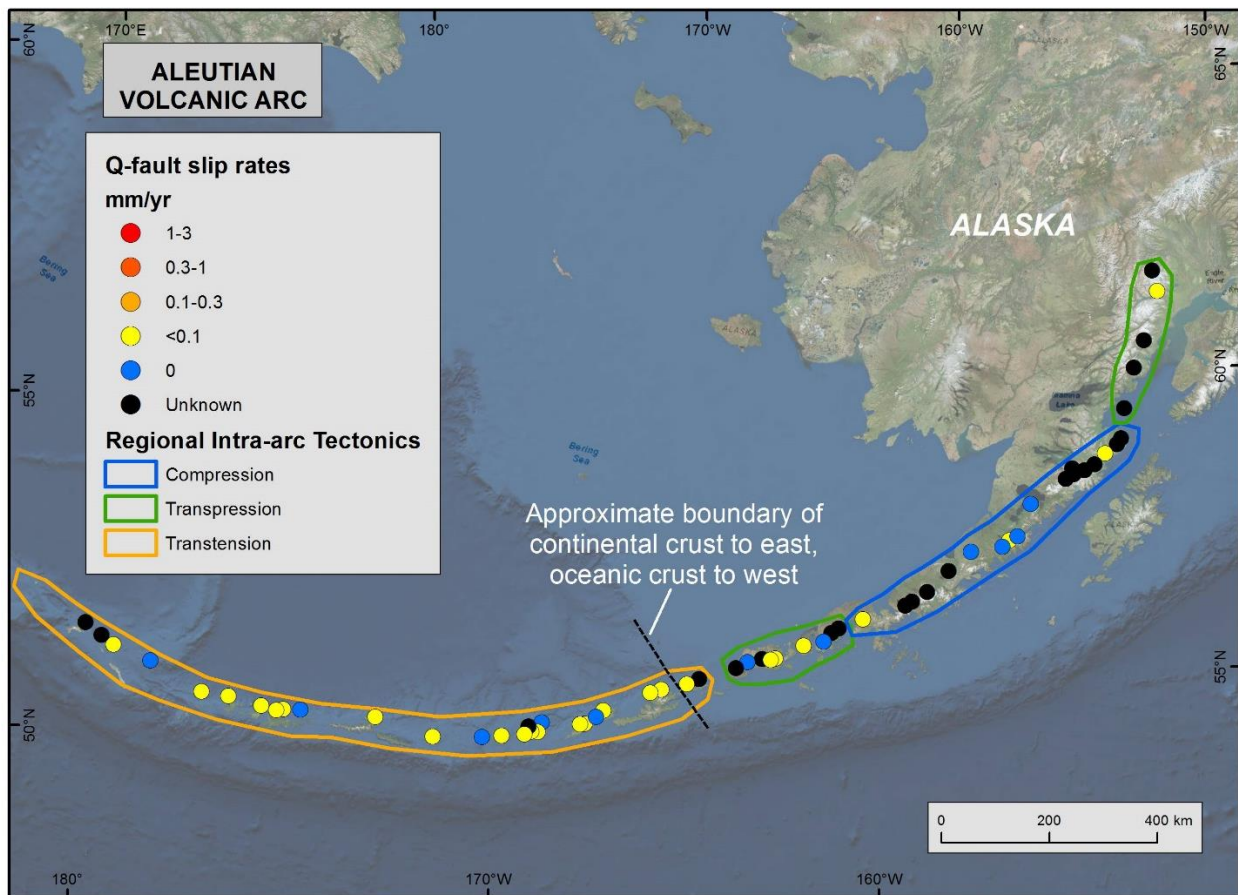


Figure 4.2-3. Quaternary fault slip rates of the Aleutian VCs.

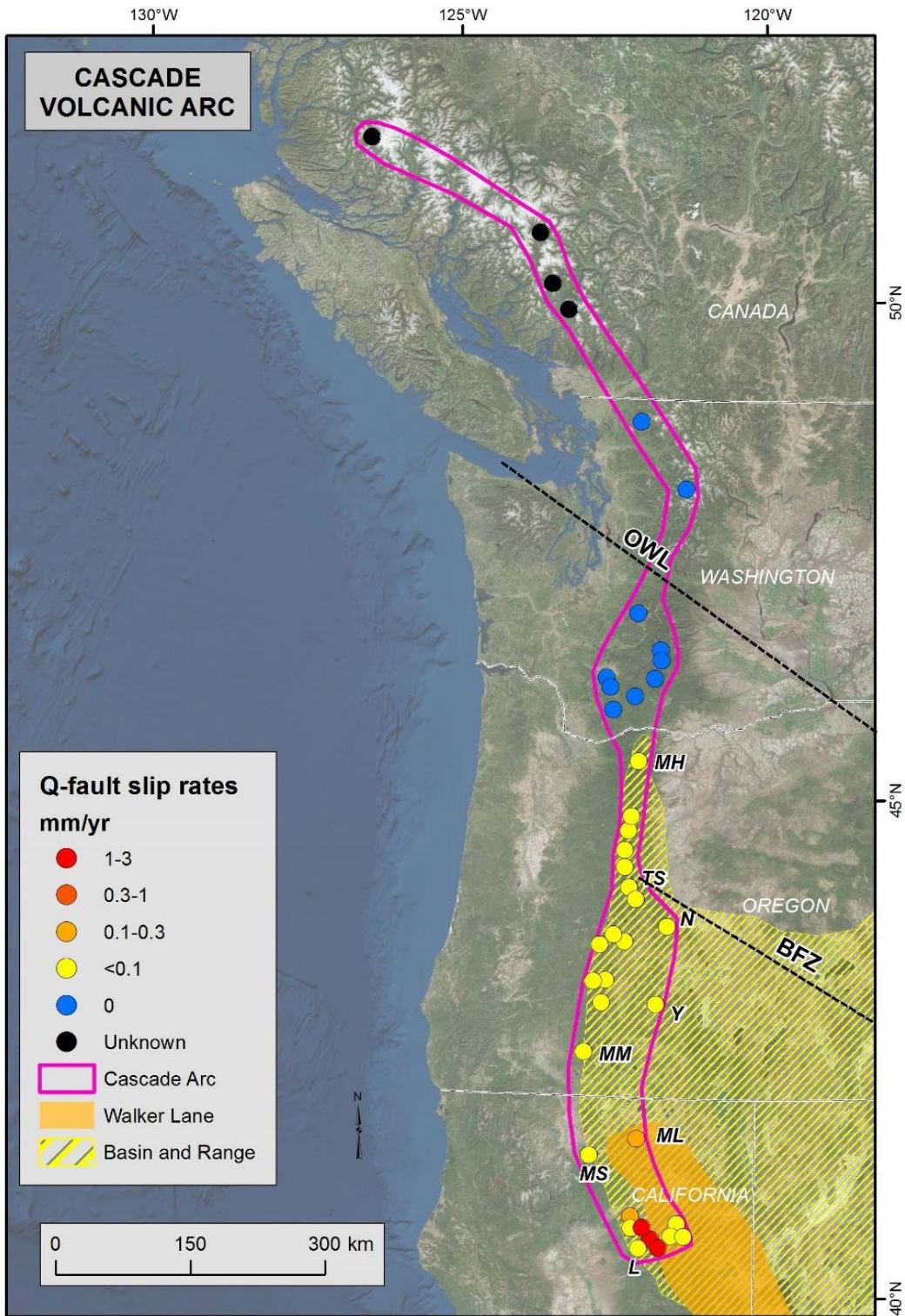


Figure 4.2-4. Quaternary fault slip rates of the Aleutian VCs. L, Lassen; MH, Mount Hood; ML, Medicine Lake; MM, Mount McLaughlin; MS, Mount Shasta; N, Newberry; TS, Three Sisters, OWL, Olympic Wallowa Lineament; Y, Yamsay.

Quaternary Fault Scarp Concentration

In a similar pattern to the distribution of Quaternary fault slip rate data, the concentration of Quaternary faults associated with VCs also correlates with regional intra-arc tectonic settings (Figs. 4.2-5, 4.2-6, Table 4.2-3). Quaternary fault scarp concentrations associated with Aleutian VCs are greater in the western half than the eastern half, coincident with the boundary between oceanic and continental crust in the overriding plate, and coincident with the regional tectonic setting (Fig. 4.2-1). The VCs with the highest density of Quaternary fault scarps fall within the western one third of the Aleutian Arc in an area where the obliquity of the plate convergence is the greatest.

Quaternary fault scarp concentrations in the Cascades are greatest in the south where the arc overlaps with the northern Walker Lane and (Fig. 4.2-6). In Oregon, the arc overlaps with Basin and Range extension and all volcanic centers are associated with Quaternary faults, however there is greater Quaternary fault activity associated with VCs coincident with and south of the Three Sisters. This pattern is in alignment with greater Basin and Range activity south of the Brothers fault zone. Quaternary faults have not been identified in association with Cascade VCs in Washington or Canada.

Table 4.2-3. Quaternary fault scarp concentration for the Aleutian, Cascade, and Global Benchmark VCs with MWe per category and average MWe/VC.

Aleutians	# of VCs	% of VCs	Total MWe	% MWe of Total	Ave MWe/System
High	0	0%	--	--	--
Medium	4	7%	--	--	--
Low	21	36%	--	--	--
Zero	13	22%	--	--	--
Unknown	21	36%	--	--	--
Totals	59	100%	0		
Cascades	# of VCs	% of VCs	Total MWe	% MWe of Total	Ave MWe/System
High	8	20%	0	--	--
Medium	7	17%	0	--	--
Low	12	29%	25	--	--
Zero	10	24%	0.0	--	--
Unknown	4	10%	5	--	--
Totals	41	100%	30		
BenchMarks	# of VC	% of VCs	Total MWe	% MWe of Total	Ave MWe/System
High	9	12%	2410	32%	268
Medium	9	12%	1343	18%	149
Low	34	46%	2846	37%	84
Zero	10	14%	246	3%	25
Unknown	12	16%	760	10%	63
Totals	74	100%	7605	100%	90.5 ± 137 MW

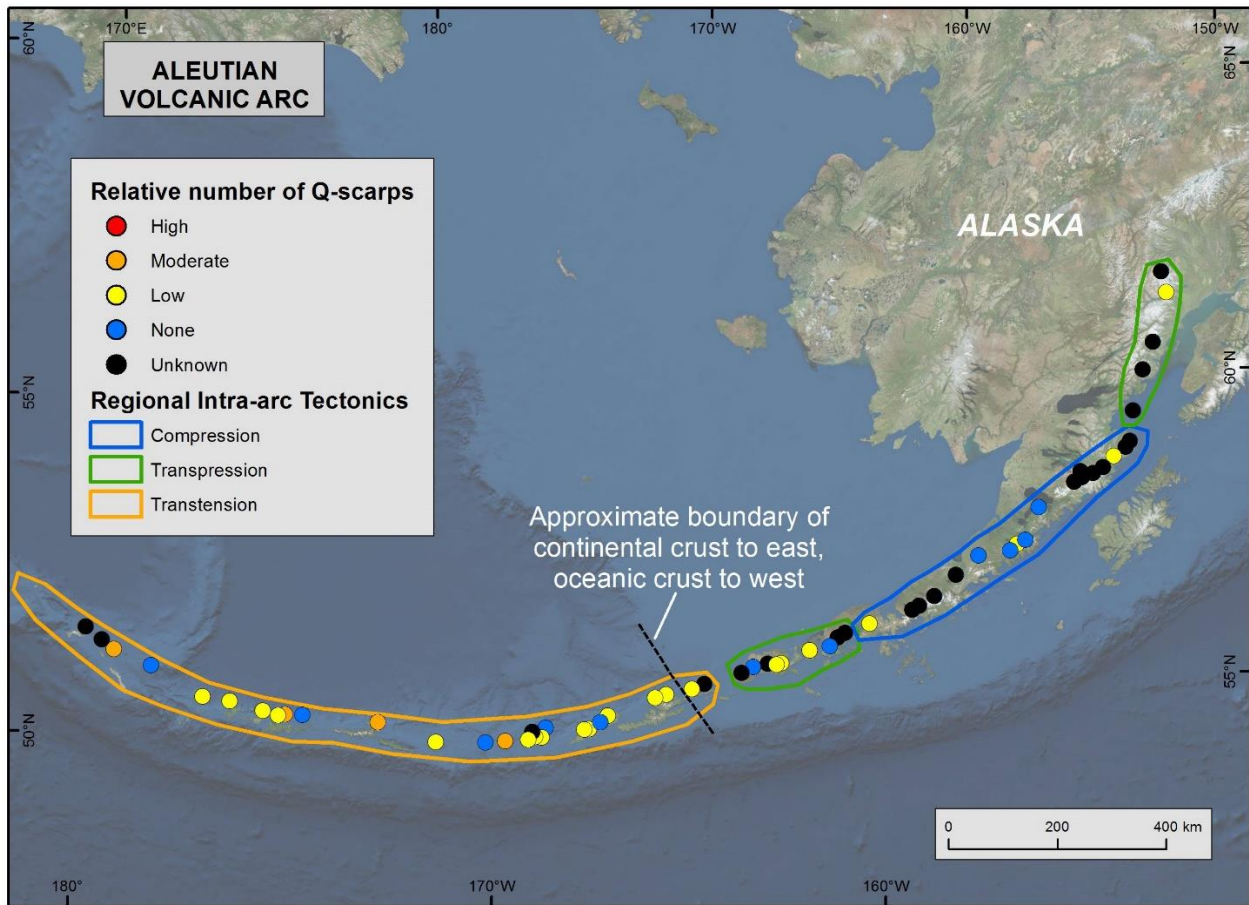


Figure 4.2-5. Quaternary fault scarp concentrations for the Aleutian VCs.

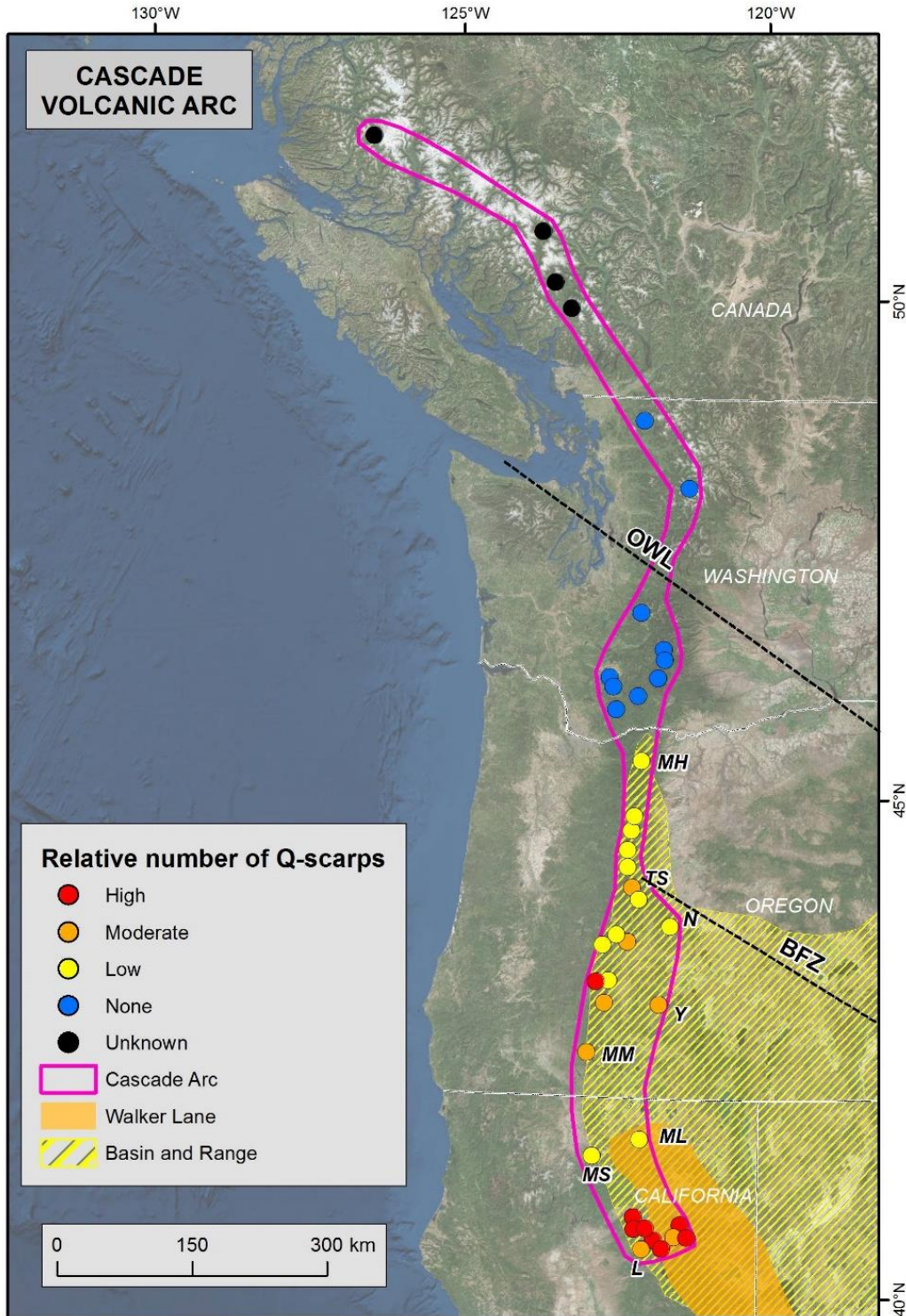


Figure 4.2-6. Quaternary fault scarp concentrations for the Cascade VCs. L, Lassen; MH, Mount Hood; ML, Medicine Lake; MM, Mount McLaughlin; MS, Mount Shasta; N, Newberry; TS, Three Sisters, OWL, Olympic Wallowa Lineament; Y, Yamsay.

Structural Setting

The structural settings of the Aleutian VCs include fault intersections (42%), other (5%), displacement transfer zones (2%), and unknown (51%; Fig. 4.2-7). The structural settings of the Cascade VCs include fault intersections (34%), step-overs (29%), accommodation zones (15%), pull-aparts (15%), displacement transfer zones (2%), and unknown (5%). The large amount of unknown structural settings for the Aleutian VCs versus the Cascade VCs and global Benchmark VCs attests to how unexplored the Aleutians are with limited available data (Table 4.2-4).

Power production in the global benchmark VC set is dominated by pull-aparts, displacement transfer zones, step-overs, and accommodation zones (Table 4.2-4, Fig. 4.2-8). These four structural settings collectively account for 49% of the VCs and 76% of the total MWe. In contrast, fault intersections account for 30% of the VCs and only 16% of the total MWe.

Table 4.2-4. Structural settings of the Aleutian, Cascade, and Global Benchmark VCs with MWe per category and average MWe/VC.

Aleutians	# of VCs	% of Total	Total MWe	% of Total	Ave Mwe/VC
Pull-apart	--	--	--	--	--
Displacement Transfer Zone	1	2%	--	--	--
Accommodation Zone	--	--	--	--	--
Step-over	--	--	--	--	--
Fault Intersection	25	42%	--	--	--
Other	3	5%	--	--	--
Unknown	30	51%	--	--	--
Total	59	100%	0		
Cascades	# of VCs	% of Total	Total MWe	% of Total	Ave Mwe/VC
Pull-apart	6	15%	--	--	--
Displacement Transfer Zone	1	2%	--	--	--
Accommodation Zone	6	15%	25	84%	--
Step-over	12	29%	--	--	--
Fault Intersection	14	34%	5	16%	--
Other	--	--	--	--	--
Unknown	2	5%	--	--	--
Total	41	100%	30	100%	
Benchmarks	# of VCs	% of Total	Total MWe	% of Total	Ave Mwe/VC
Pull-apart	10	14%	1686	22%	169
Displacement Transfer Zone	15	20%	1837	24%	122
Accommodation Zone	4	5%	907	12%	227
Step-over	7	9%	1,358	18%	194
Fault Intersection	22	30%	1,057	14%	48
Other	4	5%	273	4%	68
Unknown	12	16%	487	6%	41
Total	74	100%	7,605	100%	90.5 ± 137 MW

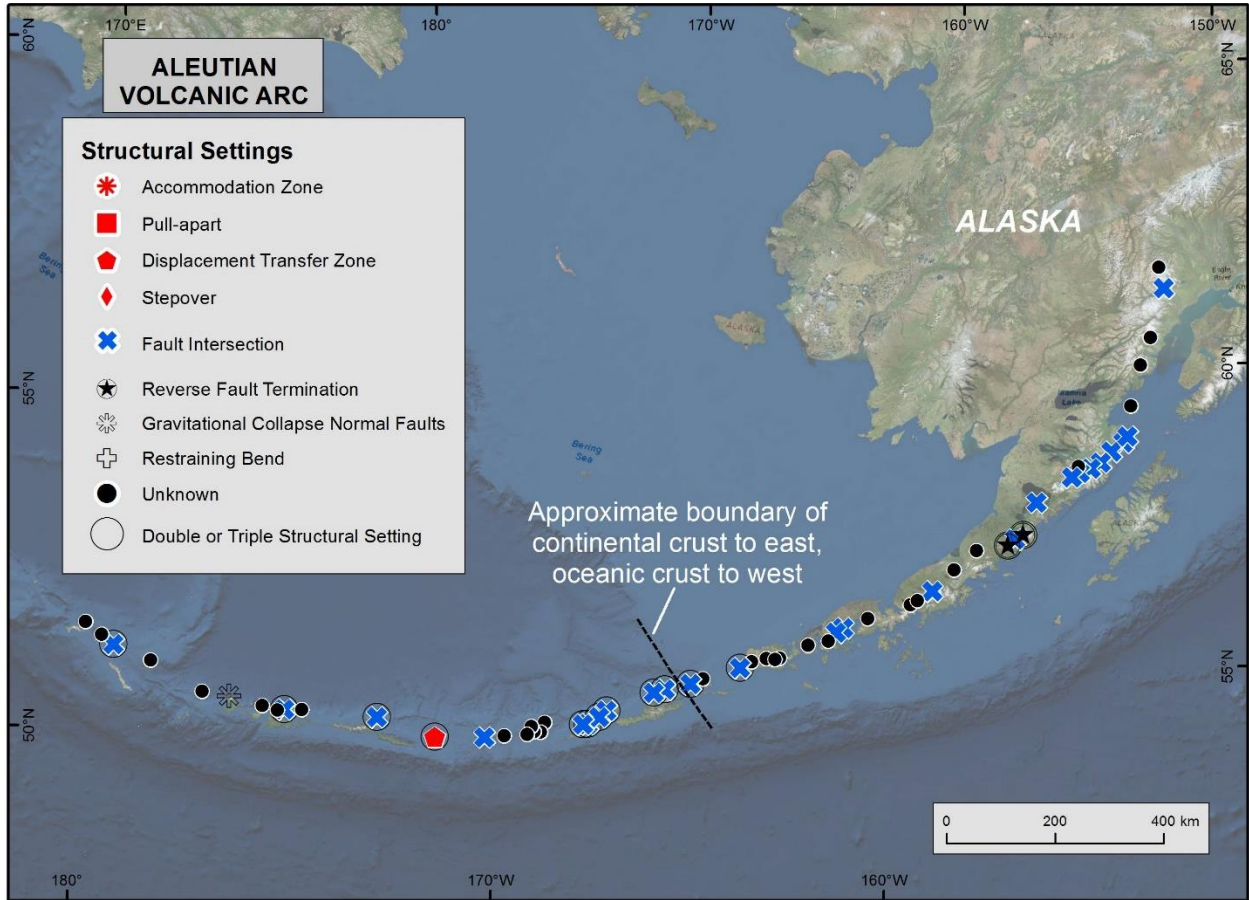


Figure 4.2-7. Structural settings of the VCs in the Aleutian arc.

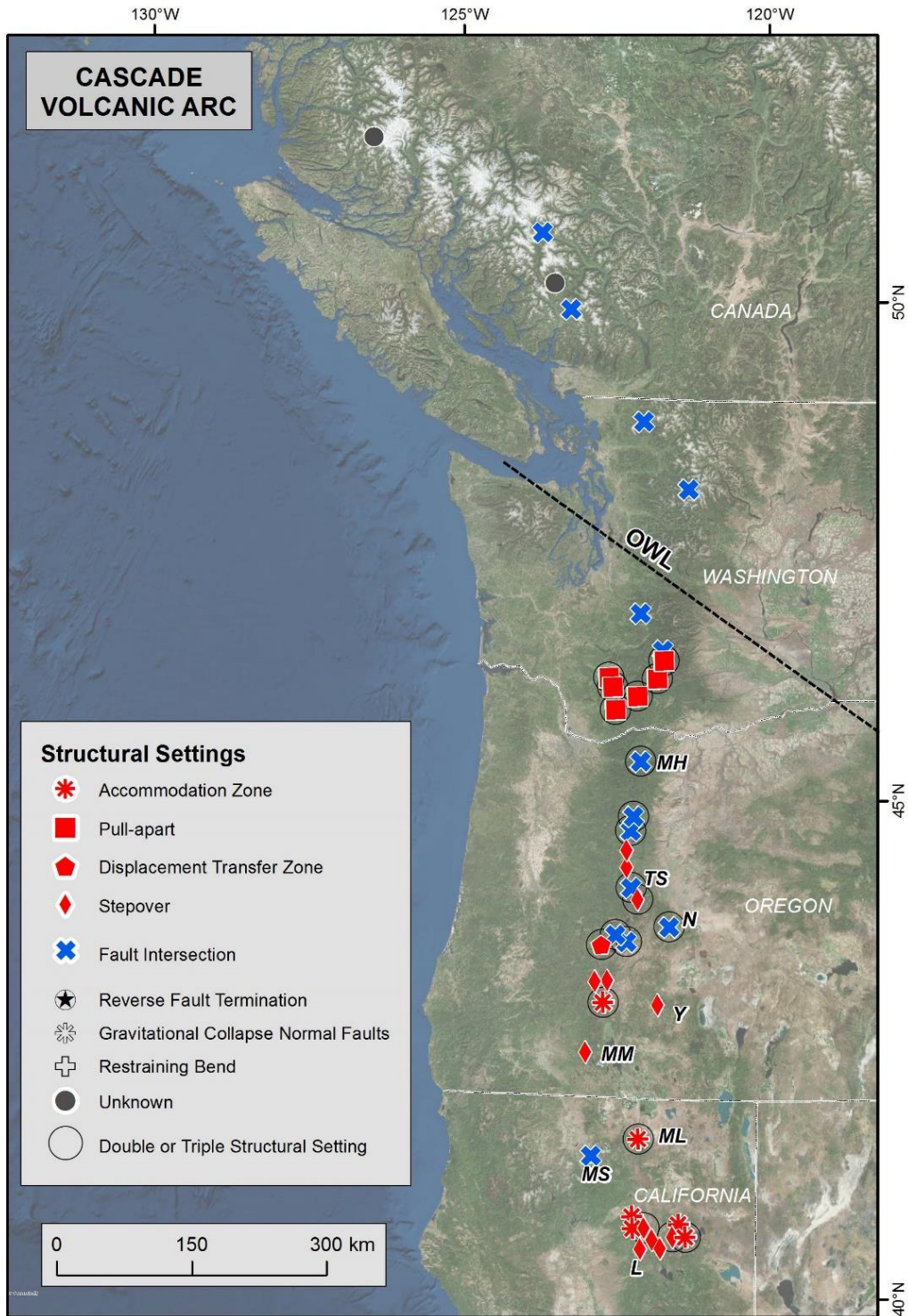


Figure 4.2-8. Structural settings of the VCs in the Cascade arc. L, Lassen; MH, Mount Hood; ML, Medicine Lake; MM, Mount McLaughlin; MS, Mount Shasta; N, Newberry; TS, Three Sisters, OWL, Olympic Wallowa Lineament; Y, Yamsay.

Dilation Potential

The orientation of S_{Hmin} was plotted relative to the strike orientation of fault(s) associated with each VC to provide a general assessment of the dilation potential (Table 4.2-5 and Fig. 4.2-9). The Aleutian VCs have a wide variability in dilation potential of faults, whereas the Cascade VCs have on average a high dilation potential. The global benchmark VCs cluster at the higher range of dilation potential and the average MWe per VC also increases with dilation potential (Fig. 4.2-9). The global benchmark VCs have 58% of the VCs and 67% of the MWe in the highest category, 75 to 90°. The next lower bin, 45-75° has 26% of the VCs and 26% of the MWe. The average MWe/VC decreases across the four categories from 119 to 106 to 57 to 17 MWe.

Table 4.2-5. Dilation potential of Aleutian, Cascade, and global benchmark VCs. Dilation potential has been summarized according to three bins: 90-75°, 75-45°, 45 to 0°.

Aleutians	# of VCs	% of Total	Total MWe	% of Total	Ave MWe/VC
1.0 to 0.95 (90-75°)	24	41%	--	--	--
0.95 to 0.75 (75-45°)	19	32%	--	--	--
0.75 to 0 (45 to 0°)	15	25%	--	--	--
Unknown	1	2%	--	--	--
Total	59	100%	--	--	
Cascades	# of VCs	% of Total	Total MWe	% of Total	Ave MWe/VC
1.0 to 0.95 (90-75°)	32	78%	30	--	--
0.95 to 0.75 (75-45°)	8	20%	--	--	--
0.75 to 0 (45 to 0°)	--	--	--	--	--
Unknown	1	2%	--	--	--
Total	41	100%	30	--	
Benchmarks	# of VCs	% of Total	Total MWe	% of Total	Ave MWe/VC
1.0 to 0.95 (90-75°)	43	58%	5110	67%	119
0.95 to 0.75 (75-45°)	19	26%	2010	26%	106
0.75 to 0 (45 to 0°)	7	9%	401	5%	57
Unknown	5	7%	84	1%	17
Total	74	100%	7605	100%	90.5 ± 137 MW

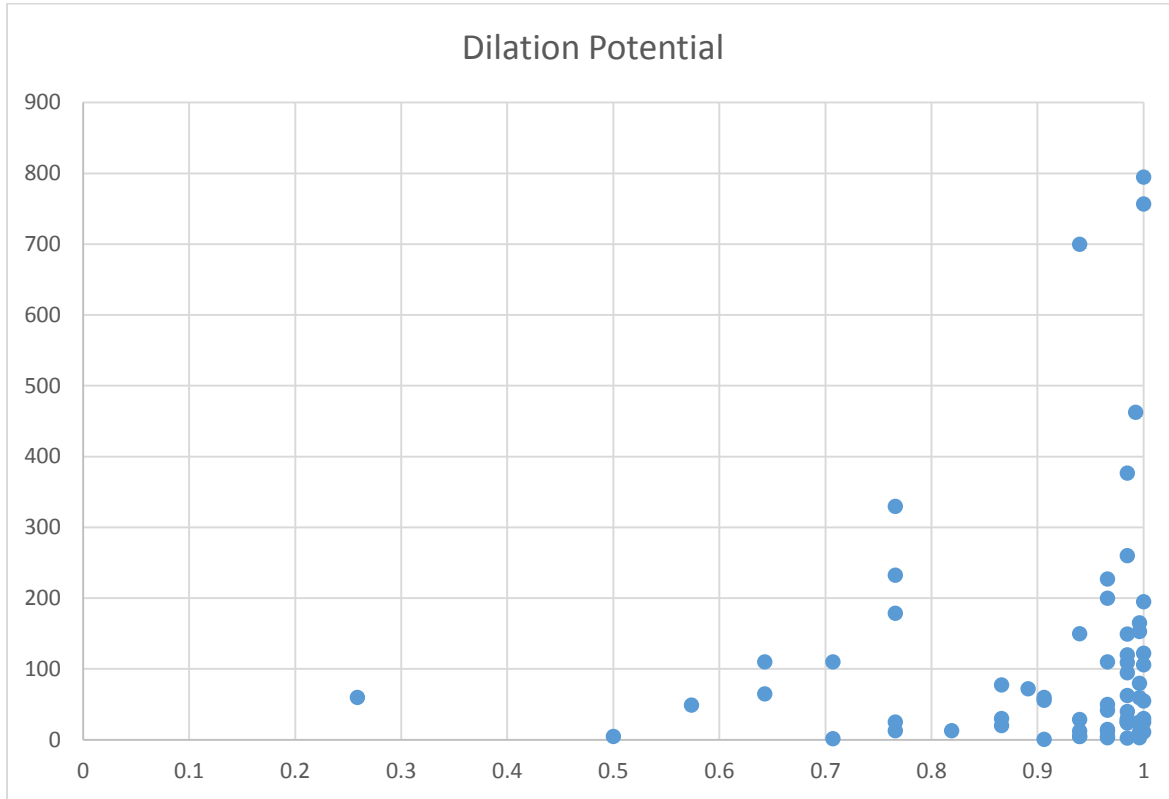


Figure 4.2-9. Dilation potential of benchmark VCs. X-axis is equal to $\sin (|S_{Hmin} - \text{Fault Strike}|)$. Y-axis is MWe.

Geodetic Data

A summary of GPS derived angle of plate convergence relative to the arc axis for the Aleutians, Cascades, and global benchmark VCs is shown in Table 4.2-6. This angle is derived from the global plate motion model (Kreemer et al., 2014) and represents the angle of obliquity between the motion of the subducting plate relative to the arc axis. Zero degrees indicates that the subducting plates is moving perpendicular to the arc axis. Ninety degrees indicates that the subducting plate is moving parallel to the arc axis. The greater the angle of obliquity, the greater the potential for arc-parallel, intra-arc shear.

Nearly 75% of the Aleutian VCs reside in areas where the subducting plate is converging at 0-22.5° from perpendicular relative to the arc axis (Table 4.2-6). About 20% and 7% of the Aleutian VCs reside in areas where the subducting plate is converging at 22.5 to 45° and 45 to 67.5° from perpendicular relative to the arc axis, respectively. In the Cascades the volcanoes are split evenly between 0 to 22.5° and 22.5 to 45° angles from perpendicular for the convergence angle relative to the arc axis. Note that Medicine Lake sits in a region with the 22.5 to 45° angle of convergence category.

In global benchmark set of VCs, 57% of the VCs reside in areas where the subducting plate is moving within 0 to 22.5° from perpendicular and these account for 31% of the total MWe (Table

4.2-6). Contrasting this, 41% of the VCs reside in areas where the subducting plate is moving >22.5° from perpendicular and these account for 58% of the total MWe. The average MWe per VC in the 22.5 to 45° category is approximately 2.5x that in the 0 to 22.5° category. This average continues to increase with greater angles of obliquity. At the top of the chart, the four VCs in the 67.5 to 90° category are also 2x the next lower category of 45 - 67.5°.

Table 4.2-6. Angle of subducting slab motion relative to the arc axis for the Aleutians, Cascade, and global benchmark VCs.

Aleutians					
Angle (°)	# of VCs	% of Total	Total MWe	% of Total	Ave MWe/VC
67.5-90	--	--	--	--	--
45-67.5	4	7%	--	--	--
22.5-45	12	20%	--	--	--
0-22.5	43	73%	--	--	--
Unknown	--	--	--	--	--
Total	59	100%	0		
Cascades					
Angle (°)	# of VCs	% of Total	Total MWe	% of Total	Ave MWe/VC
67.5-90	--	--	--	--	--
45-67.5	--	--	--	--	--
22.5-45	23	56%	25	--	--
0-22.5	18	44%	5	--	--
Unknown	--	--	--	--	--
Total	41	100%	30		
Benchmarks					
Angle (°)	# of VCs	% of Total	Total MWe	% of Total	Ave MWe/VC
67.5-90	4	5%	1381	18%	345
45-67.5	4	5%	684	9%	171
22.5-45	23	31%	3124	41%	136
0-22.5	42	57%	2355	31%	56
Unknown	1	1%	63	1%	63
Total	74	100%	7605	100%	90.5 ± 137 MW

4.3 VOLCANIC DATA EXPLORATION

Physical Geographic parameters

Scatter plots and histograms were used to evaluate correlations between physical geographic parameters (number, size and age of primary and subsidiary vents and occurrence of inter-vent volcanic features) were plotted against the total installed power (MWe) for the global training set (n=74) in order to identify meaningful trends. Results show that productive geothermal

systems can occur in a broad range of eruptive compositions, eruptive styles (calderas, stratovolcanoes, dome fields, etc.) and locations. Whereas this diversity is encouraging in terms of the ability of economic systems to form in a broad range of volcanic environments, it complicates efforts to predict geothermal potential based solely on volcanic characteristics. Below is a description of important trends that were investigated.

Important non-correlations of physical characteristics

Size of Volcanic Features

One of these physical parameters is the size of the volcanic edifice, with the assumption that a larger edifice would represent a larger, potentially longer lived magmatic system that would have greater potential to heat a larger subsurface volume. The longevity of a magmatic system has been suggested to be related to geothermal potential (Smith and Shaw, 1979). Plots of these relationships (stratocone footprint, caldera area) showed no correlation with installed power (Fig. 4.3-1).

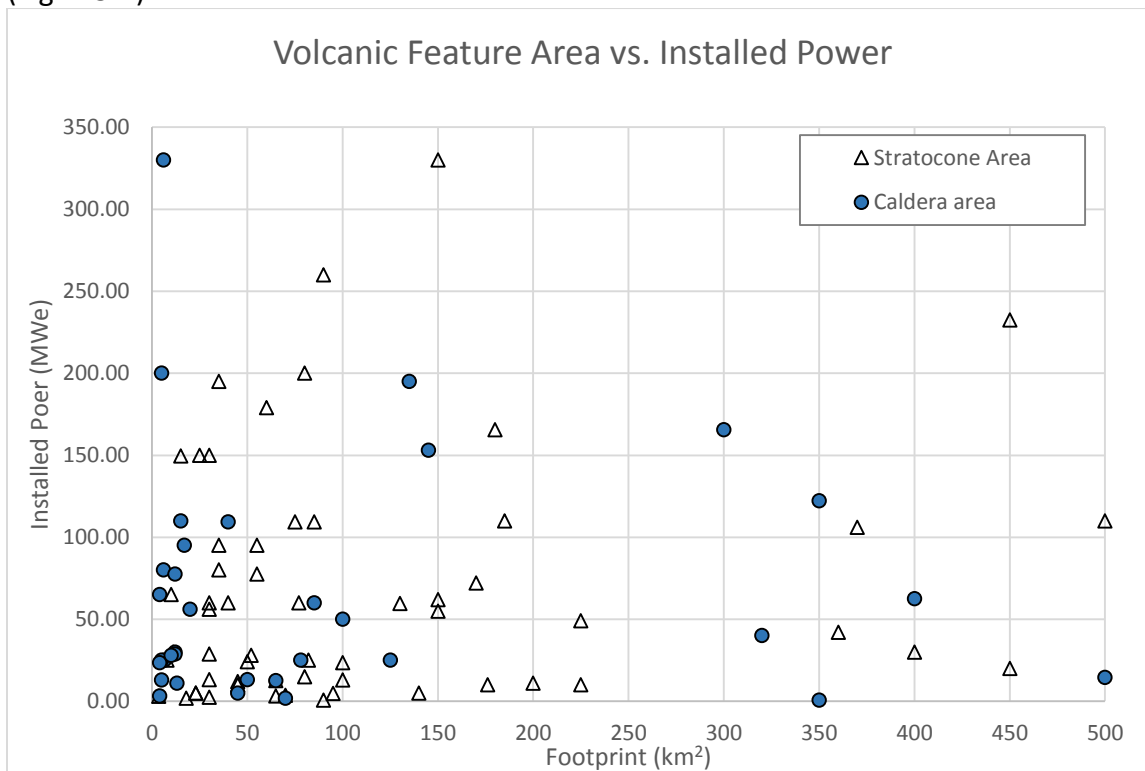


Figure 4.3-1. Areal footprint of major volcanic features (base of stratocone or caldera rim) vs. installed power. Holocene and Pleistocene VCs are plotted, and separation of Pleistocene and Holocene features showed similar results. No obvious correlation exists for either parameter.

Number of flank vents

Another anticipated correlation was between installed power and the number of cinder cones and other flank vents surrounding the main edifice. Prior to data collection, this anticipated relationship was argued in two opposing directions: a larger number of flank vents would suggest a denser fracture network that could promote permeability; or, conversely, that a larger amount

of flank vent volcanism would allow greater stress accommodation by magma injection rather than brittle failure, effectively decreasing permeability. The bivariate plots showed no trends to support either hypothesis (Fig. 4.3-2).

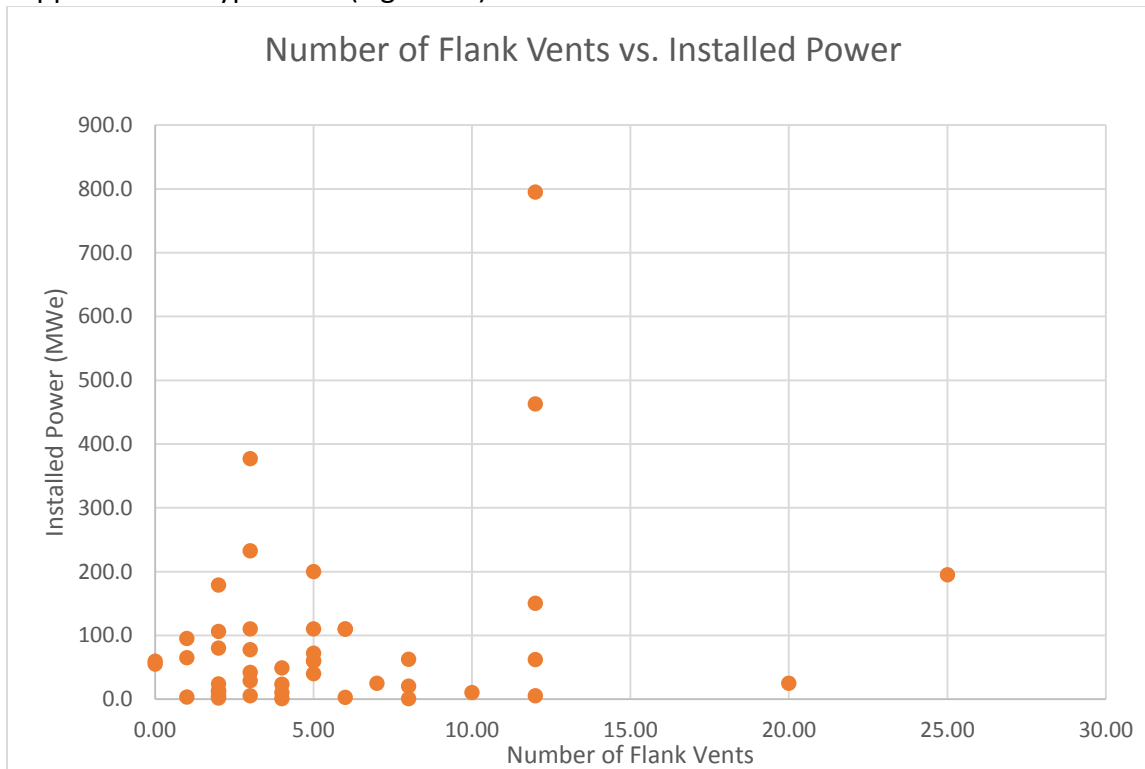


Figure 4.3-2 Number of flank vents vs. installed power. VCs with no flank vents are not plotted. No obvious correlations are present.

Recency of Eruption

The relationship between installed power and time since the last eruption was also tested, with the hypothesis that the more recently active volcanoes would have proportionally greater heat flow into the surrounding shallow crust. The data plotted for the global training set (Fig. 4.3-3) do not suggest a strong correlation between these parameters. There is an indication that geothermal systems with higher power yield are associated with VCs that have erupted in the last 1,000 years. However, of the VCs with eruptions in the last 1,000 years, 74% have installed power <100 MWe and 60% have installed power <30 MWe.

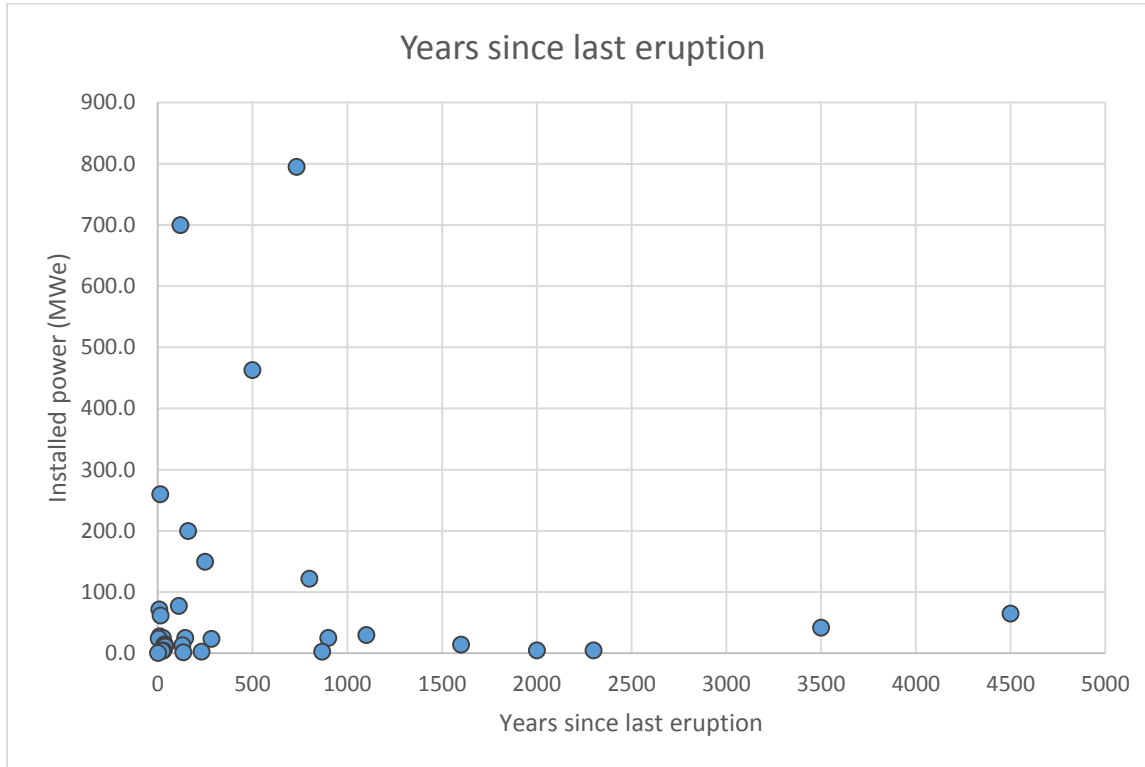


Figure 4.3-3. Years since last eruption vs. installed power. VCs for which no data exist for the most recent eruption date are not plotted. A possible link is suggested between eruptions <1,000 years and power production, but the population is too small to be statistically significant.

Inter-vent Features

An inventory was made of all volcanic features located between VCs that were not included during the primary vent inventory. These features include cinder cones, small poly-genetic Pleistocene and Holocene vents that were too small to be included in the VC list (<500 m relief, or <8 km diameter), areas of alteration, various occurrences of cinder cones (isolated, distributed fields or lineaments), and more (Fig. 4.3-4). Rigorous correlations between inter-vent features and installed power are not present, although 60% of the global training set VCs have multiple types of inter-vent features. Visually, Figure 3.4-5 shows that inter-vent shield volcanoes and Holocene vents are associated with lower power yields, but the population of these groups is too low to support a statistically significant correlation.

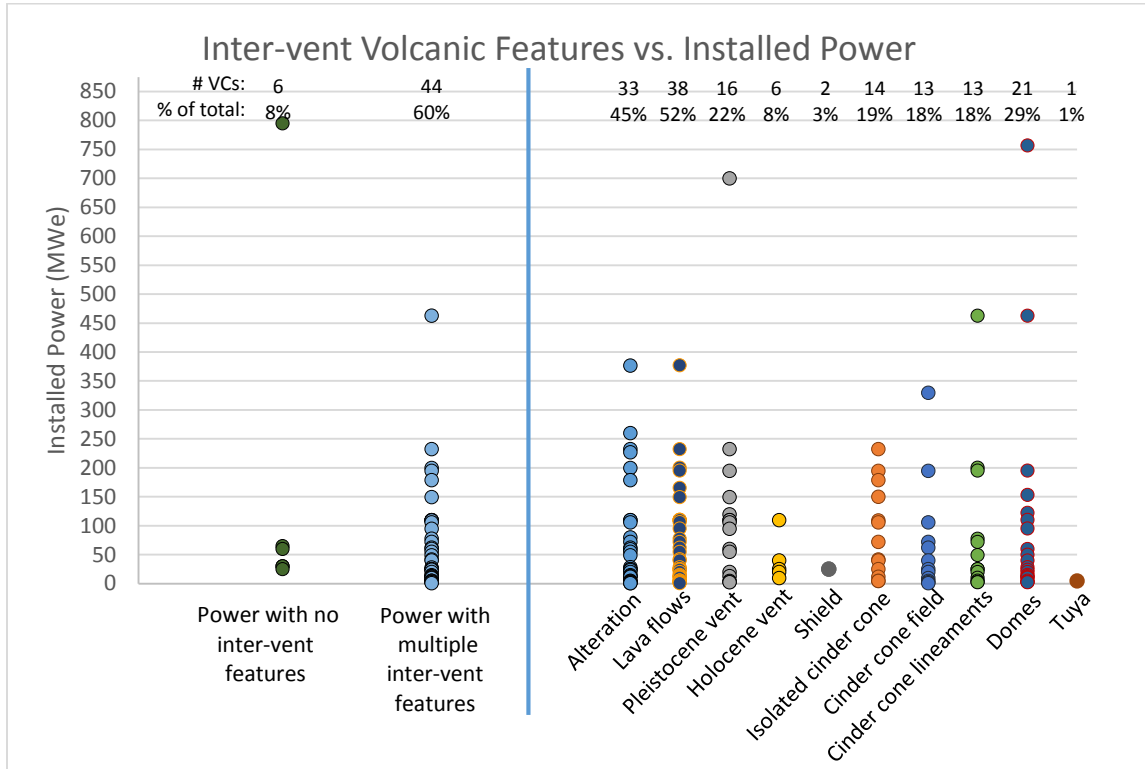


Figure 4.3-4 Inter-vent volcanic features vs installed power. The vertical blue line separates cumulative data (left) and data for individual features (right). Data for “Power with multiple inter-vent features” duplicates many of the data points separated out on the right side. Across the top are listed the number of data points in each column and the percentage of the training set VCs that contain each individual inter-vent feature. No obvious correlations are present. See text for discussion.

Rhyolite Domes

Other data were plotted to test anecdotal relationships that previous workers have identified. One notable anecdote tested is that the presence of rhyolite domes around a volcanic center is associated with productive geothermal systems. As mentioned in section 3.9, the composition of volcanic features is challenging to constrain, so the occurrence of rhyolite domes specifically cannot be addressed with the current data set. However, using the area of domes present on and around VCs in the global training set would include the rhyolite and non-rhyolite domes, and also include a factor related to the volume of material erupted. Also, domes were identified in Google Earth in part by their steep-sided morphology. Because the higher viscosity of rhyolite promotes the formation of steep-sided lava domes, this category likely includes the majority of rhyolite domes. As with many other physical and chemical parameters, a plot of dome area vs. installed power revealed no correlation (Fig. 4.3-5). The ambiguity in the data collection, however, diminishes the confidence in this conclusion.

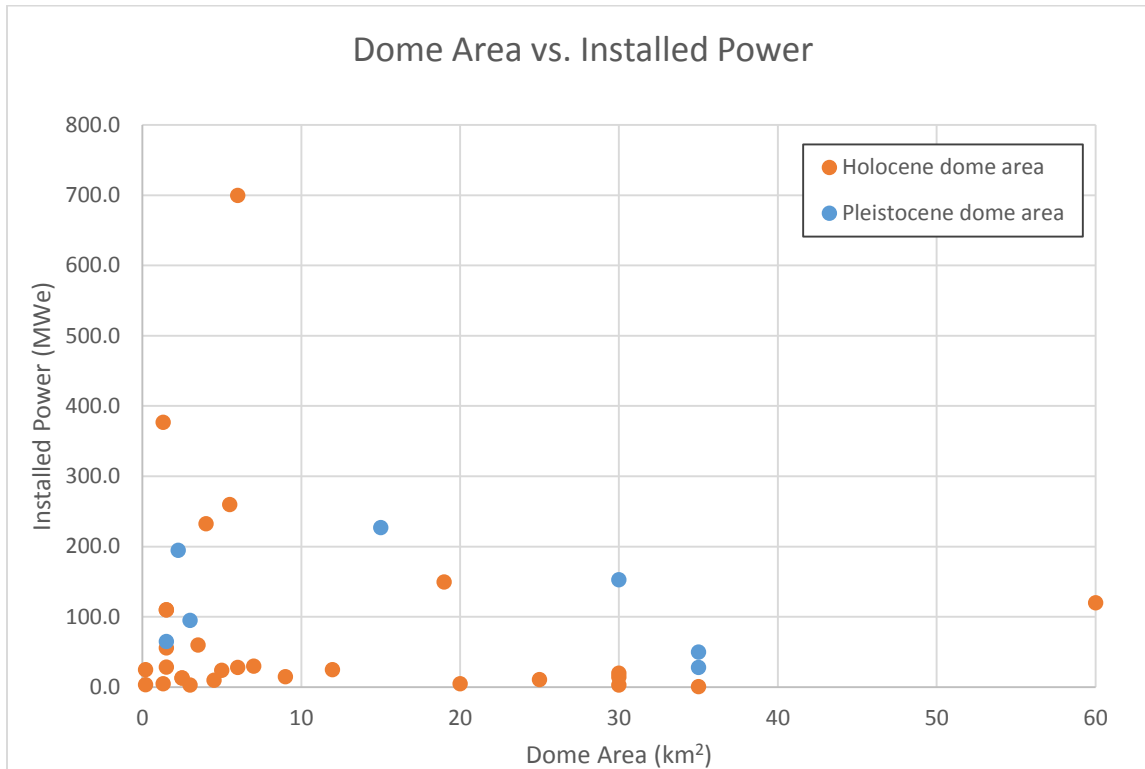


Figure 4.3-5. Dome area, or footprint vs. installed power, also separated by age. Each data point represents the sum of the areas for all domes associated with each VC. VCs without domes are not plotted. No significant correlation was observed.

Statistically significant correlations of physical characteristics

The strongest correlation between installed power and physical volcanic characteristics is the occurrence of productive geothermal systems located within or near calderas. Of the 74 global arc-related VCs that host power-producing geothermal systems (the global training set), approximately 60% are associated with caldera volcanoes (Figure 4.3-6). Further exploration of this relationship reveals that, although Pleistocene caldera volcanoes host only 26% of all power-producing systems in the global training set, they produce 36% of the power, an average of 140 MWe/system. In comparison, systems hosted by Holocene calderas represent 31% of power producers, yet yield 19% of the power (average 61 MWe/system). Non-caldera geothermal systems represent 45% of all systems and yield 43% of the power (average 108 MWe/system). Formal statistical tests of the difference between means using log-normalized populations indicate that systems associated with Pleistocene calderas have higher average energy output compared to systems in Holocene calderas or non-caldera systems (p values = 0.02 and 0.03, respectively). . This is important as the global training set, like geothermal systems worldwide, appear to obey a power-law distribution. As a result, systems with installed power >100 MWe are relatively uncommon (<30% of the global training set (benchmark sites)). But, a surface characteristic that can help discriminate potentially higher-yield systems could be valuable.

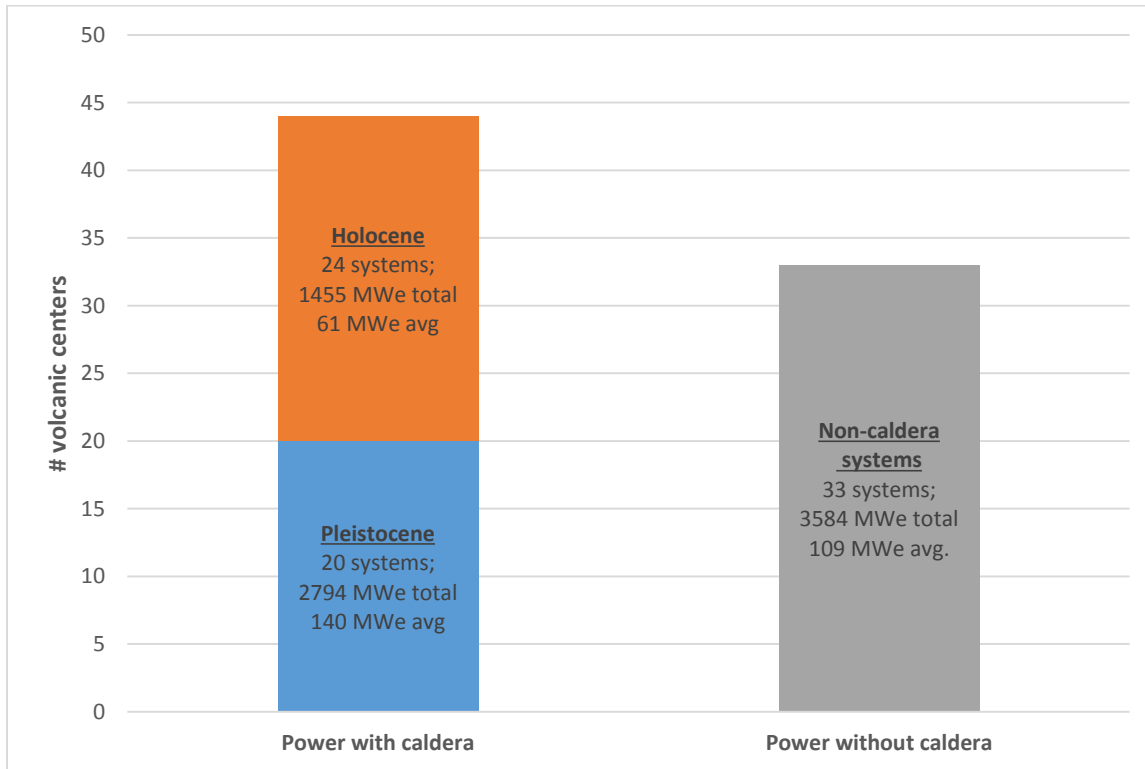


Figure 4.3-6 Global geothermal systems separated by their association with calderas. More power-producing systems are associated with calderas, and those associated with Pleistocene calderas tend to have greater power yields on average.

Eruptive Composition parameters

Overall, no strong correlations have been established between eruptive composition and installed power in our global training set. Graphical tests of relationships between the composition of the most recent eruption, compositional diversity of erupted products and the average composition of volcanic material have been made. However, most of the compositional data evaluated are based on the GeoROC database, which is not comprehensive (see section 3.9.1.3). This adds ambiguity to the importance of these conclusions.

Eruptive Diversity

An anecdotal relationship made by members of our team suggests that smooth-sided, well-formed stratovolcanoes are often somewhat distant from productive geothermal fields. Whereas the smoothness of each VC was not estimated, the morphology of “idealized” stratovolcanoes is largely due to the dominance of basaltic eruptions (Karátson et al., 2010), and volcanoes with a broader compositional diversity are less likely to have these idealized shapes. Furthermore, the lack of compositional diversity suggests limited fractionation and evolution of magma in a shallow chamber. Thus, these volcanoes are interpreted to have small, shallow magma chambers with very rapid flow-through of magma and short magma residence time in the shallow crust (Bertagnini et al, 2003). This would be consistent with a relatively low heat supply from the magma chamber into the surrounding host rock, forming poor geothermal

conditions. To test this hypothesis, we plotted eruptive diversity against installed power (Fig. 4.3-7). The result provides few robust conclusions. At first glance it appears that lower eruptive diversity (a single rock composition erupted, or a diversity score of 1) is associated with lower power yield in the training set. However, all categories of eruptive diversity scores have a similar distribution, with the majority of systems yielding <100 MWe (6-10 VCs for each diversity category), and a small number of systems >100 MWe (3-4 VCs in each diversity category). For VCs with greater eruptive diversity, there is more scatter in installed power, but the population of the groups is too small to draw any significant conclusions.

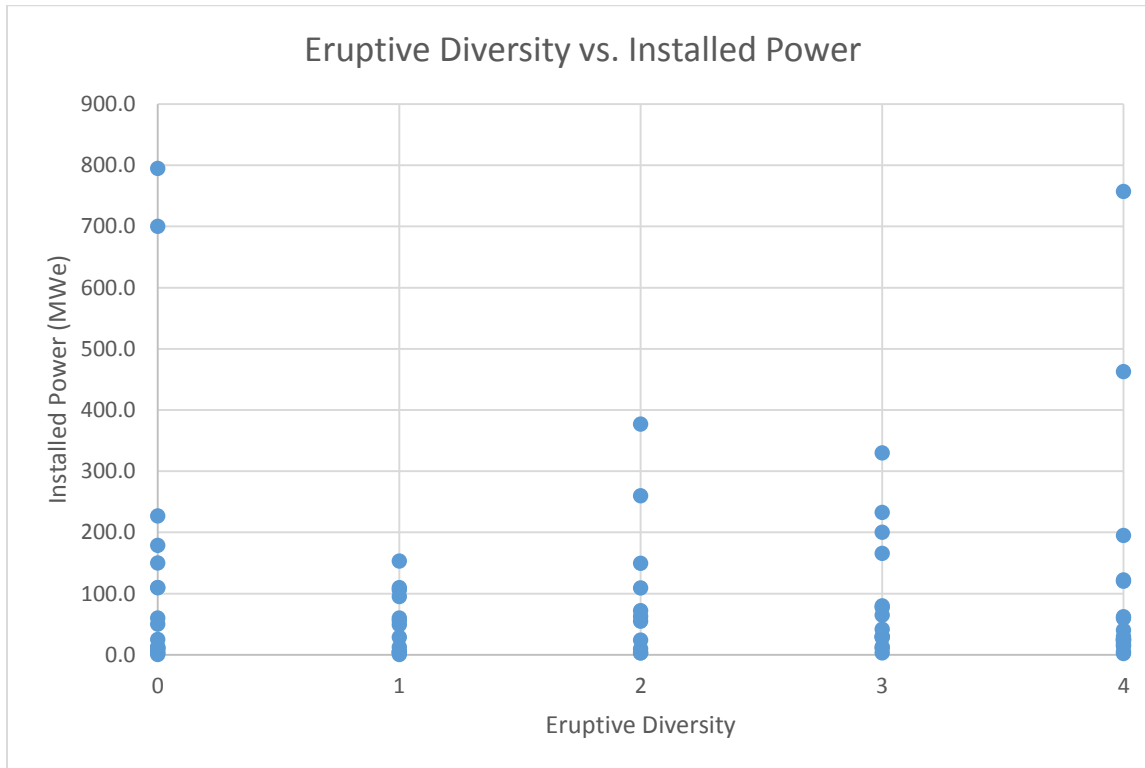


Figure 4.3-7 Eruptive diversity vs. installed power. Eruptive diversity is based on the number of different compositional groupings in the GeoROC database for each VC. A maximum score of 4 indicates that samples from all four compositional groups (basaltic, andesitic, dacitic and rhyolitic) are listed for that VC in the GeoROC database; a score of 0 means no compositional data were available. Diversity score does not reflect the actual compositions. No clear trends were observed. See text for details.

Composition of the most recent eruption

The composition on the most recent eruption was also considered (Fig. 4.3-8). These data exist for the majority of the global training set of VCs. A weak relationship between generally higher power yield (>100 MWe) and VCs for which the most recent eruption was andesitic, but the population is too low (n=5) to draw significant conclusions. Similarly, no geothermal systems with installed power >100 are associated with VCs that have most recently erupted basalt, although the sample population is too low to be statistically significant. No correlation exists

between higher silica content (more felsic) eruptive composition and installed power, as has been anecdotally suggested. Our conclusion, based on the existing training set, is that magmatic composition has little to no bearing on the likelihood of hosting a productive geothermal system. This strength of this conclusion is tempered, however, by the ambiguity present in the data collected from the GeoROC database.

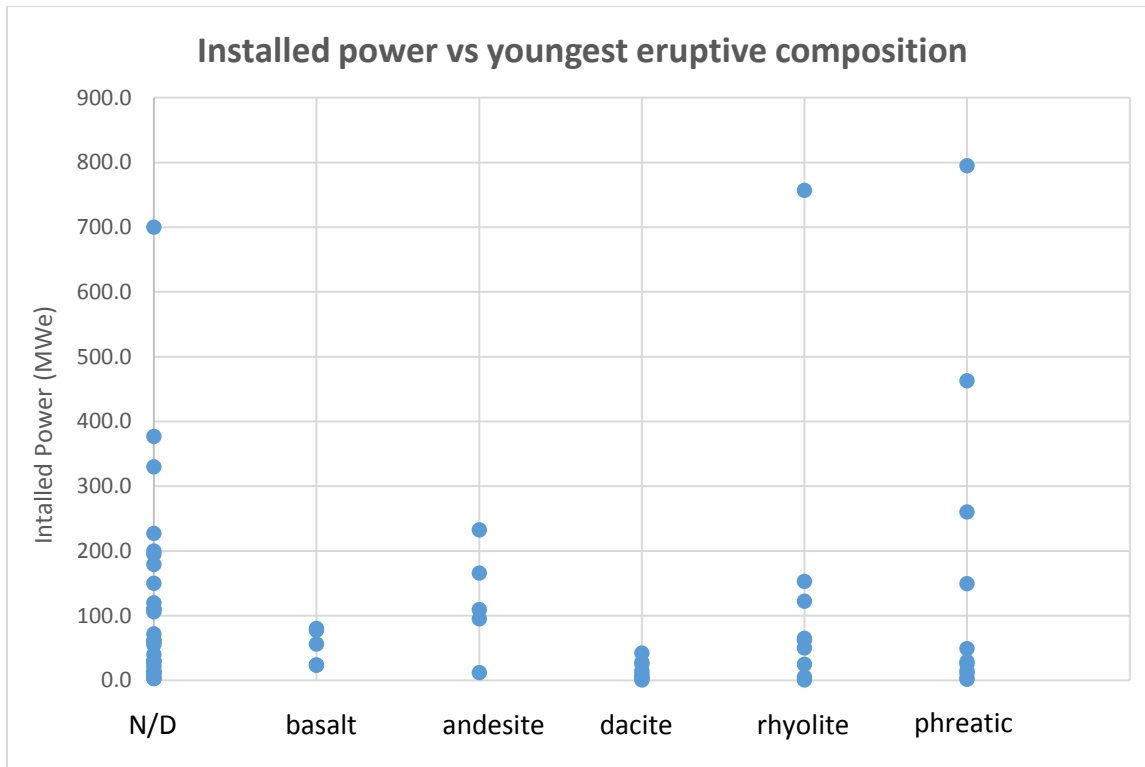


Figure 4.3-8. Composition of the most recent eruption vs. installed power. There is a potential correlation with lower power yielding geothermal systems for which the most recent eruption was a basalt, but the population numbers are very low and do not engender strong conclusions. Similarly, VCs in which the most recent eruption was andesitic appear to have a weak correlation with installed power. Ultimately, we believe this reflects the quality of the data and not a real correlation between these parameters. N/D = no data available.

4.4 WORLD STRAIN, PLATE MOTION, AND POWER DENSITY DATA

Wilmarth and Stimac (2015) recently documented systematic relationships between power density, reservoir temperature, and tectonic setting (Fig. 4.4-1). For arc settings, two distinct trends or populations of power density are apparent, one with relatively low power densities, attributed by Wilmarth and Stimac (2015) to “compressional” arc settings, and the other with higher power densities, attributed to “more complex” structural settings. The strain style index generated from the new world strain model (GSRM v.2.2) provides corroboration of this relationship (Fig. 4.4-2). Compressional to transpressional values of the strain-style index are confined to relatively low power density systems, whereas dilatational, transtensional, and shear

values of the index comprise the majority of high-density systems. The inference is that extensional, transtensional, and shear settings are more amenable to dilatational fracture permeability and widespread fracturing through shearing of larger volumes of rock, potentially forming fault-fracture meshes (Sibson, 1996), leading to high volumetric utilization (high power density) whereas in compressional settings, processes of fracturing are less efficient on a volumetric basis. Low-power-density geothermal systems might form in transtensional to dilatational settings if other factors (e.g., strain rate, lithology) are less favorable, but for the higher power density systems, a more favorable conjunction of strain style and other factors may be required.

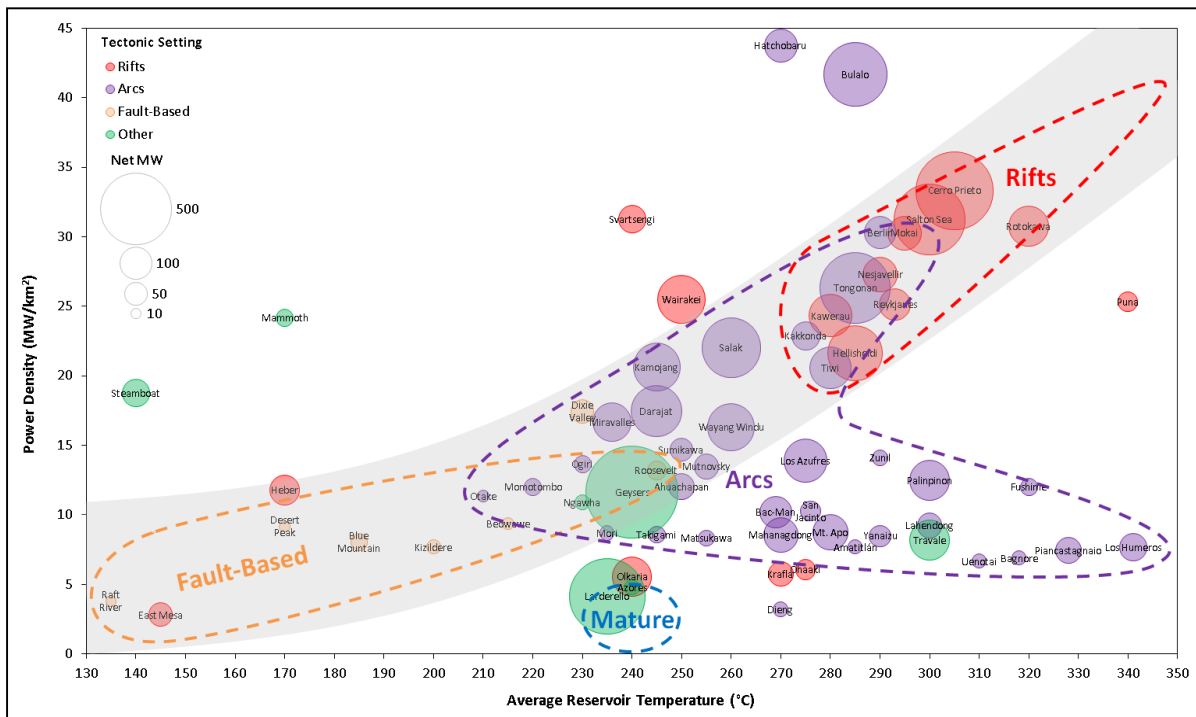


Figure 4.4-1. Power density in geothermal fields as a function of reservoir temperature and tectonic setting. Taken from Wilmarth and Stimac (2015).

A similar relationship is observed between power density and the arc-parallel velocity of the subducting plate (Fig. 4.4-3). Relatively low rates of arc-parallel motion are associated with low power density geothermal systems, whereas higher power densities are associated with higher arc-parallel velocities. Higher arc-parallel speeds could contribute to increased shearing in the volcanic arc, facilitate arc-parallel extension, and contribute to a greater structural complexity.

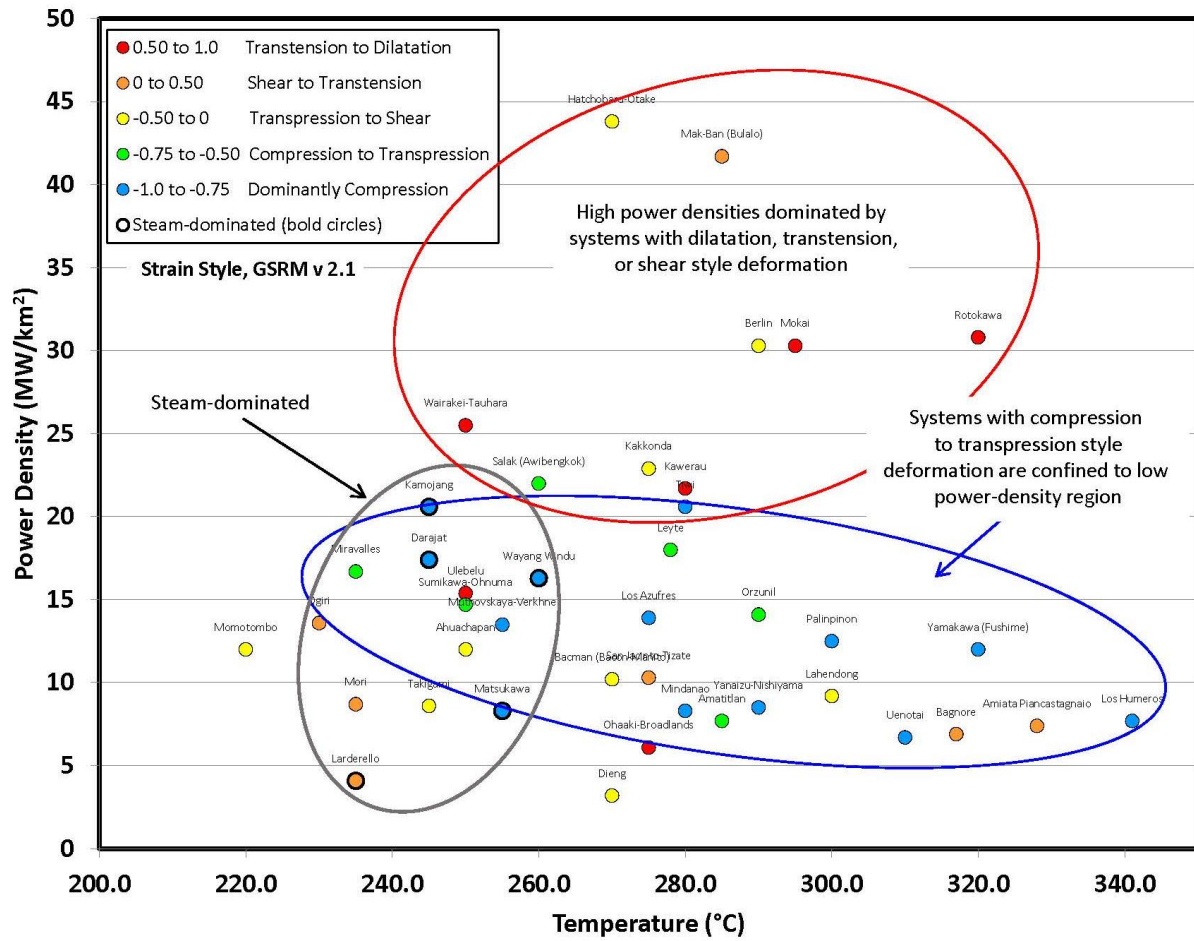


Figure 4.4-2. Relationship of power density to strain style measured from GSRM v. 2.1 for volcanic arc-hosted geothermal systems (see text for details). Power density data from Wilmarth and Stimac (2015).

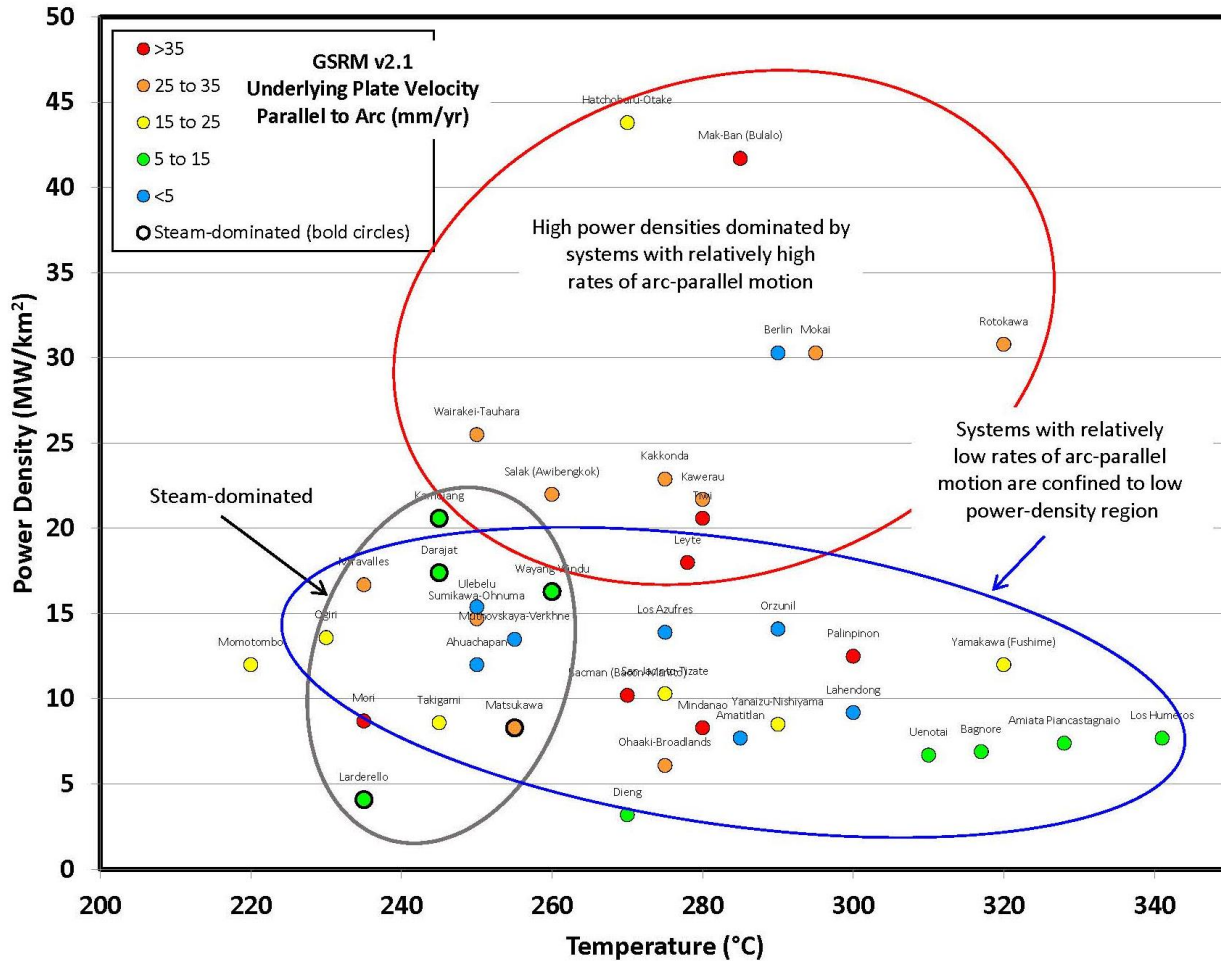


Figure 4.4-3. Relationship of power density to arc-parallel subducted plate velocities measured from GSRM v. 2.1 for volcanic arc-hosted geothermal systems (see text for details). Power density data from Wilmarth and Stimac (2015).

The strain style index and the plate motion index were linearly combined through scaled addition (index = arc-parallel motion (mm/yr) + [125 x strain style]) to create a combined strain style/motion index. The scaling factor used to convert units between arc-parallel motion and strain style was determined from examination a scatter plot of the two indices. The cumulative distribution of this combined index for all volcanic arc centers reveals a strong correlation with producing geothermal systems (Fig. 4.4-4). The binary weights-of-evidence contrast statistic for this index is 0.94 +/- 0.26, with a statistically significant studentized contrast of 3.6. This suggests that plate motion characteristics and regional strain styles have a significant impact on geothermal potential, and that perhaps with continued improvements in GPS-station network

densities and noise processing methodologies, that regional geodetic data may become more valuable in the future as a predictive tool.

Currently, high uncertainties characterize the GSRM at the scale of individual volcanic centers and some arc segments, and caution must therefore be exercised when using this parameter to predict local geothermal potential. However, these relationships provide encouragement and corroboration that the systematic compilation of structural and tectonic data at volcanic centers from multiple data sources, as discussed in section 4.2 above, is leading to the identification of significant predictive relationships for geothermal potential.

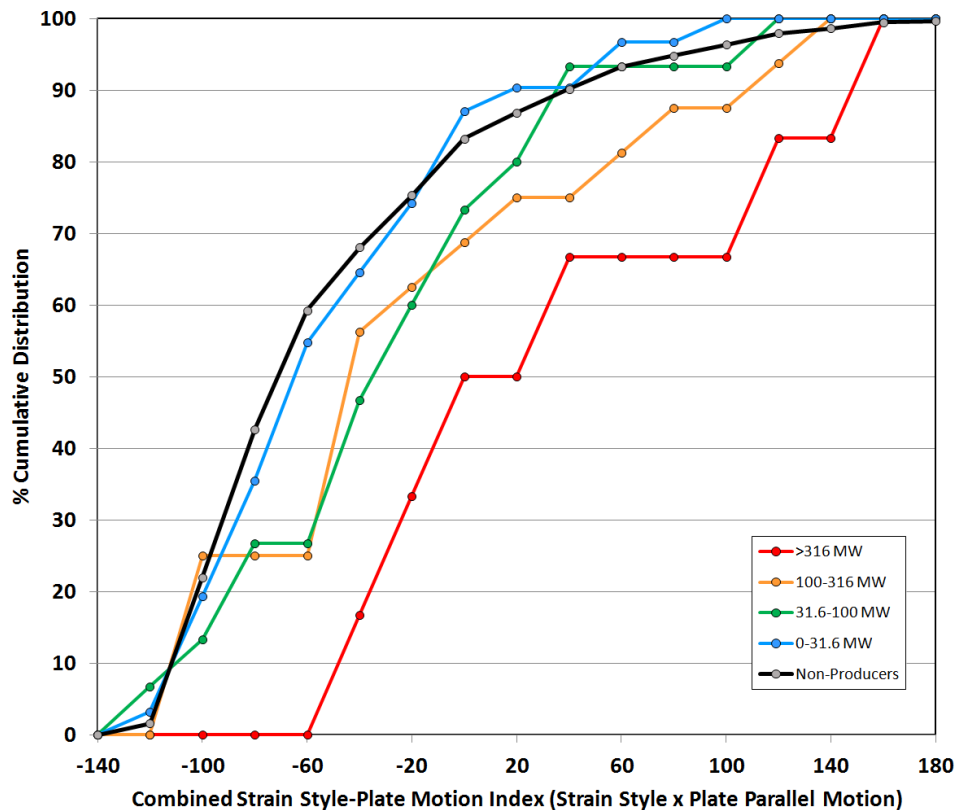


Figure 4.4-4. Cumulative distribution of an additively combined strain style-arc-parallel plate motion index for arc volcanic centers (see text for formula). Black line represents the distribution for non-producing volcanic centers, and colored lines represent distributions for the specified installed megawatt categories of geothermal systems associated with volcanic centers. Weights-of-evidence $W+ = 0.47$, $W- = -0.47$, contrast = 0.94 ± 0.26 (student contrast = 3.6).

4.5 STATISTICAL ANALYSIS

A separate statistical analysis of the database was completed to further explore and document relationships between the predictive data and geothermal potential. This work was completed by Dr. Fletcher Ibsen at Berkeley, CA.

The analysis focused on assessment of all of the Cascade and Aleutian volcanic centers plus the electricity producing volcanic centers in other arcs. Variables used in the analysis included geothermal production rates in megawatts, four plate tectonic plate velocity variables (arc-parallel velocity, arc-convergent velocity, total relative plate velocity, and angle of obliqueness), crustal thickness, the five primary structure/tectonic variables (tectonic setting, structural setting, Quaternary fault scarp density, fault slip rate, and dilation potential), and eight volcanic variables (eruption frequency, presence of calderas, composition of youngest eruption, age of youngest eruption, distance to the arc trench, the subduction angle, and the arc volcanic center spacing). In the case of the structure/tectonic variables, both the original categorical classifications (e.g., transtensional or step-overs) and the numerical scores assigned to them were evaluated.

The objective of the modeling was to identify which variables correlated best with geothermal production rates, and to identify possible interrelationships among the predictive variables. The dependent variable (megawatts) was organized in two ways. First, megawatt productivity was directly predicted as a function of the input parameters. Second, since production rates have an approximately log-normal distribution, the production was divided into two categories with approximately equal numbers of members (volcanic centers): low-rate production and high-rate production, in an effort to mimic modeling of productive and non-productive volcanic centers.

Statistical investigations included multiple regression, classification and regression decision trees (CART analysis), and visualizations including graphs and box-plots. None of the decision trees provided a meaningful improvement over the multiple regression models. Regression model selection of input variables was done by backwards deletion, such that variables with the largest p-values were removed until only those that were statistically significant remained. Log-transformed values of megawatt production were evaluated but did not improve the model fits.

Regression Results

A number of the input variables showed statistically significant correlation with geothermal power production rates. These include, in order of decreasing correlation coefficient (Table 4.5-1), angle of obliqueness (of plate convergence), Quaternary fault scarp density, fault slip rate, structural setting score, plate-parallel velocity (of underriding plate), plate convergent velocity (negatively correlated), the composition of the youngest volcanics, and crustal thickness (negatively correlated).

A number of predictive regression models were built, the three best of which were:

- 1) using categorical structural parameters,
- 2) using expert-assigned structural scores (membership functions), and,
- 3) using expert-assigned structural scores, but omitting crustal thickness.

For model one, the statistically significant input variables were reduced to fault scarp density, slip rate, and angle of obliqueness. The residual standard error is 147 MW.

For model two, the statistically significant input variables were reduced to crustal thickness, fault scarp density, and angle of obliqueness. The residual standard error is 141 MW.

For model three, in which crustal thickness was excluded, the statistically significant input variables were reduced to fault scarp density and angle of obliqueness. The residual standard error is 145 MW.

Regression Discussion

The regression models contain a limited number of statistically significant input variables. The total number of correlated variables (Table 4.5-1) is greater than the number used in the models because some of the input variables are correlated with each other. The models are also characterized by high residual errors. This is considered to be a reflection of the qualitative nature of the input data and challenges of modeling a log-normalized distribution of production rates (MW). Because of the high residual errors, the model weighting in this project primarily relied on expert knowledge and judgment regarding the appropriate combination and weighting of input variables.

One of the main contributions of the regression analysis was the confirmation that plate-subduction parameters correlate significantly with geothermal production. Foremost among these parameters is the angle of plate convergence (obliqueness), which may provide a better prediction than arc-parallel velocity. Both the angle of obliqueness and arc-parallel velocity imply transference of shear strain into the arc environment, where it can be expressed as arc-parallel strike-slip faulting, which in turn can lead to the development of transtensional tectonism and development of pull-apart blocks and other favorable structural settings.

Table 4.5-1. Correlation of input parameters with production rates.

Input Parameter	Correlation Coefficient	Lower Bound 2s	Upper Bound 2s
Plate Angle of Obliqueness	0.48	0.28	0.64
Fault Scarp Density Score	0.42	0.19	0.61
Fault Slip Score	0.38	0.13	0.58
Structural Setting Score	0.33	0.09	0.54
Plate Parallel Velocity	0.31	0.09	0.50
Composition Youngest Volcanics	0.22	-0.10	0.50
Crustal Thickness	-0.13	-0.35	0.10
Plate Convergent Velocity	-0.27	-0.47	-0.04

5.0 TRENDS AND WEIGHTING FACTORS

Weighting factors were assigned for model input into the play fairway and favorability models where structure and tectonics dominates the play fairway and direct evidence of temperatures and surface manifestations are used to adjust play fairway rankings to obtain overall geothermal favorability of the Cascade and Aleutian VCs.

5.1 STRUCTURAL AND TECTONIC DATA

In the Fairway Model (Fig. 5.1-1) these categories were individually qualitatively ranked according to their potential to host economic geothermal resources. Weights were derived through a combination of expert geologic knowledge and trends identified in the global benchmark data set (section 4.2). This combination of expert driven and data driven modeling was used for both the internal weights for each category and the relative weighting between categories. For example, the global benchmark graining data supports that the Quaternary fault slip rate and Quaternary fault density parameters are non-linear (section 4.2, Tables 4.2-2, 4.2-3). The Quaternary fault slip rates, Quaternary fault density, and GPS angle of obliquity all show very strong trends for predicting geothermal favorability and MWe in the global benchmark data set and are weighted more strongly than dilation potential, which shows a weaker capacity for predicting favorability (Table 4.2-5).

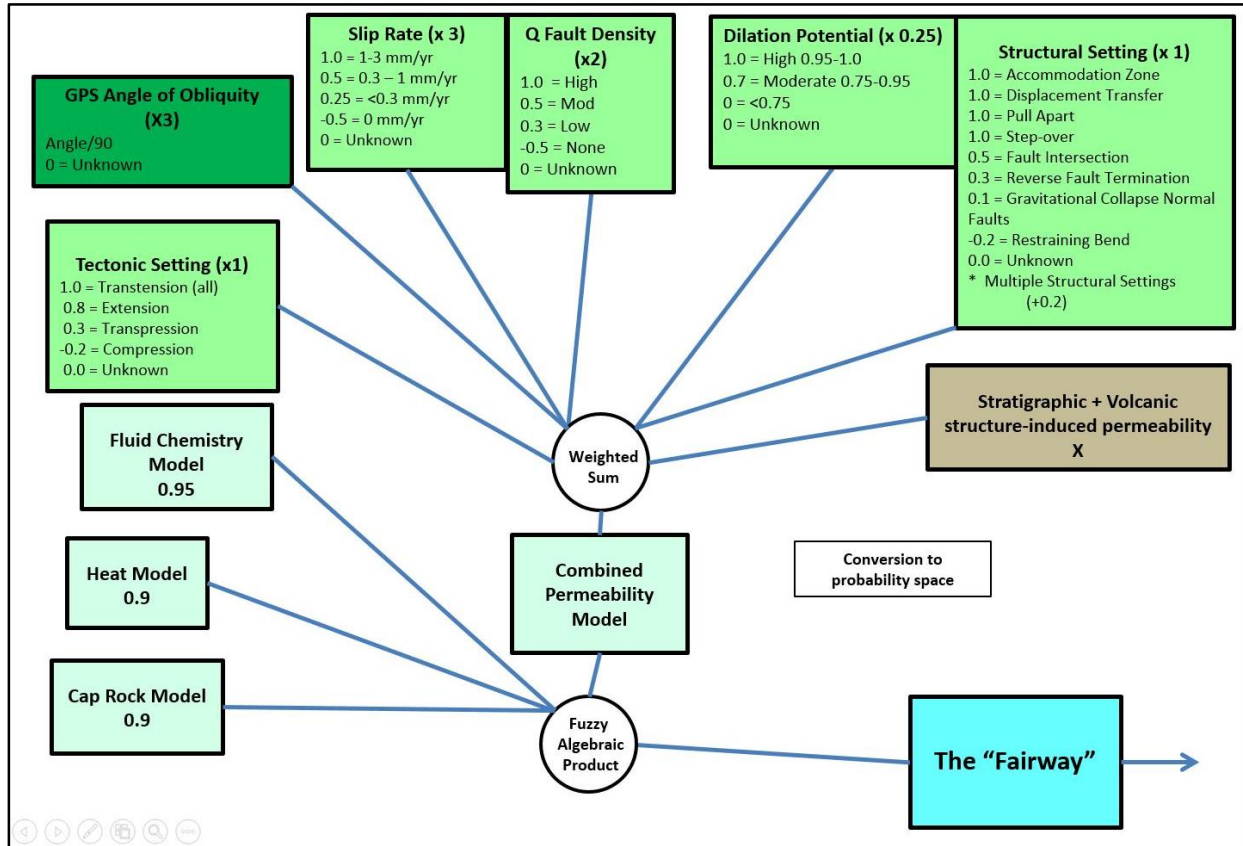


Figure 5.1-1. Fairway model with weighting per parameter and per parameter subcategory.

The power and logic of combining the data sets selected for this study is that they all demonstrate reliability in predicting geothermal favorability and they all capture different aspects of assessing strain style, strain rate, and structural style of strain accommodation. In addition, several of these key parameters integrate very closely, for example with Quaternary fault scarp concentration versus Quaternary fault slip rate (Fig. 5.1-2). In general, there is a consistent increase in favorability with each parameter individually, such that when one is held equal, the other captures another detail of favorability.

		Q Fault Density, Mean MWe/System					
mm/yr	Unknown	Zero	Low	Medium	High		
1-3			153		700	427	
0.3-1			70	100	336	198	
0.1-0.3		12	103	102		96	
<0.1			65	210	91	92	
0		29				29	
unknown	63	5	108			68	
	63	25	84	149	268		

Figure 5.1-2. Quaternary fault concentration versus Quaternary fault slip rate for the global benchmark VCs. Mean MWe/VC is plotted in the respective cells. Blank cells indicate that no benchmark VCs are known to have specific corresponding Quaternary fault density and fault slip rate for that part of the table.

5.2 GEOCHEMICAL AND SURFACE MANIFESTATION DATA

Based on considerations in Section 4.1.1, weighting factors were assigned for temperatures (measured and calculated) and surface manifestations on a scale of 0 to 1. In general, higher temperatures were assigned higher weights, regardless if measured or calculated. Measured spring temperatures in excess of 90°C are assigned a weight of 1 given that boiling springs are a strong indicator of a high temperature system, and 90°C is near boiling at many elevations. Temperature ranges are assigned to lower measured spring temperatures are noted in Figure 5.2-1 with lower temperatures associated with lower weighting factors. A maximum weight of 1 is assigned to weights assigned to the other measured and geothermometer temperatures for those >250°C so that the highest temperature systems (near the average of the world power producing systems) is given the maximum weight. Lower weights are assigned to lower temperatures based on Figure 5.2-1 values. Note that spring geothermometers of the same temperature range as well geothermometer and measured values are given a higher ranking given that the majority of spring geothermometers are expected to underestimate reservoir temperatures. Negative weights are assigned to well measured and geothermometer temperatures of <100°C as temperatures in this range are expected to be a negative indicator of the presence of a power producing system. Sites with one or more unknown geothermometer or measured temperatures are assigned a neutral weight of “0” such that lack of data does not increase or decrease the favorability of a particular VC.

Based on considerations in Section 4.1.2, fumaroles were assigned weights as noted in Figure 5.2-1. The highest weight of 1 is assigned to VC with either measured flank fumarole areas (described in Section 4.1.2), or notations in the literature that the VC had “many” or a “cluster” of flank fumaroles. If one fumarole was noted in the literature, the weight to the VC for this factor was

assigned a 0.5. If flank fumaroles are known NOT to occur, this is considered a negative indication of a power producing system based on Section 4.1.2 where it is shown that 93% of all power production originates from VC with known flank fumaroles. Hence, these VC are assigned a “-1” weight for the fumarole factor. Similarly, if a VC has ONLY a summit fumarole, and no known flank fumaroles, the weight for the fumarole factor is “-1”.

Figure 5.2-1 also notes weightings for surface deposits, although relatively few VC had notations of sinter or travertine deposits in the literature. If a VC is known to have sinter deposits, a weighting of 1 is assigned for the VC as sinter deposition occurs from systems with temperatures in excess of 180°C, which is suitable for power production. Travertines were not weighted in the final model as they may be indicators of a low temperature system or outflow from high temperature systems, which often cannot be resolved. In either case, a lower weight for travertine could erroneously negatively weight a VC if it occurs in outflow mixed with non-thermal waters. Such systems likely have a higher temperature source waters. Hence, travertines were left neutral from the perspective of weighting in the final model.

Other factors are noted in Figure 5.2-1 which could be considered in future modeling efforts. These include lithology type and variation, hydrology (recharge, depth to water table, rain curtain effect), and alteration type, patterns and size. However, the scope of this 1 year project did not allow for thorough evaluation of these factors in the data compilation and modeling efforts.

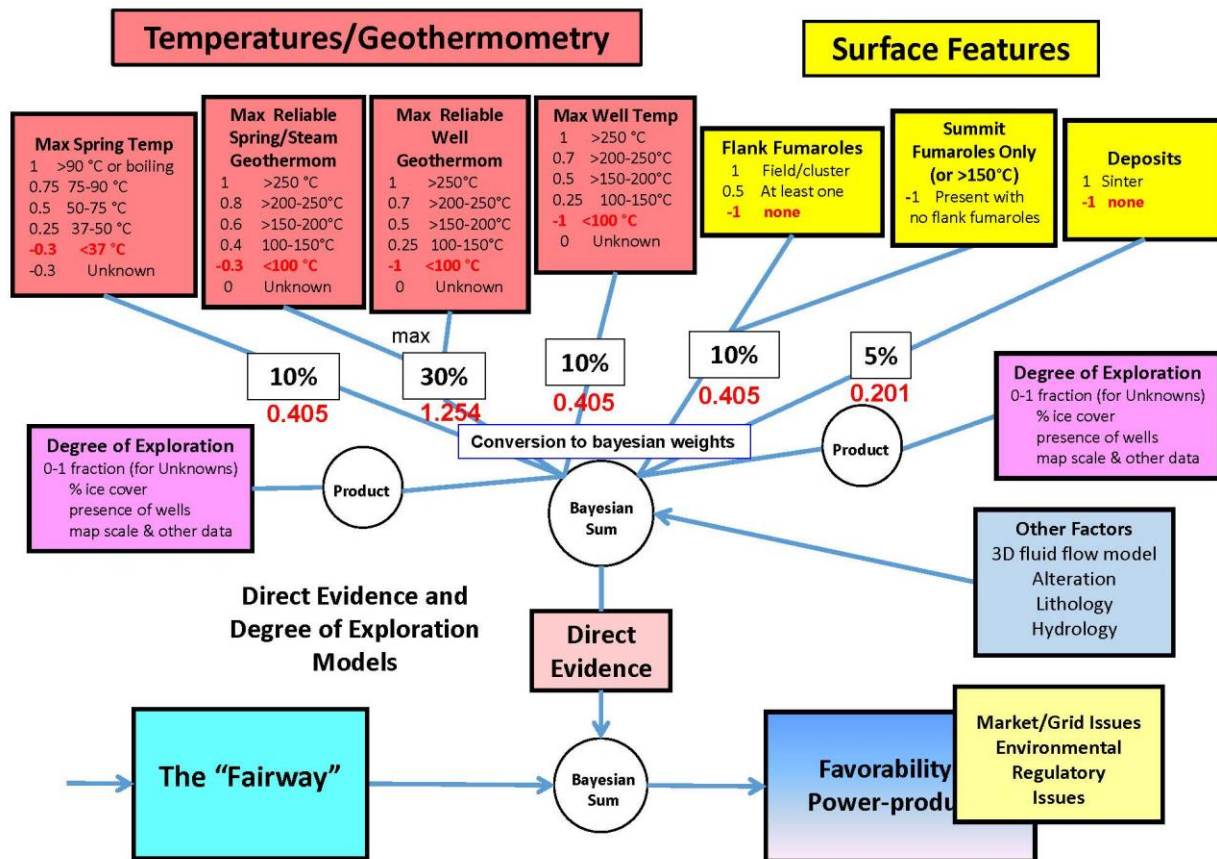


Figure 5.2-1. Weighting factors for measured and calculated temperatures and surface manifestations for the geothermal favorability model.

6.0 MODEL FORMULATION

6.1 PRINCIPAL HIERARCHICAL TIERS

The preliminary predictive geothermal models utilize the play fairway concept originally developed for petroleum exploration. In the play fairway approach, a set of key geological factors (Fugelli and Olsen, 2005) or principal hierarchical tiers (Doust, 2010) define required components or conditions considered essential for the development of resources. In the case of petroleum exploration, these tiers might consist of, for example, 1) a petroleum charge (source rocks, a maturation window, and a migration pathway), 2) a reservoir rock, 3) a topseal or caprock, and 4) suitable traps (Allen and Allen, 2005).

In the case of geothermal plays in arc terrains, four key component geological factors or hierarchical tiers are considered in this project; they are: 1) heat source, 2) permeability, 3) viable fluid chemistry, and 4) cap rock. The first component, a heat source, is commonly present to varying degrees at suitable depths beneath most active arc volcanic centers. As such, it isn't

always the most critical component, though clearly the presence of high heat flow related to large cooling magma bodies or intrusions at relatively shallow depths can have a significant impact on the heat content and size of a resource. The third component, a viable fluid composition, is also usually available in most arcs where moderate-salinity, near-neutral pH meteoric hydrothermal systems develop within or marginal to intrusive centers. In some cases, however, low-pH fluids with magmatic input, or other fluids that pose difficult-to-resolve challenges related to corrosion or mineral precipitation in well bores, can make economic exploitation difficult.

It might be argued that the fourth component, a cap rock, is not necessary for the development of hydrothermal circulation in a geothermal system; however, most successfully developed systems show well established caps (Facca and Tonani, 1967; Grant and Bixley, 2011). It may be that in order to achieve *economic* viability, some type of cap rock helps constrain the natural rate of energy release into the environment. Geothermal reservoirs are inherently more dynamic than petroleum reservoirs in the sense that, if they are not sustained by an ongoing influx of heat, they will dissipate their stored energy by conduction within a few tens of thousands of years if impermeable and much more quickly by convection if permeable. Economically viable conventional geothermal resource development requires high permeability, which would result in the rapid dissipation of a reservoir's available heat energy to the surface or near-surface environment if a cap rock was not present.

It could also be argued that clay caps commonly form in volcanic environments where geothermal systems are present, thus the presence of a clay cap might be assumed in many cases, and will not usually comprise a critical missing component. However, the ability of a clay cap to form might be complicated by an unsuitable host rock (e.g. quartzite) or hindered by the presence of alteration minerals formed during earlier periods of alteration that are resistant to the transformation into clay (e.g. hornfels?). At some locations, clay caps have initially formed, but have since been breached by rapid rates of erosion related to high topographic gradients, high uplift and/or high precipitation rates, glaciation, or volcanic sector collapse. Such breaching is interpreted to have caused significant damage to reservoirs at Karaha Bodas, Indonesia (Moore et al, 2002) and Tolhuaca, Chile (Melosh et al, 2012; Melosh, verbal communication, April, 2015). Hoagland and Bodell (1990) described a cap failure event during production that was devastating at Tiwi, Philippines. In these cases, lack of an intact cap constitutes a negative indicator.

The remaining component, permeability, is considered by many as the most critical factor for geothermal resource development (Faulds et al., 2010, Melosh, 2015, Hinz et al., 2011), from the perspective of its relative scarcity compared to the other factors mentioned above. Economic levels of permeability can be challenging to predict, and are influenced by structural and tectonic settings, lithology (as it influences both primary and secondary permeability) and lithologic diversity (Melosh, 2015), as well as geologic history. Accordingly, permeability has received the greatest attention in the geothermal modeling processes described herein.

6.2 FAIRWAY MODEL

The predictive models comprise principal two stages (Fig. 6.2-1.): a fairway model and a favorability model. The first stage is the fairway model; it models the combined occurrence of the four geologic factors or hierarchical tiers considered necessary for an economic geothermal system to form, and as such, constitutes the “fairway” when plotted on maps. The fairway model does not consider any direct evidence of geothermal activity (e.g. hot springs). Direct evidence is added later in the favorability model (see below).

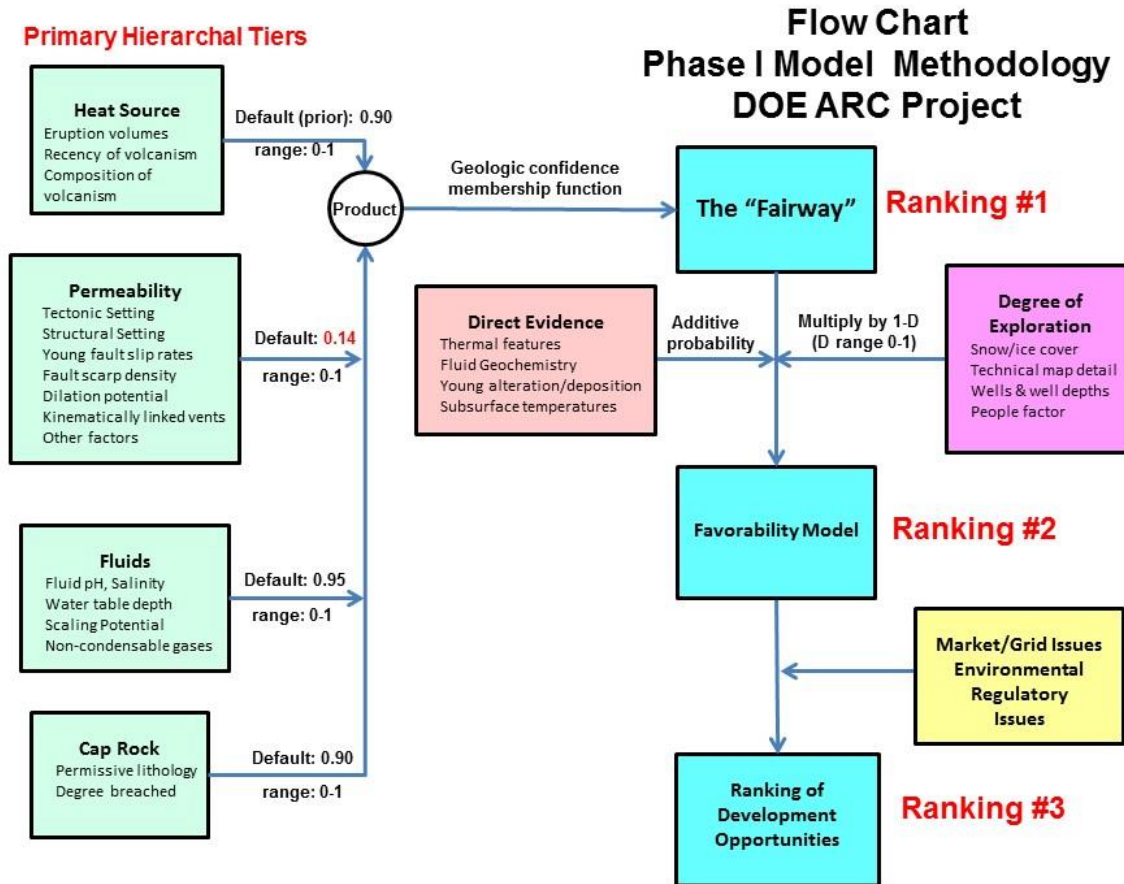


Figure 6.2-1. Overall flow chart of predictive model methodology. The model includes calculation of the fairway and favorability models. Development opportunities are ranked after consideration of market/grid, environmental, and regulatory considerations (see section 7).

In the modeling process, the four hierarchical tiers or principal geologic factors described above (see initial section on “Model Construction”) were assigned numerical values that qualitatively indicate the probability that each key component is present at each volcanic center. The numerical range for each component is from 0 to 1. These probability assignments are non-quantitative in part because the scale of the project and data availability and quality issues for less well-explored volcanic arcs prevented accurate characterization of geologic factors in non-

producing volcanic arc segments around the world. The probability assignments for each of the four hierarchical tiers were then multiplied together to form a fairway prediction (Fig. 6.2-1.), in accordance with the play concept that each of these key factors should be present in order for a viable geothermal system to form.

In the fairway model, sufficient data has not been gathered to differentiate between the quality of heat source, fluid chemistry, or cap rock for each of the Aleutian and Cascade volcanic centers. Accordingly, default probabilities have been assigned to these three tiers or geologic factors. These default probabilities are high, ranging from 0.9 to 0.95 (Fig. 6.2-1.), reflecting the expectation that at most active arc volcanic centers, these three factors are either present or could develop in response to geothermal activity.

A mean default probability value for the permeability component of the model was chosen such that the resultant mean value for the play fairway equaled the fraction of arc volcanic centers that are currently producing electrical energy (the prior probability). In other words, in the current model, approximately 730 arc volcanic centers have been defined (around the world), and ~10% are known to host productive geothermal systems. Calculation of the mean permeability probability based on this number, and based on the default probabilities assigned for the other three hierarchical tiers, yields a mean permeability value of 0.14 (so that 0.14 (mean permeability) \times 0.90 (mean heat source) \times 0.95 (mean fluid chemistry) \times 0.90 (mean cap rock) = 0.10). The intention is to work with plausible probabilities, so that when other similarly scaled components are added to the model, the resulting output is more likely to be weighted properly.

Permeability

The permeability component constitutes the core of the preliminary fairway model, based on its demonstrated importance in determining geothermal potential. Permeability is influenced by many factors that include lithologic as well as structural/tectonic parameters. Because of challenges in accurately representing subsurface lithology at reservoir depths on a regional basis, it has not been added.

The permeability model comprises six components (Fig. 5.1-1); tectonic setting, structural setting, plate angle of obliqueness, slip rate, Quaternary fault density, and dilation potential. The selection of these components and the determination of weighting factors for them are described in detail in the preceding section.

Scaling to Probability Space and Creation of the Predictive Fairway

The membership functions and weights for each of the six classes of evidence in the permeability model (Fig. 5.1-1) were combined in a simple linear weighted sum. For example, if a given volcanic center has an estimated fault slip rate of 0.3-1 mm/yr, a membership function of 0.5 would be multiplied by a weighting factor of 3 to produce a slip-rate contribution of 1.5 (Fig. 5.1-1). This contribution would be added to similarly calculated contributions from the remaining five classes of evidence to produce an overall permeability model score for that volcanic center.

The permeability scores for all of the volcanic centers were then rescaled into approximate probability space so that the mean fairway score equaled 0.11 (approximately equal to the prior probability) and so that all scores were positive. In this model, the rescaling involved addition of a constant value of 7.0 and multiplication by a constant factor of 0.155. The resulting fairway scores for each of the volcanic centers are listed in Table 6.2-1.

Errors

As described in section 3, errors were estimated for each data parameter input into the permeability model. A +/- error range was based in part on data quality, but was also based on an assessment of how much the parameter value could change due to misclassification. These errors were then propagated to a total error of the permeability score by summing variances weighted by the square of the weighting factors. The relative error (permeability error divided by permeability score) was then assumed as the relative error for the overall fairway score, since input values for heat, fluids, and cap rock were constant across the model.

Calculated fairway errors are quite high for some volcanic centers, equaling or exceeding 100% for seven volcanic centers in the Aleutians and four volcanic centers in the Cascades (Table 6.2-1). This is an expected result, because data availability issues are significant for some of the more remote and isolated volcanic centers, and these high scores underscore the need for additional studies to better understand these areas and their geothermal potential.

Table 6.2-1. Fairway and Favorability relative scores along with relative error estimates of each. VC listed in order of decreasing Fairway ranking.

VC #	Volcano Name	Fairway Ranking	Fairway Relative Error	Total Degree of Exploration	Favorability Ranking	Favorability Relative Error
	Aleutian Arc					
1052	Little Sitkin	0.147	0.12	0.25	0.400	0.67
1044	Korovin	0.142	0.13	0.08	0.331	0.79
1046	Adagdak	0.139	0.13	0.32	0.262	0.59
1043	Seguam	0.136	0.14	0.49	0.099	0.42
1060	Vsididov	0.132	0.14	0.07	0.126	0.74
1035	Recheschnoi	0.132	0.14	0.09	0.419	0.80
1034	Okmok	0.131	0.15	0.07	0.191	0.79
1050	Gareloi	0.131	0.19	0.29	0.109	0.58
1033	Makushin	0.130	0.15	0.35	0.497	0.60
1049	Tanaga	0.129	0.19	0.25	0.110	0.61
1047	Moffett	0.128	0.20	0.25	0.109	0.61
1048	Kanaga	0.128	0.20	0.25	0.109	0.61
1041	Yunaska	0.126	0.20	0.07	0.121	0.75
1001	Spurr	0.126	0.17	0.14	0.201	0.74
1032	Table Top	0.124	0.16	0.07	0.140	0.77
1031	Akutan	0.124	0.14	0.63	0.508	0.39
1040	Herbert	0.122	0.21	0.07	0.117	0.75
1037	Tana	0.122	0.21	0.06	0.168	0.79
1038	Cleveland	0.122	0.21	0.07	0.117	0.76
1054	Kiska	0.121	0.34	0.24	0.103	0.62
1053	Segula	0.121	0.34	0.24	0.103	0.62
1007	Kaguyak	0.111	0.22	0.07	0.154	0.80
1025	Frosty	0.109	0.38	0.04	0.126	0.81
1058	Isanotski	0.108	0.39	0.05	0.104	0.79
1026	Roundtop	0.108	0.39	0.04	0.105	0.79
1015	Chiginagak	0.107	0.23	0.15	0.221	0.76
1002	Hayes	0.105	0.57	0.01	0.104	0.82
1021	Dana	0.104	0.42	0.06	0.100	0.79
1039	Carlisle	0.104	0.44	0.06	0.100	0.79
1003	Redoubt	0.102	0.47	0.02	0.101	0.82
1030	Gilbert	0.101	0.61	0.06	0.166	0.82
1022	Pavlof	0.100	0.59	0.05	0.097	0.80
1029	Westdahl	0.099	0.60	0.06	0.095	0.79
1004	Iliamna	0.099	0.64	0.01	0.098	0.83
1023	Emmons Lake	0.099	0.61	0.06	0.215	0.85
1005	Augustine	0.097	0.67	0.06	0.093	0.80
1056	Douglas	0.095	0.66	0.01	0.146	0.88
1006	Fourpeaked	0.095	0.67	0.01	0.094	0.84
1009	Snowy Mountain	0.095	0.67	0.01	0.094	0.84
1008	Kukak	0.094	0.67	0.01	0.094	0.84

Table 6.2-1. (Continued)						
VC #	Volcano Name	Fairway Ranking	Fairway Relative Error	Total Degree of Exploration	Favorability Ranking	Favorability Relative Error
1010	Katmai	0.094	0.67	0.01	0.134	0.86
1012	Mageik	0.094	0.68	0.01	0.188	0.89
1019	Veniaminof	0.093	0.70	0.04	0.090	0.82
1027	Shishaldin	0.090	0.77	0.05	0.087	0.81
1051	Semisopochnoi	0.089	0.77	0.28	0.181	0.68
1011	Griggs	0.089	0.81	0.01	0.088	0.85
1020	Stepovak Bay 4	0.086	0.86	0.02	0.085	0.85
1059	Unnamed	0.086	0.80	0.07	0.216	0.84
1018	Black Peak	0.085	0.88	0.06	0.082	0.82
1057	Kupreanof	0.084	0.91	0.04	0.100	0.85
1042	Amukta	0.083	0.86	0.07	0.079	0.81
1045	Great Sitkin	0.080	0.98	0.24	0.227	0.72
1036	Kagamil	0.074	1.00	0.07	0.105	0.85
1024	Dutton	0.064	1.00	0.03	0.119	0.90
1014	Ugashik-Peulik	0.064	1.00	0.25	0.106	0.71
1028	Fisher	0.060	1.00	0.07	0.058	0.84
1055	Kialagvik	0.060	1.00	0.07	0.057	0.85
1016	Yantarni	0.058	1.00	0.42	0.044	0.56
1017	Aniakchak	0.055	1.00	0.07	0.083	0.89
	Cascade Arc					
2041	Sugarloaf	0.176	0.14	0.59	0.122	0.33
2028	Prospect Peak	0.176	0.14	0.59	0.122	0.33
2029	Red Cinder Chain	0.176	0.14	0.59	0.122	0.33
2039	Mt. Bailey	0.153	0.09	0.45	0.201	0.49
2025	Magee Peak	0.149	0.09	0.59	0.103	0.34
2023	Burney Mtn	0.149	0.11	0.45	0.112	0.44
2027	Antelope Mtn	0.149	0.09	0.59	0.102	0.34
2024	Harvey Mtn	0.148	0.11	0.59	0.102	0.35
2015	South Sister	0.142	0.13	0.58	0.099	0.36
2018	Davis Lake	0.142	0.13	0.44	0.107	0.45
2019	Crater Lake	0.142	0.13	0.63	0.086	0.35
2020	McLoughlin	0.141	0.11	0.45	0.106	0.45
2040	Yamsay Mountain	0.141	0.11	0.43	0.107	0.46
2030	Lassen	0.138	0.12	0.59	0.545	0.41
2037	Diamond Peak	0.138	0.12	0.58	0.095	0.36
2036	Maiden Peak	0.137	0.13	0.44	0.103	0.46
2016	Bachelor	0.137	0.10	0.58	0.094	0.36
2026	Crater Mtn	0.137	0.10	0.59	0.094	0.35
2038	Mt. Theilson	0.136	0.10	0.45	0.102	0.45
2014	Belknap	0.136	0.13	0.59	0.184	0.40
2035	Three-fingered Jack	0.136	0.14	0.59	0.094	0.35
2013	Jefferson	0.136	0.14	0.63	0.095	0.33

Table 6.2-1. (Continued)						
VC #	Volcano Name	Fairway Ranking	Fairway Relative Error	Total Degree of Exploration	Favorability Ranking	Favorability Relative Error
2034	Olallie Butte	0.136	0.14	0.41	0.286	0.55
2021	Medicine Lake	0.136	0.12	0.85	0.163	0.29
2012	Hood	0.135	0.14	0.80	0.156	0.55
2017	Newberry	0.130	0.14	0.80	0.392	0.25
2022	Shasta	0.123	0.16	0.42	0.286	0.57
2002	Meager	0.092	0.40	0.83	0.338	0.24
2004	Garibaldi	0.091	0.42	0.07	0.087	0.79
2001	Silverthorne	0.089	0.49	0.02	0.088	0.84
2003	Cayley	0.084	0.57	0.31	0.121	0.69
2011	West Crater	0.082	0.87	0.45	0.061	0.52
2009	St. Helens	0.082	0.88	0.50	0.177	0.51
2033	Marble Mountain	0.082	0.88	0.45	0.060	0.52
2010	Indian Heaven	0.082	0.88	0.53	0.059	0.46
2008	Adams	0.081	0.90	0.57	0.056	0.43
2032	Lakeview Mountain	0.080	0.94	0.45	0.050	0.54
2031	Goat Rocks	0.074	1.00	0.50	0.054	0.49
2007	Rainier	0.073	1.00	0.36	0.114	0.65
2006	Glacier Peak	0.065	1.00	0.09	0.146	0.86
2005	Baker	0.063	1.00	0.17	0.124	0.81
	Average	0.111	0.45	0.28	0.145	0.64
	Maximum	0.176	1.00	0.85	0.545	0.90
	Minimum	0.055	0.09	0.01	0.044	0.24

6.3 DEGREE-OF-EXPLORATION

The degree-of-exploration index is designed to qualitatively characterize the thoroughness of geothermal exploration at each volcanic center. If thorough exploration has not yielded a 'discovery', it is less likely that an economic geothermal system exists. The degree-of-exploration index also attempts to account for the ability of a geothermal system to remain blind or hidden. If the potential for a blind system is considered high, the degree-of-exploration will be lower. Degree-of-exploration is scaled in probability space from 0 (no exploration) to 1 (complete exploration). Degree-of-exploration is difficult to estimate because many factors play a role, including geomorphic factors related to surface manifestations, climate/vegetation, population density, drilling, geological, geochemical, and geophysical surveys, and ease of access. An example of the use of degree-of-exploration is provided by Coolbaugh et al. (2007) who used this index to revise geothermal evidence weights in Nevada and estimate the magnitude of undiscovered resources.

Consideration was given to including a 'rain curtain' effect in the degree-of-exploration model which would account for the often quoted tendency of geothermal manifestations in the Cascade and Aleutian Arcs to remain concealed or disguised due to high rates of precipitation and shallow cold groundwater flow, which, it is envisioned, could capture and entrain rising thermal fluids. However, many arc volcanic settings in similarly wet, mountainous climates in the southwestern and western Pacific show strong surface geothermal manifestations, and surface water mass balance calculations in the Cascades do not reveal significant rates of hidden geothermal contributions to streams and rivers (Muffler and Guffanti, 1995). For this reason, a rain-curtain effect was not included.

Degree-of-exploration was divided into two main components, sub-surface degree-of-exploration and surface exploration. Each of these was intersected with different parts of the direct evidence model discussed in a later section.

Sub-surface Degree-of-Exploration

A rough, qualitative measure of the degree-of-sub-surface exploration was made by compiling a list of the number of wells drilled within 10 km of each volcanic center. These wells were divided into two categories: 1) temperature gradient wells, and 2) larger diameter test wells and/or deeper slim holes. Degree-of-exploration was considered to increase with the number of wells drilled according to the formula,

$$\text{Degree-of-exploration} = 1 - [(1-p)^n]$$

where n = number of wells drilled of a given category, and p = the degree-of-exploration per well. In the case of temperature gradient wells, n was set to 0.025 and the magnitude of degree-of-exploration was capped at 50% (0.50). For deeper wells, n was set to 0.050 and degree-of-exploration was capped at 75% (0.75). The overall subsurface degree-of-exploration was taken as the maximum of the two well categories of degree-of-exploration. This type of estimate does not consider the spatial distribution of the wells around the volcanic center, because of the time

constraints in quantitatively assessing that type of spatial information for the entire Cascade and Aleutian arcs.

Surface Degree-of-Exploration

Parameters used to estimate surface degree-of-exploration include 1) the availability of geologic maps, 2) the quality of available data for estimating permeability scores, 3) a people factor, and 4) percent ice cover.

Geologic mapping at each volcanic center was scored from 0 to 1 according to the mapping scale, percent coverage, and availability of LiDAR.

The quality of available data for estimating structural scores consists of the average of the quality/availability scores for the structure, Quaternary fault scarp density, and fault slip rate scores described in section 3 of this report. Each of these three scores ranges from 0 (poor quality/availability) to 1 (excellent quality/availability), so the average of the three scores similarly ranges from 0 to 1.

The people factor reflects the degree to which each of the volcanic centers is visited by people regardless of whether these visits are related to scientific investigation, exploration, hiking, or tourism. Two “people factors” were used; a low factor of 0.05 used for the Aleutians and the northernmost, ice-covered volcanic center of the Cascades (Silverthron), and a higher factor (0.35) for the remaining portion of the Cascades.

Percent ice cover represents an estimate of the fraction of permanent ice cover at each volcanic center based on an examination of Google Earth images.

These above four factors were combined into a single degree-of-surface exploration factor in the following steps:

- 1) creation of a weighted sum of the geologic map factor and permeability quality/availability factor using respective weights of 0.75 and 0.10,
- 2) combination of the above map/data score with the people factor using the equation: $\text{degree-of-exploration} = 1 - [(1-p_1) * (1-p_2)]$, where p_1 and p_2 equal the map/data score and people score, respectively, and,
- 3) multiplying the score from 2) above by the fraction of ice-free ground (which equals $1 - \text{the fraction of ice cover}$).

Total Degree-of-Exploration

Total degree-of-exploration was calculated using same form of equation used above. Total degree-of-exploration = $1 - [(1-p_1) * (1-p_2)]$, where in this case, p_1 and p_2 equal the subsurface and surface degree-of-exploration scores. Degrees-of-exploration for the Cascade and Aleutian arcs are listed in Table 6.2-1.

Errors

Estimation of error associated with degree-of-exploration is difficult because of the uncertain and qualitative aspect of the input data and inherently qualitative nature of converting those parameters into an exploration index. An across-the-board +/- 25% relative error was ultimately assigned to this index with the idea that three successive +/- 25% ranges is approximately equivalent to the ability to distinguish three broad categories of degree-of-exploration: low, medium, and high.

6.4 DIRECT EVIDENCE AND ESTIMATION OF THE FAVORABILITY MODEL

Direct evidence incorporated into the model includes well and spring temperatures, well and spring geothermometry (including gas and liquid geothermometers), and presence of fumaroles and sinter deposits. Methods of compiling these parameters and assigning membership functions (scaled from 0 to +/-1) are described in sections 3 and 4, respectively, and depicted in Fig. 5.2-1.

Conversion of these parameters into an overall direct evidence index and estimation of the favorability model involved the following steps:

- 1) assignment of incremental probabilities associated with each of the component parameters,
- 2) use of the degree-of-exploration to scale negative membership functions where the input parameters do not support the presence of geothermal activity,
- 3) conversion of the probabilities into equivalent weights-of-evidence, and,
- 4) combination of the individual weights with the fairway probability to produce the favorability index.

Assignment of Incremental Probabilities

Incremental probabilities represent the perceived amount that the probability of an economic geothermal occurrence increases when the parameter in question is present at its maximum level. These probabilities were arrived at based on input from the explorationist members of the research team. As a specific example, the presence of fluid geothermometry indicative of reservoir temperatures in excess of 250°C is considered to increase the probability of occurrence of an economic geothermal system to 70% from a starting point of 40%. The incremental probabilities used for each of the input parameters for direct evidence range from 5 to 30% and are listed in Fig. 5-2.1.

Scaling Negative Membership with Degree-of-Exploration

Negative membership functions are assigned to some of the input parameters where the values are not encouraging for the presence of a geothermal system (e.g., where the highest spring temperature is less than 37°C (Fig. 5-2.1)). These negative values are considered more significant if exploration has been sufficiently thorough to have found the highest values (e.g., the highest temperature springs). For this reason, negative membership functions were scaled by the degree-of-exploration (that is, multiplied by the degree-of-exploration), such that areas with a

high degree of exploration incorporate a stronger negative weight for lack of encouraging data, whereas areas with little exploration have minimal negative weights assigned. Subsurface degree-of-exploration factors were scaled to subsurface well data (e.g., temperatures and geothermometry) and surface degree-of-exploration factors were applied to surface-related data (fumaroles, springs, geothermometry, sinter).

Conversion of Incremental Probabilities into Equivalent Weights-of-Evidence

The incremental probabilities were scaled into equivalent weights-of-evidence using the standard Bayesian statistics-based logit (natural log of odds ratio) equation (Bonham-Carter, 1996). The equivalent weight equals the weight necessary to move a pre-existing probability from a base of 40% to a higher level percentage level, where the change in percentage is listed Fig. 5-2.1 and ranges from 5 to 30%. For example, the weight necessary to move a pre-existing probability from 40% to 50% (an increase of 10 percentage points) is 0.405. The equivalent weights are shown in red font in Fig. 5-2.1. The actual weight assigned for a given parameter at a given volcanic center is also scaled by the membership function. For example, if the maximum spring temperature is 70°C, the membership function is 0.5 and the scaled weight is one-half of 0.405, or 0.2025.

Generation of the Favorability Index

After conversion to weights of evidence, a standard weights-of-evidence probability equation can be used to calculate the output, or posterior probability. For this purpose, the fairway model is considered as equivalent to prior probability and converted to a prior logit. The prior logit can then be added to the sum of the direct evidence weights, and the resulting sum converted back to probability space as the “posterior probability”. Favorability indices for the Cascade and Aleutian arcs are listed in Table 6.2-1.

Errors

Two types of errors were considered in the estimation of direct evidence. The first type is measurement and/or observational error associated with the input parameters of temperature, geothermometers, and presence of fumaroles and sinter. The error type is related to the completeness or representativeness of the data for each volcanic center and is a function of degree-of-exploration.

Measurement/observational Errors

Measurement/observational errors were estimated for the six parameters of spring temperatures, spring and well geothermometry, well temperatures, and occurrence of fumaroles and sinter. In the case of temperature measurements, direct measurement error is normally small. However, questions can arise in regards to whether a measured temperature has fully equilibrated in the case of wells, or whether a spring temperature was measured properly in the vent area, or whether a spring temperature represents the maximum temperature from a group of springs over time. Silica sinter deposits are not always identified correctly (sometimes

confused with travertine), and fumaroles are transient. A nominal 10% error was assigned to these measurement types to cover these variable circumstances.

Geothermometer temperature measurements can have more significant errors related to the quality of the geochemical sampling, the type of geothermometer used, and the hydrologic history of the sampled waters. The team geochemist, Dr. Shevenell, estimated geothermometer prediction error for wells and springs based on the reliability of the geochemical data and the reliability of geothermometer used.

The geochemical data were also evaluated and categorized for use in the predictive fairway model. In order to weight the various geothermometer calculations, a confidence factor was assigned to each analysis based on measured temperature, maturity indices, charge balance, and the difference between the Na-K-Ca and Quartz geothermometers (Table 6.4-1). These confidence factors provide one measure of uncertainty incorporated into the numerical model.

Table 6.4-1. Confidence values assigned to geothermometer estimates based on data quality.

Available Analysis	Confidence	MI	Sub-criteria
Good Balance (<10%)	0.95	MI≥2	Na-K-Ca ≈ Qtz
Good Balance (<10%)	0.9	MI≥2	OR available gas for spring
Good Balance (<10%)	0.8	MI<2	if using Na-K-Ca only
Fair Balance (<20%)	0.75		
Poor Balance (>20%)	0.5		
Low pH (<3)	0.1		
Low pH (3-5.5)	0.3		
No Available Analysis; Reference			
Specifies geothermometer	0.75		
Does not Specify geothermometer	0.25		

Errors on geochemical analyses and geothermometer estimates were expert-based and data-driven. Error assignment for calculated geothermometers were based in consideration of the level of agreement between the Na-K-Ca and Quartz geothermometers for each analysis. No geothermometer was assumed to be in error by >25% or <5%, and errors were estimated in increments of 5%.

The relative errors for each measurement and/or observation parameter were scaled to their respective weights, converted to variance and summed in order to estimate total measurement/observational error.

Degree-of-exploration-related Error

Degree-of-exploration errors were also considered in the analysis of direct evidence, and this type of error is much more significant in most cases than measurement error. For example, a temperature of a thermal spring may be measured accurately, but if only 10% of a volcanic

complex has been explored, then the spring temperature may not be representative of the maximum spring temperature from the entire area. In this study, degree-of-exploration-related direct evidence error was assumed to vary inversely with degree-of-exploration, from a maximum of 100% error at 0% degree-of-exploration to a minimum of 10% error at 100% degree-of-exploration.

Propagation of Errors to Favorability Model

Error propagation for the favorability model was accomplished in the following steps;

- 1) degree-of-exploration-related error was converted to a weight-scale by multiplying the summed weights of direct evidence,
- 2) in “weight-space”, degree-of-exploration error was combined with direct measurement errors by taking the square root of the sum of variances,
- 3) the revised total error in “weight-space” was then extracted from weight-space by dividing by the summed weights of direct evidence, and,
- 4) to estimate relative favorability error, the total relative direct evidence error was combined with the fairway relative error by summing variances weighted by the relative magnitudes of the fairway prediction and the direct evidence, both measured in probability space.

The resulting error estimates are included in Table 6.2-1.

The favorability error estimates are high, averaging 64%. This is largely driven by the high uncertainties of direct evidence related to degree-of-exploration. This suggests, logically enough, that direct evidence is most significant where it is strongly positive, near the upper end of the probability scale, unless a given volcanic center has been well explored.

7.0 RESULTS

7.1 PLAY FAIRWAYS

One utility of this study is development of a foundation for a global set of subduction arc geothermal play types. Each of these has a pattern relative to the size of systems, abundance of systems, strain style and rate, and types of local structural controls.

Benchmarks

EXTENSION, broad area, slow to moderate strain rate

- Mexico (TMVB)

EXTENSIONAL, narrow “rifts”, high strain rate

- New Zealand (TVZ), Southwest Japan (Kyushu)

TRANSTENSION STRIKE-SLIP, moderate to high strain rate

- Philippines, Sumatra, West Java

STRIKE-SLIP, low strain rate

- Northern and Central Chile, Northern El Salvador, Guatemala, East Java

STRIKE-SLIP, moderate to high strain rate, with slab roll-back

- Northern Costa-Rica, Nicaragua, Southern El Salvador

COMPRESSION, low to moderate strain rates

- Northeast Japan (Honshu)

TRANSPRESSION/COMPRESSION, lowest strain rate or inactive

- No known producing VCs globally

From this list, analogues can be drawn for the Aleutians and Cascades that may help further refine resource potential and specific exploration strategies.

Analogues for the Aleutians and Cascades

NORTH CASCADES

- eastern Aleutians
- Kamchatka
- Other non-producing global analogs

SOUTH CASCADES

- TMVB

EASTERN ALEUTIANS

- Kamchatka
- North Cascades
- Southern Chile
- Northern Japan
- Other non-producing global analogs

CENTRAL ALEUTIANS

- Chile
- Northern Japan
- Other non-producing global analogs

WESTERN ALEUTIANS

- Other oceanic arcs with moderate to high angles of plate convergence

These different play types defined by tectonic setting are evaluated based on the number of MW currently being produced in each setting (Figure 7.1-1). The “extensional plays” capture 21% of the total MW, the “transtensional plays” capture 73% of the MW, the “compressional-transpressional plays” capture 4% of the MW, and unknown captures 2% of the MW. This categorization shows that 94% of the world MW production in arc settings is in play types in transtensional or transpressional settings, with some of the production areas being in areas of Sumatra and the Philippines where there are local areas of transpression.

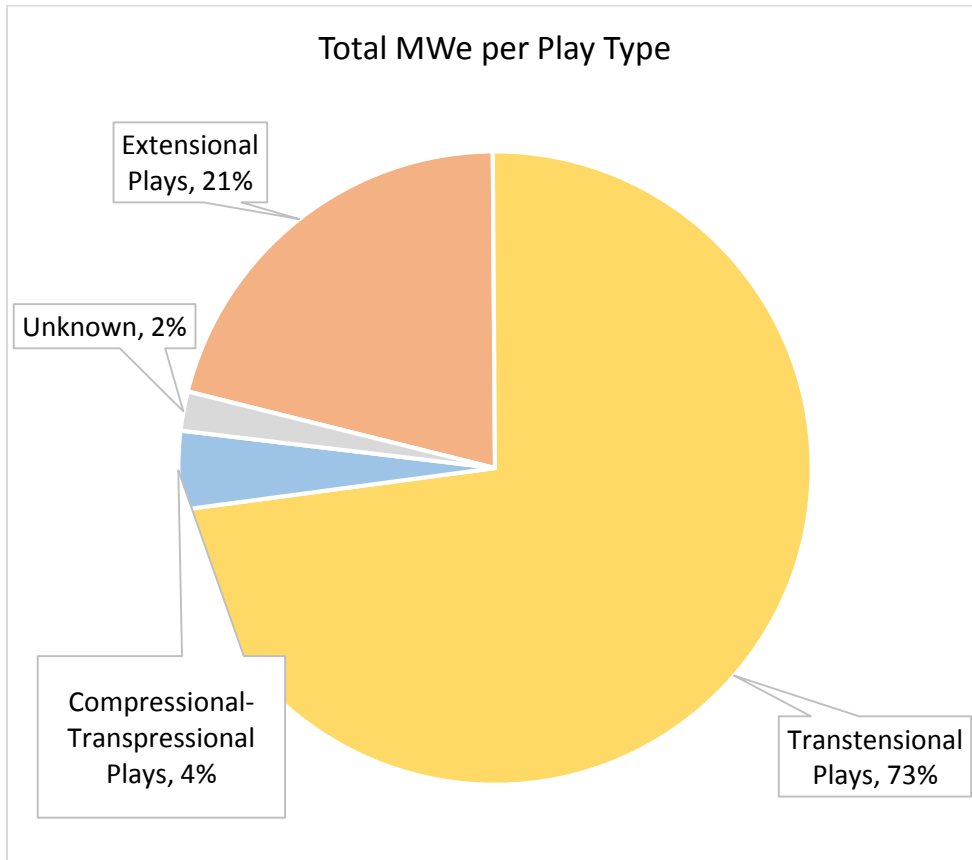


Figure 7.1-1. Pie chart illustrating the total MW current production in the benchmark VC dataset by play type.

7.2 PRELIMINARY MODEL

Preliminary predictive maps were completed in Q2 and Q3 and presented at the DOE peer review in May 2015, and reproduced below. These maps show that the initial model was suitable for predicting high geothermal potential areas both previously known and unknown. Known sites in Alaska at which considerable geothermal exploration has been conducted are predicted to have high potential: Makushin and Akutan. Four additional sites (Recheschnoi, unnamed volcano east of Recheschnoi, Korovin, and Great Sitkin (from east to west)) were predicted to have high geothermal potential using the preliminary model in the Aleutians (see Fairway and Favorability maps reproduced here from Q2).

Similarly, the fairway and favorability model results using the same model as for the Aleutians was successful in predicting the known higher geothermal potential areas in the Cascades: Lassen, Medicine Lake and Mt St Helens (see maps below), two of which are largely off limits based on land-use considerations (National Park/Monument). Additional sites were also predicted to have high, medium and low geothermal potential based on the fairway parameters used in the preliminary model.

In the team meetings, permeability was identified as the key predictive parameter for geothermal potential for which data were available and could be obtained. The other key factors for geothermal potential, which include 1) heat source, 2) cap rock, and 3) fluid composition, either had challenges associated with data collection, or they are considered to be commonly present in most volcanic centers. Experimentation with data parameters derived from Google Earth to characterize the presence of clay caps yielded mixed results (task 3). Similarly, correlations between characteristics of volcanism and geothermal potential proved difficult to establish (task 3). Permeability, as reflected by both structure and lithology, was accordingly assigned a focus for task 5 final data acquisition.

Lithologic influences on permeability are significant but difficult to quantify and the regional scale of this project. Accordingly, structure/tectonics became the focus for relevant data gathering.

7.3 FINAL MODEL

The modeled results are compared to the prior probability of a geothermal occurrence (in the absence of any supporting data) of 10%, which is the approximate percent of VC with power plants on world VC that constitute the training set. Table 7.3-1 and 7.3-2 list the probabilities of a productive geothermal system by VC using both the play fairway and favorability model results. The column labeled “Difference” subtracts the favorability from the fairway probability to indicate if the probabilities increased or decreased between the fairway and favorability models. A positive number indicates the probability assigned to the VC improved with the favorability model, whereas a negative number indicates the VC probability became worse in the favorability model that incorporated the direct evidence from springs, wells and fumaroles along with the degree of exploration factors. The column labeled “Rank” indicates if the favorability model results were better (higher probability) or worse (lower probability) than the play fairway model. The final column (> Prior Probability) indicates if the site has a probability greater than the prior probability (10.5% or greater) in either of the two models. This represents a minimal, lower level at which sites are indicated to have geothermal potential slightly in excess of the prior probability. Sites for which the modeled probability is <10.5% (at or below the prior probability) are eliminated from further consideration in the subsequent sections (Table 7.3-1). Sites further evaluated in subsequent sections as having some minimal probability of a productive geothermal system in excess of the prior probability are listed in Table 7.3-2. Both tables list VC in order of increasing probabilities based on the play fairway model results, combining both the Aleutian and Cascade VC such that a consistent comparison can be made among all VC in both volcanic arcs.

Table 7.3-1. Ranking of Cascade and Aleutian VC by order of increasing probability of a productive system based on the play fairway model. All VC noted in this table have predicted probabilities less than the prior probability of encountering a productive VC and are not considered prospective.

		Fairway	Favorability	Difference	Rank	> Prior Probability
Aniakchak	Aleutians	0.055	0.083	0.028	Better	N
Yantarni	Aleutians	0.058	0.044	-0.015	Worse	N
Kialagvik	Aleutians	0.060	0.057	-0.003	No Change	N
Fisher	Aleutians	0.060	0.058	-0.003	No Change	N
Goat Rocks	Cascades	0.074	0.054	-0.020	Worse	N
Lakeview Mountain	Cascades	0.080	0.050	-0.030	Worse	N
Adams	Cascades	0.081	0.056	-0.026	Worse	N
Indian Heaven	Cascades	0.082	0.059	-0.022	Worse	N
Marble Mountain	Cascades	0.082	0.060	-0.022	Worse	N
West Crater	Cascades	0.082	0.061	-0.022	Worse	N
Amukta	Aleutians	0.083	0.079	-0.004	No Change	N
Kupreanof	Aleutians	0.084	0.100	0.016	Better	N
Black Peak	Aleutians	0.085	0.082	-0.004	No Change	N
Stepovak Bay 4	Aleutians	0.086	0.085	-0.001	No Change	N
Griggs	Aleutians	0.089	0.088	-0.001	No Change	N
Silverthrone	Cascades	0.089	0.088	-0.001	No Change	N
Shishaldin	Aleutians	0.090	0.087	-0.003	No Change	N
Garibaldi	Cascades	0.091	0.087	-0.004	No Change	N
Veniaminof	Aleutians	0.093	0.090	-0.002	No Change	N
Kukak	Aleutians	0.094	0.094	-0.001	No Change	N
Snowy Mountain	Aleutians	0.095	0.094	-0.001	No Change	N
Fourpeaked	Aleutians	0.095	0.094	-0.001	No Change	N
Augustine	Aleutians	0.097	0.093	-0.004	No Change	N
Iliamna	Aleutians	0.099	0.098	-0.001	No Change	N
Westdahl	Aleutians	0.099	0.095	-0.004	No Change	N
Pavlof	Aleutians	0.100	0.097	-0.003	No Change	N
Redoubt	Aleutians	0.102	0.101	-0.001	No Change	N
Carlisle	Aleutians	0.104	0.100	-0.004	No Change	N
Dana	Aleutians	0.104	0.100	-0.004	No Change	N

Table 7.3-2. Ranking of Cascade and Aleutian VC by order of increasing probability of a productive system based on the play fairway model. All VC noted in this table have predicted probabilities greater than the prior probability of encountering a productive VC and are considered prospective.

		Fairway	Favorability	Difference	Rank	> Prior Probability
Ugashik-Peulik	Aleutians	0.064	0.106	0.042	Better	Y
Dutton	Aleutians	0.064	0.119	0.055	Better	Y
Kagamil	Aleutians	0.074	0.105	0.031	Better	Y
Great Sitkin	Aleutians	0.080	0.227	0.146	Better	Y
Unnamed	Aleutians	0.086	0.216	0.130	Better	Y
Semisopchnoi	Aleutians	0.089	0.181	0.092	Better	Y
Mageik	Aleutians	0.094	0.188	0.094	Better	Y
Katmai	Aleutians	0.094	0.134	0.040	Better	Y
Douglas	Aleutians	0.095	0.146	0.052	Better	Y
Emmons Lake	Aleutians	0.099	0.215	0.117	Better	Y
Gilbert	Aleutians	0.101	0.166	0.064	Better	Y
Hayes	Aleutians	0.105	0.104	-0.001	No Change	Y
Chiginagak	Aleutians	0.107	0.221	0.114	Better	Y
Roundtop	Aleutians	0.108	0.105	-0.003	No Change	Y
Isanotski	Aleutians	0.108	0.104	-0.003	No Change	Y
Frosty	Aleutians	0.109	0.126	0.016	Better	Y
Kaguyak	Aleutians	0.111	0.154	0.044	Better	Y
Segula	Aleutians	0.121	0.103	-0.018	Worse	Y
Kiska	Aleutians	0.121	0.103	-0.018	Worse	Y
Cleveland	Aleutians	0.122	0.117	-0.005	No Change	Y
Tana	Aleutians	0.122	0.168	0.046	Better	Y
Herbert	Aleutians	0.122	0.117	-0.005	No Change	Y
Akutan	Aleutians	0.124	0.508	0.384	Better	Y
Table Top	Aleutians	0.124	0.140	0.016	Better	Y
Spurr	Aleutians	0.126	0.201	0.075	Better	Y
Yunaska	Aleutians	0.126	0.121	-0.006	Worse	Y
Kanaga	Aleutians	0.128	0.109	-0.019	Worse	Y
Moffett	Aleutians	0.128	0.109	-0.019	Worse	Y
Tanaga	Aleutians	0.129	0.110	-0.019	Worse	Y
Makushin	Aleutians	0.130	0.497	0.367	Better	Y
Gareloi	Aleutians	0.131	0.109	-0.022	Worse	Y
Okmok	Aleutians	0.131	0.191	0.060	Better	Y
Recheschnoi	Aleutians	0.132	0.419	0.288	Better	Y
Vsididov	Aleutians	0.132	0.126	-0.006	Worse	Y
Seguam	Aleutians	0.136	0.099	-0.037	Worse	Y
Adagdak	Aleutians	0.139	0.262	0.123	Better	Y
Korovin	Aleutians	0.142	0.331	0.189	Better	Y
Little Sitkin	Aleutians	0.147	0.400	0.254	Better	Y
Meager	Cascades	0.092	0.338	0.247	Better	Y
Cayley	Cascades	0.084	0.121	0.037	Better	Y
Baker	Cascades	0.063	0.124	0.062	Better	Y
Glacier Peak	Cascades	0.065	0.146	0.081	Better	Y
Rainier	Cascades	0.073	0.114	0.041	Better	Y
St. Helens	Cascades	0.082	0.177	0.095	Better	Y
Hood	Cascades	0.135	0.156	0.021	Better	Y
Jefferson	Cascades	0.136	0.095	-0.041	Worse	Y
Belknap	Cascades	0.136	0.184	0.047	Better	Y
South Sister	Cascades	0.142	0.099	-0.043	Worse	Y
Bachelor	Cascades	0.137	0.094	-0.043	Worse	Y
Newberry	Cascades	0.130	0.392	0.262	Better	Y
Davis Lake	Cascades	0.142	0.107	-0.035	Worse	Y
Crater Lake	Cascades	0.142	0.086	-0.055	Worse	Y
McLoughlin	Cascades	0.141	0.106	-0.035	Worse	Y
Medicine Lake	Cascades	0.136	0.163	0.027	Better	Y
Shasta	Cascades	0.123	0.286	0.163	Better	Y
Burney Mtn	Cascades	0.149	0.112	-0.037	Worse	Y
Harvey Mtn	Cascades	0.148	0.102	-0.046	Worse	Y
Magee Peak	Cascades	0.149	0.103	-0.047	Worse	Y
Crater Mtn	Cascades	0.137	0.094	-0.043	Worse	Y
Antelope Mtn	Cascades	0.149	0.102	-0.047	Worse	Y
Prospect Peak	Cascades	0.176	0.122	-0.054	Worse	Y
Red Cinder Chain	Cascades	0.176	0.122	-0.054	Worse	Y
Lassen	Cascades	0.138	0.545	0.407	Better	Y
Olallie Butte	Cascades	0.136	0.286	0.150	Better	Y
Three-fingered Jack	Cascades	0.136	0.094	-0.042	Worse	Y
Maiden Peak	Cascades	0.137	0.103	-0.034	Worse	Y
Diamond Peak	Cascades	0.138	0.095	-0.043	Worse	Y
Mt. Theilson	Cascades	0.136	0.102	-0.034	Worse	Y
Mt. Bailey	Cascades	0.153	0.201	0.048	Better	Y
Yamsay Mountain	Cascades	0.141	0.107	-0.034	Worse	Y
Sugarloaf	Cascades	0.176	0.122	-0.054	Worse	Y

Table 7.3-2. Ranking of Cascade and Aleutian VC by order of increasing probability of a productive system based on the play fairway model. All VC noted in this table have predicted probabilities greater than the prior probability of encountering a productive VC.

As can be seen from Table 7.3-2, modeling results show 38 VCs (60%) in the Aleutians and 33 VCs (89%) in the Cascades have probabilities of a geothermal occurrence capable of power production that is greater than the prior probability. This indicates that at least some factors such as structural setting, geothermometer temperatures, or fumarole occurrences are suggestive of productive geothermal systems at most of the VC in both the Cascades and Aleutians.

7.4 RANKING OF CASCADE VOLCANIC CENTERS

The data from Table 7.3-1 and 7.3-2 are reorganized to include only the data from the Cascade VCs with fairway or favorability probabilities in excess of the prior probability, and these VC are listed in Table 7.4-1. Six of the 33 Cascade VC that had either a fairway or favorability probability greater than the prior probability have a fairway probability of <10.5%. This shows that the direct evidence along with degree of exploration data helped improve the modeled probabilities based on known geothermal occurrences at many sites. Also, when comparing Fairway to Favorability model results, six sites show the lowest probabilities (Lowest in Table 7.4-1) based on play fairways alone, but are re-categorized with considerably higher probabilities in the favorability model that includes direct observations. However, most (21 VC, 64%) of the Cascade VC rank lower in the favorability than with the fairway model alone.

Table 7.4-1. Play Fairway and Favorability modeled probabilities of occurrence of a power-productive geothermal system. VC are ranked in decreasing probabilities based on the favorability model.

VC	Fairway	Rank	Favorability	Rank	Difference
Lassen	0.138	Low	0.545	Highest	0.407
Newberry	0.130	Low	0.392	High	0.262
Meager	0.092	Lowest	0.338	High	0.247
Olallie Butte	0.136	Low	0.286	Medium	0.150
Shasta	0.123	Low	0.286	Medium	0.163
Mt. Bailey	0.153	Low	0.201	Medium	0.048
Belknap	0.136	Low	0.184	Low	0.047
St. Helens	0.082	Lowest	0.177	Low	0.095
Medicine Lake	0.136	Low	0.163	Low	0.027
Hood	0.135	Low	0.156	Low	0.021
Glacier Peak	0.065	Lowest	0.146	Low	0.081
Baker	0.063	Lowest	0.124	Low	0.062
Sugarloaf	0.176	Low	0.122	Low	-0.054
Prospect Peak	0.176	Low	0.122	Low	-0.054
Red Cinder Chain	0.176	Low	0.122	Low	-0.054
Cayley	0.084	Lowest	0.121	Low	0.037
Rainier	0.073	Lowest	0.114	Low	0.041
Burney Mtn	0.149	Low	0.112	Low	-0.037
Yamsay Mountain	0.141	Low	0.107	Low	-0.034
Davis Lake	0.142	Low	0.107	Low	-0.035
McLoughlin	0.141	Low	0.106	Low	-0.035
Maiden Peak	0.137	Low	0.103	Low	-0.034
Magee Peak	0.149	Low	0.103	Low	-0.047
Mt. Theilson	0.136	Low	0.102	Low	-0.034
Antelope Mtn	0.149	Low	0.102	Low	-0.047
Harvey Mtn	0.148	Low	0.102	Low	-0.046
South Sister	0.142	Low	0.099	Lowest	-0.043
Jefferson	0.136	Low	0.095	Lowest	-0.041
Diamond Peak	0.138	Low	0.095	Lowest	-0.043
Bachelor	0.137	Low	0.094	Lowest	-0.043
Three-fingered Jack	0.136	Low	0.094	Lowest	-0.042
Crater Mtn	0.137	Low	0.094	Lowest	-0.043
Crater Lake	0.142	Low	0.086	Lowest	-0.055

Figure 7.4-1 shows the distribution of these rankings for the. The categories of high to low used in grouping VC in the tables by probabilities are:

Ranking	Probability	Color
Lowest	0-0.1	Blue
Low	>0.1-0.2	Green
Medium	>0.2-0.3	Yellow
High	>0.3-0.4	Orange
Highest	>0.4	Red

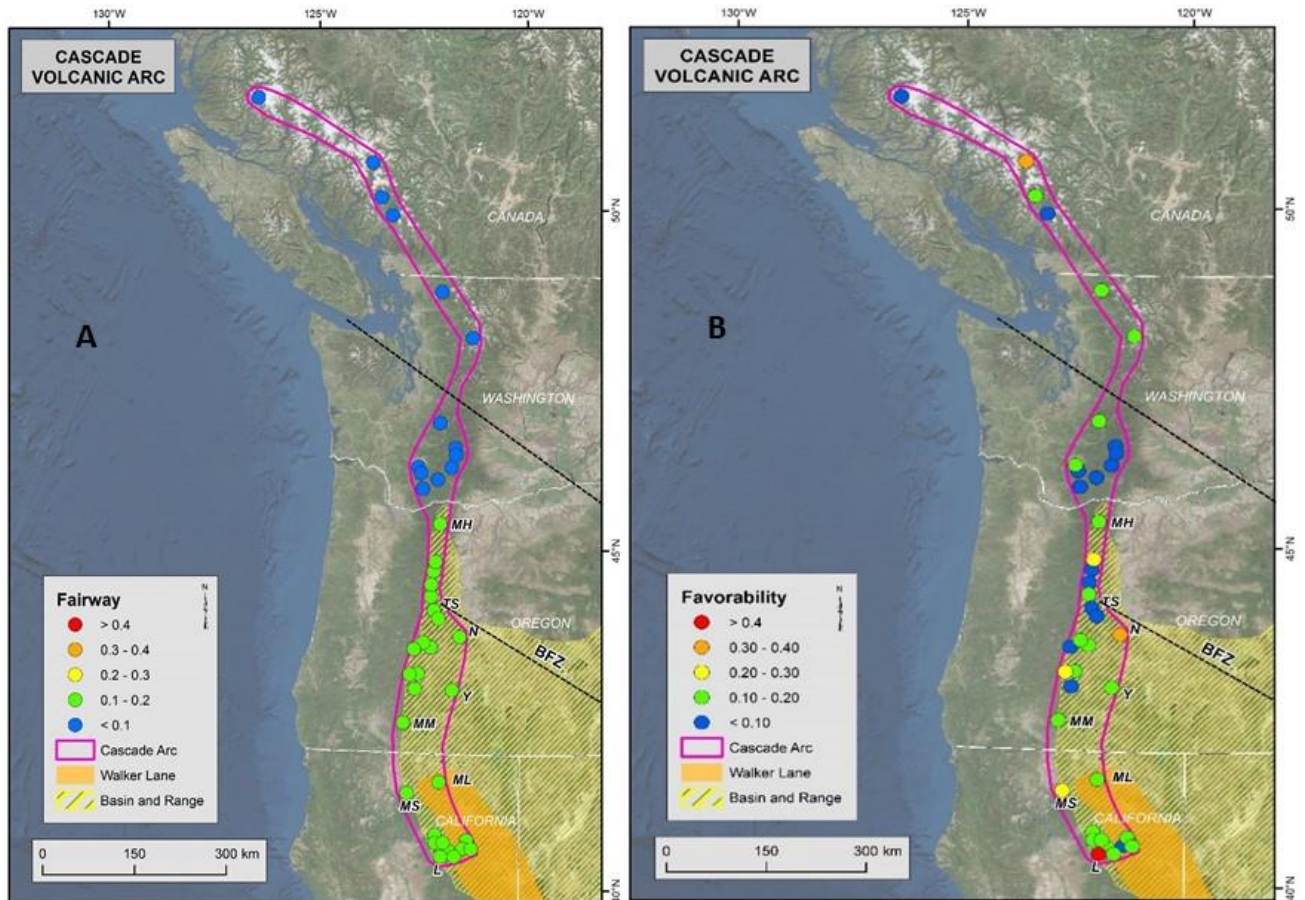


Figure 7.4-1. Distribution of Fairway (A) and Favorability (B) model results in the Cascades, with modeled probability ranges noted in the legend using the same scale for both maps.. L, Lassen; MH, Mount Hood; ML, Medicine Lake; MM, Mount McLaughlin; MS, Mount Shasta; N, Newberry; TS, Three Sisters, OWL, Olympic Wallowa Lineament; Y, Yamsay.

Mt Bailey, Olallie Butte, Newberry, Oregon, Shasta and Lassen, California, and Meager, Canada show the greatest probability of hosting a productive geothermal system (Medium to Highest ranking in favorability model of >20%), whereas the fairway model suggests lower probabilities of <15.3% for these systems. This indicates that fairway models alone cannot predict all VC with a high probability of a productive geothermal system, and direct evidence from field data

collection and evaluation is needed to target the highest potential systems. Whether considering the play fairway or favorability model results, Lassen and Newberry show the highest geothermal potential of any of the Cascade VC and are most likely to be productive based on the play fairway model along with available direct evidence.

Many (19) of the Cascade VC show a lower probability of a productive geothermal system when direct evidence and degree of exploration are considered in the favorability model. These results point to the need to conduct greater exploration at these sites in which the play fairway suggests the probability of a productive geothermal occurrence is greater than the prior probability. These VC are listed in Table 7.4-2 and may host hidden geothermal systems.

Table 7.4-2. Highly ranked VC based on play fairway modeling, but ranked less favorably with the favorability model suggesting a relatively high probability of the occurrence of a productive geothermal system, but that additional field data are required from these sites.

California	Oregon	Washington
Antelope Mtn	Bachelor	None
Burney Mtn	Crater Lake	
Crater Mtn	Davis Lake	
Harvey Mtn	Diamond Peak	
Magee Peak	Jefferson	
Prospect Peak	Maiden Peak	
Red Cinder Chain	McLoughlin	
Sugarloaf	Mt. Theilson	
	South Sister	
	Three-fingered Jack	
	Yamsay Mountain	

Note that none of the rankings in the preceding tables take land ownership/use into consideration and these rankings are based solely on scientifically based model results. The final ranking of sites available for geothermal development appears in Section 7.6.

7.5 RANKING OF ALEUTIAN VOLCANIC CENTERS

The data from Table 7.3-2 are reorganized to include only the data from the Aleutian VCs with fairway or favorability probabilities in excess of the prior probability, and appear in Table 7.5-1, and locations illustrated in Figure 7-5.1. Eleven of the 38 Aleutian VC that had either a fairway or favorability probability greater than the prior probability show have a fairway probability of <10.5%. As with the Cascade VC, this shows that the direct evidence along with degree of exploration data helped improve the modeled probabilities based on known geothermal occurrences. This indicates that fairway models alone are not likely to predict all VC with a high probability of a productive geothermal system, and direct evidence from field data collection and

evaluation is needed to target the highest potential systems. Thus, the favorability model results are used to highlight these systems with at least some direct evidence of geothermal potential.

Table 7.5-1. Play Fairway and Favorability modeled probabilities of occurrence of a power-productive geothermal system. VC are ranked in decreasing probabilities based on the favorability model.

Volcanic Center	Fairway	Rank	Favorability	Rank	Difference
Akutan	0.124	Low	0.508	Highest	0.384
Makushin	0.130	Low	0.497	Highest	0.367
Recheschnoi	0.132	Low	0.419	Highest	0.288
Little Sitkin	0.147	Low	0.400	High	0.254
Korovin	0.142	Low	0.331	High	0.189
Adagdak	0.139	Low	0.262	Medium	0.123
Great Sitkin	0.080	Lowest	0.227	Medium	0.146
Chiginagak	0.107	Low	0.221	Medium	0.114
Unnamed	0.086	Lowest	0.216	Medium	0.130
Emmons Lake	0.099	Lowest	0.215	Medium	0.117
Spurr	0.126	Low	0.201	Medium	0.075
Okmok	0.131	Low	0.191	Low	0.060
Mageik	0.094	Lowest	0.188	Low	0.094
Semisopchnoi	0.089	Lowest	0.181	Low	0.092
Tana	0.122	Low	0.168	Low	0.046
Gilbert	0.101	Low	0.166	Low	0.064
Kaguyak	0.111	Low	0.154	Low	0.044
Douglas	0.095	Lowest	0.146	Low	0.052
Table Top	0.124	Low	0.140	Low	0.016
Katmai	0.094	Lowest	0.134	Low	0.040
Vsididov	0.132	Low	0.126	Low	-0.006
Frosty	0.109	Low	0.126	Low	0.016
Yunaska	0.126	Low	0.121	Low	-0.006
Dutton	0.064	Lowest	0.119	Low	0.055
Herbert	0.122	Low	0.117	Low	-0.005
Cleveland	0.122	Low	0.117	Low	-0.005
Tanaga	0.129	Low	0.110	Low	-0.019
Moffett	0.128	Low	0.109	Low	-0.019
Kanaga	0.128	Low	0.109	Low	-0.019
Gareloi	0.131	Low	0.109	Low	-0.022
Ugashik-Peulik	0.064	Lowest	0.106	Low	0.042
Roundtop	0.108	Low	0.105	Low	-0.003
Kagamil	0.074	Lowest	0.105	Low	0.031
Hayes	0.105	Low	0.104	Low	-0.001
Isanotski	0.108	Low	0.104	Low	-0.003
Kiska	0.121	Low	0.103	Low	-0.018
Segula	0.121	Low	0.103	Low	-0.018
Seguam	0.136	Low	0.099	Lowest	-0.037

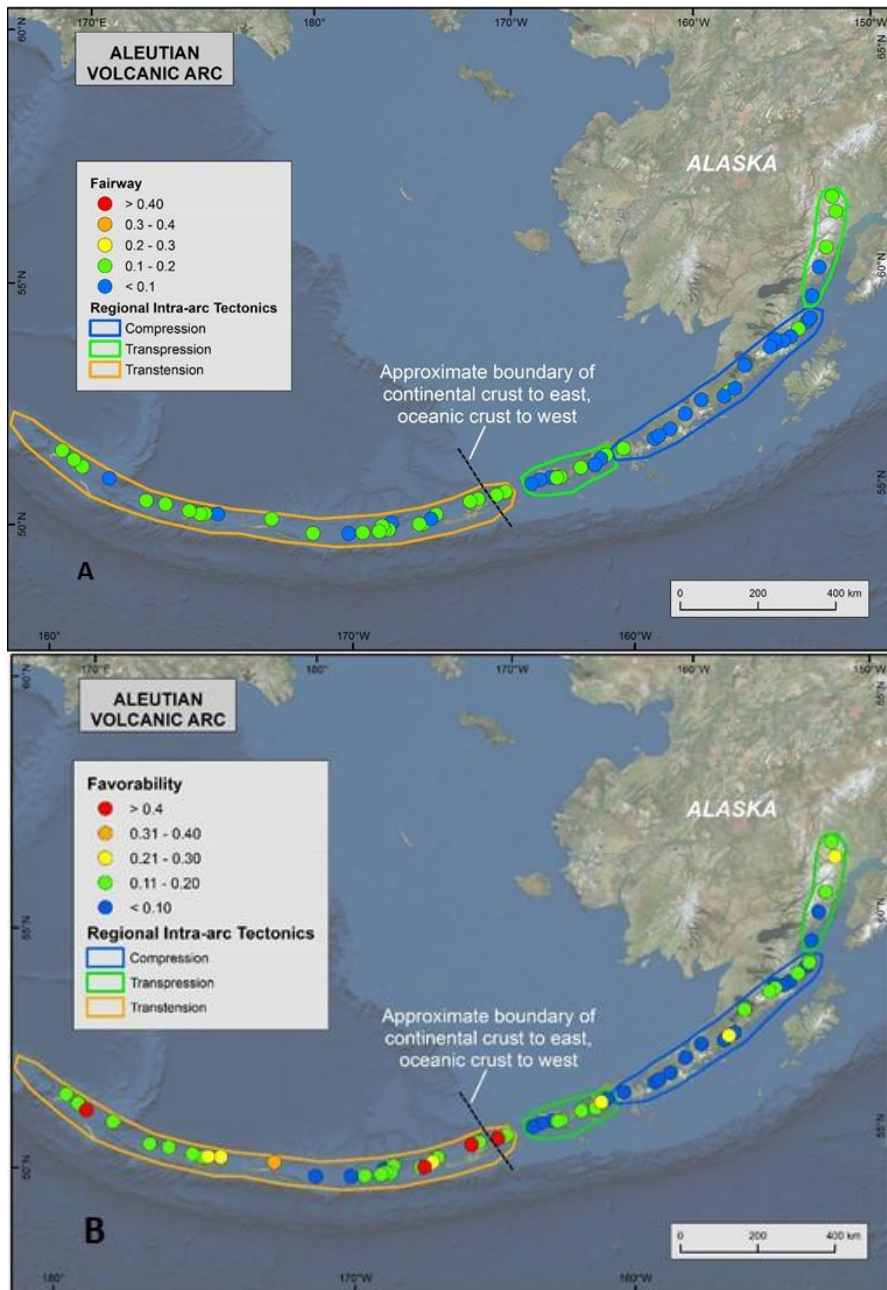


Figure 7.5-1. Distribution of Fairway (A) and Favorability (B) model results in the Aleutians, with modeled probability ranges noted in the legend using the same scale for both maps.

Korovin, Little Sitkin, Rechesnoi, Makushin and Akutan show the greatest probability of hosting a productive geothermal system (High ranking in favorability model of >30%), whereas the fairway model suggests lower probabilities of $\leq 14.7\%$ for these systems. This indicates that fairway models alone cannot predict all VC with a high probability of a productive geothermal

system, and direct evidence from field data collection and evaluation is needed to target the highest potential systems. Makushin, Akutan, Little Sitkin, and Recheschnoi show the highest geothermal potential ($\geq 40\%$ probability with favorability model) of any of the Aleutian VC and are most likely to be productive based on the play fairway model along with available direct evidence. Notably, these VC rank higher than any of the Cascade VC except for Lassen, which has a probability of $>50\%$

Many (14) of the Aleutian VC show a lower probability of a productive geothermal system when direct evidence and degree of exploration are considered in the favorability model. These results point to the need to conduct greater exploration at these sites in which the play fairway suggests the probability of a productive geothermal occurrence is greater than the prior probability. These VC are listed in Table 7.5-2 and may host hidden geothermal systems.

Table 7.5-2. Highly ranked VC based on play fairway modeling, but ranked less favorably with the favorability model suggesting a relatively high probability of the occurrence of a productive geothermal system, but that additional field data are required from these sites.

Volcanic Center	Volcanic Center
Cleveland	Moffett
Gareloi	Roundtop
Hayes	Seguam
Herbert	Segula
Isanotski	Tanaga
Kanaga	Vsididov
Kiska	Yunaska

Note that none of the rankings in the preceding tables take land ownership/use into consideration and these rankings are based solely on scientifically based model results. The final ranking of sites available for geothermal development appears in Section 7.6.

7.6 LAND STATUS CONSIDERATIONS

Land use (digital data from the BLM) was superimposed on the model results to determine which of the highly ranked systems in the Cascades and Aleutians are within land designations allowing development. Figures 7.6-1 and 7.6-2 show the location of selected VC in the Cascades relative to land classification for California and Oregon, and Table 7.6-1 and 7.6-2 lists each Cascade and Aleutian VC, respectively, along with the predominant land category occupied by the VC. None of the VC in Washington rank highly, and no separate figure is included for this state.

For the Cascades, 51% of the VC are off-limits to development based on their dominant land status in wilderness or national parks. The most notable VC that is off-limits to development is Lassen, which is the highest ranked site of all of the Aleutian and Cascade VCs. Of those on which development is not prohibited, the following have the highest potential for geothermal power generation based on the Play Fairway model: Sugarloaf, Prospect Peak, Burney Mt, Antelope Mt,

Harvey Mt, Crater Mt (all in close proximity to Lassen; Figure 7.6-1), and Mt Bailey, Davis Lake, and Maiden Peak (southern Oregon; Figure 7.6-2).

Table 7.6-1. Dominant land status of Cascade VC along with their fairway and favorability probabilities. The top 6 ranked sites based on the play fairway model that are wholly or partially available based on land status consideration are highlighted in red text.

VC	State	Land Status	Fairway	Favorability
Sugarloaf	N. California	National Forest	0.176	0.122
Prospect Peak	N. California	National Forest/ National Park (50%)	0.176	0.122
Red Cinder Chain	N. California	Wilderness/Park Service	0.176	0.122
Mt Bailey	Oregon	National Forest	0.153	0.201
Magee Peak	N. California	Wilderness (25%)	0.149	0.103
Burney Mt	N. California	National Forest	0.149	0.112
Antelpe Mtn	N. California	National Forest	0.149	0.102
Harvey Mt	N. California	National Forest	0.148	0.102
South Sister	Oregon	Wilderness	0.142	0.099
Davis Lake	Oregon	National Forest	0.142	0.107
Crater Lake	Oregon	National Park	0.142	0.086
McLoughlin	Oregon	Wilderness	0.141	0.106
Yamsay Mtn	Oregon	National Forest	0.141	0.107
Lassen	N. California	National Park	0.138	0.545
Diamond Peak	Oregon	Wilderness	0.138	0.095
Maiden Peak	Oregon	National Forest	0.137	0.103
Bachelor	Oregon	National Forest	0.137	0.094
Crater Mtn	N. California	National Forest	0.137	0.094
Mt Theilson	Oregon	Wilderness	0.136	0.102
Belknap	Oregon	Wilderness	0.136	0.184
Three Fingered Jack	Oregon	Wilderness	0.136	0.094
Jefferson	Oregon	Wilderness and Indian	0.136	0.095
Olalie Butte	Oregon	Reservation & National Forest	0.136	0.286
Medicine Lake	N. California	National Forest	0.136	0.163
Hood	Oregon	Wilderness	0.135	0.156
Newberry	Oregon	National Forest	0.130	0.392
Shasta	N. California	Wilderness	0.123	0.286
West Crater	Washington	National Forest	0.082	0.061
Mt St Helens	Washington	National Forest/Monument	0.082	0.177
Marble Mt	Washington	Not Federal	0.082	0.060
Indian Heaven	Washington	Wilderness	0.082	0.059
Adams	Washington	Wilderness/Reservation	0.081	0.056
Lakeview Mtn	Washington	Wilderness/Reservation	0.080	0.050
Goat Rocks	Washington	Reservation/Wilderness	0.074	0.054
Rainier	Washington	National Park	0.073	0.114
Glacier Peak	Washington	Wilderness	0.065	0.146
Baker	Washington	Wilderness	0.063	0.124

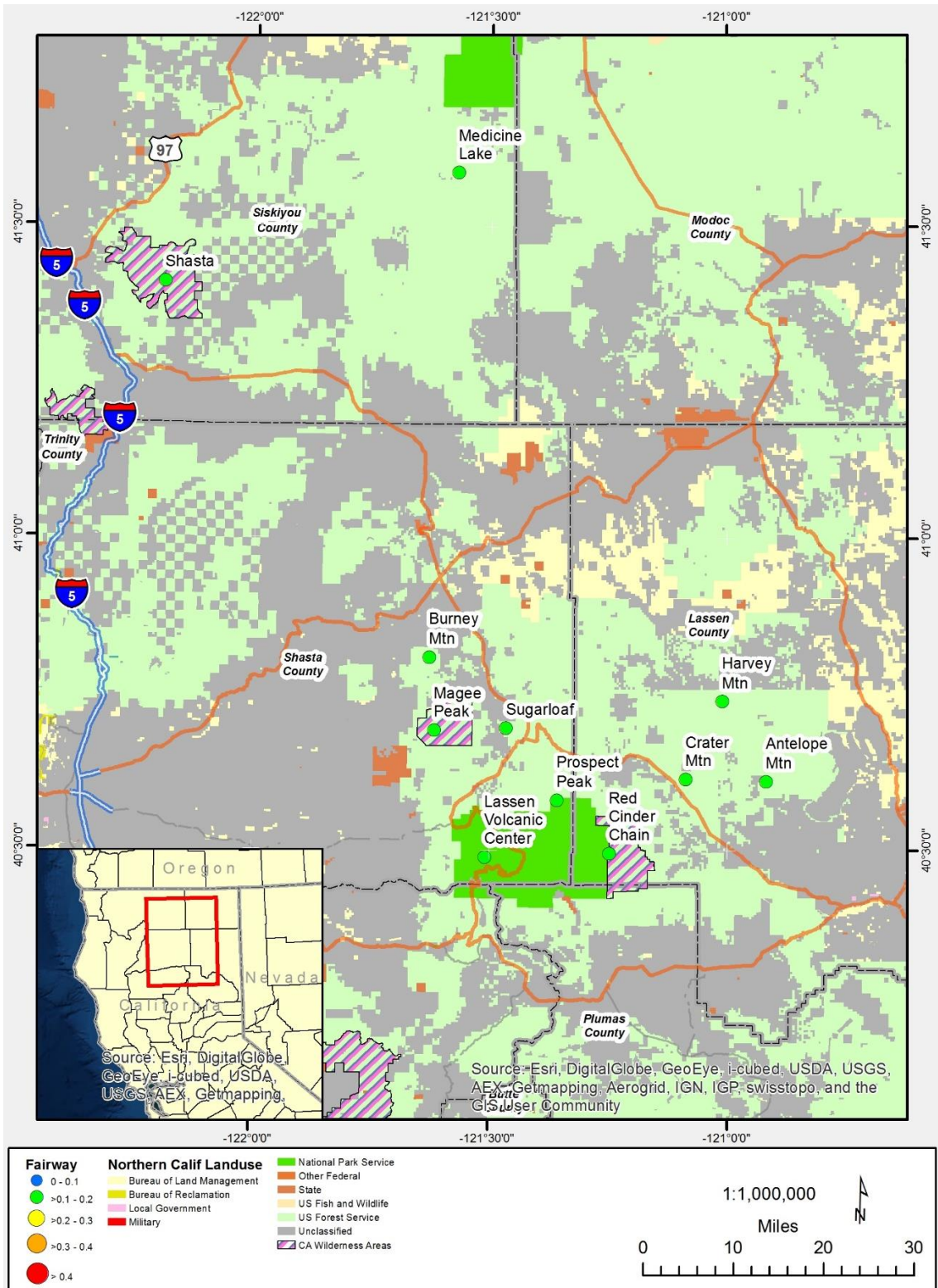


Figure 7.6-1. Location of most prospective sites with highest Play Fairway probability model results for VC surrounding the Lassen VC showing land status.

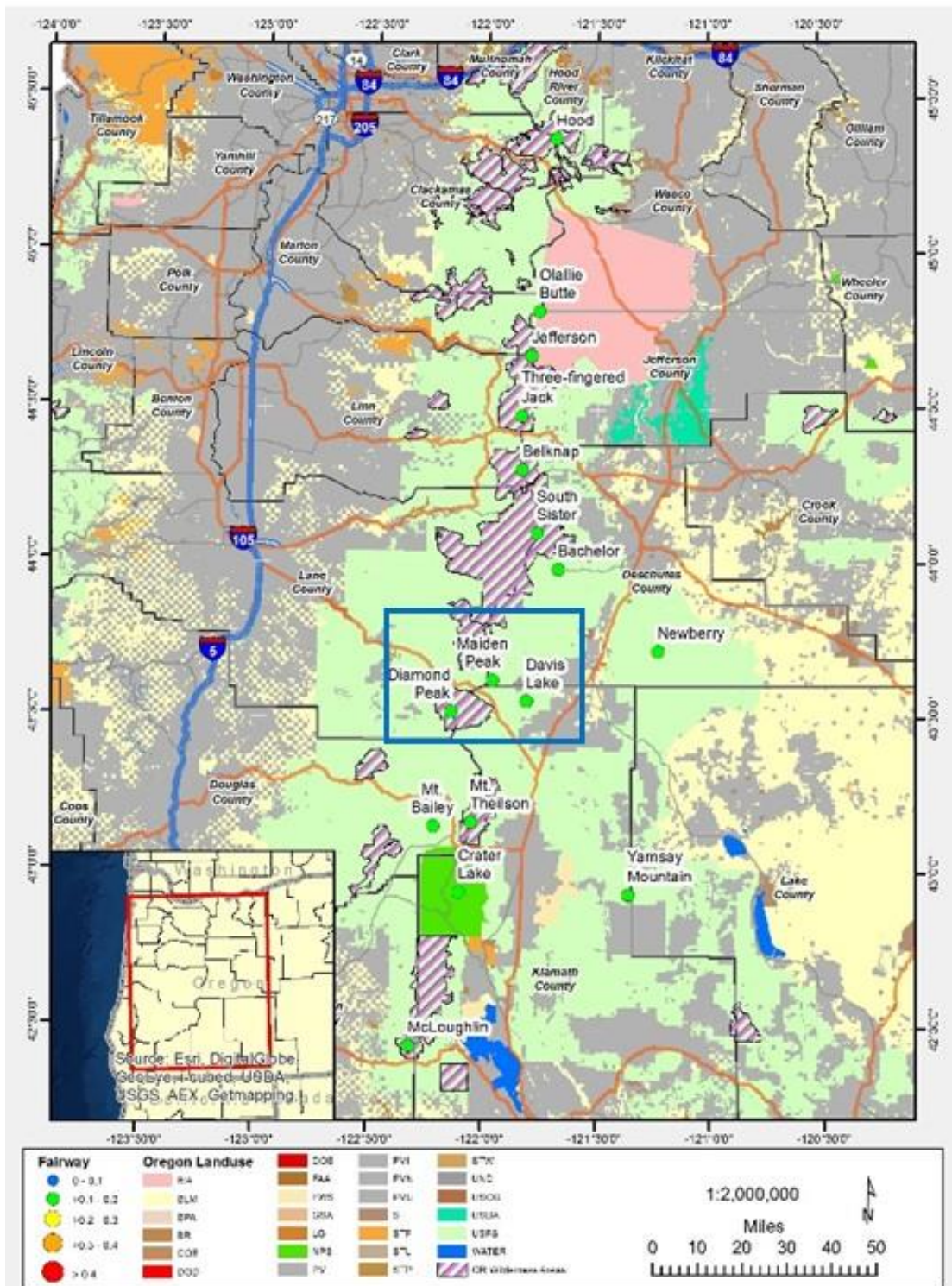


Figure 7.6-2. Location of most prospective sites with highest Play Fairway probability model results (blue box in center of Figure) for VC in Oregon showing land classification.

Table 7.6-2 lists the land status of the Aleutian VC, showing a majority are on Fish and Wildlife lands. Most (71%) of Aleutian VC are not explicitly excluded from geothermal development based on a land status of Fish and Wildlife Service, although there may be local considerations limiting development in some areas. Several VC are in National Park or Monuments (19%), whereas an additional 10% occur on State of Native Patented lands. Only one of the higher ranked sites (Douglas) listed in Table 7.5-2 is excluded from further development based on land withdrawals (National Park Service).

Table 7.6-2. Dominant land status of Aleutian VC along with their fairway and favorability probabilities. The top 21 VC in this table (Little Sitkin through Segula), ranked based on the play fairway model, are available for development based on land status considerations.

VC	Land Status	Fairway	Favorability	VC	Land Status	Fairway	Favorability
Little Sitkin	Fish and Wildlife Service	0.147	0.400	Gilbert	Fish & Wildlife Service	0.101	0.166
Korovin	Fish & Wildlife Service	0.142	0.331	Pavlof	Fish & Wildlife Service	0.100	0.097
Adagdak	Fish & Wildlife Service + Military	0.139	0.262	Westdahl	Fish & Wildlife Service	0.099	0.095
Seguam	Fish & Wildlife Service	0.136	0.099	Iliamna	National Park Service	0.099	0.098
Vsididov	State Patent	0.132	0.126	Emmons Lake	Fish & Wildlife Service	0.099	0.215
Recheschnoi	Fish & Wildlife Service	0.132	0.419	Augustine	State Patent	0.097	0.093
Okmok	Fish & Wildlife Service	0.131	0.191	Douglas	National Park Service	0.095	0.146
Gareloi	Fish & Wildlife Service	0.131	0.109	Fourpeaked	Katmai Natl Park & Preserve	0.095	0.094
Makushin	Native Patent	0.130	0.497	Snowy Mountain	Katmai Natl Park & Preserve	0.095	0.094
Tanaga	Fish & Wildlife Service	0.129	0.110	Kukak	Katmai Natl Park & Preserve	0.094	0.094
Moffett	Fish & Wildlife Service + Military	0.128	0.109	Katmai	Katmai Natl Park & Preserve	0.094	0.134
Kanaga	Fish & Wildlife Service	0.128	0.109	Mageik	Katmai Natl Park & Preserve	0.094	0.188
Yunaska	Fish & Wildlife Service	0.126	0.121	Veniaminof	Fish & Wildlife Service	0.093	0.090
Spurr	State Patent	0.126	0.201	Shishaldin	Fish & Wildlife Service	0.090	0.087
Table Top	Fish & Wildlife Service	0.124	0.140	Semisopochnoi	Fish and Wildlife Service	0.089	0.181
Akutan	Fish & Wildlife Service	0.124	0.508	Griggs	Katmai Natl Park & Preserve	0.089	0.088
Herbert	Fish & Wildlife Service	0.122	0.117	Stepovak Bay 4	Fish & Wildlife Service	0.086	0.085
Tana	Fish & Wildlife Service	0.122	0.168	Unnamed	Fish & Wildlife Service	0.086	0.216
Cleveland	Fish & Wildlife Service	0.122	0.117	Black Peak	Fish & Wildlife Service	0.085	0.082
Kiska	Fish and Wildlife Service	0.121	0.103	Kupreanof	Fish & Wildlife Service	0.084	0.100
Segula	Fish and Wildlife Service	0.121	0.103	Amukta	Fish & Wildlife Service	0.083	0.079
Kaguyak	Katmai Natl Park & Preserve	0.111	0.154	Great Sitkin	Fish & Wildlife Service	0.080	0.227
Frosty	Fish & Wildlife Service	0.109	0.126	Kagamil	Fish & Wildlife Service	0.074	0.105
Isanotski	Fish & Wildlife Service	0.108	0.104	Dutton	Fish & Wildlife Service	0.064	0.119
Roundtop	Fish & Wildlife Service	0.108	0.105	Ugashik-Peulik	Fish & Wildlife Service	0.064	0.106
Chiginagak	Fish & Wildlife Service	0.107	0.221	Fisher	Fish & Wildlife Service	0.060	0.058
Hayes	State Patent	0.105	0.104	Kialagvik	Fish & Wildlife Service	0.060	0.057
Dana	Fish & Wildlife Service	0.104	0.100	Yantarni	Native Patent	0.058	0.044
Carlisle	Fish & Wildlife Service	0.104	0.100	Aniakchak	Aniakchak National Monument	0.055	0.083
Redoubt	National Park Service	0.102	0.101				

7.7 TRANSMISSION

Most Aleutian VC have no access to transmission, and the few that do are very localized. Thus, the lack of power transmission is a serious impediment to geothermal development on unpopulated or underpopulated islands. Because development of these systems is not economically viable at this point and developers willing to invest likely to be scarce, near-term, future work on geothermal exploration and development should focus on the VC in the Cascade Arc. However, many viable targets exist in the Aleutians which should be evaluated if market conditions change.

The Cascades, on the other hand, have major transmission lines among states and significant power demand, only to increase as California increases its renewable portfolio standard to 50%. Figure 7.7-1 shows the location of power lines relative to the position of the VC, and although there are major transmission corridors, the VC tend to lie between two major corridors due to their mountainous terrain. Note, digital files of power lines could not be obtained and the VC data are plotted on top of a .tiff image.

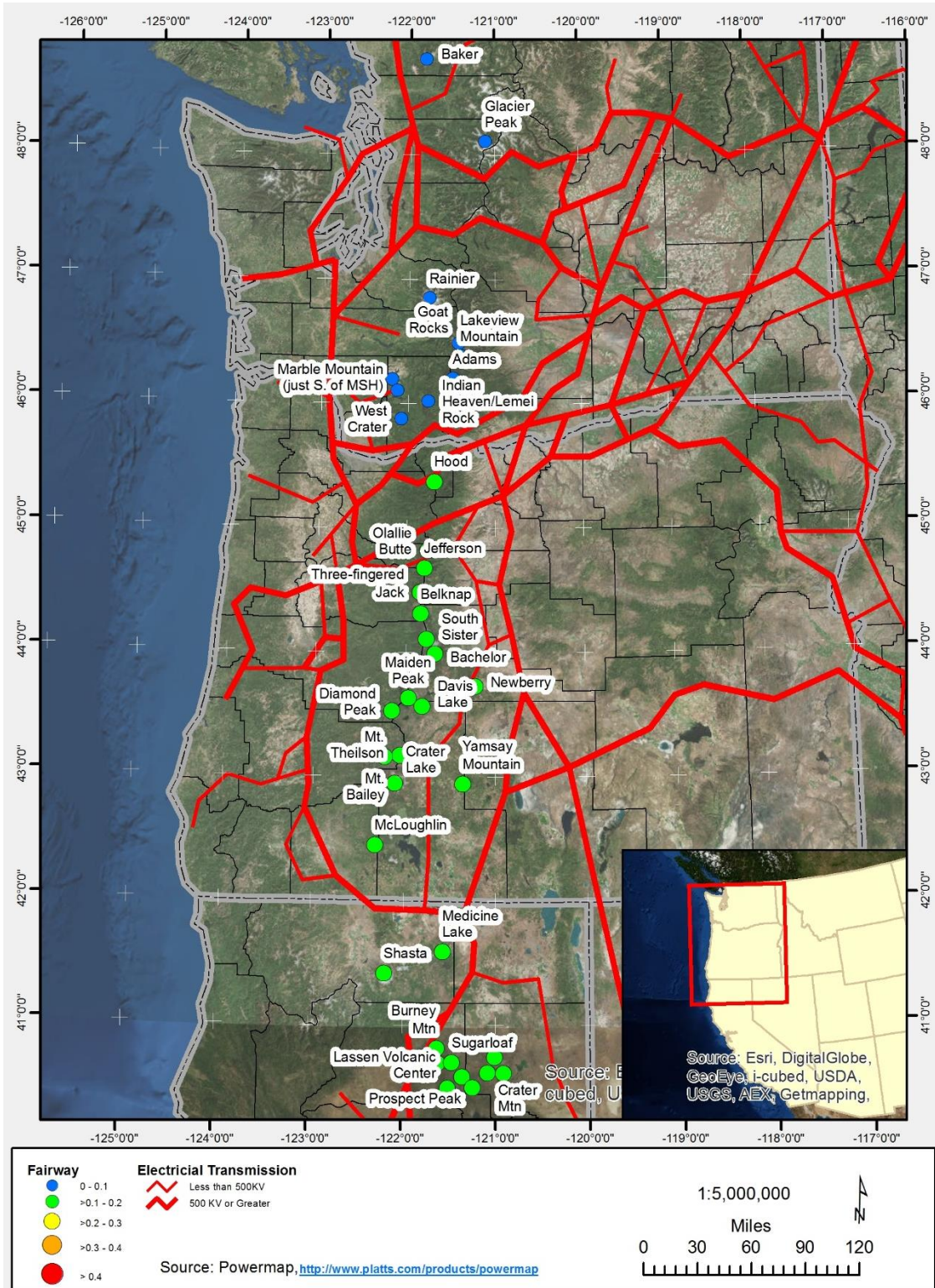


Figure 7.7-1 Location of power lines relative to the position of the VC and play fairway model results in the Cascades.

8.0 DISCUSSION

8.1 TECHNICAL

Potentially Blind Geothermal Systems

One of the fundamental goals of a Play-Fairway approach was the use of a rigorous statistical approach to identify targets that wouldn't have been identified in other ways. These blind resource are a particularly important aspect of this project, as the most obvious geothermal targets are not associated with the two volcanic arcs in the United States. This is either because the Cascade and Aleutian arcs are uniquely poor regions for geothermal systems to develop, or the commonly used identifiers of geothermal systems are absent for other reasons. Our investigation has shown that the latter is more accurate.

Our Play-Fairway analysis of global geothermal systems on arc volcanoes has shown that structural controls on permeability are the primary predictors of geothermal potential, and that volcanic features to a large degree exert little control over geothermal systems. Success of our analysis can be measured by the high rankings for systems already identified to have high geothermal potential in both volcanic arcs (e.g., Newberry and Medicine Lake in the Cascades, Akutan and Makushin in the Aleutians). In addition to identifying known systems as having high potential, we have also identified the southern Cascades as a region with relatively high Fairway scores. The VCs in this area have had very little exploration and, as a result, have little direct evidence for active geothermal systems. Our Fairway study also showed that, to a large extent, geothermal favorability is not related to volcanic parameters, and that the heat source is not a substantial obstacle to development of geothermal systems in the US arcs.

Figure 10.1-1 shows the direct evidence score plotted against Fairway score for the Cascades. Nearly all of the VCs between Mt. Jefferson and Mt. Lassen have very high Fairway scores and little direct evidence, plotting in the lower right quadrant. Highlighted in red on Fig. 10.1-1 are VCs selected independently through the Fairway analysis as the most likely targets in Cascades, primarily based on structural controls on permeability. These VCs also happen to have among the lowest direct evidence scores. Additional investigation of these VCs to target these potentially blind geothermal systems should be conducted in Phase 2 will narrow down the list of targets for MT and thermal gradient well drilling for Phase 3.

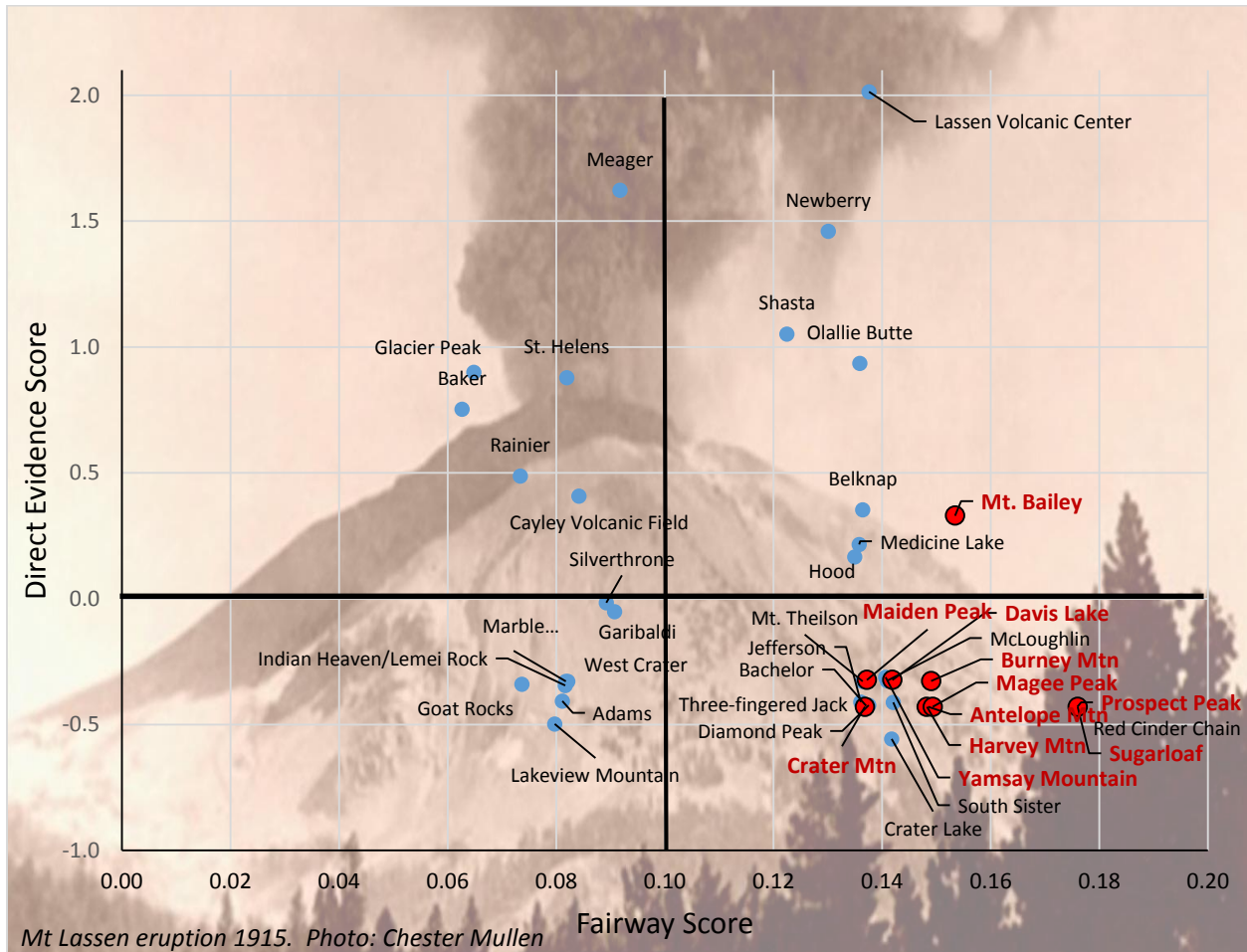


Figure 8.1-1. Direct evidence (vertical axis) vs Fairway score (horizontal axis). Areas in the lower right quadrant represent the highest Fairway scores and the least direct evidence, interpreted as the highest potential blind systems. Highlighted in red are VCs that Play-Fairway analysis independently identified as the best targets for additional investigation.

Figure 8.1-1 also shows which of the studied VC have little likelihood of hosting a productive geothermal system. VC plotted in the lower left quadrant have low Fairway scores, indicative of low permeability, as well as lack of direct evidence of the presence of a productive system. VC plotting in the upper left quadrant have higher direct evidence scores, but lower fairway scores suggesting insufficient permeabilities may be present to support an electric-grade geothermal production facility. The upper right quadrant plots systems with high probability of hosting an electric-grade geothermal system based on both high fairway and direct evidence scores.

Global Benchmarks by Arc Segment – Looking for Analogues

One additional and potentially powerful tool that can be derived from the database of global benchmark VCs is to identify analogues for use in refining specific exploration strategies. The benchmark VCs have been subdivided into major contiguous arc segments according to the tectonic setting and further subdivided by strain rate categories. Relatively consistent trends

over broad arc segments could be expected because a region with a common tectonic setting type/region is typically associated with a common suite of local structures accommodating the style of strain present. Transtensional terranes are mostly dominated by strike-slip faults which are linked locally to normal faults, forming pull-aparts and displacement transfer zones. Extensional terranes are mostly dominated by normal faults which develop step-overs, fault terminations, and accommodation zones. Compressive and transpressive terranes are dominated by reverse faults and oblique reverse faults, respectively.

The total MWe per arc segment, average MW/VC, average permeability fairway score, and collective suite of local structural setting types were used to evaluate for trends between the arc segments (Table 8.1-1 and Fig. 8.1-2). The results are broadly consistent with the results section 4.2, and illustrates that the majority of the MW produced in subduction arcs are related to transtension or extension strain style and higher strain rates correlate with greater MW/VC. While many of these broad arc segments only have a few benchmark VCs, there is still an overall correlation between average MW/VC and the permeability fairway.

Drawing from details in the global benchmark database and from the arc segment patterns illustrated in Table 8.1-1, analogues can be drawn for the Aleutians and Cascades that may help further refine resource potential and specific exploration strategies. Honshu, Japan is the only broad arc segment undergoing compression and transpression with producing geothermal systems (7 total). Both the eastern Aleutians and the north Cascades also reside in compression and transpressional tectonic settings. Granted, nearly 90% of the MWe produced in subduction arc settings worldwide come from VCs located in extensional and transtensional settings, there must be some unique characteristics that coalesce in Honshu for those volcanoes to be so productive in a largely compressive environment. Tectonically, the western Aleutians behave similarly to Sumatra and Chile, however in contrast to those regions, the western Aleutians are an oceanic arc, and other productive oceanic arc segments like the Mariana or Kuril arcs may provide the best analogs. Notably the Trans-Mexico volcanic belt presents a close analog to the southern Cascades, including numerous similarities between Lassen, CA and Los Azufres, Mexico. Both the southern Cascades and the Trans-Mexico volcanic belt are collocated with broad regional extensional terranes and with localized transtension, have similar volcanic signatures, and have similarities in known resources in the US. A summary of the structural and stratigraphic control of the reservoirs, geochemistry, geothermal manifestations, volcanology, and overall structural-tectonic data from these analog regions could help further improve future exploration programs in the Aleutian and Cascade arcs.

Table 8.1-1. Summary of arc segments organized by tectonic setting and intra-arc strain rate in the first and second columns, respectively. Average MW per benchmark are color coded by even thirds at log scale: blank = low, yellow = medium, orange = high. Fairway score is also color coded by even thirds: orange = high, yellow = medium, blank = low. Structural settings of benchmark VCs: AZ, accommodation zone; DTZ, displacement transfer zone; FI, fault intersection; FT, fault termination; PA, pull-apart; RB, restraining bend; SO, step-over; U, Unknown.

Tectonic Setting	Strain Rate	Arc Segment	Benchmark VCs (#)	Total MWe	Ave MWe/VC	Fairway Score	Structural Settings of VCs
Extensional - Narrow Rifts	H	TVZ	5	1082	216	0.212	AZ (3), SO (1), FI (1)
	H, M	Kyushu, Japan	4	213	53	0.166	DTZ (2), FI (1), U (1)
Extensional - Broad Regional	M, L	S. Cascades	1 (of 27)	25	25	0.188	AZ (6), DTZ (1), SO (12), FI (8)
	L	TMVB	4	270	68	0.182	SO (3), FI (1)
Transtension	H, M	Philippines	7	2030	290	0.210	PA (2), DTZ (3), U (2)
	H, M	Sumatra and W. Java	14	1784	127	0.168	PA (4), DTZ (7), FI (2), RB (1)
Transtension	M	Costa Rica, Nicaragua, S. El Salvador	6	561	94	0.177	PA (3), DTZ (2), FI (1)
Transtension	L	Italy	2	915	458	0.222	SO (1), FI (1)
	L	Guatemala, N. El Salvador	3	57	19	0.163	DTZ (1), FI (2)
	L	New Ireland	1	56	56	0.166	FI (1)
	L	Caribbean	2	26	13	0.166	PA (1), FI (1)
	L	N. Chile	4	85	21	0.179	FI (4)
	L	S. Chile	3	18	6	0.147	DTZ (1), FI (2)
	L	Taiwan	1	3	3	0.206	U (1)
Compression-Transpression	L	Western Aleutians	0 (of 27)	0	--	0.155	DTZ (1), FI (11), U (14), O (1)
	L	Honshu, Japan	7	294	42	0.105	FI (4), FT (3)
	L	N. Cascades	1 (of 14)	5	5	0.105	PA (6), FI (6), U (2)
Unknown	L	Eastern Aleutians	0 (of 32)	0	--	0.119	FI (14), FT (2), U (16)
	L	Kamchatka	4	102	26	0.120	U (4)
	L	Kuril	2	5	3	0.127	U (2)
	L	East Nusa Tenggara	2	8	4	0.113	FI (1), U (1)
	L	Sulawesi	1	63	63	0.112	U (1)
L	Marianas	1	3	3	0.112	U (1)	

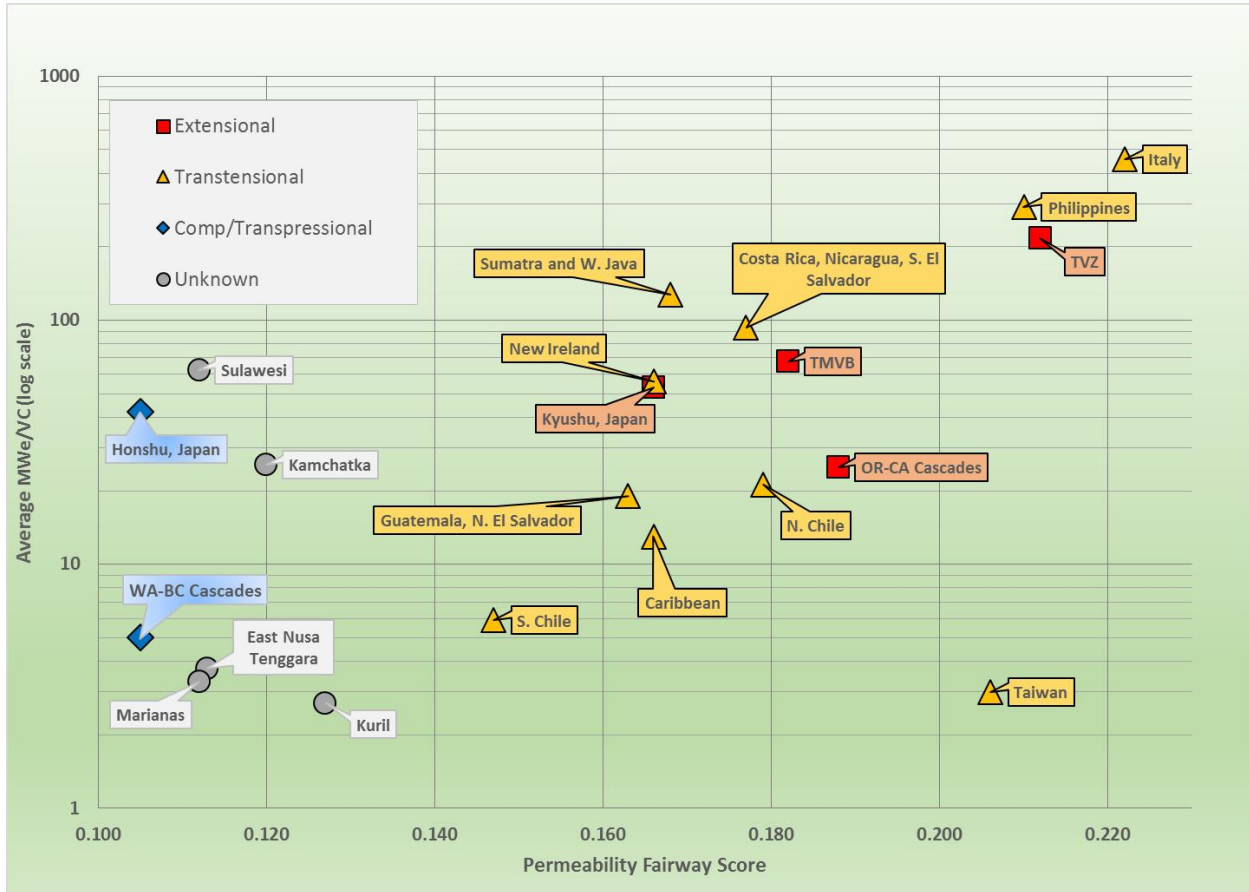


Figure 8.1-2. Plot of average permeability fairway scores versus average MW/VC for separate arc segments from Table 8.1-1. Increasing fairway score correlates well with increasing average MW production showing the fairway model reliably models the relative ranking of these systems.

8.2 ADMINISTRATIVE

This project successfully achieved the goal of providing a robust play fairway model application that identified traditional and blind geothermal systems in the Cascades and Aleutians. Probabilities of occurrence of and electric-grade geothermal reservoir were calculated for the 59 Aleutian VC and 37 (US) Cascade VC from which a ranking of sites by favorability resulted. All milestones were met, as noted in table 8.2-1, for successful complete of Phase I of this project.

Table 8.2-1. Project milestones table for Phase I. (appears on following page)

Major Task Schedule								
SOPO Task #	Item: Task = T Milestone = M Deliverable = D	Task Title or Milestone/Deliverable Description	Original Planned Start Date	Actual Start Date	Planned Completion Date	Actual Completion Date	% Complete	Progress Notes
1	T	Background Data Evaluation	10/1/2014	9/1/2014	10/31/2014			
1.1	T	Literature Search	10/1/2014	9/1/2014	10/31/2014	on-going	100%	Ongoing as new data and sites are defined
1.2	T	Collaborator meetings (2)	10/1/2014	10/1/2014	Nov-14	Nov-14	100%	3 collaborator (GoToMeetings) held; 2 in person
1.3	T	ID Geothermal Play Fairway types	10/1/2014	10/1/2014	10/31/2014	Nov-14	100%	Broad categorization of types defined
1.4	T	ID Power production parameters	10/1/2014	10/1/2014	10/31/2014	Oct-14	100%	Table of power plants completed
1.5	T	Define "young volcanic center"	10/1/2014	10/1/2014	10/31/2014	Oct-14	100%	Young (<500 Ka), focus on Holocene
1.6	T	Regional predictive data types	10/1/2014	10/1/2014	10/31/2014	Oct-14	100%	Researched and identified
1.7	T	Local predictive data types	10/1/2014	10/1/2014	10/31/2014	Nov-14	100%	Many identified, some to be discarded upon data collection and review in later phases
1.8	T	Definition of "Degree-of-Exploration"	10/1/2014	10/1/2014	10/31/2014	ongoing	100%	
1	M	Document	11/1/2014	11/1/2014	1/25/2015	12/15/2014	100%	Document describing Task 1 subtask summary; included as part of Q1 report
2	T	Data Compilation	11/1/2014	11/1/2014	1/30/2015	9/15/2015	100%	Conducted throughout project
2.1	T	Table of producing power plants globally in arc settings	11/1/2014	11/1/2014	1/15/2015	1/22/2015	100%	Table included in Quarterly (Q1); additional information to be added Q2
2.2	T	Table of volcanic centers	11/1/2014	11/1/2014	1/15/2015	1/22/2015	100%	Table to be included in Quarterly (Q1); major features: rock type, subduction type, etc.). additional information to be added Q2
2.3	T	Compilation of evidential data	11/1/2014	11/1/2014	1/15/2015	3/30/2015	100%	Compilation of various data; revised in Task 5
2	M	Tables: Power plants, world volcanic centers included in project	10/1/2014	9/1/2014	12/31/2015	1/15/2015	100%	From tasks 2.1 and 2.2
2	D	Quarterly Report	1/1/2015	1/1/2005	1/30/2015	1/22/2015	100%	Q1
3	T	Preliminary Predictive Modeling	1/1/2015	2/1/2015	3/30/2015	3/29/2015	100%	
3.1	T	Data mining/data exploration	1/1/2015	3/1/2015	3/30/2015	3/29/2015	100%	Data compilation and initial data evaluation
3.2	T	Regional predictive indices	1/1/2015	3/1/2015	3/30/2015	3/29/2015	100%	Preliminary indices developed for refinement in final model
3.2	T	Local predictive indices	1/1/2015	3/1/2015	3/30/2015	3/29/2015	100%	Preliminary indices developed for refinement in final model
3.4	T	Degree of exploration	1/1/2015	3/1/2015	3/30/2015	3/31/2015	100%	Began addressing data gaps in the context of degree of exploration
3.5	T	Prelim Maps & Sensitivity analysis	1/1/2015	3/1/2015	3/30/2015	3/29/2015	100%	Preliminary maps completed
3	M	Maps	2/15/2015	3/1/2015	3/30/2015	3/29/2015	100%	Preliminary maps
4	T	Collaborator Meeting	3/30/2015	4/10/2015	4/20/2015	7/8/2015	100%	GoToMeeting - part 3 of Task 4 completed
4.1	T	Evaluate and interpret initial model results	3/30/2015	4/10/2015	4/20/2015	5/20/2015	100%	Group discussion and decisions
4.2	T	Assess data quality/completeness	3/30/2015	4/10/2015	4/20/2015	6/1/2015	100%	Group discussion and decisions
4.3	T	Refine models and definitions	3/30/2015	4/10/2015	4/20/2015	6/20/2015	100%	Group discussion and decisions
4	M	Go/No Go	3/1/2015	4/1/2015	4/30/2015	7/25/2015	100%	Document of proceeding with project
4	D	Quarterly Report	4/15/2015	4/12/2015	4/30/2015	4/27/2015	100%	Q2 Report
5	T	Final Stage Data Compilation	4/1/2015	4/1/2015	7/15/2015			
5.1	T	Complete volcanic center identification & data acquisition	4/1/2015	4/1/2015	7/15/2015	6/30/2015	100%	several Exce spreadsheets
5.2	T	Adjust model parameters & ID key evidential data	4/1/2015	4/1/2015	7/15/2015	6/29/2015	100%	review prelim model; make adjustments
5	M	Report on the final data collection	5/1/2015	6/1/2015	7/15/2015	7/25/2015	100%	Included in quarterly report (Q3)
5	D	Quarterly Report	7/1/2015	7/6/2015	7/30/2015	7/25/2015	100%	Q3 Report
6	T	Final Model	7/1/2015	6/1/2015	9/30/2015	10/16/15%	100%	
6.1	T	Data mining/data exploration	7/1/2015	6/1/2015	9/30/2015	9/15/2015	100%	various plots and maps to evaluate data
6.2	T	Regional predictive indices	7/1/2015	9/1/2015	9/30/2015	9/30/2015	100%	probability weighting factors
6.3	T	Local predictive indices	7/1/2015	9/10/2015	9/30/2015	9/30/2015	100%	probability weighting factors
6.4	T	Degree of exploration	7/1/2015	9/15/2015	9/30/2015	10/10/2015	100%	data collection and weighting to assess uncertainty
6.5	T	Final Maps & Sensitivity analysis	7/1/2015	9/1/2015	9/30/2015	10/16/2015	100%	Final Report
6	M	Maps/Tables	10/1/2015	9/20/2015	10/30/2015	10/16/2015	100%	maps and tables showing predictive results
7	T	Ranking of Volcanoes	10/1/2015	9/20/2015	10/30/2015	10/16/2015	100%	Ranking tables
7	M	Document discussing the ranked volcanoes	10/1/2015	9/20/2015	10/30/2015	10/16/2015	100%	Final Report
8	T	Project Management/Reporting	10/1/2014	9/25/2015	10/31/2015	10/16/2015	100%	Final Report
8	M	Presentation at DOE peer review	5/1/2015	5/1/2015	5/15/2015	5/13/2015	100%	Peer Review - May 2015
9	T	Commercialization	9/1/2015	10/1/2015	10/30/2015	10/16/2015	100%	Final Report
9.1	T	Final Report	9/1/2015	9/15/2015	10/30/2015	10/16/2015	100%	Final Report
9.2	T	DOE Review	5/1/2015	9/20/2015	10/30/2015	10/26/2015	100%	Final presentation to DOE
9.3	T	Public paper/presentation (e.g., GRC)	9/1/2015	4/1/2015	10/30/2015	9/23/2015	100%	Final papers submitted to EERE
9	M	Paper/Presentation (GRC)	4/1/2015	4/1/2015	10/1/2015	10/12/15	100%	Presentations at GRC
9	D	Final Report	10/1/2015	9/15/2015	11/30/2015	10/16/2015	100%	Final Report
		Financial Reporting	10/23/2015	10/22/2015	11/19/2015			

9.0 CONCLUSIONS

Our evaluation of global energy producing arc systems has shown that a number of factors are associated with productive geothermal systems. Chief among these factors is active extensional intra-arc strain. Dilatant structures that facilitate fluid flow are common in extensional and transtensional terranes, but are less well developed in regions of compression or transpression. Additional factors that correlate with electricity generating potential include: 1) regions of oblique plate convergence, 2) high Quaternary fault slip rates, 3) high densities of Quaternary fault scarps, and 4) local extensional structural settings that include pull-aparts, step-overs, accommodation zones, or displacement transfer zones. Together, these favorable factors combine in an expert-driven and data-driven weighting system to produce a significant fairway analysis tool with which to evaluate the electricity-generating potential of arc volcanic centers in the U.S. and around the world. The methodologies developed can be easily adapted to other tectonic environments.

Data Trends and Correlations

This project involved a large data collection effort, from which some general trends were observed. Relationships not already noted above include:

- Most productive World Arc reservoirs are $>250^{\circ}\text{C}$ (73%)
- Most Cascade (93%) and Aleutian (96%) systems are $<200^{\circ}\text{C}$, based on available information.
- The presence of flank fumaroles (hydrothermal as opposed to magmatic) was found to be an important indicator of the presence and approximate size of a productive geothermal system.
- Most productive systems have known flank fumarole manifestations (70%), and flank fumaroles may be present at some of the remaining 30% of productive systems but are not documented.
- Systems with mapped flank fumaroles produce 90% of the power globally from arc systems.
- Fewer Cascade (11%) or Aleutian (41%) systems volcanic centers have known flank fumaroles.
- Larger fumarole areas are correlated with higher measured and geothermometer temperatures, Quaternary faults, and more prospective tectonic setting, structural setting and regional strain characteristics.
- Larger fumarole areas are typically associated with higher MW per system world-wide.
- There are limited surface manifestations in the Cascades; those areas with known surface manifestations have been heavily explored. Most of the Cascades are relatively well explored by outdoor enthusiasts and the existence of such surface manifestations is likely to have been documented.
- The Aleutians, on the other hand, have not been extensively explored and the occurrence of flank fumaroles may still remain undocumented at many of the VCs given that fewer people have explored the islands.
- Various geochemical, manifestation, and structural/tectonic plots shows that few of the US arc VCs are of the same size as the higher MW producing systems in the global training set.

However, Lassen and Akutan routinely rank nearest to the global training set, higher than other Aleutian and Cascade systems.

- Data trends indicate many other VCs in both U.S. arcs have elevated geothermal potential, although probably at lower levels of output (<50 MW).
- Volcanic characteristics such as dominant eruptive compositions, compositional diversity, edifice size, inter-vent features and eruption timing and frequency show no obvious correlations with MW production in the global training set. These factors are not predictive of potentially productive geothermal prospects, and thus, were not included in the play fairway model.
- Tectonic Setting, Quaternary fault slip rate, Quaternary fault density, structural setting and dilation potential correlate favorably with the global training set, which, by design, captures the characteristics of high productivity systems.
- Extension accommodated through magmatic intrusion is inversely related to geothermal favorability

Summary of Arc Settings

Several tectonic settings were identified for the world volcanic arcs based on structural analysis relevant to permeability assessment. These settings are summarized here with more prospective fairways listed first.

Fairway Model

We have developed a very robust fairway analysis that highlights the southern Cascades of CA and OR as having high potential relative to northern Cascade VCs. This is an area with which has a large power demand, sufficient open land access, good power line corridors and significant future power market opportunities in light of the new CA RPS of 50% renewables by 2030.

This method of fairway analysis is applicable to all geothermal areas in the world and can be tuned accordingly. In essence, we model permeability, co-located with heat and fluids to generate a hydrothermal system. Permeability is largely influenced by crustal dilation accomplished through either tectonically driven extension (rifting or pull-aparts, along strike-slip faults) or through gravitational collapse on mid-plate VCs (e.g. Hawaii).

- Several Aleutian systems rank highly, but most are from Akutan and westward, not in areas with likely commercial applications outside of Akutan and Makushin, both of which have had previous drilling and DOE interest.
- Aleutian VCs are likely more prospective than Cascade VCs but due to remoteness, lack of transmission and market, most systems are not economically viable at this time. Many viable targets exist in the Aleutians that should be evaluated if market conditions change.
- These fairways can be used to focus future exploration as opportunities exist to and fine-tune regional relationships and fairway definitions with additional data integration of structure, lithology, and geochemistry.

Relative Potential of the Cascade and Aleutian Volcanic Arcs

Fumaroles, hot springs and active altered ground are direct indicators of the potential existence of geothermal reservoirs. Almost all developed geothermal fields in arc settings have such indicators. Identification of such features in the Cascades is probably complete (less so in the Aleutians) and they indicate a lower density of prospective areas than in Java, Sumatra, and the Philippines. Several candidate reasons have been proposed for this: reservoirs could exist but they are more “hidden” than those elsewhere or systems are of smaller size. The Cascade and Aleutian Arcs have many positive indications of a favorable structural setting for creating reservoir permeability. Based on a statistical assessment of the criteria that are available, numerous areas have been identified as being attractive in the US arcs for further investigation of suitable host formations, cap integrity, alteration and similar low cost exploration prior to geophysical surveys that could be used to characterize resource capacity or target wells.

Model results show that 60% of the volcanic centers in the Aleutians and 89% of those in the Cascades have probabilities of a geothermal occurrence capable of power production that is greater than the prior probability of 10% (rankings are detailed in Section 7.0). That is, many sites are within favorable structural and tectonic settings anticipated to have sufficient heat and permeability for development. Four sites in the Cascades (Lassen, Newberry, Olallie Butte, and Shasta) show probabilities of >25% based on favorability model results, with Lassen and parts of Shasta being unavailable for development based on land use designations. Six of the centers in the Aleutians (Akutan, Makushin, Recheschnoi, Little Sitkin, Korovin, and Adagdak) have probabilities >25%, with all nominally available for development based on land status considerations. Although these and many other Aleutian volcanic centers could be developed based on technical considerations, most will likely not be developed unless/until market and/or population dynamics change (except for at Akutan, which is currently being evaluated in other projects, Makushin, and possibly Korovin, each of which have small population bases and industries to support a power market). Most of the other Aleutians volcanic centers are remote with no population or access to transmission.

MW Capacities: Based on various relationships identified during data exploration, ranges in system MW capacities can be assessed.

- Based on Fumarole areas and structure relationships, most systems in Aleutians and Cascades will be <100 MW (except for Lassen, which is unavailable for development).
- Many Cascade and Aleutian VCs could provide up to 50 MW.
- It is unlikely that many VCs in the Cascades or Aleutians are associated with large (>150 MW), high temperature (>250°C) world-class systems. However, for systems <100 MW, much of the southern Cascades and western Aleutians is quite prospective as most have very good permeability scores in the Fairway Model.
- The area around Lassen has high permeability values but limited direct evidence, and may be the most prospective area in the Cascades and Aleutians. The lack of direct evidence and high modeled permeability values points to the success for the Play Fairway model in identifying potentially blind geothermal areas.

Although most Cascade and Aleutian VC have modeled play fairway scores within the range modeled for the world VC benchmark sites (i.e., high permeability scores), the data trends and analyses suggest the US systems will be somewhat smaller and cooler. Nevertheless, the modeling identified many lower MW (<50 MW) systems as well some areas of likely blind geothermal systems requiring increased attention in the effort to increase renewable energy resources capacities. Among the most compelling regions of potentially hidden resources is the southern Cascades in the area surrounding, but exclusive of, Lassen. This area includes six separate VC over a 6,400 km² are, none of which have existing information on surface features: Antelope Mt, Burney Mt, Crater Mt, Harvey Mt, Prospect Peak, and Sugarloaf,

10.0 RECOMMENDATIONS – PHASE 2

10.1 BACKGROUND

One of the fundamental goals of a Play-Fairway approach is the use of rigorous statistics to identify geothermal targets that conventional methods miss (blind resources). This is particularly important for this project, because the two active volcanic arcs in the United States (Cascades and Aleutians) have very few recognized geothermal targets. This lack of recognized targets is either due to these arcs having uniquely poor geothermal potential, or because the commonly used identifiers of geothermal systems are absent for other reasons. Our investigation has shown that the latter is more accurate.

Our Play-Fairway analysis of global geothermal systems on arc volcanoes shows that structural controls on permeability are the best predictors of geothermal potential. While geothermal systems are commonly located around volcanoes, there typically is not potential for reservoir development without structural controls to transit hot fluids. Another important aspect of permeability assessment in volcanic areas involves the lithology and lithologic variability at depth. This information has an impact both on the likelihood of occurrence of a cap rock and the expectations for reservoir permeability. Lithology type is known to correlate with higher permeability in geothermal wells according to the worldwide database of geothermal wells assembled by the International Finance Cor. This database as well as study of geologic maps in the Cascades and Aleutians are included in a phase 2 proposed work.

Success of our analysis can be measured by the high rankings for systems already identified to have high geothermal potential in both volcanic arcs (i.e., Newberry and Medicine Lake in the Cascades; Akutan and Makushin in the Aleutians). Along with these known systems, the southern Cascades as a region also have very high Fairway scores. The VCs in the southern Cascades have had very little exploration and, as a result, have very low direct evidence for active systems. Figure 10.1-1 shows Direct Evidence score plotted against Fairway score for the Cascades. Nearly all of the VCs between Mt. Jefferson and Mt. Lassen have very high Fairway scores and very little direct evidence, and thus plot in the lower right quadrant. Highlighted on Fig. 10.1-1 are VCs selected independently through the Play-Fairway analysis as the most promising targets in the Cascades, primarily based on structural controls on permeability. Our Fairway study also shows that, to a large extent, geothermal favorability is not related to volcanic parameters, and that the

heat source alone is not a sufficient guide to geothermal potential. Additional investigation of these VCs in Phase II will narrow down the list of targets for MT and thermal gradient well drilling in Phase III by better defining the structural controls and obtaining direct evidence from thermal features.

Based on the positive results obtained in the Phase I Play-Fairway model, we recommend the following be conducted as part of Phase II of this project to better define highly favorable areas in the southern Cascades, which have access to a significant power market. Further, CA Senate Bill 350 enacted 10/7/15 raises California's renewable portfolio standard from 33% to 50% by 2030.

The area in and around Lassen has the highest Fairway score and favorability ranking of all Cascade VCs (Section 7.4). All VCs in a 6300 km² block of area surrounding Lassen also have relatively high or moderately high rankings in terms of Play-Fairway settings, primarily as a result of permeability favorability. These VCs around Lassen are locally associated with relatively high strain rates, transtension, and complex Quaternary fault patterns. Half of these VCs are associated with accommodation zones and half are associated with normal fault step-overs. Only the Lassen VC itself ranks highest in overall geothermal favorability, largely due to there being insufficient or no direct evidence at the other VCs. The other three VC to be considered in Phase II are located in southern Oregon. All three (Davis Lake, Maiden Peak, and Mt. Bailey) have relatively high modeled fairway scores, but low degree of detailed exploration.

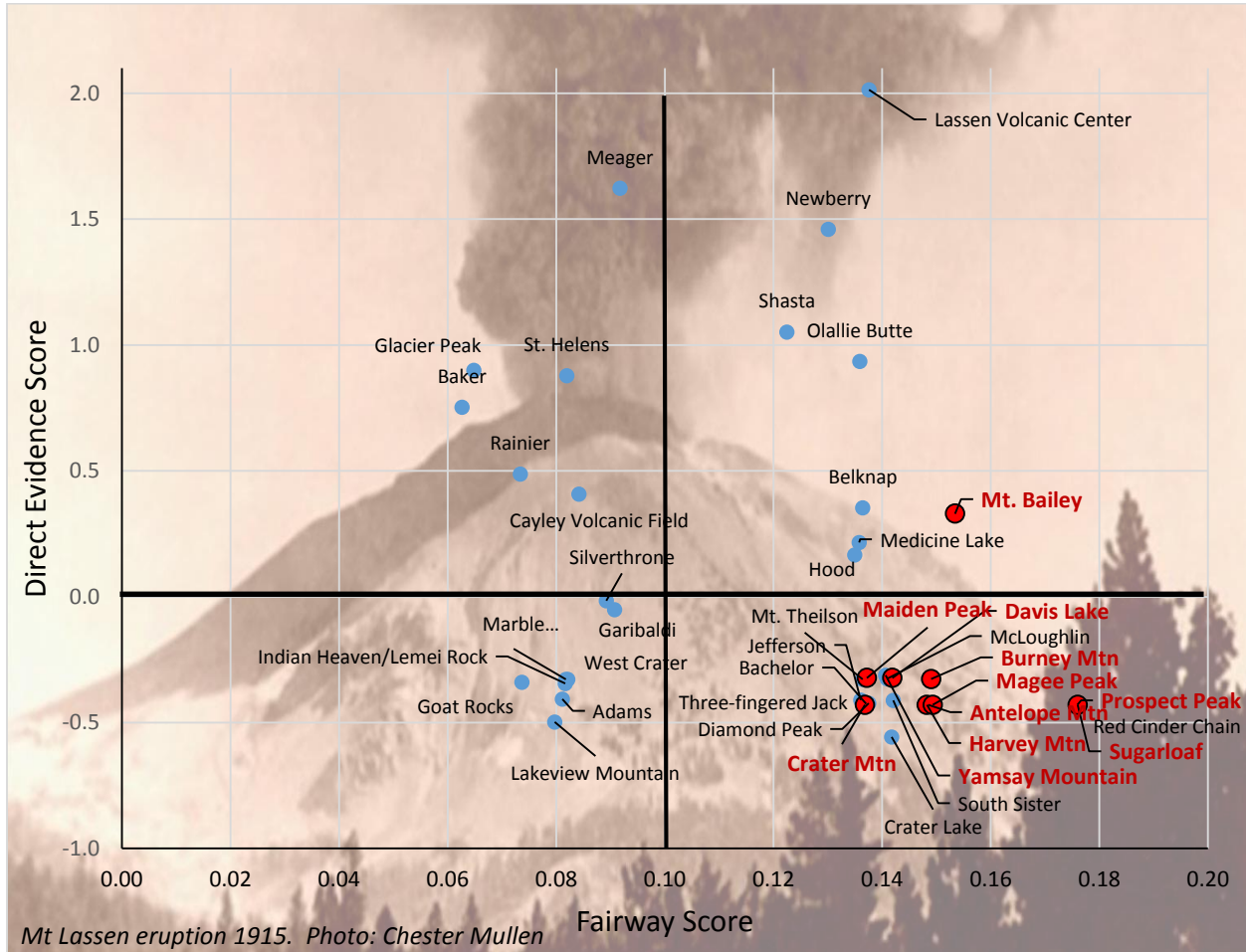


Figure 10.1-1. Direct Evidence (vertical axis) vs Fairway score (horizontal axis). Areas in the lower right quadrant, with the highest Fairway scores and the least direct evidence, are interpreted as the highest potential blind systems. Highlighted in red are VCs that our Play-Fairway analysis independently identified as the best targets for additional investigation. Other high-scoring VCs are not considered due to land-use constraints or existing development.

10.2 PROPOSED WORK

Objectives

We propose to build directly on our Play-Fairway Analysis, Direct Evidence, and Degree of Exploration models that we have constructed in Phase I and will carry forward into Phase II. We will employ a number of tools that the team has been successfully employing and perfecting through years of work in places like the Aleutians (e.g., Stelling et al., 2015) and the Great Basin (e.g., Hinz et al., 2013; 2014). Specifically, the methods proposed for Phase II of this study include water and whole rock geochemistry, LiDAR acquisition and analysis, field mapping, structural analysis, and developing conceptual models based on geothermal data for targeting wells for Phase III.

We will conduct reconnaissance mapping of structure, Quaternary faults, alteration, and surface manifestations at highly ranked VCs in the southern Cascades. Using the results of this step we will further refine our list of targets to two or three VCs near Lassen and southern Oregon. We then propose to collect sufficient data from the selected VCs to refine the Fairway and favorability models with direct, observed evidence. This work will help identify geothermal systems currently hidden and/or insufficiently defined at the VCs in the southern Cascades within National Forests.

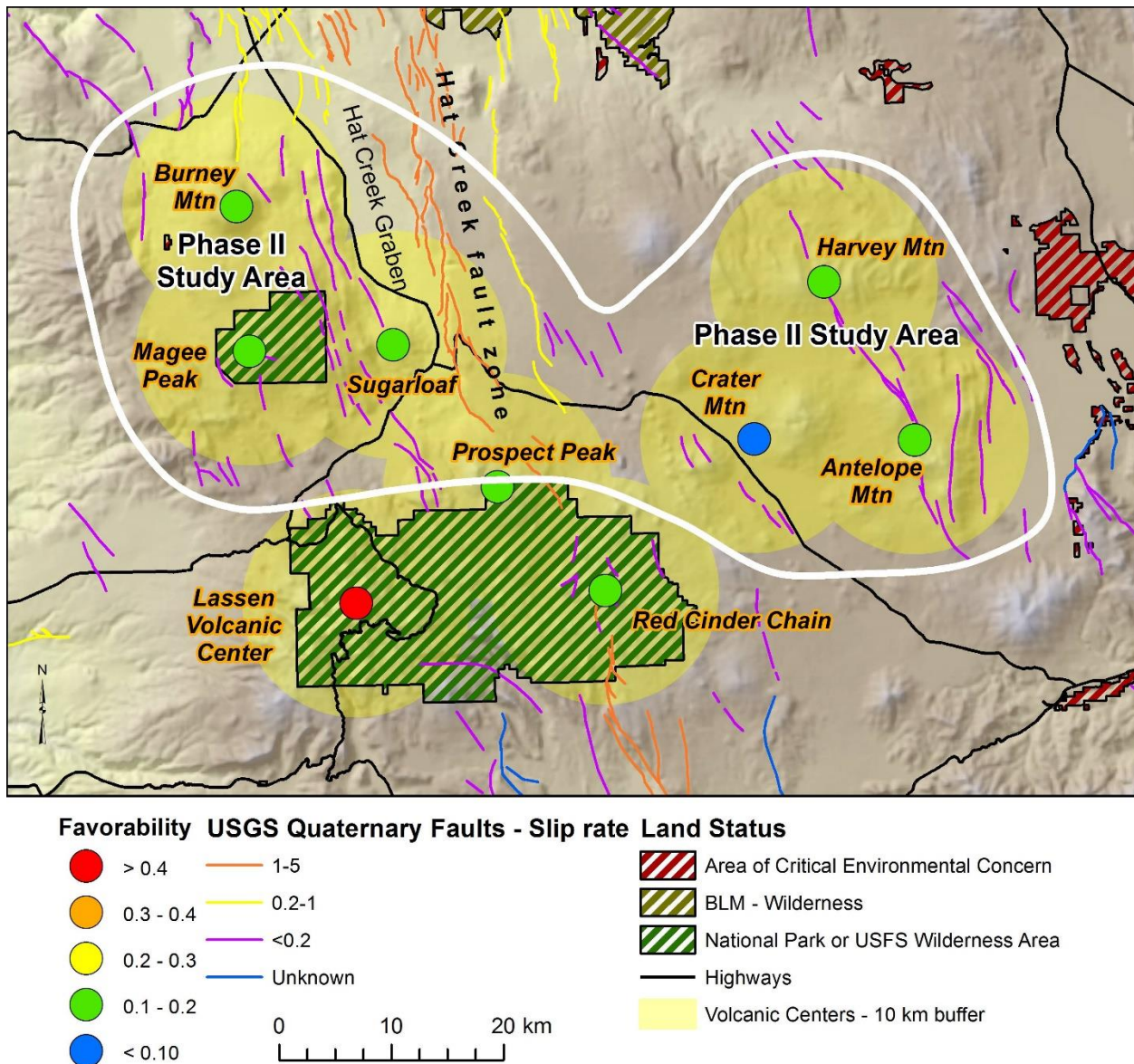


Figure 10.1-2. Proposed Phase II study area near Lassen showing the study area outline in white, excluded areas in cross-hatch, and Quaternary fault data (mm/yr slip rate).

We also propose to conduct detailed field mapping and geochemistry analysis around the highest ranked systems in the southern Cascades to narrow these favorable Fairway areas to those most

likely to produce the most power (Figures 10.1-2, and 7.6-2, which shows outline of southern Oregon study area). This phase of the work will identify which sites warrant an MT study and gradient well drilling in Phase III. The sites to be investigated in Phase II are seven VCs around Lassen (Fig. 10.1-2) and three in southern Oregon (Davis Lake, Maiden Peak, and Mt. Bailey). The seven VCs near Lassen (Prospect Peak, Magee Peak, Burney Mtn, Sugarloaf, Crater Mtn, Antelope Mtn, and Harvey Mtn) all rank highly in the Play-Fairway model, but drop in ranking in the favorability model due to lack of direct evidence (geochemistry, surface features, alteration). While the lack of direct evidence is partly due to these being blind systems, it also owes to a lack of exploration and data collection.

10.3 PLANNED ACTIVITIES

Task 1: Reconnaissance Field Mapping (ATLAS, UNR, WWU, Sawyer)

Using existing LiDAR data and imagery, and field visits to all 10 VC in the southern Cascades, conduct a preliminary inventory of structure, Quaternary faulting, alteration and location of surface manifestations or potential sites with no current geochemical data (e.g., fumaroles, springs and wells not currently in any known database). Initial reconnaissance will be accomplished through evaluating existing LiDAR data for Davis Lake and Maiden Peak. Reconnaissance for other areas will utilize high resolution air photos available through the USFS and other available imagery (e.g., NAIP). Field reconnaissance will be conducted at all VCs. GPS locations of all fumaroles, springs, wells and deposits (e.g., sinter) encountered during initial reconnaissance will be compiled.

Outcome: The goal of Task 1 is to narrow the number of VCs to the most favorable few to investigate in greater detail in subsequent tasks.

Task 2: Geochemistry of fluids (ATLAS)

None of the seven VCs in the Lassen area have any reported geochemistry in NGDS, nor could references on geochemistry be located in GeoRef, GRC, OSTI, IGA or Geothermics. We propose to collect 5 samples from each site for major and trace element chemistry and δD and $\delta^{18}O$, collecting any available thermal waters and at least one cold water per VC from the sites being considered. This task will include evaluation of geothermometers and calculation of multicomponent chemical equilibria from the sampled waters. In the absence of thermal waters, we will evaluate cold waters for indications of thermal leakage (elevated geothermometers, B, Li, etc.). Note that the high and low budgets reflect greater and lesser acquisition and evaluation of fluid geochemical data, such that fewer VC could be evaluated in the low budget scenario.

Outcome: Task 2 will significantly increase the direct evidence for the reduced set of VCs identified in Task 1.

Task 3: Clay Caps (ATLAS)

Clay caps could be partly responsible for lack of surface expressions and can also be investigated in some detail to better define the fairway model. This task will include review of well logs for all

available wells at and near the VC identified above. Where possible, we will identify depth of clay/impermeable layers, type, thickness, and extent.

Outcome: Task 3 will generate an estimate of clay cap presence and integrity for the selected VCs. This will be an important factor in deciding targets in Phase III.

Task 4: LiDAR Acquisition and Evaluation (UNR, Sawyer)

Prior to detailed field work (Task 5), we propose to acquire LiDAR for two to four VCs to augment detailed mapping in Task 5. Note that the high and low budgets reflect greater and lesser acquisition and evaluation of LiDAR, such that fewer VC could be evaluated in the low budget scenario. All of the VCs proposed for phase II are in forested terrane, so LiDAR acquisition will be key to the success of Phase II of this study. The density of vegetation will require Q1-level LiDAR quality per USGS standards. Each of the NBMG team members has 5 to 10 years of experience in using LiDAR for field studies, including rigorous manipulation of combined slopeshades and hillshades to maximize data interpretation.

Outcome: New LiDAR of specific VCs will help focus targeted fieldwork in Task 5, significantly increasing the efficiency and effectiveness of Task 5.

Task 5: Structural Geology

Task 5a: Field mapping and structural analysis (UNR, Sawyer, WWU)

Conduct Quaternary fault and alteration mapping at VCs selected in Task 1 for detail study using the newly acquired and processed LiDAR. Approximately 200 to 300 square km will be covered across two to four volcanic centers depending upon the budget for Phase II. Structural data, including detailed assessment of the structural framework, the distribution of Quaternary faults and folds, recency of faulting, slip rates, and kinematics will be evaluated to identify structural targets for integration with geochemistry for Phase III targeting. Key structures known to be fruitful for geothermal potential such as accommodation zones, fault step-overs, fault terminations, fault intersections, displacement transfer zones, and pull-parts will be studied in detail. Fault kinematic data will be analyzed separately and then combined with analysis of earthquake data (Task 5b) to collectively assess the tectonic stress field and help identify the most favorable dilatant areas.

For example, recent work by Unruh and Humphrey (2013) identified a transtension belt extending northwest from Lake Almanor that includes the Lassen, Magee Peak, Sugar Loaf, and western Hat Creek graben region using inverted focal mechanisms. Complementing the work of Unruh and Humphrey (2013), fault kinematic data has been collected and interpreted to show dextral transtension along the Hat Creek fault zone (Walker, 2008; Walker and Kattenhorn, 2008; Blakeslee and Kattenhorn, 2010, 2012; Blakeslee, 2012).

Task 5b: Earthquake seismology (UNR, Sawyer)

Acquire earthquake seismicity data from the USGS database and plot these relative to the geologic mapping and other structural data to help assess fault activity, stress orientations, geothermal favorability, and the kinematic framework of faults in the vicinity of each VC. In particular, we will optimally relocate earthquakes in the project region using HypoDD (<http://www.ldeo.columbia.edu/~felixw/hypoDD.html>; e.g., Unruh and Humphrey, 2013).

Outcome: Targeted mapping of key geological and geophysical indicators identified as important in our Fairway model will refine the Fairway model and constrain specific areas on each VC for MT and gradient well drilling in Phase III.

Task 6: Administrative (ATLAS)

Task 6 includes project administration and coordination, project meetings to discuss progress and scientific issues, DOE required reporting, review meetings and presentation of results at the 2016 GRC.

Outcome: Project administration will ensure the timely and effective completion of Phase II and preparation for Phase III work.

Task 7: Analog Study – Trans-Mexico Volcanic Belt (ATLAS, UNR, WWU)

There is remarkable similarity between the structural-tectonic and volcanologic characteristics between the Trans-Mexico volcanic belt (TMVB) and the Oregon-California Cascades. The TMVB has producing systems and the Cascades do not, although successful flow tests at Medicine Lake suggest 25 MWe capacities and theoretical calculations for Lassen support at least 100 MWe. Is land access and market access the primary reason that there are no producing systems in the Cascades? Or is there something we are missing from an exploration standpoint?

We proposed to complete a literature review, field review, and conceptual model summary of the four producing TMVB systems. This would allow us to hone our methodology in looking for new undiscovered and accessible resources in the Cascades.

Outcome: Better understanding of the Cascade geothermal potential.

Timeline – Q1 only

Products – Refined metrics and conceptual models for CA-OR Cascade and TMVB type plays.

Table 10.1-1. Structural-tectonic, volcanologic, and geothermal characteristics of the Trans Mexico volcanic belt and the Oregon-California Cascades.

Characteristics		TMVB	OR-CA Cascades
Structure-Tectonics	Tectonic Setting	Extensional, local transtension (e.g., Los Azufres)	Extensional, local transtension (e.g., Lassen)
	Fault slip rates	<0.1 mm/yr	<0.1 mm.yr (locally up to 1-3 mm/yr)
	Q-fault concentration	Variable - Low, Medium, or High	Variable - Low, Medium, or High
	Structures	Step-overs, Accommodation Zones, Fault Intersections, Displacement Transfer Zones	Step-overs, Accommodation Zones, Fault Intersections, Displacement Transfer Zones
Volcanic Centers	# of VCs	21	27
	# of Benchmarks	4	2*
	Total MWe	270	>125*
	Ave MWe/VC	68	63
	Ave # inter-vent features (global ave: 2.2)	5	3.3
*Assuming that Lassen is probably capable of at least 100 MWe			

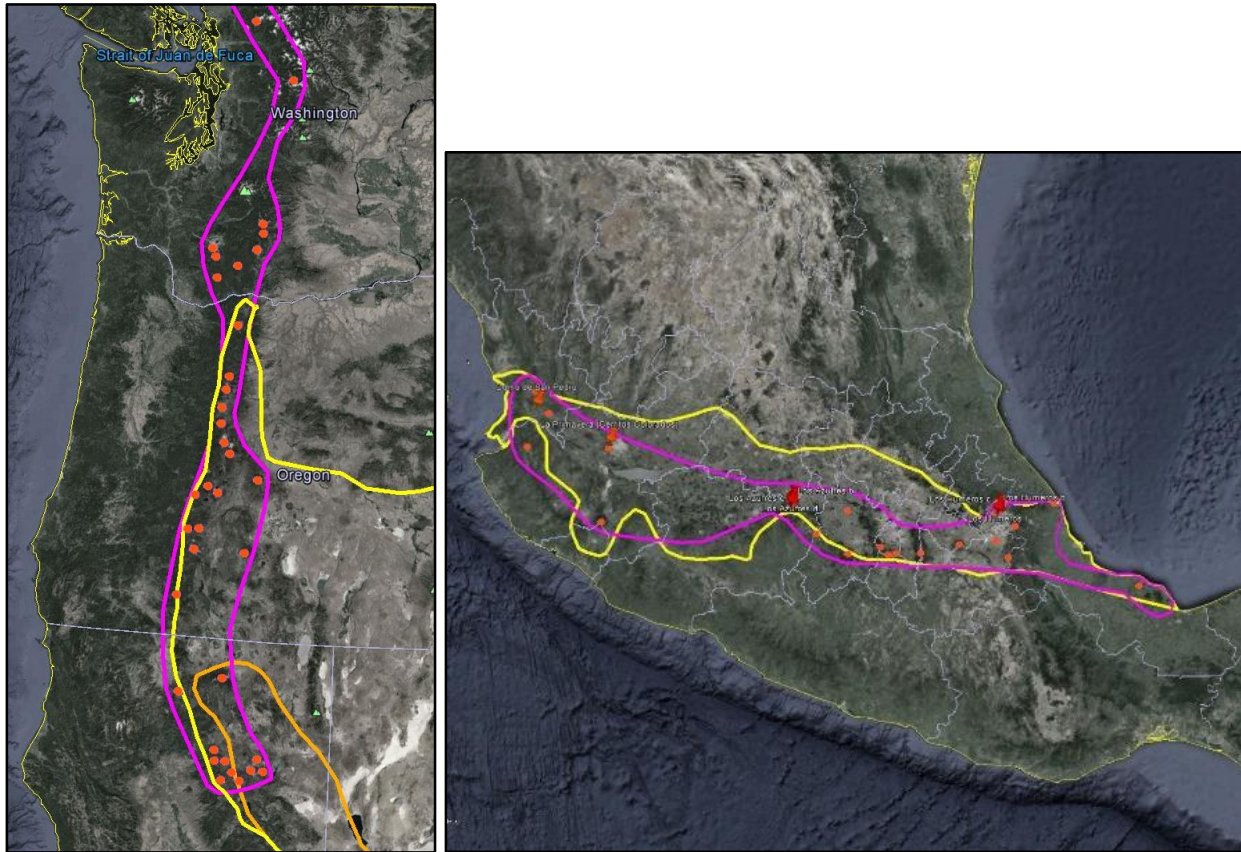


Figure 10.1-3. Tectonic play maps for the Cascades and Trans-Mexico volcanic arcs. Arcs are outlined in purple, Basin and Range and Trans-Mexico extensional tectonic belts outlined in yellow, Walker Lane in the western Basin and Range outlined in orange. Benchmark VCs shown by red and orange push-pins for the TMVB.

10.4 PARTNERS AND ROLES

ATLAS Geosciences Inc – Project coordinator and overall project management. Reconnaissance mapping of surface features. Geochemical sampling and analysis. Clay cap evaluation from well logs. Project management and reporting.

Lisa Shevenell – PI, Hydrogeochemist

Mark Coolbaugh - Geologist

Gary Johnson - GIS specialist

University of Nevada, Reno – Structural mapping and analysis in volcanic terrane, Quaternary fault mapping and analysis, LiDAR analysis, extensive experience with Walker Lane and Basin and Range tectonics, geothermal exploration and modeling.

Nick Hinz – Structural geologist, field geologist, lead of the UNR team

Seth Dee – Field geologist specializing in Quaternary fault studies and geologic mapping

Alan Ramelli – Field geologist specializing in Quaternary fault studies and geologic mapping

Irene Seelye – Cartographer and geospatial analyst

Western Washington University – Volcanics and alteration mapping and analysis, investigation of volcanic, lithologies, features and compositions.

Pete Stelling – Volcanologist, field geologist

Tom Sawyer – Neotectonics specialist with extensive experience in northern California

10.5 DRAFT BUDGET AND TIMELINE

Below is a draft budget to complete the seven tasks noted above based on a high and low dollar scenario. These budget numbers are the requested federal dollars and do not include cost share dollars in this estimate. The lower dollar scenario primarily differs in the amount of LiDAR and geochemical data acquired and interpreted, and thus fewer VC would have detailed assessments. Detailed budgets and appropriate adjustments will be provided during contract negotiations, if Phase II is selected for funding.

	Admin Role	High Estimate	Low Estimate
ATLAS Geosciences Inc	Primary	\$300,000	\$230,000
University of Nevada, Reno	Subcontractor	\$575,000	\$340,000
Tom Sawyer, Independent	Subcontractor	\$45,000	\$35,000
Western Washington University	Subcontractor	\$50,000	\$35,000
Total Federal Dollar Request:		\$970,000	\$640,000

Estimated Timeline (proposed start 1/1/16):

Months	Tasks
1-3	Reconnaissance mapping using publically available LiDAR and aerial photography, plan LiDAR acquisition
	Plan LiDAR acquisition
	Acquire publicly available well logs for clay cap evaluation
4-6	Locate all springs and wells on USGS topo sheets for possible sampling
	Build maps
	Acquire LiDAR when the snow melts
7-9	Finalize clay cap data evaluation
	Reconnaissance mapping - locate springs, fumaroles, wells and deposits
	Field work - surface feature mapping and geochemical sampling
10-12	Processing and detailed evaluation of LiDAR, initiate detailed mapping
	Finalize field mapping
	Geochemical analysis and interpretation
13-15	Map construction
	Categorize surface feature and geochemical data
	Refinement of fairway models
16-17	Final report, recommendations

11.0 DIGITAL DATA SUBMITTED TO GDR

Compiled data submitted to GDR at the completion of the project are from six major sources.

1. Geochemical, temperature and geothermometer data from springs and wells – Excel file
2. Fumarole data sheet noting presence or absence and surface area of manifestation where available – Excel file
3. Structural data and assignments for each VC, including regional tectonics – Excel file
4. Volcanic information data sheet to include eruption frequencies and types and numbers of volcanic vents and primary eruption compositions – Excel file
5. Summary of world Power Plants – Excel file
6. Model input data to consist of selected geochemical, structural, tectonic, volcanic, surface manifestation, and fumarole area data used in the final model. – Excel file
7. ArcMap mxd with related shapefiles

Data entered into #6 above will primarily be constructed from selected data from the previous 5 data sets based on a determination of the most relevant data types required for the play fairway analysis modeling. Weighting factors discussed in section 5.0 are also included in the final file. These data will also be supplied in shapefiles combined with a common .mxd in ArcMap.

Because many of the data sets used in this work such as crustal thickness and geodetic strain data (and many others) are published by other sources by other authors/investigators not associated with this project, these data sets are not submitted GDR, although they provide valuable data to the play fairway model, and links to the original data are noted in Table 3.10-1.

Publications

- Coolbaugh, M., L. Shevenell, P. Stelling, W. Cumming, N. Hinz, G. Melosh, and J. Faulds, 2014. Geothermal Potential of the Cascade and Aleutian Arcs Based on Comparison with other Productive Arc Settings around the World. Geological Society of America Abstracts with Programs.
- Coolbaugh, M., L. Shevenell, N.H. Hinz, P. Stelling, G. Melosh, W. Cumming, and C. Kreemer, 2015. Preliminary Ranking of Geothermal Potential in the Cascade and Aleutian Volcanic Arcs, Part III: Preliminary Model. Geothermal Resources Council Transactions 39: 677-690.
- Hinz, N., M. Coolbaugh, L. Shevenell, G. Melosh, W. Cumming, and P. Stelling, 2015. Preliminary Ranking of Geothermal Potential in the Cascade and Aleutian Volcanic Arcs, Part II: Structural-tectonic settings of the Volcanic Centers. Geothermal Resources Council Transactions 39: 717-725.
- Shevenell, L., M. Coolbaugh, N.H. Hinz, P. Stelling, G. Melosh, W. Cumming, and C. Kreemer, 2015. Preliminary Ranking of Geothermal Potential in the Cascade and Aleutian Volcanic Arcs, Part I: Data collection. Geothermal Resources Council Transactions 39: 771-784.

Presentations

- Coolbaugh, M., 2015. Preliminary Ranking of Geothermal Potential in the Cascade and Aleutian Volcanic Arcs, Part III: Preliminary Model. Presented at Geothermal Resources Council 2015 Annual Meeting, September 23, 2015.
- Hinz, N., 2015. Preliminary Ranking of Geothermal Potential in the Cascade and Aleutian Volcanic Arcs, Part II: Structural-tectonic settings of the Volcanic Centers. Presented at Geothermal Resources Council 2015 Annual Meeting, September 23, 2015.
- Hinz, N.H., Coolbaugh, M., Shevenell, L., Melosh, G., Cumming, W., and Stelling, P., *in prep - 2016*, Structural-tectonic settings of 74 “global benchmark” volcanic centers in subduction arc settings – defining permeability fairways: Proceedings 41st Workshop on Geothermal Reservoir Engineering Stanford University, Stanford, California.
- Shevenell, L., 2015. Preliminary Ranking of Geothermal Potential in the Cascade and Aleutian Volcanic Arcs, Part I: Data collection. Presented at Geothermal Resources Council 2015 Annual Meeting, September 23, 2015.

Networks/Collaborations Fostered:

- Discussions have been held with experts in a variety of fields:
Maria Richards (SMU) & Dave Blackwell (SMU, retired) - discussed regional heat flow and Cascades volcanism. Provided additional data.

Dick Benoit (TMT) – Exploration and drilling history in the Cascades and Aleutians.

William Evans (USGS, retired) – provided discussions and digital data from a new USGS report to be published in the fall of 2015 on Alaska.

Corné Kreemer (UNR) – discussed and acquired regional GPS data to evaluate strain.

Janet Schafer (DNR) – data links to digital data, fumarole information for AK and participation in project meetings. Discussions w/Schafer continue to be helpful and informative.

Tom Powell – meetings to discuss fumaroles, hot springs and other thermal manifestations in Philippines and Indonesia.

12.0 REFERENCES

- Allen, P. A. and Allen, J.R., 2005, Basin Analysis, Principles and Applications, 2nd ed., Blackwell Publishing, Malden, MA, USA, 549 p.
- Ave Lallemand, H.G., 1996, Displacement partitioning and arc-parallel extension in the Aleutian volcanic arc: Tectonophysics, v. 256, p. 279-293.
- Ave Lallemand, H.G., and Oldow, J.S., 2000, Active displacement partitioning and arc-parallel extension of the Aleutian volcanic arc based on Global Positioning System geodesy and kinematic analysis: Geology, v. 28, no. 8, p. 739-772.
- Bertagnini A., Metrich N., Landi P., Rosi M., 2003. Stromboli Volcano (Aeolian Archipelago, Italy): An Open Window On The Deep-Feeding System Of A Steady State Basaltic Volcano. J. Geophys. Res. B108.
- Blackwell, D.D., and D.S., Chapman, 1977. Interpretation of geothermal gradients and heat flow data for Basin and Range geothermal systems. Geothermal Resources Council Transactions 1: 19-20.
- Bonham-Carter, G.F., 1996, Geographic Information Systems for Geoscientists, Modelling with GIS: Elsevier Science Inc., Tarrytown, NY, 398 p.
- Buurman, H., Nye, C.J., West, M.W., and Cameron, C., 2014, Regional controls on volcano seismicity along the Aleutian arc: Geochemistry, Geophysics, Geosystems, v. 15, p. 1-17.
- Coolbaugh, M.F., Raines, G.L., and Zehner, R.E., 2007, Assessment of exploration bias in data-driven predictive models and the estimation of undiscovered resources: Natural Resources Research, v. 16, n. 2, p. 199-207.
- Doust, H., 2010, The exploration play: what do we mean by it?: AAPG Bulletin, v. 94, n. 11, p. 1657-1672.
- Facca, G. and Tonani, F., 1967, The self-sealing geothermal field; Bulletin Volcanologique, v. 30, p. 271-273.
- Faulds, J., Coolbaugh, M., Bouchot, V., Moeck, I., and Oğuz, K., Characterizing structural controls of geothermal reservoirs in the Great Basin, USA, and western Turkey: developing successful exploration strategies in extended terranes: World Geothermal Congress 2010, Bali, Indonesia, April 25-29, 2010, 11 p.
- Faulds, J.E., Hinz, N.H., Kreemer, C., and Coolbaugh, M., 2012, Regional patterns of geothermal activity in the Great Basin region, western USA: Correlation with strain rates: Geothermal Resources Council Transactions, v. 36, p. 897-902.
- Faulds, J.E., Hinz, N.H., Dering, G.M., and Siler, D.L., 2013, The hybrid model – the most accommodating structural setting for geothermal power generation in the Great Basin, western USA: Geothermal Resources Council Transactions, v. 37, p. 3-10.
- Faulds, N.H., and Hinz, N.H., 2015, Favorable tectonic and structural settings of geothermal settings in the Great Basin Region, western USA: Proxies for discovering blind geothermal systems: Proceedings, World Geothermal Congress 2015, Melbourne, Australia.

- Ferrill, D.A., Winterle, J., Wittmeyer, G., Sims, D., Colton, S. and Armstrong, A., 1999, Stressed rock strains groundwater at Yucca Mountain, Nevada: *GSA Today*, v. 9, no. 5, p. 1-8.
- Fournier, R.O., Truesdell, A.H., 1973. An Empirical Na-K-Ca Geothermometer for Natural Waters. *Geochimica et Cosmochimica Acta* 37: 1255-1275.
- Fournier, R.O., and Potter, II, R.W., 1979. Magnesium correction to the Na-K-Ca chemical geothermometer. *Geochim. Cosmochim. Acta* 43: 1543-1550.
- Fournier, R.O., 1981. Application of Water Geochemistry to Geothermal Exploration and Reservoir Engineering. In: Rybach, L. and Muffler, L.J.P., *Geothermal Systems: Principals and Case Histories*. Wiley, Chichester, pp. 109-143.
- Fugelli, E.M.G. and Olsen, T.R., 2005, Risk assessment and play fairway analysis in frontier basins: part 2 - examples from offshore mid-Norway: *AAPG Bulletin*, v. 89, n. 7, p. 883-896.
- Giggenbach, W.F., 1988. Geothermal Solute Equilibria. Derivation of Na-K-Mg-Ca Geoindicators. *Geochimica et Cosmochimica Acta* 52: 2749-2765.
- Giggenbach, W.F., 1992, "Chemical Techniques in Geothermal Exploration: Chapter 5", in, Franco D'Amore, coordinator, *Application of Geochemistry in Geothermal Reservoir Development*, Series of Technical Guides on the use of Geothermal Energy, UNITAR/UNDP Centre on Small Energy Resources, Rome-Italy, 1991, p. 119-144.
- Grant, M.A. and Bixley, P.F., 2011, *Geothermal Reservoir Engineering*: Academic Press, 359 p.
- Heidbach, O., Tingay, M., Barth, A., Reinecker, J., Kurfe, D. and Müller, B., 2008, The World Stress Map database release 2008 doi:10.1594/GFZ WSM Rel2008.
- Hinz, N.H., Faulds, J.E., and Stroup, C., 2011, Stratigraphic and structural framework of the Reese River geothermal area, Lander County, Nevada: a new conceptual structural model: *Geothermal Resources Council Transactions*, v. 35, p. 827-832.
- Hoagland, J.R. and Bodell, J.M., 1990, The Tiwi geothermal reservoir; geology, geochemistry, and response to production: *AAPG Bulletin*, v. 74, n. 6, p. 979, Fifth Circum-Pacific energy and mineral resources conference; abstracts, 1990.
- Karátson, D., Favalli, M., Tarquini, S., Fornaciai, A., & Wörner, G. 2010. The regular shape of stratovolcanoes: a DEM-based morphometrical approach. *Journal of Volcanology and Geothermal Research* 193(3): 171-181.
- Kreemer, C., Blewitt, G., and Klein, E.C., 2014, A geodetic plate motion and global strain rate model: *Geochimica et Cosmochimica Acta*, v. 15, p. 3849-3889. doi: 10.1002/2014GC005407.
- Laske, G., Masters, G., Ma, Z. and Pasyanos, M., 2013, Update on CRUST1.0 - A 1-degree Global Model of Earth's Crust, *Geophysical Research Abstracts*, 15, Abstract EGU2013-2658, 2013, (made available Aug. 2014).
- Mariner, R.H., Presser, T.S., and Evans, W.C., 1983, *Geochemistry of active geothermal systems in the northern Basin and Range Province*; Geothermal Resources Council Special Report No. 13.
- McCaffrey, R., King, R.W., Payne, S.J., and Lancaster, M., 2013, Active tectonics of the northwestern U.S. inferred from GPS-derived surface velocities: *Journal of Geophysical Research: Solid Earth*, v. 118, p. 709-723.
- Melosh, G., Moore, J., and Stacey, R., 2012, Natural reservoir evolution in the Tolhuaca geothermal field, southern Chile: *Proceedings, 36th Workshop on Geothermal Reservoir Engineering*, Stanford University, Stanford, CA, Jan. 30-Feb. 1, 2012, SGP-TR-194.
- Melosh, G., 2015, Geothermal well targeting method using structural irregularities: *Proceedings, 40th Workshop on Geothermal Reservoir Engineering*, Stanford University, Stanford, CA, Jan. 26-28, 2015, SGP-TR-204.
- Micklethwaite, S., and Cox, S.F., 2004, Fault-segment rupture, aftershock-zone fluid flow, and mineralization: *Geology*, v. 32, p. 813-816. doi:10.1130/G20559.1.
- Moore, J.N., Allis, R., Renner, J.L., Mildenhall, D., and McCulloch, J., 2002, Petrologic evidence for boiling to dryness in the Karaha-Telaga Bodas geothermal system, Indonesia: *Proceedings, 27th Workshop on Geothermal Reservoir Engineering*, Stanford University, Stanford, CA, Jan. 28-30, 2002, SGP-TR-171.
- Muffler, L.J.P. and Guffanti, M., 1995, Are there significant hydrothermal resources in the U.S. part of the Cascade Range?: *Proceedings, 20th Workshop on Geothermal Reservoir Engineering*, Stanford University, Stanford, CA, Jan. 24-26, 1995, SGP-TR-150, p. 9-16.
- Sibson, R.H., 1987, Earthquake rupturing as a mineralizing agent in hydrothermal systems: *Geology*, v. 15, p. 701-704.
- Sibson, R.H., 1994, *Crustal stress, faulting and fluid flow*: Geological Society, London Special Publication 78: 69-84.

- Sibson, R.H., 1996, Structural permeability of fluid-driven fault-fracture meshes: *Journal of Structural Geology*, v. 18, n. 8, p. 1031-1042.
- Siler, D.L., Faulds, J.E., and Hinz, N.H., 2015, Earthquake-related stress concentration in fault zones and permeability generation in geothermal systems: *Geothermal Resources Council Transactions* 39 437-446
- Smith, R. L., & Shaw, H. R., 1979. Igneous-related geothermal systems. *US Geol Surv Circ* 790, 12-17.
- USGS, 2010, United States Geological Survey Quaternary Fault and Fold Database of the United States: <http://earthquake.usgs.gov/hazards/qfaults/>, retrieved 2013.
- Wells, R.E., and McCaffrey, R., 2014, Steady rotation of the Cascade arc: *Geology*, v. 41, no. 9, p. 1027-1030.
- Wilmarth, M. and Stimac, J., 2015, Power density in geothermal fields: *Proceedings World Geothermal Congress*, Melbourne, Australia, Apr. 19-25, 2015.

13.0 TMT QUARTERLY REVIEW

13.1 Q1 Review

Comment: *Overall comment is that “NO action items requested in the assessment.”*

There is some concern about the readiness of the team to proceed to modelling as soon as has been proposed.

Response: Although the timing for the project was very tight, the team did proceed to modeling and produced results by the 10/16/15 deadline.

13.2 Q2 Peer Review

The following is excerpted from the Response to Review Comments submitted in response to the Peer Review held in May 2015.

Comment: *This project is unique among the play fairway group of projects in that it is not intending to discover prospect sized areas for future work. Instead it is identifying volcanic centers which are semi regional locations.*

Parts of the work performed as of the time of the Peer Review are truly worldwide in scale. In that sense it appears that it can break significant new ground in understanding which volcanic arcs or parts of volcanic arcs are most likely to host viable geothermal resources. It should result in papers that will be widely read and noted by the world-wide geothermal industry and generate considerable discussion and probably spawn further large scale research so it is expected to have a high impact.

Unfortunately, due to the location choice of the project it appears that this project is also unlikely to result in new exploration or recognize new site specific plays. That is the reason for the score that seems to be erroneously low relative to the previous comments.

This is the only play fairway project that could have significant impacts on another two play fairway projects.

The project is reported to be progressing on schedule.

Response: Thanks for your comments regarding the research aspect of this project. In regards to paragraph 3, we think this project is highlighting specific portions of the Aleutian and Cascade arcs that justify further exploration, and the play fairway methodology being developed will lend itself to identifying

a specific volcanic center or cluster of volcanic centers that warrant exploration in phase 2. Stage 3 could ultimately drill-test specific sites identified during phase 2 exploration.

Comment: *Need to do a better job of aligning their project with the GTO goals. May need to use a modified approach that is applicable to play fairway analysis in general so their methodology is transferable from one geologic setting to another.*

The awardees have developed preliminary fairway models and preliminary favorability models for both the Aleutians and the Cascades, but if the same models cannot even be used for the two areas of interest in this specific study, how can they be applied to geothermal play fairway analysis in general?

Along these same lines, the majority of the slides refer to arc systems and volcanic centers with only a few slides mentioning "generic" geothermal systems and "different play types". How are the awardees going to take a study that focuses primarily on arc systems and volcanic centers and then apply these data and analyses to play fairway analysis for different types of geothermal systems?

The results being shown in this presentation may be too narrow to be generally applicable to geothermal play fairway analyses in other tectonic settings. It seems that, at this point, the awardees should be directing their efforts toward results that have broader applications.

Slide 25 states, "Parameters of the power distribution curve can be modified for different play types." This statement seems to indicate that the awardees may have broader applications in mind, but how were the data in this slide obtained and analyzed, what are the uncertainties in the data, and exactly how can the parameters in this slide be modified and applied to different play types?

They do not appear to have identified the most promising prospects for development. What have they done to attract investors, potential users, and/or to publicize their work?

The awardees seem to be knowledgeable and have done a significant amount of data analysis at this point, but I'm not sure that their approach and the work they have done have broad applicability. I'm not sure that the money spent on this project has been money well spent given the GTO goals.

Response: Paragraph 1: Our ranking system builds directly on the play fairway concept, and the favorability rankings are directly applicable to all the volcanic centers in the Cascade and Aleutian Arcs, which is a huge area, much larger than the other project study areas, so we don't think approach or methodology is too limiting.

Paragraph 2: The reviewer is confused about what we are doing, perhaps because we did not explain it clearly during the time available in the presentation. In fact, the fairway modeling

approach we are using for the Cascade and Aleutian arcs is the same for each arc. The model consists of several stages, the first two of which were presented during the peer review. The first stage, which we term the 'Fairway', represents geothermal favorability based on intrinsic evidence before direct evidence such as hot springs and drill data are included. The second stage, which we term the 'Favorability Model', is a modified version of the 'Fairway Model' after direct evidence and degree-of-exploration have been factored in.

Paragraph 3: Our methodology incorporates all types of geothermal plays expected to be encountered in volcanic arcs, by employing appropriate indices based on geologic characteristics that could signal any particular recognized geothermal play. Our study area is much broader than most, if not all, of the study areas of the other research projects, so we feel the results are broadly applicable. In addition, our use of four key types of geologic tiers or hierarchies in the fairway modeling (permeability, heat, fluid composition, and cap rock), facilitates the modification of our approach so that it could be used for exploration of any geothermal play type, even those outside of active arcs.

Paragraph 4: See comments to paragraph 3 above.

Paragraph 5: Each geothermal play type could have a different size-frequency distribution. Because the peer review only reports on preliminary results, we have not yet calculated size-frequency distributions for different play types, but only showed the size-frequency distribution for all producing arc systems. We intend, to the extent allowable by the data, to calculate size-frequency distributions for each play type of the volcanic arcs.

Paragraph 6: We clearly did identify volcanic centers much more promising for geothermal development than others, as indicated by the color-coded rankings shown in slides 18-21. These indices can be used to select specific volcanic centers for more detailed exploration.

Paragraph 7: At the time of the peer review, we had presented one poster and abstract (GSA, Canada) and had submitted two papers (GRC, 2015). Since the peer review, we have submitted a third paper (GRC, 2015).

Paragraph 8: Again, we feel that these results are applicable to large regions (see above), even to larger regions than those of the other projects, which tend to have more spatially focused efforts.

Comment: *Their study area is scarcely populated and has no geothermal power generation facilities. They are seriously data limited and while they are building a fairway concept, the PI's admit that it may be "too general to be of much value." Fairly similarly systematically evaluating the geothermal potential of their area, but don't have any unique approaches.*

On the plus side they have collected data from all arc systems worldwide.

They have submitted 3 abstracts and have one publication.

Given the scarcity of data, the team's biggest contributions may be in new data correlations such as the one that resulted from their volunteer collaboration with Nevada Geodetic Laboratory and Max Wilmarth. The team has demonstrated a positive relationship between crustal deformation style (extension and shear) and power density and size of geothermal resources. Even if the team does not develop a complete play fairway concept, advances such as this could impact the research of others.

Response:

Paragraph 1: While our study area includes some sparsely populated areas, such as the Aleutian Islands, it also includes volcanic centers close to heavily populated areas, including Seattle, WA, Portland, OR, and Anchorage, AK.

Paragraph 2: There may have been a misunderstanding during the presentation. We believe our work to hold significant value, not only in predicting geothermal potential in the Cascades and Aleutians, but also because we are learning more about what types of tectonic and structural conditions are most important for the formation of viable geothermal systems. We do have some challenges in regard to data availability, but we are focusing our study to use types of data that have sufficient availability to be valuable, and are building into the model estimates of reliability of the data, as well as estimates of the degree of past exploration.

Paragraph 3: We believe that many of our approaches have not been used previously and thus we are braking some new ground. For the first time, we are using world models of strain rate, plate motion, and crustal thickness. We are also developing detailed assessments of structural and tectonic settings for each volcanic center with the help of structural specialists who are leaders in their field for making such assessments for geothermal systems. So on the contrary, we argue that we are using new data in a unique way to assess geothermal potential better than previously possible.

Paragraph 6: Yes, thank-you. We believe our research will have an impact on geothermal research and models elsewhere.

Comment: *The overall approach to this project is breaking new ground on a regional or continental scale utilizing new data that have become available since Muffler et al. 2000 first compared the Cascades with the Japanese Arc.*

Response: Yes, thanks. A number of years have passed since the Muffler work, and much more data are available now than before. So we think this is an overdue research project that can leverage better data sets to refine our knowledge of the factors that control the development of viable geothermal systems.

Comment: *Seem to be assessing data in arc settings and volcanic centers around the world. However, on a number of slides displaying these global data, data from the Cascades and Aleutian arcs are not shown for comparison.*

Slide #18 in the presentation shows the differences in the Aleutian arc preliminary fairway model and states that the "Higher indices driven by more complex/favorable structural settings". Could the awardees be more specific about what these more complex/favorable structural settings are? In the SOPO, the awardees state that estimated productivity will be drawn from volumetric-based Monte Carlo simulations. Is this what is being shown in slide #18? Why aren't the Cascades shown in slide #18? Why are the indices lower to the east? Is the technology used to create this map easily transferable to other areas and projects?

In the next slide, the awardees state, "Relative weighting changes (updates) when direct evidence (geothermometry, well data, and surface features) are considered", but the indices still generally get lower to the east. Why?

What are the differences between slide #18 ("Aleutian Arc Preliminary Fairway Model") and slide #19 ("Aleutian Arc Preliminary Favorability Model")? Why are Atka, Akutan, and Makushin pointed out on slides 18 and 19?

Slide #20 is "Cascade Arc Preliminary Fairway Model" and slide #21 is "Cascade Arc Preliminary Favorability Model". Why are different models being used for the Aleutians versus the Cascades? If the same models cannot even be used for the two areas of interest in this study, how can they be applied to geothermal play fairway analysis in general?

Why are Mt. Meager, Mt. Hood, Medicine Lake, and Mt. Lassen pointed out on slides 20 and 21?

Response:

Paragraph 1: Okay, given the scale of a world map, it is sometimes challenging to display all features from volcanic arcs around the world simultaneously. We will try to do better in the future.

Paragraph 2: Yes, to be more specific, the more complex/favorable structural settings in this region are composed of transtensional tectonics with multiple fault intersections. Given the regional scale of our project, we now believe that volumetric Monte Carlo simulations may not be practical (so we are not showing a Monte Carlo ranking in slide 18, instead the rankings are based on the methodologies documented in slides 14, 15, and 16). However, we will use some type of error estimation to characterize the perceived accuracy and reliability of our index rankings. The Cascades are not shown in slides 18 and 19 because they are shown in slides 20 and 21. The indices are lower in the east on slide 18 in significant part because of a more transpressional setting. The technology used to create the map are immediately transferable to all other volcanic arcs in the world, including the Cascades (see slides 20 and 21), and the approach can be readily modified to assess other types of geothermal plays.

Paragraph 3: The indices are lower in the east largely because the tectonic setting appears to be more transpressional in nature.

Paragraph 4: Sorry for not making this clear. Slide 18 represents our "Fairway Model" (see slide 14) based on the presence of geologic characteristics, and slide 19 represents an updated estimate based on direct evidence of geothermal activity, such as hot springs, geothermal wells, etc., and modified by the degree of exploration (again, see slide 14 to see how these two models are related to each other). The Fairway Model represents the favorable terrain based on geological characteristics (the "Fairway"), while slide 19 (the 'Favorability Model') represents an updated prediction based on direct evidence. Atka, Akutan, and Makushin were pointed out on the slides because they are known sites of geothermal activity, so they serve as points of reference so that the viewer can see how these systems rank compared to nearby areas.

Paragraph 5: The models for the Aleutians and Cascades are exactly the same. They are the same models. The only reason they are being shown on different slides is because of the scale. If we showed them on the same slides, everything would be much smaller and more difficult to see.

Paragraph 6: Mt. Meager, Mt. Hood, Medicine Lake, and Mt. Lassen were pointed out on the slides because they are known sites of geothermal activity, so they serve as points of reference so that the viewer can see how these systems rank compared to nearby areas.

Comment: *Given the scarcity of data in their study region, they have collected data from arcs globally. They are using a GIS system putting multiple datasets in using a tiered modeling approach. Key hierarchical tiers have weighting factors for different types of data.*

Worldwide, they have found 84 systems in arc systems and acquired data on those power plants. 733 volcanic centers are available, but only 74 have a productive power system. They have collected 160 data fields and are working to determine what is most important. They have identified their key factors: structure, strain, clay caps, volcanism, permeability/lithology, geochemistry, surface manifestations. Surface features including fumaroles and deposits will be included. Issues of social concern, land use, etc. will be incorporated into their evaluation.

Cascades and Aleutians seem less prospective. No evidence for huge systems. One modeling approach may apply is some kind of direct analog. Looked at regional data to find an analog. Will develop an index and see how existing systems score.

Looking at many subduction related parameters. Best thus far is the magnitude of arc parallel subduction. "It is challenging" to define regional parameters in arc settings. "Gets down to what's happening in each individual center."

Empirical approach. Established cut-offs to include things and lumped things.

Possible approach is defining play sub-types with different size type distributions.

Response: Yes, we are considering some of these possibilities.

STRENGTHS

Comment: *This is a very strong project from an academic perspective. It has the potential to be perhaps the most interesting of all the play fairway projects.*

In the Cascades this project appears to be leading to an understanding of why the southern portion of the arc has higher quality resources. It also provides an explanation as to why all of the drilling at Meager Mountain has been unsuccessful in locating commercial permeability. Unfortunately, this apparent understanding has come too late for the funders of that project.

Comment: *The experience and knowledge of the individuals making up this team.*

Comment: *Since they have limited data on their region, the project is leveraging data on island arcs worldwide. Leveraging networking to secure new data sets ("Nevada Geodetic Laboratory and Max Wilmarth have joined the collaboration team on a volunteer basis: Kreemer has contributed a new global strain rate and plate tectonic model and Wilmarth has contributed world data on geothermal system power densities.")*

WEAKNESSES

Comment: *The primary weakness of this project is that it is unlikely to lead to new geothermal developments in the Aleutians or Cascades in the next decade. The Aleutians are just too remote and under populated to support a significant geothermal industry in the foreseeable future and the most obvious Aleutian resources have already been identified. This project is unlikely to lead to drilling in the Aleutians.*

It is unclear as to whether this project will lead to a revival of exploration in the southern part of the Cascade Range as it is hampered by environmental issues and land use restrictions in the most promising areas.

It is difficult to see how this project could lead to siting of temperature-gradient holes in the overall time frame of the program.

Response:

Paragraphs 1 and 2: The Cascades and Aleutians have been problematic with their lack of established geothermal energy production. We believe that if we can better explain why this is the case from a geological perspective, and at the same time illustrate which portions of these arcs have the best potential for geothermal energy development, it could serve to help reinvigorate exploration in the most appropriate areas. If we can reduce the risk of exploration, through a better understanding of which portions of the arcs warrant exploration and development, a new stage of exploration could begin. There are certainly challenges in terms of accessibility and land use restrictions in some portions of these arcs, but other areas are more accessible.

Paragraph 3: We foresee the selection of one or more volcanic centers for exploration work in phase 2, which could easily lead to the selection of temperature gradient sites for drilling in phase 3.

Comment: *Although the PI presenting the talk has considerable experience in geothermal resources, she seemed not to have practiced her talk. At one point, when she was about 2/3 through the 20 minutes allocated for the talk but only about 40% through the slides, she made a comment about how she, "... guessed she better get moving." From that point on, she appeared to rush through the remaining slides. In addition, although the instructions to presenters clearly stated that, excluding the title page, the presentation could be a maximum of 15 slides, at the time the PI finished the presentation, she was on slide #19, and the total number of slides in the presentation was 30.*

Much regional exploration data used in this study has relatively high uncertainties. Among the greatest challenges in this project are the large amount of data search and compilation that are required and the incomplete and uneven nature of the data. Given the variability of the data, how reliable are the various cut offs being applied to determine what will and what won't be productive?

There are no power generation facilities in either of these arcs, so how are the awardees going to determine sites that are appropriate for testing their models? Have they found any good existing analogs for either the Aleutians or Cascades?

Response:

Paragraph 1: Sorry, we will try to do better next time. Please note that these are only preliminary results and that the slides were required to be finalized well before the half-way point in the project timeline. This has been especially challenging for us because of the huge amount of data-collection activities necessary because of the world-wide scope of our investigation. We still managed to generate some preliminary model results prior to the deadline for submitting the PowerPoint presentation.

Paragraph 2: We will be characterizing uncertainties as part of this project.

Paragraph 4: We are not using cut offs.

Paragraph 5: This is why we are looking at volcanic arcs elsewhere in the world. You could think of this as a worldwide analogy. We are identifying the key geologic features for a productive system elsewhere in the world, and then looking for those same characteristics in the Aleutians and Cascades.

Comment: *Limited data within their geographic region. Inconsistency in the data that is available.*

Response:

We are designing the project to use the data that are the most available and reliable, and we are monitoring the degree of data availability for each area. It is true that data availability is frustrating in some places, but yet, there is a huge amount of data and information available overall, and data quality is improving from year to year.

IMPROVEMENTS

Comment: *I have no recommended improvements for this project.*

Response: Okay.

Comment: *The project needs to change its emphasis to develop applications that are more broadly applicable and transferable to play fairway analysis in general.*

During her presentation, the PI stated that "This is basically permeability" model, but none of the slides address this statement. If their work is indeed basically a permeability model, it might have broader applications than what were indicated in the presentation.

In addition, how does their model, which is basically a "permeability" model contrast and compare with geothermal models that consider permeability, heat, and fluids in their play fairway analysis?

Response:

Paragraphs 1 and 2: We believe our results are broadly applicable to geothermal play fairway analysis in other areas. Yes, permeability is the key factor in our model, and as you indicate, since permeability is a key factor in other geothermal play types outside of volcanic arcs, the approaches we have developed could be valuable for better assessing geothermal potential in much broader regions.

Paragraph 3: To enhance the applicability of our model throughout the world for all geothermal areas, we have carefully considered four geologic factors in our model (permeability, heat, fluids, and cap rock). In the specific case of volcanic arcs, heat is usually present (because of active or recent volcanism), adequate fluids are usually available (near-neutral pH), and cap rock is usually present (due to the ability of volcanic rocks in high levels of these systems to form clay). For these reasons, the remaining factor, permeability, is especially important in volcanic arcs, and has therefore received the greatest attention in our model. So to answer the question, we are considering all factors in our model, and weighting them accordingly. Even though our model relies most heavily on permeability, we are considering all of the factors.

Comment: *The PI's note that volunteer collaboration with Nevada Geodetic Laboratory and Max Wilmarth have resulted in contribution of a new global strain rate and plate tectonic model and new data on geothermal system power densities that enabled the team to demonstrate a positive relationship between crustal deformation style (extension and shear) and power density and size of geothermal resources. Even if the team does not develop a complete play fairway concept, advances such as this one could be important. The team should continue to leverage their network and develop new data correlations.*

Response: Thanks. We would like to do this.

13.3 Q3 Review

Comment: The written Quarterly Report shows that the project is basically on track to complete Phase I. This work is a valuable contribution to a worldwide geothermal audience

Comment: *Project appears to have little information on reservoir rocks and insufficient data on clay caps—fluid, heat and seals don't seem to appear in the evaluation. Few correlations between producing systems and 294 columns of other data were found.*

Response: Clay caps were not explicitly modeled in Phase I due to lack of available data from which to quantitatively model their presence/absence, thickness, extent and composition. There seems to be a misunderstanding regarding the second comment in that *many* correlations were found between the producing systems and the Cascade and Aleutian systems (See Sections 3.0 and 4.0). The PI likely noted that we saw limited correlations with respect to volcanic characteristics such as composition, compositional diversity, eruptive style and frequency and volcanic vent types. Considerable and consistent correlations were identified related to other factors such as temperature, structural styles, regional tectonics and strain rates, fumarole areas and others.

Comment: *The PI appears to believe that this project will not move onto phase 2, and appears to have lost some enthusiasm. The proposal for Phase II is fraught with land use issues in the Cascades, remoteness of the hotter Aleutian Islands, and difficulty of getting an industry match except at Akutan. The suggestion of focusing Phase II on Northern California was not supported by the rest of the PI's presentation. It isn't clear how the proposed Phase II work to identify 3-4 play fairways having power-producing potential will be conducted.*

Response: The PI apologizes for confusion as she believes the project can and should move to Phase 2 based on the significant, positive results indicating multiple power producing systems occur in the Cascades and Aleutians. The PI merely intended to indicate that it would be difficult to obtain industry cost share for the Aleutians as there are few viable markets from which a company could anticipate profits. This was one consideration in selecting parts of the southern Cascades for Phase II. The PI acknowledges the land use issues in the Cascades, but the results suggest significant potential may exist in poorly explored areas around Lassen and in Southern Oregon where increased renewable power production will become increasingly important in light of the new California RPS of 50%.

14.0 DOWNSELECT CRITERIA

1. The technical strength of the methodology employed in the analysis – 25%
 - Are assumptions clearly stated and reasonable – **See Sections 5.0 and 6.0**
 - Are sound scientific principles being used – **All Sections**
 - Have methods been validated in other areas (e.g. O&G, minerals) – **See Section 6.0**

- Is the approach the same as was proposed or were there modifications – **The same approach was used with minimal modifications. Variance noted in Section 13.3 Q3 Review, first response to comment**
2. The degree to which the Phase 1 report presents a rigorous quantification of project risk – 25%
- Is data (quantity and quality) sufficient to make a meaningful analysis, and how was this demonstrated – **Section 5.0 details data quality and uncertainties used in the Model of Section 6.0, which includes additional factors related to risk based on degree of exploration.**
 - Are (quantitative) probabilities of success presented along with uncertainty – **Yes, see Section 7.0**
3. Utility of the methods for application at other sites – 25%
- How specific is the analysis to the region it was developed for, is it transferable to other areas of interest. **Overall model formulation and rationale is applicable to other regions, although additional or fewer specific data types may be necessary for other regions (e.g., ranking of structural settings may vary by region).**
 - Report package makes available all data and custom codes used in the analysis (and code is properly commented and organized). **All compiled and modeled data are to be submitted to GRD by the 10/31/15 deadline. Modeling was conducted in Excel (and ArcGIS using statistical packages).**
 - Is there a training dataset that is usable at other areas? **The 74 training sites are a global training set from 16 countries (outside the US) and are used as benchmark sites in modeling the Cascades and Aleutians, and as such, are applicable world-wide. This is the first publically available training set of its kind available world-wide and it is a relatively large one.**
 - Are there adjustable parameters in the tools to allow for others to tweak and re-run the analysis. **Most weightings can be re-evaluated and re-specified by subsequent users. The training data set from 16 countries can be used world-wide in other volcanic arc settings and is largely transferable to other volcanic settings such as the East African Rift.**
 - Software Platform – standard software, transferable data types. **Data sets to be submitted are primarily in Excel format, easily used by all. Modeling is conducted in ArcGIS, also a common platform, with the data from the Excel sheets input into the model.**
4. Commercial viability of the play – 25%
- Does the analysis indicate presence of a resource? **The analyses indicate the presence of multiple resources (see section 7.0) in both the Cascades and Aleutians**
 - What is the potential size of the resource, and are anticipated temperatures sufficient for development. **Many of the volcanic centers are capable of small power production (<50 MW), and several are capable of up to 100 MW power production (see Section 7.0).**
 - Are there local factors supporting development (local price of electricity, etc.). **California has recently increased its renewable portfolio standard to 50%, which will make the**

targets identified in Northern California and Southern Oregon particularly attractive in this currently geothermally underdeveloped region of the US.

- What is the land position of the identified fairways? **See Sections 7.4-7.6 where land status is used to adjust the rankings based on land availability for development. Some highly ranking sites (e.g., Lassen) are removed from the final ranking due to the inability to develop on those lands.**
- Does the analysis include project economics (with support for assumptions)? **No.**
- Are any other hurdles addressed (environmental, proximity to markets, transmission, water, etc.) and how significant are those hurdles? **Over several decades, the hurdles in Northern California and Southern Oregon have consistently been related to land access and time to acquire permits on Forest Service land, on which most of the volcanic centers are located (See Section 7.4). Distances to transmission are noted in Section 7.7. Many of the volcanic centers are in relatively remote areas, but in a very populated state with large power demands.**
- Are there potential industry partners identified, or currently involved. Is there any other commercialization plan presented? **No current developers are included as partners, but three of the five partner organizations conducting the Phase I work are private companies.**

APPENDICES

APPENDIX I: References used in Constructing Databases (34 pages).

APPENDIX II: Basic information of volcanic centers (VC) evaluated in this work (13 pages).

APPENDIX III: Listing of international VC with power plants that are used as the training set (benchmarks) in this work (2 pages).

APPENDIX IV. Known flank fumarole occurrences, with noted surface area of disturbance if available, for the Cascade, Aleutian and international benchmark VC (4 pages).

APPENDIX V. Play Fairway and Favorability Maps for the Cascades showing land use designations and major transmission corridors (8 pages).

APPENDIX I

References used in Constructing Databases

Part 1 – Geochemistry References

- Acuña J.A., Stimac J., Sirad-Azwar L., Pasikki R.G., 2008. Reservoir management at Awibengkok geothermal field, West Java, Indonesia. *Geothermics* 37: 332-346.
- Adams A., Dennis B., Van Eeckhout E., Goff F., Lawton R., Trujillo P.E., Counce D., Medina V., Archuleta J., 1991. Results of Investigations at the Zunil Geothermal Field, Guatemala: Well Logging and Brine Geochemistry. Los Alamos National Laboratory: 48 pp.
- Adams A.I., Aycinena S., Castañeda O., Chipera S., Counce D., Duffield W., Fahlquist L., Gardner J., Goff S., Goff F., Heiken G., Janik C., Laughlin A.W., Martinelli L., Moore J.N., Musgrave J., Revolorio M., Roldan A., Trujillo P.E. Jr., 1992. Results of Geothermal Gradient Core Hole TCB-1 Tecuamburro Volcano Geothermal Site Guatemala, Central America. Los Alamos National Laboratory: 79 pp.
- Adams M.C., Moore J.N., 1987. Hydrothermal Alteration and Fluid Geochemistry of the Meager Mountain Geothermal System, British Columbia. *Am J of Sci* 287: 720-755.
- Adams M.C., Moore J.N., Forster C., 1985. Fluid Flow in Volcanic Terrains - Hydrogeochemistry of the Meager Mountain Thermal System. *Geoth. Res. Council Trans.* 9 Part II: 377-382.
- Ajima S., Todaka N., Akasaka C., 2010. Multivariate Analysis for Chemical Evolution of Reservoir Water for 35-year Operation of the Onikobe Geothermal Plant, Japan. *WGC 2010*: 6 pp.
- Akaku K., Reed M.H., Yagi M., Kai K., Yasuda Y., 1991. Chemical and physical processes occurring in the Fushime geothermal system, Kyushu, Japan. *Geochemical Journal* 25: 315-333.
- Allen E.T., Zies E.G., 1923. A Chemical Study of the Fumaroles of the Katmai Region. *Contributed Technical Papers, Katmai Series, National Geographic Society* 2: 75-155.
- Alvis-Isidro R.R., Solaña R.R., D'Amore F., Nuti S., Gonfiantini R., 1993. Hydrology of the Greater Tongonan Geothermal System, Philippines, as Deduced From Geochemical and Isotopic Data. *Geothermics* 22, No. 5/6: 435-449.
- Anderson E.B., Jacobo H.R., Ussher G.N.H., 1994. The Berlin Geothermal System - From the Surface to the Magma Chamber? *NZ Geoth Workshop* 16: 127-132.
- Angcoy Jr. E.C., 2010. Geochemical Modelling of the High-Temperature Mahanagdong Geothermal Field, Leyte, Philippines. Master's thesis, Faculty of Science, University of Iceland: 126 pp.
- Angcoy Jr. E.C., 2011. Geochemical Modeling of Wells Discharging Excess Enthalpy by Mechanism of Phase Segregation in Mahanagdong, Leyte, Philippines. *Stanford Geoth. Workshop* 36: 808-816.
- Aragon G.M., Sambrano B.M., 2010. Assessment of Boiling Processes and Initial Steam Fractions of the Mindanao Geothermal Production Field, PHILIPPINES. *WGC 2010*: 6 pp.
- Aravena D., Villalón I., Sánchez P., 2015. Igneous Related Geothermal Resource in the Chilean Andes. *WGC 2015*: 8 pp.
- Ariki K., Kato H., Ueda A., Bamba M., 2000. Characteristics and management of the Sumikawa geothermal reservoir, northeastern Japan. *Geothermics* 29: 171-189.
- Ariki K., Kawakami Y., 2000. Production History of the Ohnuma Geothermal Field, Northeast Japan. *WGC 2000*: 2031-2036.
- Asturias F., Grajeda E.C., 2010. Geothermal Resources and Development in Guatemala Country Update. *WGC 2010*: 7 pp.
- Atmojo J.P., Itoi R., Tanaka T., Sudarman S., Widiyarso A., 2000. Modeling Studies of Sibayak Geothermal Reservoir, Northern Sumatra, Indonesia. *WGC 2000*: 2037-2043.
- Austin J.A., 2014. The State of California's GeoSteam Database & Well Finder On-line Mapping System. *Stanford Geoth. Workshop* 38: 9 pp.

- Baldi P., Ferrara G.C., Masselli L., Pieretti G., 1973. Hydrogeochemistry of the Region Between Monte Amiata and Rome. *Geothermics* Vol. 2: 124-141.
- Baldi P., Ferrara G.C., Masselli L., Pieretti G., 1973. Hydrogeochemistry of the Region Between Monte Amiata and Rome. *Geothermics* Vol. 2: 124-141.
- Barnes I., Johnston D.A., Evans W.C., Presser T.S., Mariner R.H., White L.D., 1981. Properties of waters and gases of deep origin. In Lipman P.W., and Mullineaux D.R., eds., 1981. *The 1980 eruptions of Mount St. Helens, Washington*. U S Geol Surv Prof Pap 1250: 233-237.
- Barnett B., Korosec M.A., 1986. Geothermal Exploratory Drilling by the State of Washington in 1985. *Washington State Geological Newsletter* 14, 1-2: 21-28.
- Barragán R.M., Arellano V.M., Nieva D., Portugal E., Garcia A., Aragón A., Tovar R., Torres-Alvarado I., 2000. Gas Geochemistry of the Los Humeros Geothermal Field, México. *WGC 2000*: 2527-2532.
- Beall J.J., 1981. A Hydrologic Model Based on Deep Test Data from the Walker "O" No. 1 Well, Terminal Geyser, California. *Geoth. Res. Council Trans.* 5: 153-156.
- Bellani S., Brogi A., Lazzarotto A., Liotta D., Ranalli G., 2004. Heat flow, deep temperatures and extensional structures in the Larderello geothermal field (Italy): constraints on geothermal fluid flow. *J. Vol. Geoth. Res.* 132: 15-29.
- Benoit W.R., 1977. Report on the Newberry Crater, Oregon Geothermal Prospect. Phillips Petroleum Co. Geothermal Division Technical Report: 38 pp., 5 plates.
- Benoit W.R., 1983. An Explorationist Viewpoint of the High-Temperature Geothermal Potential of the Cascade Range in Oregon. *Geoth. Res. Council Trans.* 7: 227-232.
- Bergfeld D., Evans W.C., McGee K.A., Spicer K.R., 2008. Pre- and post-eruptive investigations of gas and water samples from Mount St. Helens, Washington, 2002 to 2005. In Sherrod D.R., Scott W.E., Stauffer P.H., eds., 2008. *A volcano rekindled: The renewed eruption of Mount St. Helens, 2004–2006*: U S Geol Surv Prof Pap 1750: 523-542.
- Bergfeld D., Lewicki J.L., Evans W.C., Hunt A.G., Revesz K., Huebner M., 2014. Geochemical investigation of the hydrothermal system on Akutan Island, Alaska, July 2012. *U S Geol Surv Sci Invest Rpt 2013-5231*: 20 pp.
- Bergfeld D., Lewicki J.L., Evans W.C., Hunt A.G., Revesz K., Huebner M., 2014. Geochemical investigation of the hydrothermal system on Akutan Island, Alaska, July 2012. *U S Geol Surv Sci Invest Rpt 2013-5231*: 20 pp.
- Bertini G., Cappetti G., Dini I., Lovari F., 1995. Deep Drilling Results and Updating of Geothermal Knowledge on the Monte Amiata Area. *WGC 1995*: 1283-1286.
- Blackwell D.D., Baker S.L., 1988. Thermal Analysis of the Breitenbush Geothermal System. *Geoth. Res. Council Trans.* 12: 221-227.
- Blackwell D.D., Bowen R.G., Hull D.A., Riccio J., Steele J.L., 1982. Heat Flow, Arc Volcanism, and Subduction in Northern Oregon. *J. Geophys. Res.* 87(B10): 8735-8754.
- Blackwell D.D., Bowen R.G., Hull D.A., Riccio J., Steele J.L., 1982. Heat Flow, Arc Volcanism, and Subduction in Northern Oregon. *J. Geophys. Res.* 87(B10): 8735-8754.
- Blackwell D.D., Priest G.R., 1996. Comment on "Rates and patterns of groundwater flow in the Cascade Range volcanic arc and the effect on subsurface temperatures". *J. Geophys. Res.* 101(B8): 17561-17568.
- Blackwell D.D., Steele J.L., 1987. Geothermal Data from Deep Holes in the Oregon Cascade Range. *Geoth. Res. Council Trans.* 11: 317-322.
- Blackwell D.D., Steele J.L., Kelley S., 1990. Heat Flow in the State of Washington and Thermal Conditions in the Cascade Range. *J. Geophys. Res.* 95(B12): 19495-19516.
- Bogie I., Kusumah Y.I., Wisnandary M.C., 2008. Overview of the Wayang Windu geothermal field, West Java, Indonesia. *Geothermics* 37: 347-365.

- Bogie I., Kusumah Y.I., Wisnandary M.C., 2008. Overview of the Wayang Windu geothermal field, West Java, Indonesia. *Geothermics* 37: 347-365.
- Bortnikova S.B., Bessonova E.P., Gavrilenko G.M., Vernikovskaya I.V., Bortnikova S.P., Palchik N.A., 2008. Hydrogeochemistry of Thermal Sources, Mutnovsky Volcano, South Kamchatka (Russia). *Stanford Geoth. Workshop 33*: 350-358.
- Bortnikova S.B., Bortnikova S.P., Manstein Yu.A., Kiryuhin A.V., Vernikovskaya I.V., Palchik N.A., 2009. Thermal Springs Hydrogeochemistry and Structure at North-Mutnovskoe Fumarole Field (South Kamchatka, Russia). *Stanford Geoth. Workshop 34*: 291-299.
- Bortnikova S.P., Bortnikova S.B., Gora M.P., Shevko A.Y., Lesnov F.P., Kiryuhin A.V., 2010. Boiling Mud Pots: Origin and Hydrogeochemistry (Donnoe and North-Mutnovsky Fumarolic Fields, Mutnovsky Volcano; South Kamchatka, Russia). *WGC 2010*: 7 pp.
- Brotheridge J.M.A., Browne P.R.L., Hochstein M.P., 1995. The Ngatamariki Geothermal Field, NZ: Surface Manifestations - Past and Present. *NZ Geoth. Workshop 17*: 61-66.
- Brown K.L., Bixley P.F., 2005. Geochemistry of the Lihir Geothermal Field, Papua New Guinea. *WGC 2005*: 6 pp.
- Browne P.R.L., Rodgers K.A., 2006. Occurrence and significance of anomalous chloride waters at the Orakei Korako geothermal field, Taupo Volcanic Zone, New Zealand. *Geothermics* 35: 211-220.
- Bruton C.J., Moor J.N., Powell T.S., 1997. Geochemical Analysis of Fluid-Mineral Relations in the Tiwi Geothermal Field, Philippines. *Stanford Geoth. Workshop 22*: 457-463.
- Burgassi P.D., Ceron P., Ferrara G.C., Sestini G., Toro B., 1970. Geothermal Gradient and Heat Flow in the Radicofani Region (East of Monte Amiata, Italy). *Geothermics Special Issue 2, Vol. 2, Part 1*: 443-449.
- Butler D.L., Keller G.V., 1975. Appendix B Exploration on Adak Island, Alaska. In Grose L.T., Keller G.V., 1975. *Geothermal Energy in the Pacific Region*. U.S. Office of Naval Research: B1-B31
- Caicedo A.A., Palma A.J., 1990. Present Status of Exploration and Development of the Geothermal Resources of Guatemala. *Geoth. Res. Council Trans.* 14: 97-105.
- Capuno V.T., Maria R.B.S., Minguez E.B., 2010. Mak-Ban Geothermal Field, Philippines: 30 Years of Commercial Operation. *WGC 2010*: 7 pp.
- Chavarría L., Rodríguez A., 2010. Geothermal Reconnaissance of the Caribbean Flank of the Rincón de la Vieja Volcano, Costa Rica. *WGC 2010*: 7 pp.
- Chelnokov G., 2004. Interpretation of Geothermal Fluid Compositions from Mendeleev Volcano, Kunashir, Russia. *UNU-GTP Reports 2004, Number 5*: 57-82.
- Chen C., Sanyal S.K., 2006. Power Generation Potential at Chingshui Geothermal Field, Taiwan. *Stanford Geoth. Workshop 31*: 83-93.
- Cherng, F., 1979. Geochemistry of the Geothermal Fields in the Slate Terrane. *Geoth. Res. Council Trans.* 3: 107-111.
- Clark I.D., Phillips R.J., 2000. Geochemical and $^3\text{He}/^4\text{He}$ evidence for mantle and crustal contributions to geothermal fluids in the western Canadian continental margin. *J. Vol. Geoth. Res.* 104: 261-276.
- Clemente W.C., Villadolid-Abrigo F.L., 1993. The Bulalo Geothermal Field, Philippines: Reservoir Characteristics and Response to Production. *Geothermics* 22 No. 5/6: 381-394.
- Clynne M.A., Janik C.J., and Muffler L.J.P., 2003. "Hot water" in Lassen Volcanic National Park – Fumaroles, steaming ground, and mudpots. *U S Geol Surv Fact Sheet 101-02*: 4 pp.
- Cortecci G., Boschetti T., Mussi M., Lameli C.H., Mucchino C., Barbieri M., 2005. New chemical and original isotopic data on waters from El Tatio geothermal field, northern Chile. *Geochemical Journal* 39: 547-571.
- Crisostomo J.N.R., Villaseñor L.B., Calibugan A.A., 2015. Developing the Acid Reservoir at Tiwi Geothermal Field, Philippines. *WGC 2015*: 10 pp.
- Cuéllar G., 1990. Country Update Report for El Salvador, *Geoth. Res. Council Trans.* 14: 41-45.

- Daco-ag L.M., Cabahug M.R., Fernandez I.M., Dancillo D., Alcober E., 2015. Update on the Stable Isotope Geochemistry of the Leyte Geothermal Production Field. WGC 2015: 5 pp.
- D'Amore F., Fancelli R., Saracco L., Truesdell A.H., 1987. Gas Geothermometry Based on CO Content -- Application in Italian Geothermal Fields. Stanford Geoth. Workshop 12: 247-252.
- D'Amore F., Maniquis-Buenviaje M., Solis R.P., 1993. An Evaluation of the Deep Reservoir Conditions of the Bacon-Manito Geothermal Field, Philippines Using Well Gas Chemistry. Stanford Geoth. Workshop 18: 235-240.
- D'Amore F., Mejia J.T., 1999. Chemical and physical reservoir parameters at initial conditions in Berlin geothermal field, El Salvador: A first assessment. *Geothermics* 28: 45-73.
- D'Amore F., Ramos-Candelaria M.N., Seastres Jr. J.S., Ruaya J.R., Nuti S., 1993. Applications of Gas Chemistry in Evaluating Physical Processes in the Southern Negros (Palinpinon) Geothermal Field, Philippines. *Geothermics* 22, No. 5/6: 535-553.
- Daud Y., Atmjo J.P., Sudarman S., Ushijima K., 1999. Reservoir Imaging of the Sibayak Geothermal Field, Indonesia using Borehole-to-Surface Resistivity Measurements. NZ Geoth. Workshop 21: 139-144.
- Dawson G.B., Dickinson D.J., 1970. Heat Flow Studies in Thermal Areas of The North Island of New Zealand. *Geothermics Special Issue 2, Vol. 2, Part 1*: 466-473.
- Dennis B., Goff F., Van Eeckhout E., Hanold B., 1989a, Results of Investigations at the Ahuachapan Geothermal Field, El Salvador, Part 1: Well Logging and Brine Geochemistry. Los Alamos National Laboratory: 68 pp.
- Detterman R.L., Wilson F.H., Yount M.E., Miller T.P., 1987. Quaternary geologic map of the Ugashik, Bristol Bay, and western part of Karluk quadrangles, Alaska. U S Geol Surv Map, I-1801.
- Di Paola M., Luccioli F., Rico Calderon G., 1990. Geothermal Feasibility Study of Laguna Colorada - Bolivia. *Geoth. Res. Council Trans.* 14: 867-872.
- DiPippo R., Moya P., 2013. Las Pailas geothermal binary power plant, Rincón de la Vieja, Costa Rica: Performance assessment of plant and alternatives. *Geothermics* 48: 15 pp.
- Duchi V., Minissale A.A., Rossi R., 1986. Chemistry of thermal springs in the Larderello-Travale geothermal region, southern Tuscany, Italy. *Applied Geochemistry* 1: 659-667.
- Evans W.C., Mariner R.H., Ingebritsen S.E., Kennedy B.M., van Soest M.C., Huebner M.A., 2002b. Report of hydrologic investigations in the Three Sisters area of central Oregon, summer 2001. U S Geol Surv Water-Resour. Invest. Rept 02-4061: 13 pp.
- Evans W.C., van Soest M.C., Mariner R.H., Hurwitz S., Ingebritsen S.E., Wicks Jr. C.W., Schmidt M.E., 2004. Magmatic intrusion west of Three Sisters, central Oregon, USA: The perspective from spring geochemistry. *Geology* 32(1): 69-72.
- Evans, W.C., Bergfeld, D., Neal, C.A., McGimsey, R.G., Werner, C.A., Waythomas, C.F., Lewicki, J.L., Lopez, T., Mangan, M.T., Miller, T.P., Diefenbach, A., Schaefer, J., Coombs, M.L., Wang, B., Nicolaysen, K., Izbekov, P., Maharrey, Z., Huebner, M., Hunt, A.G., Fitzpatrick, J., and Freiburg, G., 2015, Aleutian Arc geothermal fluids: chemical analyses of waters and gases sampled in association with the Alaska Volcano Observatory, U.S. Geological Survey Data Release, <http://dx.doi.org/10.5066/F78G8HR1>
- Fahrurrozie A., Saputra M.P., Nugraha T., 2015. The Application of Na-K-Mg, Na-K/Mg-Ca and K-Mg/Quartz Diagram to Evaluate Water Geochemistry in West Java Geothermal Prospects, Indonesia. WGC 2015: 8 pp.
- Fierstein J., Hildreth W., 2008. Kaguyak dome field and its Holocene caldera, Alaska Peninsula. *J. Vol. Geoth. Res.* 177: 301-312.
- Firmansyah W., Sujarmaitanto H., Mulyanto, Hartanto D.B., Wicaksono T., 2015. Geochemistry Monitoring in the Kamojang Vapor-dominated Geothermal Field from 2010 to 2013. WGC 2015: 6 pp.
- Flowers C., 1997. Observations of Geothermal Activity near Pavlof Volcano on the Alaska Peninsula During March and April of 1996. U S Geol Surv Open-File Rept 97-146: 13 pp.

- Frank D., Surficial extent and conceptual model of hydrothermal system at Mount Rainier, Washington. J. Vol. Geoth. Res. 65: 51-80.
- Fujimitsu Y., Ehara S., Oki R., Kanou R., 2008. Numerical model of the hydrothermal system beneath Unzen Volcano, Japan. J. Vol. Geoth. Res. 175: 35-44.
- Furuya S., Aoki M., Gotoh H., Takenaka T., 2000. Takigami geothermal system, northeastern Kyushu, Japan. Geothermics 29: 191-211.
- Gambill D.T., Beraquit D.B., 1993. Development History of the Tiwi Geothermal Field, Philippines. Geothermics 22, No. 5/6: 403-416.
- Ganda S., Sunaryo D., Hantono D., Tampubolon T., 1992. Exploration Progress of High Enthalpy Geothermal Prospect in Indonesia. Geoth. Res. Council Trans. 16: 83-88.
- Gherardi F., Panichi C., Yock A., Gerardo-Abaya J., 2002. Geochemistry of the surface and deep fluids of the Miravalles volcano geothermal system (Costa Rica). Geothermics 31: 91-128.
- Ghomshei M., Sanyal S., MacLeod K., Henneberger R., Ryder A., Meech J., Fainbank B., 2004. Status of the South Meager Geothermal Project British Columbia, Canada: Resource Evaluation and Plans for Development. Geoth. Res. Council Trans. 28: 339-344.
- Ghomshei M., Sanyal S., MacLeod K., Henneberger R., Ryder A., Meech J., Fainbank B., 2004. Status of the South Meager Geothermal Project British Columbia, Canada: Resource Evaluation and Plans for Development. Geoth. Res. Council Trans. 28: 339-344.
- Ghomshei M.M., 2010. Canadian Geothermal Power Prospects. WGC 2010: 5 pp.
- Ghomshei M.M., Croft S.A.S., Stauder J.C., 1986. Geochemical Evidence of Chemical Equilibria in the South Meager Creek Geothermal System, British Columbia, Canada. Geothermics 15: 49-61.
- Giggenbach W.F., 1993. Redox Control of Gas Compositions in Philippine Volcanic-Hydrothermal Systems. Geothermics 22, No. 5/6: 575-587.
- Giggenbach W.F., Glover R.B., 1992. Tectonic Regime and Major Processes Governing the Chemistry of Water and Gas Discharges from the Rotorua Geothermal Field, New Zealand. Geothermics 21, No. 1/2: 121-140.
- Giggenbach W.F., Sheppard D.S., Robinson B.W., Stewart M.K., Lyon G.L., 1995. Geochemical Structure and Position of the Waiotapu Geothermal Field, New Zealand. Geothermics 23, No. 5/6: 599-644.
- Glover R.B., 1966. The Chemistry of Thermal Waters at Rotorua. N.Z. J. Sci. 10: 70-96.
- Glover R.B., 1966. The Chemistry of Thermal Waters at Rotorua. N.Z. J. Sci. 10: 70-96.
- Glover R.B., Mroczek E.K., 2008. Chemical changes in natural features and well discharges in response to production at Wairakei, New Zealand. Geothermics 38: 117-133.
- Glover R.B., Stewart M.K., 1996. Chemical and Isotopic Changes in Shallow Groundwater Caused By Exploitation of the Wairakei Geothermal Field, New Zealand. Geothermics 25, No. 6: 647-661.
- Goko K., 2000. Structure and hydrology of the Ogiri field, West Kirishima geothermal area, Kyushu, Japan. Geothermics 29: 127-149.
- Gonzalez-Partida E., Birkle P., Torres-Alvarado I.S., 2000. Evolution of the hydrothermal system at Los Azufres, Mexico, based on petrologic, fluid inclusion and isotopic data. J. Vol. Geoth. Res. 104: 277-296.
- Grigsby C.O., Goff F., Trujillo Jr. P.E., Counce D.A., Dennis B., Kolar J., Corrales R., 1989. Results of Investigation at the Miravalles Geothermal Field, Costa Rica, Part 2: Downhole Fluid Sampling. Los Alamos National Laboratory: 51 pp.
- Gunderson R., Ganefianto N., Riedel K., Sirad-Azwar L., Suleiman S., 2000. Exploration Results in the Sarulla Block, North Sumatra, Indonesia. WGC 2000: 1183-1188.
- Gunderson R.P., Dobson P.F., Sharp W.D., Pudjianto R., Hasibuan A., 1995. Geology and Thermal Features of the Sarulla Contract Area, North Sumatra, Indonesia. WGC 1995: 687-692.
- Gutiérrez-Negrín L.C.A., 1988. The La Primavera, Jalisco, Mexico, Geothermal Field. Geoth. Res. Council Trans. 12: 161-165.

- Gutiérrez-Negrin L.C.A., Ramírez-Silva G.R., Martínez-Ménez M., López-López C., 2002. Hydrographic Characterization of the La Primavera, Mexico, Geothermal Field. *Geoth. Res. Council Trans.* 26: 17-21.
- Hamza V.M., Munoz M., 1996. Heat Flow Map of South America. *Geothermics* 25: 599-646.
- Hanano M., Kajiwara T., Hishi Y., Arai F., Asanuma M., Sato K., Takanohashi M., 2005. Overview of Production at the Mori Geothermal Field, Japan. *WGC 2005*: 10 pp.
- Hanano M., Matsuo G., 1990. Initial State of the Matsukawa Geothermal Reservoir: Reconstruction of a Reservoir Pressure Profile and Its Implications. *Geothermics* 19: 541-560.
- Healy J., Mahon W.A.J., 1982. Kawah Kamojang Geothermal Field, West Java. *NZ Geoth. Workshop 4 Part 2*: 313-319.
- Hedenquist J.W., 1990. The Thermal and Geochemical Structure of the Broadlands-Ohaaki Geothermal System, New Zealand. *Geothermics* 19, No. 2: 151-185.
- Heiken G., Duffield W., 1990. An Evaluation of the Geothermal Potential of the Tecuamburro Volcano Area of Guatemala. *Los Alamos National Laboratory*: 227 pp.
- Henley R.W., Middendorf K.I., 1985. Geothermometry in the Recent Exploration of Mokai and Rotokawa Geothermal Fields, New Zealand. *Geoth. Res. Council Trans.* 9: 317-324.
- Hernandez D., Clearwater J., Burnell J., Franz P., Azwar L., Marsh A., 2015. Update on the Modeling of the Rotokawa Geothermal System: 2010 - 2014. *WGC 2015*: 12 pp.
- Herrera R., Montalvo F., Herrera A., 2010. El Salvador Country Update. *WGC 2010*: 6 pp.
- Hidayatika A., Utami P., Suharno, Amukti R., 2015. Analysis of Thermal Manifestation in Suoh West Lampung Indonesia. *WGC 2015*: 5 pp.
- Hildreth W., Fierstein J., 1990. Geologic Map and Geothermal Assessment of the Mount Adams Volcanic Field, Cascade Range of Southern Washington. *Geoth. Res. Council Trans.* 14: 1455-1456.
- Hildreth W., Fierstein J., 2000. Katmai volcanic cluster and the great eruption of 1912. *Geol Soc Am Bull* 112: 1594-1620.
- Hinojosa E.T., 1997. Geochemical Model Update of the Los Azufres, Mexico, Geothermal Reservoir. *Geoth. Res. Council Trans.* 21: 441-448.
- Hochstein M.P., Sudarman S., 1993. Geothermal Resources of Sumatra. *Geothermics* 22: 181-200.
- Hochstein M.P., Sudarman S., 2008. History of geothermal exploration in Indonesia from 1970 to 2000. *Geothermics* 37: 220-266.
- Hochstein M.P., Sudarman S., 2015. Indonesian Volcanic Geothermal Systems. *WGC 2015*: 11 pp.
- Hook J.W., 1982. History of geothermal exploration in the Mount Hood area. *Oregon Dept of Geol and Mineral Industries Special Paper* 14: 3-5.
- Horton T.W., Atkinson L., Oze C., 2012. Hydrothermal Carbonate Geochemistry of the Ngatamariki Subsurface Reservoir, New Zealand. *Stanford Geoth. Workshop 37*: 1002-1009.
- Horton T.W., Atkinson L., Oze C., 2012. Hydrothermal Carbonate Geochemistry of the Ngatamariki Subsurface Reservoir, New Zealand. *Stanford Geoth. Workshop 37*: 1002-1009.
- Horwell C.J., Patterson J.E., Gamble J.A., Allen A.G., 2005. Monitoring and mapping of hydrogen sulphide emissions across an active geothermal field: Rotorua, New Zealand. *J. Vol. Geoth. Res.* 139: 259-269.
- Hulston J.R., Henley R.W., Glover R.B., Cox M.A., 1981. Stable Isotope and Geochemical Reconnaissance of the Mokai Geothermal System, Taupo Volcanic Zone. *NZ Geoth. Workshop 1981*: 81-86.
- Hurwitz S., Mariner R.H., Fehn U., Snyder G.T., 2005. Systematics of halogen elements and their radioisotopes in thermal springs of the Cascade Range, Central Oregon, Western USA. *Earth Planet. Sci. Lett.* 235: 700-714.
- Iglesias E.R., Arellano V.M., 1985. The Natural Thermodynamic State of the Fluids in the Los Azufres Geothermal Reservoir. *Stanford Geoth. Workshop 10*: 241-246.
- Ingebritsen S.E., Carothers W.W., Mariner R.H., Gudmundsson J.S., Sammel E.A., 1986. Flow testing of the Newberry 2 research drillhole, Newberry volcano, Oregon. *U S Geol Surv Water-Resour. Invest. Rept* 86-4133: 23 pp.

- Ingebritsen S.E., Galloway D.L., Colvard E.M., Sorey M.L., Mariner R.H., 2001. Time-variation of hydrothermal discharge at selected sites in the western United States: implications for monitoring. *J. Vol. Geoth. Res.* 111: 1-23.
- Ingebritsen S.E., Gelwick K.D., Randolph-Flagg N.G., Crankshaw I.M., Lundstrom E.A., McCulloch C.L., Murveit A.M., Newman A.C., Mariner R.H., Bergfeld D., Tucker D.S., Schmidt M.E., Spicer K.R., Mosbrucker A., Evans W.C., 2014. Hydrothermal monitoring data from the Cascade Range, northwestern United States. *U S Geol Surv Data Set*, doi:10.5066/F72N5088.
- Ingebritsen S.E., Mariner R.H., 2010. Hydrothermal heat discharge in the Cascade Range, northwestern United States. *J. Vol. Geoth. Res.* 196: 208-218.
- Ingebritsen S.E., Paulson K.M., 1990. Numerical Simulation of Hydrothermal Circulation in the Cascade Range, North-Central Oregon. *Geoth. Res. Council Trans.* 14(1): 692-698.
- Ingebritsen S.E., Randolph-Flagg N.G., Gelwick K.D., Lundstrom E.A., Crankshaw I.M., Murveit A.M., Schmidt M.E., Bergfeld D., Spicer K.R., Tucker D.S., Mariner R.H., Evans W.C., 2014. Hydrothermal monitoring in a quiescent volcanic arc: Cascade Range, northwestern United States. *Geofluids* 14: 326-346.
- Ingebritsen S.E., Sherrod D.R., Mariner R.H., 1992. Rates and Patterns of Groundwater Flow in the Cascade Range Volcanic Arc, and the Effect on Subsurface Temperatures. *J. Geophys. Res.* 97(B4): 4599-4627.
- International Engineering Company, 1982. The Momotombo Geothermal Field, Nicaragua: Exploration and Development Case History Study. *USDOE Report IEC-82-1-Z*: 198 pp.
- Isselhardt C.F., Matlick J.S., Parmentier P.P., Bamford R.W., 1983. Temperature Gradient Hole Results from Makushin Geothermal Area, Unalaska Island, Alaska. *Geoth. Res. Council Trans.* 7: 95-98.
- Isselhardt C.F., Motyka R., Matlick J.S., Parmentier P.P., Huttner G.W., 1983. Geothermal Resource Model for the Makushin Geothermal Area, Unalaska Island, Alaska. *Geoth. Res. Council Trans.* 7: 99-102.
- Janik C.J., McLaren M.K., 2010. Seismicity and fluid geochemistry at Lassen Volcanic National Park, California: Evidence for two circulation cells in the hydrothermal system. *J. Vol. Geoth. Res.* 189: 257-277.
- Kalacheva E.G., Koroleva G.P., Rychagov S.N., 2010. Geochemistry of Thermal Waters of Pauzhetsky-Kambalny-Koshelev Geothermal Area (Southern Kamchatka, Russia). *WGC 2010*: 5 pp.
- Karpov G., Esikov A., Esikov D., 2000. Isotopic Geochemistry of Acid Lakes in the Uzon-Geyserny and Karymsky Geothermal Areas (Kamchatka). *WGC 2000*: 2115-2119.
- Kasai K., Sakagawa Y., Komatsu R., Sasaki M., Akaku K., Uchida T., 1998. The Origin of Hypersaline Liquid in the Quaternary Kakkonda Granite, Sampled from Well WD-1a, Kakkonda Geothermal System, Japan. *Geothermics* 27, No. 5/6: 631-645.
- Kawazoe S., Shirakura N., 2005. Geothermal Power Generation and Direct Use in Japan. *WGC 2005*: 7 pp.
- Kaya E., Hochstein M.P., Yeh A., O'Sullivan M.J., 2015. Aspects of Natural Heat Transfer of a Geothermal System in Moderate Terrain: the Greater Waiotapu Geothermal System, New Zealand. *WGC 2015*: 12 pp.
- Keith T.E.C., Thompson J.M., Hutchinson R.A., White L.D., 1992. Geochemistry of waters in the Valley of Ten Thousand Smokes region, Alaska. *J. Vol. Geoth. Res.* 49: 209-231.
- Keller W.D., Valduga A., 1946. The Natural Steam at Larderello, Italy. *J. Geol.* 54(5): 327-334.
- Kimbara K., 1999. Geothermal resources survey in the volcanic fields of Japan; a review. *地球科學* 53(5): 325-339.
- Kiryukhin A., Xu T., Pruess K., Apps J., Slotvsov I., 2004. Thermal-hydrodynamic-chemical (THC) modeling based on geothermal field data. *Geothermics* 33: 349-381.
- Kissling W.M., Weir G.J., 2005. The spatial distribution of the geothermal fields in the Taupo volcanic zone, New Zealand. *J. Vol. Geoth. Res.* 145: 136-150.
- Kodosky L., Keskinen M., 1990. Fumarole distribution, morphology, and encrustation mineralogy associated with the 1986 eruptive deposits of Mount St. Augustine, Alaska. *Bull Volc* 52: 175-185.

- Koestono H., 2010. Lahendong Geothermal Field, Indonesia: Geothermal Model Based on Wells LHD-23 and LHD-28. Thesis (MSc) UNU-GTP Report 3: 90 pp.
- Koestono H., Siahaan E.E., Silaban M., Franzson H., 2010. Geothermal Model of the Lahendong Geothermal Field, Indonesia. WGC 2010: 6 pp.
- Koga A., 1970. Geochemistry of the Waters Discharged from Drillholes in the Otake and Hatchobaru Areas. Geothermics Special Issue 2, Vol. 2, Part 2: 1422-1425.
- Kolker A., Bailey A., Howard W., 2011. The 2010 Akutan Exploratory Drilling Program: Preliminary Findings. Geoth. Res. Council Trans. 35: 847-851.
- Kolker A., Cumming W., Stelling P., 2010. Geothermal Exploration at Akutan, Alaska: Favorable Indications for a High-Enthalpy Hydrothermal Resource near a Remote Market. Geoth. Res. Council Trans. 34: 561-566.
- Kolker A., Stelling P., Cumming W., Rohrs D., 2012. Exploration of the Akutan Geothermal Resource Area. Proc Workshop Geotherm Reservoir Eng 37: 1234-1243.
- Kononov V.I., Polyak B.G., Khutorskoy M.D., 2003. Hydrogeothermal Resources of Russia. International Geoth. Workshop: 11 pp.
- Kruger P., Semprini L., Nieva D., Verma S., Barragán R., Molinar R., Aragón A., Ortiz J., Miranda C., Garfias A., Gallardo M., 1985. Analysis of Reservoir Conditions During Production Startup at the Los Azufres Geothermal Field. Geoth. Res. Council Trans. 9: 527-532.
- Kruger P., Semprini L., Verma S., Barragán R., Molinar R., Aragón A., Ortiz J., Miranda C., Garfias A., Gallardo M., 1985. Initial Chemical and Reservoir Conditions at Los Azufres Wellhead Power Plant Startup. Stanford Geoth. Workshop 10: 219-226.
- Kusumasari B.A., Yonezu K., Herdianita N.R., Taguchi S., Watanabe K., 2013. Fluid Geochemistry Characteristics of Simbolon and Pusuk Bukit Geothermal Area in Toba Caldera, North Sumatra Province, Indonesia. NZ Geoth. Workshop 35: 6 pp.
- La Fleur J.G., 1987. Legend of the Crater Lake Hot Springs A Product of Model Mania. Geoth. Res. Council Trans. 11: 267-279.
- Lahsen A., 1988. Chilean Geothermal Resources and Their Possible Utilization. Geothermics 17: 401-410.
- Lawless J.V., Bromley C.J., Leach T.M., Licup Jr. A.C., Cope D.M., Recio C.M., 1983. Bacon-Manito Geothermal Field: A Geoscientific Exploration Model. NZ Geoth. Workshop 5: 97-102.
- Legmann, H., 2015. The 100-MW Ngatamariki Geothermal Power Station A Purpose-Built Plant for High Temperature, High Enthalpy Resource. WGC 2015: 6 pp.
- Lima E., Fujino T., 1996. A Hydrogeological and Geochemical Model of the High-Temperature Geothermal System of Amatitlán, Guatemala. Geoth. Res. Council Trans. 20: 347-352.
- Litvinenko V.S., Boguslavsky E.I., Khakhaev B.N., 2010. Deep Seated and Near-Surface Geothermal Resources of Russia. WGC 2010: 8 pp.
- Lopez M.R.T., Arriaga M.C.S., 2000. Geochemical Evolution of the Los Azufres, Mexico, Geothermal Reservoir. Part I: Water and Salts. WGC 2000: 2257-2262.
- Lowenstern J.B., Mariner R.H., 1998. Three-dimensional visualization of the geology, hydrology and geochemistry of the medicine lake highland and surrounding region. DOE Geothermal Energy R&D Program Executive Summary 1998: 2-77 - 2-80.
- Lu Y., Song S., Liu C., Yeh E., 2011. Factors Controlling the Termination of a 3-Mw-Pilot Power Plant in the Chingshui Geothermal Field, Taiwan. Geoth. Res. Council Trans. 35: 1195-1200.
- Lutz S.J., Hulen J.B., Schriener Jr. A., 2000. Alteration, Geothermometry, and Granitoid Intrusions in Well GMF 31-17, Medicine Lake Volcano Geothermal System, California. Stanford Geoth. Workshop 25: 7 pp.
- Mahon W.A.J., 1962. A Chemical Survey of the Steam and Water Discharged from Drillholes and Hot Springs at Kawerau. N.Z. J. Sci. 5: 417-433.

- Mahon W.A.J., 1962. A Chemical Survey of the Steam and Water Discharged from Drillholes and Hot Springs at Kawerau. *N.Z. J. Sci.* 5: 417-433.
- Mahon W.A.J., 1970. Chemistry in the Exploration and Exploitation of Hydrothermal Systems. *Geothermics Special Issue 2, Vol. 2, Part 2*: 1310-1322.
- Mainieri A., 2000. Costa Rica Country Update. *WGC 2000*: 313-318.
- Mainieri A.P., Robles E.F., 1995. Costa Rica Country Update Report. *WGC 1995*: 81-85.
- Malate R.C.M., O'Sullivan M.J., 1991. Modelling of Chemical and Thermal Changes in Well PN-26 Palimpinon Geothermal Field, Philippines. *Geothermics* 20, No. 5/6: 291-318.
- Manga M., Berensnev I., Brodsky E.E., Elkhoury J.E., Elsworth D., Ingebritsen S.E., Mays D.C., Wang C., 2012. Changes in Permeability Caused by Transient Stresses: Field Observations, Experiments, and Mechanisms. *Rev. Geophys.* 50, RG2004: 24 pp.
- Mariner R.H., Evans W.C., Presser T.S., White L.D., 2003. Excess nitrogen in selected thermal and mineral springs of the Cascade Range in northern California, Oregon, and Washington: sedimentary or volcanic in origin? *J. Vol. Geoth. Res.* 121: 99-114.
- Mariner R.H., Lowenstern J.B., 1999. The Geochemistry of Waters from Springs, Wells, and Snowpack On and Adjacent to Medicine Lake Volcano, Northern California. *Geoth. Res. Council Trans.* 23: 319-326.
- Mariner R.H., Presser T.S., Evans W.C., 1982. Chemical and Isotopic Composition of Water from Thermal and Mineral Springs of Washington. *U S Geol Surv Open-File Rpt 82-98*: 18 pp.
- Mariner R.H., Swanson J.R., Orris G.J., Presser T.S., Evans W.C., 1980. Chemical and Isotopic Data for Water From Thermal Springs and Wells of Oregon. *U S Geol Surv Open-File Rept 80-737*: 50 pp.
- Mariner R.H., Swanson J.R., Orris G.J., Presser T.S., Evans W.C., 1980. Chemical and Isotopic Data for Water From Thermal Springs and Wells of Oregon. *U S Geol Surv Open-File Rept 80-737*: 50 pp.
- Marini L., Cioni R., Guidi M., 1998. Water Chemistry of San Marcos Area, Guatemala. *Geothermics* 27: 331-360.
- Marini L., Yock Fung A., Sanchez E., 2003. Use of reaction path modeling to identify the process governing the generation of neutral Na-Cl and acidic Na-Cl-SO₄ deep geothermal liquids at Miravalles geothermal system, Costa Rica. *J. Vol. Geoth. Res.* 128: 363-387.
- Martinez-Olivar M.V.M., See F., Solis R., 2005. Isotopic Response to Changes in the Reservoir in Bacman Geothermal Production Field, Philippines. *WGC 2005*: 7 pp.
- Martini B.A., Lide C., Owens L., Walsh P., Delwiche B., Payne A., 2011. Geothermal Resource Definition at Mt. Spurr, Alaska. *Geoth. Res. Council Trans.* 35: 897-904.
- Matlick J.S., Parmentier P.P., 1983. Geothermal Manifestations and Results of a Mercury Soil Survey in the Makushin Geothermal Area, Unalaska Island, Alaska. *Geoth. Res. Council Trans.* 7: 305-309.
- Matsuyama K., Narita N., Tomita K., Majima T., 2000. Geothermal resources of Hachijojima. *Geothermics* 29: 213-232.
- Maunder B.R., Brodie A.J., Tolentino B.S., 1982. The Palimpinon Geothermal Resource Negros, Republic of the Philippines: An Exploration Case History. *NZ Geoth. Workshop 4 Part 1*: 87-92.
- Mazot A., Bernard A., Fischer T., Inguaggiato S., Sutawidjaja I.S., 2008. Chemical evolution of thermal waters and changes in the hydrothermal system of Papandayan volcano (West Java, Indonesia) after the November 2002 eruption. *J. Vol. Geoth. Res.* 178: 276-286.
- Mazot A., Bernard A., Fischer T., Inguaggiato S., Sutawidjaja I.S., 2008. Chemical evolution of thermal waters and changes in the hydrothermal system of Papandayan volcano (West Java, Indonesia) after the November 2002 eruption. *J. Vol. Geoth. Res.* 178: 276-286.
- Mazot A., Bernard A., Fischer T., Inguaggiato S., Sutawidjaja I.S., 2008. Chemical evolution of thermal waters and changes in the hydrothermal system of Papandayan volcano (West Java, Indonesia) after the November 2002 eruption. *J. Vol. Geoth. Res.* 178: 276-286.
- Melosh G., Moore J., Stacey R., 2012. Natural Reservoir Evaluation in the Tolhuaca Geothermal Field, Southern Chile. *Stanford Geoth. Workshop 36*: 7 pp.

- Meneses III S.F.M., 2015. Thermal Remote Sensing at Leyte Geothermal Production Field using Mono-window Algorithms. WGC 2015: 9 pp.
- Menzies A., Villaseñor L., Sunio E., Lim W., 2010. Characteristics of the Matalibong Steam Zone, Tiwi Geothermal Field, Philippines. WGC 2010: 6 pp.
- Menzies A.J., Sanyal S.K., Granados E.E., Pham M., Lima E., Cuevas A., Torres J., 1996. Analysis of Well Test Data From the High-Temperature Geothermal System of Amatitlán, Guatemala. Geoth. Res. Council Trans. 20: 821-827.
- Miller T.P., 1973. Distribution and chemical analyses of thermal springs in Alaska. U S Geol Surv Open-File Rept 73-187, Scale 1:2,500,000, 1 map, 5 pp.
- Miller T.P., Chertkoff D.G., Eichelberger J.C., Coombs M.L., 1999. Mount Dutton volcano, Alaska: Aleutian arc analog to Unzen volcano, Japan. J. Vol. Geoth. Res. 89: 275-301.
- Miller T.P., McGimsey R.G., Richter D.H., Riehle J.R., Nye C.J., Yount M.E., Dumoulin J.A., 1998. Catalogue of the historically active volcanoes of Alaska. U S Geol Surv Open-File Rept 98-582: 104 pp.
- Moiseenko U.I., Duchkov A.D., Sokolova L.S., 1973. Heat Flow in Some Regions of Siberia and the Far Eastern USSR. Geothermics 2: 17-23.
- Moran S.C., Zimbelman D.R., Malone S.D., 2000. A model for the magmatic-hydrothermal system at Mount Rainier, Washington, from seismic and geochemical observations. Bull Volc 61: 425-436.
- Morgan D.S., Tanner D.Q., Crumrine M.D., 1997. Hydrologic and Water-Quality Conditions at Newberry Volcano, Deschutes County, Oregon, 1991-95. U S Geol Surv Water-Resour. Invest. Rept 97-4088: 66 pp.
- Motyka R.J., Liss S.A., Nye C.J., Moorman M.A., 1993. Geothermal Resources of the Aleutian Arc. Alaska Div of Geol and Geophys Surv Prof Rept 114: 17 pp.
- Motyka R.J., Liss S.A., Nye C.J., Moorman M.A., 1993. Geothermal Resources of the Aleutian Arc (Central Arc). Alaska Div of Geol and Geophys Surv Prof Rept 114: 17 pp.
- Motyka R.J., Liss S.A., Nye C.J., Moorman M.A., 1993. Geothermal Resources of the Aleutian Arc (Eastern Arc). Alaska Div of Geol and Geophys Surv Prof Rept 114: 17 pp.
- Motyka R.J., Liss S.A., Nye C.J., Moorman M.A., 1993. Geothermal Resources of the Aleutian Arc (Western Arc). Alaska Div of Geol and Geophys Surv Prof Rept 114: 17 pp.
- Motyka R.J., Liss S.A., Nye C.J., Moorman M.A., 1993. Geothermal Resources of the Aleutian Arc. Alaska Div of Geol and Geophys Surv Prof Rept 114: 17 pp.
- Motyka R.J., Moorman M.A., Liss S.A., 1981. Assessment of Thermal Springs Sites Aleutian Arc, Atka Island to Becherof Lake --Preliminary Results and Evaluation. Alaska Div of Geol and Geophys Surv Open-File Rept 144: 173 pp.
- Motyka R.J., Moorman M.A., Poreda R., 1982a. Fluid Geochemistry of Hot Springs Bay Valley, Akutan Island, Alaska. Geoth. Res. Council Trans. 6: 103-106.
- Motyka R.J., Moorman M.A., Poreda R., 1982b. Fluid Geochemistry of the Makushin Geothermal Area, Unalaska Island, Alaska. Geoth. Res. Council Trans. 6: 107-110.
- Motyka R.J., Moorman M.A., Poreda R., 1982b. Fluid Geochemistry of the Makushin Geothermal Area, Unalaska Island, Alaska. Geoth. Res. Council Trans. 6: 107-110.
- Motyka R.J., Nye C.J., Turner D.L., Liss S.A., 1993. The Geyser Bight Geothermal Area, Umnak Island, Alaska. Geothermics 22: 301-327.
- Motyka R.J., Wescott E.M., Turner D.L., Swanson S.E., Romick J.D., Moorman M.A., Poreda R.J., Witte W., Petzinger B., Allely R.D., Larsen M., 1985. A Geological, Geochemical, and Geophysical Survey of the Geothermal Resources at Hot Springs Bay Valley, Akutan Island, Alaska. Alaska Div of Geol and Geophys Sur, 2 plates, scale 1:20,000, 167 pp.
- Moxham R.M., Crandell D.R., Marlatt W.E., 1965, Thermal Features at Mount Rainer, Washington, as Revealed by Infrared Surveys. In Geological Survey Research 1965 Chapter D. U S Geol Surv Prof Pap, 525-D: 93-100.

- Mulyanto, Nani A., Zuhro A.A., Ahmad Y., 2010. Surface Thermal Manifestation Monitoring of Kamojang Geothermal Field West Java, Indonesia. WGC 2010: 3 pp.
- Mulyanto, Puspadianti A., Giriarmo J.P., Hartanto D.B., 2015. The Initial-State Geochemistry as a Baseline for Geochemical Monitoring at Ulubelu Geothermal Field, Indonesia. WGC 2015: 5 pp.
- Nakamura H., Sumi K., Katagiri K., Iwata T., 1970. The Geological Environment of Matsukawa Geothermal Area, Japan. Geothermics Special Issue 2, Vol. 2, Part 1: 221-231.
- Nanlohy F., Kusnadi D., Sulaeman B., 2001. Geology and Geochemistry of Mataloko Geothermal Field Central Flores - East Nusa Tenggara. INAGA 5: 4 pp.
- Nasution A., Takashima I., Muraoka H., Takahashi H., Matsuda K., Akasako H., Futagoishi M., Kusnadi D., Nanlohi F., 2000. The Geology and Geochemistry of Mataloko-Nage-Bobo Geothermal Areas, Central Flores, Indonesia. WGC 2000: 2165-2170.
- Nasution A., Takashima I., Muraoka H., Takahashi H., Matsuda K., Akasako H., Futagoishi M., Kusnadi D., Nanlohi F., 2000. The Geology and Geochemistry of Mataloko-Nage-Bobo Geothermal Areas, Central Flores, Indonesia. WGC 2000: 2165-2170.
- Nathenson M., 2004. Springs on and in the vicinity of Mount Hood volcano, Oregon: U S Geol Surv Open-File Rept 2004-1298: 43 pp.
- Nathenson M., Thompson J.M., White L.D., 2003. Slightly thermal springs and non-thermal springs at Mount Shasta, California: Chemistry and recharge elevations. J Vol Geotherm Res 121: 137-153.
- Nehring N.L., Wollenberg H.A., Johnston D.A., 1981. Gas analysis of fumaroles from Mount Hood, Oregon. U S Geol Surv Open-File Rept 81-236: 9 pp.
- Nieva D., Verma M.P., Santoyo E., Portugal E., Campos A., 1997. Geochemical exploration of the Chipilapa Geothermal Field, El Salvador. Geothermics 26, No. 5/6: 589-612.
- Nye C.J., Keith T.E.C., Eichelberger J.C., Miller T.P., McNutt S.R., Moran S., Schneider D.J., Dehn J., Schaefer J.R., 2002. The 1999 eruption of Shishaldin volcano, Alaska: monitoring a distant eruption. Bull Volc 64: 507-519.
- O'Brian J., Mroczek E., Boseley C., 2011. Chemical Structure of the Ngatamariki Geothermal Field, Taupo Volcanic Zone, N.Z. NZ Geoth. Workshop 2011: 6 pp.
- Ohren M., Bailey, A., Hinz N., Oppliger G., Hernandez J., Rickard W., Dering G., 2013, Akutan Geothermal Area Exploration Results and Pre-Drilling Resource Model. Geoth. Res. Council Trans. 37: 301-308.
- Okada H., Yasuda Y., Yagi M., Kai K., 2000. Geology and fluid chemistry of the Fushime geothermal field, Kyushu, Japan. Geothermics 29: 279-311.
- Okrugin V., Chernev I., 2015. Correlation of Epithermal and Geothermal Deposits (an Example of Mutnovsky Geothermal Area, Southern Kamchatka). WGC 2015: 7 pp.
- Okrugin V., Chernev I., 2015. Correlation of Epithermal and Geothermal Deposits (an Example of Mutnovsky Geothermal Area, Southern Kamchatka). WGC 2015: 7 pp.
- Osborn W., Hernández J., George A., 2014. Successful Discovery Drilling in Roseau Valley, Commonwealth of Dominica. Stanford Geoth. Workshop 39: 10 pp.
- Ostapenko S., Spektor S., Dávila H., Porras E., Pérez M., 1996. A Reservoir Engineering Assessment of the San Jacinto-Tizate Geothermal Field, Nicaragua. Stanford Geoth. Workshop 21: 21-28.
- Ostapenko S., Spektor S., Netesov Y., Romero F., 1997. Geothermal Exploration of El Najo Field, Nicaragua. Stanford Geoth. Workshop 22: 511-518.
- Ostapenko S.V., Spektor S.V., Netesov Y.P., 1998. San Jacinto-Tizate Geothermal Field, Nicaragua: Exploration and Conceptual Model. Geothermics 27, No. 3: 361-378.
- Palma J., Garcia O., 1995. Updated Status of the Geothermal Development in Guatemala. WGC 1995: 135-140.
- Pambudi N.A., Itoi R., Yamashiro R., Alam B.Y. CSS S., Tusara L., Jalilinasrady S., Khasani J., 2015. The behavior of silica in geothermal brine from Dieng geothermal power plant, Indonesia. Geothermics 54: 109-114.

- Parini M., Pisani P., Monterrosa M., 1995. Resource Assessment at the Berlin Geothermal Field (El Salvador). WGC 1995: 1537-1542.
- Patrick M.R., Dehn J., Papp K.R., Lu Z., Dean K., Moxey L., Izbekov P., Guritz R., 2003. The 1997 eruption of Okmok volcano, Alaska: a synthesis of remotely sensed imagery. *J. Vol. Geoth. Res.* 127: 87-105.
- Permana T., Mulyanto, Hartanto D.B., 2015. Geochemical Changes during 12 Year Exploitation of the Southern Reservoir Zone of Lahendong Geothermal Field, Indonesia. WGC 2015: 6 pp.
- Poeschel K.R., Rowe T.G., Blodgett J.C., 1986. Water-Resources Data for the Mount Shasta Area, Northern California. U S Geol Surv Open-File Rept 86-65: 73 pp.
- Poeschel K.R., Rowe T.G., Blodgett J.C., 1986. Water-Resources Data for the Mount Shasta Area, Northern California. U S Geol Surv Open-File Rept 86-65: 73 pp.
- Pope J., Brown K.L., 2014. Geochemistry of discharge at Waiotapu geothermal area, New Zealand - Trace elements and temporal changes. *Geothermics* 51: 253-269.
- Povarov K.O., Svalova V.B., 2010. Geothermal Development in Russia: Country Update Report 2005-2009. WGC 2010: 4 pp.
- Powell T., Moore J., Cumming B., 2002. Conceptual Models of Karaha-Telaga Bodas and The Geysers. *Geoth. Res. Council Trans.* 26: 369-373.
- Powell T., Moore J., DeRocher T., McCulloch J., 2001. Reservoir Geochemistry of the Karaha-Telaga Bodas Prospect, Indonesia. *Geoth. Res. Council Trans.* 25: 363-367.
- Power J.A., Jolly A.D., Nye C.J., Harbin M.L., 2002. A conceptual model of the Mount Spurr magmatic system from seismic and geochemical observations of the 1992 Crater Peak eruption sequence. *Bull Volc* 64: 206-218.
- Prasetyo R., Laksmi N., Pratikno B., 2015. Gas Geochemistry and Carbon-13 Systematics of Ungaran Geothermal Field, Central Java, Indonesia. WGC 2015: 6 pp.
- Priest G.R., 1982. Overview of the Geology and Geothermal Resources of the Mount Hood Area, Oregon. Oregon Dept of Geol and Mineral Resources Special Paper 14: 6-15.
- Priest G.R., Beeson M.H., Gannett M.W., Berri D.A., 1982. Geology, Geochemistry, and Geothermal Resources of the Old Maid Flat Area, Oregon. Oregon Dept of Geol and Mineral Industries Special Paper 14: 16-30.
- Priest G.R., Blackwell D.D., 1984. Understanding thermal energy and dynamic processes in subduction-related volcanic arcs: Proposed studies in the Cascades. *Eos* 65(39): 722-722.
- Priest G.R., Vogt B.F., Black G.L., eds., 1983. Survey of Potential Geothermal Exploration Sites at Newberry Volcano, Deschutes County, Oregon. Oregon Dept of Geol and Mineral Ind OFR O-83-3: 174 pp.
- Purnomo B.J., Pichler T., 2014. Geothermal systems on the island of Java, Indonesia. *J. Vol. Geoth. Res.* 285: 47-59.
- Purnomo B.J., Pichler T., 2014. Geothermal systems on the island of Java, Indonesia. *J. Vol. Geoth. Res.* 285: 47-59.
- Ramirez L.E., Rae A.J., Bardsley C., Bignall G., 2009. Spatial Variation of High Temperature Hydrothermal Activity at Mokai Geothermal Field, Taupo Volcanic Zone, New Zealand. *Geoth. Res. Council Trans.* 33: 855-857.
- Ramos M.E.S., Espartinez C.M.R., 2015. The Bacon-Manito Surface Thermal Features - Geochemical and Physical Changes After Three Decades (1983-2013) of Monitoring. WGC 2015: 5 pp.
- Ramos M.E.S., Espartinez C.M.R., 2015. The Bacon-Manito Surface Thermal Features - Geochemical and Physical Changes After Three Decades (1983-2013) of Monitoring. WGC 2015: 5 pp.
- Read P.B., 1978. Meager Creek geothermal area. Geol Surv Can, Open-File 603: 1:20,000 geol map and text.
- Reeves R.R., Bromley C.J., Milloy S.F., 2015. Using Time-Series Aerial Thermal Surveys to Determine Near-Surface Thermal Processes at the Ohaaki Geothermal Field, New Zealand. WGC 2015: 6 pp.

- Robison J.H., Forcella L.S., and Gannett, M.W., 1981. Data from geothermal test wells near Mount Hood, Oregon. U S Geol Surv Open-File Rept 81-1002: 24 pp.
- Romagnoli P., Cuellar G., Jimenez M., Ghezzi G., 1976. Hydrogeological Characteristics of the Geothermal Field of Ahuachapan, El Salvador. Second UN Symposium on the Development and Use of Geothermal Resources: 571-574.
- Romagnoli P., Cuellar G., Jimenez M., Ghezzi G., 1976. Hydrogeological Characteristics of the Geothermal Field of Ahuachapan, El Salvador. Second UN Symposium on the Development and Use of Geothermal Resources: 571-574.
- Ruggieri G., Gianelli G., 1999. Multi-stage fluid circulation in a hydraulic fracture breccia of the Larderello geothermal field (Italy). *J. Vol. Geoth. Res.* 90: 241-261.
- Salgado G., Raasch G., 2002. Recent Geothermal Industry Activity and the Market for Electric Power in Chile. *Geoth. Res. Council Trans.* 26: 55-58.
- Sambrano B.G., 2001. Geochemical Changes and Reservoir Processes Resulting from Mass Extraction in the Mindanao Geothermal Production Field, Philippines. *Geoth. Res. Council Trans.* 25: 687-692.
- Sammel E.A., 1981. Results of Test Drilling at Newberry Volcano, Oregon. *Geoth. Res. Council Trans.* 10: 3-8.
- Sammel E.A., 1981. Results of Test Drilling at Newberry Volcano, Oregon. *Geoth. Res. Council Trans.* 10: 3-8.
- Sammel E.A., 1983. The Shallow Hydrothermal System at Newberry Volcano, Oregon: A Conceptual Model. *Geoth. Res. Council Trans.* 7: 325-330.
- Sanchez D.R., 2010. Calcite Deposition of Wells Affected by Re-injected Fluids in Palinpinon II, Southern Negros Geothermal Production Field, Philippines. *WGC 2010*: 5 pp.
- Sánchez-Velasco R.A., 2003. Update of the Cerritos Colorados Geothermal Project, Mexico. *Geoth. Res. Council Trans.* 27: 453-457.
- Sanjuan B., Jousset P., Pajot G., Debeglia N., De Michele M., Brach M., Dupont F., Braibant G., Lasne E., Duré F., 2010. Monitoring of the Bouillante Geothermal Exploitation (Guadeloupe, French West Indies) and the Impact on Its Immediate Environment. *WGC 2010*: 11 pp.
- Schaefer J.R., Cameron C.E., Nye C.J., 2014. Historically active volcanoes of Alaska. Alaska Div of Geol and Geophys Surv Digital Data Series 6, http://maps.dggs.alaska.gov/historically_active_volcanoes/.
- Schuster J.E., 1974. Geothermal energy potential of Washington. in *Energy Resources of Washington*. Washington State Div of Geol and Earth Resources Info. Circular No. 50: 1-20.
- Schuster J.E., 1981. A Geothermal Exploration Philosophy for Mount St. Helens (and other Cascade Volcanoes?). *Geothermal Direct Heat Program: Glenwood Springs Technical Conference Proceedings, Volume I, Papers Presented State Coupled Geothermal Resource Assessment Program*: 297-300.
- Sepúlveda F., Lahsen A., Powell T., 2007. Gas geochemistry of the Cordón Caulle geothermal system, Southern Chile. *Geothermics* 36: 389-420.
- Sheppard D.S., Giggenbach W.F., 1980. Chemistry of the Well Discharges at Ngawha. *NZ Geoth. Workshop 1980*: 91-95.
- Shoji T., 1999. Minor element geochemistry in the Yanaizu-Nishiyama geothermal field, northeastern Japan. *Geoth. Res. Council Trans.* 23: 405-406.
- Shoji T., 2005. Geostatistical Analysis of Geothermal Temperatures in Yanaidzu-Nishiyama Geothermal Field, Northeastern Japan. *J Geoth Research Soc of Japan* 27(3): 233-247.
- Sifford A., 2014. Geothermal Energy in Oregon 2014. *Geoth. Res. Council Trans.* 38: 99-106.
- Silitonga T.H., Siahaan E.E., Sasradipoera D.S., Pelmelay C., Timisela D.P., 2015. Exploration Strategy in Kerinci Geothermal Prospect located inside the National Park of Indonesia. *WGC 2015*: 6 pp.
- Simatupang C.H., Intani R.G., Suryanta M.R., Irfan R., Golla G., Cease C., Molling P., 2015. Evaluation of Water Produced from a Stream Dominated System, a Case Study from the Darajat Field. *WGC 2015*: 8 pp.

- Smith R.L., Shaw H.R., Luedke R.G., Russell S.L., 1978. Comprehensive tables giving physical data and thermal energy estimates for young igneous systems of the United States. U S Geol Surv Open-File Rept 78-925: 25 pp.
- Solie D.N., Tannian F., Eds., 1993. Short Notes on Alaskan Geology 1993. Alaska Dept of Natural Res Prof Pap 113: 101 pp.
- Souther J.G., 1980. Geothermal Reconnaissance in the Central Garibaldi Belt, British Columbia. In Current Research, Part A, Geological Survey of Canada, Paper 80-1a. 11 pp.
- Souther J.G., Dellechiaie F., 1984. Geothermal Exploration at Mt. Cayley - A Quaternary Volcano in Southwestern British Columbia. Geoth. Res. Council Trans. 8: 463-468.
- Sriwana T., van Bergen M.J., Varekamp J.C., Sumarti S., Takano B., van Os B.J.H., Leng M.J., 2000. Geochemistry of the acid Kawah Putih lake, Patuha Volcano, West Java, Indonesia. J. Vol. Geoth. Res. 97: 77-104.
- Stimac J., Nordquist G., Suminar A., Sirad-Azwar L., 2008. An overview of the Awibengkok geothermal system, Indonesia. Geothermics 37: 300-331.
- Stimac J., Sugiawan F., 2000. The AWI 1-2 Core Research Program: Part I, Geologic Overview of the Awibengkok Geothermal Field, Indonesia. WGC 2015: 2221-2226.
- Strelbitskaya S., 2005. Interpretation of Chemical Composition of Geothermal Fluid from the Geothermal Field of Baransky Volcano, Iturup Island, Russia. UNU-GTP Reports 2005, Number 17: 333-351.
- Sugai S., Baba K., 1996. Geothermal Development in Hachijojima, Japan. Geoth. Res. Council Bull. 25: 339-348.
- Sulasdi D., 1996. Exploration of Ulumbu Geothermal Field, Flores-East Nusa Tenggara Indonesia. Stanford Geoth. Workshop 21: 51-54.
- Sulistiyardi, H.B., 2015. An Update on the Basic Design of Lumut Balai Geothermal Power Plant, Indonesia. WGC 2015: 5 pp.
- Sunaryo, Hantono D., Ganda S., Nugroho, 1993. Exploration Results of the Ulubelu Geothermal Prospect, South Sumatra, Indonesia. NZ Geoth. Workshop 15: 103-106.
- Suryantini, 2015. Volcanological Approach for Evaluation of Geothermal Potential in Volcanic Associated Hydrothermal System at the Early Stage of Exploration. WGC 2015: 5 pp.
- Svalova V., Povarov K., 2013. Geothermal Energy Use in Russia, Country Update for 2007-2012. European Geoth. Congress 2013: 7 pp.
- Takenaka T., Furuya S., 1991. Geochemical model of the Takigami geothermal system, northeast Kyushu, Japan. Geochemical Journal 25: 267-281.
- Takeo N., 2000. Thermal and geochemical structure of the Uenotai geothermal system, Japan. Geothermics 29: 257-277.
- Tamanyu S., Sakaguchi K., Murata Y., 2010. Image Database of Geothermal Drill Core Samples in Japan. WGC 2010: 5 pp.
- Tello H.E., Verma M.P., Tovar A.R., 2000. Chemical and Isotopic Study to Define the Origin of Acidity in the Los Humeros (México) Geothermal Reservoir. Geoth. Res. Council Trans. 24: 441-449.
- Terceros Z.D., 2000. State of the Geothermal Resources in Bolivia Laguna Colorada Project. WGC 2000: 153-158.
- Thompson A., 2010. Geothermal Development in Canada: Country Update. WGC 2010: 3 pp.
- Thompson J.M., 1982. Preliminary Chemical Studies of Thermal Waters in Lassen Volcanic National Park and Vicinity. Geoth. Res. Council Trans. 6: 115-118.
- Thompson J.M., 1983. Chemical analyses of thermal and nonthermal springs in Lassen Volcanic National Park and vicinity, California. U S Geol Surv Open-File Rept 83-311: 26 pp.
- Tiffer E.M., Ostapenko S., 1995. San Jacinto-Tizate Geothermal Field in Nicaragua First Results of Feasibility Study. Geoth. Res. Council Bull. 24(10): 345-350.

- Till A.B., Yount M.E., Bevier M.L., 1994. The geologic history of Redoubt volcano, Alaska. *J. Vol. Geoth. Res.* 62: 11-30.
- Tonani F.B., Teilman M.A., 1980. Geochemistry at Momotombo, Nicaragua: One Aspect in a Geothermal Field Case History. *Geoth. Res. Council Trans.* 4: 193-196.
- Torres-Mora Y., Axelsson G., 2015. Chemical Tracer Test in Las Pailas Geothermal Field, Costa Rica. *WGC 2015*: 8 pp.
- Torres-Rodriguez M.A., Flores-Armenta M., 1998. Pressure and Enthalpy Evolution in Wells of the Los Azufres Geothermal Field. *Geoth. Res. Council Trans.* 22: 339-358.
- Traineau H., Sanjuan B., Deaufort D., Brach M., Castaing C., Correia H., Genter A., Herbrich B., 1997. The Bouillante Geothermal Field (F.W.I.) Revisited: New Data on the Fractured Geothermal Reservoir in Light of a Future Stimulation Experiment in a Low Productive Well. *Stanford Geoth. Workshop 22*: 97-103.
- Truesdell A.H., Aunzo Z., Bodvarsson G., Alonso J., Campos A., 1989. The Use of Ahuachapan Fluid Chemistry to Indicate Natural State Conditions and Reservoir Processes during Exploitation. *Stanford Geoth. Workshop 14*: 6 pp.
- Turner, D.L., Wescott, E.M., Eds., 1986. Geothermal Energy Resource Investigations at Mt. Spurr, Alaska. *Univ of Alaska Geophys Inst UAG R-308*: 98 p., 5 plates, scales 1:2680 and 1:6250.
- Turner, D.L., Wescott, E.M., Eds., 1986. Geothermal Energy Resource Investigations at Mt. Spurr, Alaska. *Univ of Alaska Geophys Inst UAG R-308*: 98 p., 5 plates, scales 1:2680 and 1:6250.
- Ueda A., Kubota Y., Katoh H., Hatakeyama K., Matsubaya O., 1991. Geochemical characteristics of the Sumikawa geothermal system, northeast Japan. *Geochemical Journal* 25: 223-244.
- Vakin E.A., Polak B.G., Sugrobov V.M., Erlikh E.N., Belousov V.I., Pilipenko G.F., 1970. Recent Hydrothermal Systems of Kamchatka. *Geothermics Special Issue 2, Vol. 2, Part 2*: 1116-1133.
- Varekamp J.C., Ouimette A.P., Herman S.W., Bermudez A., Delpino D., 2001. Hydrothermal element fluxes from Copahue, Argentina: A "beehive" volcano in turmoil. *Geology* 29(11): 1059-1062.
- Vice D.H., 2010. A History of Geothermal Exploration in Washington. *Geoth. Res. Council Trans.* 34: 653-658.
- Viggiano-Guerra J.C., Gutierrez-Negrin L.C.A., 1994. First Results of Deep Exploratory Drilling in the El Ceboruco Geothermal Zone. *Geoth. Res. Council Trans.* 18: 297-302.
- Vigliano J.A., Harmon R.S., Borthwick J., Nehring N.L., Motyka R.J., White L.D., Johnston D.A., 1985. Stable-Isotope Evidence for a Magmatic Component in Fumarole Condensates from Augustine Volcano, Cook Inlet, Alaska, U.S.A.. *Chem Geol* 49: 141-157.
- Waibel A.F., Frone Z., Jaffe T., 2012. Geothermal Exploration at Newberry Volcano, Central Oregon. *Geoth. Res. Council Trans.* 36: 803-810.
- Waldron H.H., 1961. Geologic Reconnaissance of Frosty Peak Volcano and Vicinity, Alaska. *U S Geol Surv Bulletin* 1028-T: 677-708.
- Werner C., Evans W.C., Poland M., Tucker D.S., Doukas M.P., 2009. Long-term changes in quiescent degassing at Mount Baker volcano, Washington, USA; evidence for a stalled intrusion in 1975 and connection to a deep magma source. *J. Vol. Geoth. Res.* 186: 379-386.
- Wharton Jr. R.A., Vinyard W.C., 1979. Summit Thermal Springs Mount Shasta, California. *California Geology* 32: 38-41.
- Wisnandary M.C., Alamsyah O., 2012. Zero Generation of Muara Laboh Numerical Model: Role of Heat Loss and Shallow Wells Data on Preliminary Natural State Modeling. *Geoth. Res. Council* 36: 825-830.
- Yamasaki T., Hayashi M., 1976. Geologic Background of Otake and Other Geothermal Areas in North-Central Kyushu, Southwestern Japan. *Second United Nations Symposium on the Development and Use of Geothermal Resources* 1: 673-384.
- Yamashita M., Majima T., Tsujita M., Matsuyama K., 2000. Geothermal Development in Hachijojima. *WGC 2000*: 2989-2994.

- Yasuda Y., 1998. Studies on the Fluid Chemistry in the Fushime Geothermal System, Japan. Stanford Geoth. Workshop 23: 196-203.
- Yoshida Y., 1981. Chemical Study on Deep Hot Water of the Nigorikawa Geothermal Field. Geoth. Res. Council Trans. 5: 217-220.
- Yoshida Y., 1991. Geochemistry of the Nigorikawa geothermal system, southwest Hokkaido, Japan. Geochemical Journal 25: 203-222.
- Youngquist W., 1980. Geothermal Gradient Drilling, North-Central Cascades of Oregon, 1979. Oregon Dept of Geol and Mineral Industries Open-File Rept O-80-12: 47 pp.
- Youngquist W., 1981. Geothermal Potential of the Cascades. In Geothermal Potential of the Cascade Mountain Range: Exploration and Development. Geoth. Res. Council Special Report 10: 25-29.
- Yuniar D.M., Hastuti P., Silaban M., 2015. Ulubelu, First Year Reservoir Monitoring. WGC 2015: 5 pp.
- Zen M.T., Radja V.T., 1970. Result of the Preliminary Geological Investigation of Natural Steam Fields in Indonesia. Geothermic Special Issue 2, Vol. 2, Part 1: 130-135.
- Zimbelman D.R., Rye R.O., Landis G.P., 2000. Fumaroles in ice caves on the summit of Mount Rainier- preliminary stable isotope, gas, and geochemical studies. J. Vol. Geoth. Res. 97: 457-473.
- Excel spreadsheet compiled by Glenn Melosh from published literature

Part 2 – Volcanology References

The compilation of the volcanologic data relied heavily on the GeoRoc database that contains over 3400 references (165 pages) from the published literature. For brevity, this list is not included in its entirety here, but is uploaded to the GDR as part of this appendix. The sources of data include:

<http://georoc.mpch-mainz.gwdg.de/georoc/> - This is the most complete global clearinghouse of igneous rock geochemistry.

www.EarthChem.org

www.earthref.org/GERM/

Part 3 – Structure/Tectonic References

- Acocella, V., Vezzoli, L., Omarini, R., Matteini, M., Mazzuoli, R., 2009, Reply to comment on “Kinematic variations across Eastern Cordillera at 24°S (Central Andes): Tectonic and magmatic implications”: *Tectonophysics*, v. 469, p. 155–159, doi:10.1016/j.tecto.2008.02.005
- Agostini, S., Corti, G., Doglioni, C., Carminati, E., Innocenti, F., Tonarini, S., Manetti, P., Di Vincenzo, G., Montanari, D., 2006, Tectonic and magmatic evolution of the active volcanic front in El Salvador: insight into the Berlín and Ahuachapán geothermal areas: *Geothermics*, v. 35, p. 368–408, doi:10.1016/j.geothermics.2006.05.003
- Allmendinger, R.W., Jordan, T.E., Kay, S.M., Isacks, B.L., 1997, The Evolution of the Altiplano-Puna Plateau of the Central Andes: *Annu. Rev. Earth Planet Science*, v. 25, p.139–174.
- Allmendinger, R.W., Strecker, M., Eremchuk, J.E., Francis, P., 1989, Neotectonic Deformation of the Southern Puna Plateau, Northwestern Argentina: *Journal of South American Earth Sciences*, v. 2, p. 111–130.
- Alvarado, D., DeMets, C., Tikoff, B., Hernandez, D., Wawrzyniec, T.F., Pullinger, C., Mattioli, G., Turner, H.L., Rodriguez, M., Correa-Mora, F., 2011, Forearc motion and deformation between El Salvador and Nicaragua: GPS, seismic, structural, and paleomagnetic observations: *Lithosphere*, v. 3, p. 3–21, doi:10.1130/L108.1
- Aravena, D., Villalón, I., Sánchez, P., 2015, Igneous Related Geothermal Resource in the Chilean Andes: *Proceedings World Geothermal Congress*, p. 1–8.
- Arellano, V.M., Barragán, R.M., Ramírez, M., López, S., Paredes, A., Aragón, A., Tovar, R., 2015, The Response to Exploitation of the Los Humeros (México) Geothermal Reservoir: *Proceedings World Geothermal Congress*, p. 1–7.
- Arias, A., Bertani, R., Ceccarelli, A., Dini, I., Fiordelisi, A., Marocco, B.M., Scandiffio, G., Volpi, G., Barrios, L., Handal, S., Monterrosa, M., Quezada, A., Santos, P., 2003, Conceptual Model Review of the Berlín Geothermal System (El Salvador): *GRC Transactions*, v. 27, p. 755–759.
- Asanuma, H., Mitsumori, S., Adachi, M., Saeki, K., Aoyama, K., Ozeki, H., 2012, Estimation of Stress State at Yanaizu-Nishiyama Geothermal Field Using Microseismic Multiplets: *GRC Transactions*, v. 36, p. 989–994.
- Asanuma, H., Mitsumori, S., Saeki, K., Aoyama, K., Ozeki, H., Mukuhira, Y., Niitsuma, H., 2011, Characteristics of Microearthquakes at Yanaizu-Nishiyama Geothermal Field: *GRC Transactions*, v. 35, p.1613–1616.
- Asturias, F., 2015, Reservoir Assessment of Zunil I and II Geothermal Fields, Guatemala: *Proceedings World Geothermal Congress*, p. 1–5.
- Austria, D.C.S., Tugawin, R.J., Pastor, M.S., Morillo, L.B., Los Banos, C.F., Layugan, D.B., 2015, Subsurface Characterization of the Leyte Geothermal Field, Philippines Using Magnetotellurics: *Proceedings World Geothermal Congress*, p. 1–7.
- Authemayou, C., Brocard, G., Teyssier, C., Simon-Labric, T., Guttierrez, A., 2011, The Caribbean-North America-Cocos Triple Junction and the dynamics of the Polochic-Motagua Fault Systems: Pull-Up and Zipper Models: *Tectonics*, v. 20, p. 1–23.
- Avé Lallemant, H.G., 1996, Displacement partitioning and arc-parallel extension in the Aleutian volcanic arc: *Tectonophysics*, v. 256, p. 279-293.
- Avé Lallemant, H.G., and Oldow, J.S., 2000, Active displacement partitioning and arc-parallel extension of the Aleutian volcanic arc based on Global Positioning System geodesy and kinematic analysis: *Geology*, v. 28, no. 8, p. 739-372.
- Avellán, D.R., Macías, J.L., Pardo, N., Scolamacchia, T., Rodriguez, D., 2012, Stratigraphy, geomorphology, geochemistry and hazard implications of the Nejapa Volcanic Field, western Managua, Nicaragua:

- Journal of Volcanology and Geothermal Research, v. 213-214, p. 51–71, doi:10.1016/j.jvolgeores.2011.11.002
- Barelli, A., Ceccarelli, A., Dini, I., Fiodelisi, A., Giorgi, N., Lovari, F., Romagnoli, P., 2010, A Review of the Mt. Amiata Geothermal System (Italy): Proceedings World Geothermal Congress, p. 1–6.
- Barton, C. A., Zoback, M. D., and Moos, D., 1995, Fluid flow along potentially active faults in crystalline rock: *Geology*, v. 23, p. 683-686.
- Beikman, H.M., 1980, Geologic Map of Alaska: Alaska Department of Natural Resources, Division of Geological and Geophysical Surveys, Scale 1:2,500,000
- Bell, J.W., and Ramelli, A.R., 2007, Active faults and neotectonics at geothermal sites in the western Basin and Range: Preliminary results: *Geothermal Resources Council Transactions*, v. 31, p. 375-378.
- Blackwell, J.L., Cooke, D.R., McPhie, J., Simpson, K.A., 2014, Lithofacies Associations and Evolution of the Volcanic Host Succession to the Minifie Ore Zone: Ladolam Gold Deposit, Lihir Island, Papua New Guinea: *Economic Geology*, v. 109, p. 1137–1160.
- Bogie, I., Kusumah, Y.I., Wisnandary, M.C., 2008, Overview of the Wayang Windu geothermal field, West Java, Indonesia: *Geothermics*, v. 37, p. 347–365, doi:10.1016/j.geothermics.2008.03.004
- Broggi, A., 2008, Fault zone architecture and permeability features in siliceous sedimentary rocks: Insights from the Rapolano geothermal area (Northern Apennines, Italy): *Journal of Structural Geology*, v. 30, p. 237–256, doi:10.1016/j.jsg.2007.10.004
- Buonassorte, G., Cameli, G.M., Fiordelisi, A., Parotto, M., Perticone, I., 1995, Results of Geothermal Exploration in Central Italy (Latium-Campania): *World Geothermal Congress*, p. 1–6.
- Buurman, H., Nye, C.J., West, M.W., and Cameron, C., 2014, Regional controls on volcano seismicity along the Aleutian arc: *Geochemistry, Geophysics, Geosystems*, v. 15, p. 1-17
- Cabezas, D.H., 2015, Resistivity Structure of the SE Sector of the Miravalles Caldera: *Proceedings World Geothermal Congress*, p. 1–10.
- Cabezas, D.H., 2010, Precision Gravity Data of the Miravalles Geothermal Field an Ongoing Assessment: *Proceedings World Geothermal Congress*, p. 1–4.
- Cáceres, D., Monterroso, D., Tavakoli, B., 2005, Crustal deformation in northern Central America: *Tectonophysics*, v. 404, p. 119–131, doi:10.1016/j.tecto.2005.05.008
- Cailleau, B., LaFemina, P.C., Dixon, T.H., 2007, Stress accumulation between volcanoes: an explanation for intra-arc earthquakes in Nicaragua?: *Geophysical Journal International*, v. 169, p. 1132–1138, doi:10.1111/j.1365-246X.2007.03353.x
- Calamita, F., Coltorti, M., Piccinini, D., Pierantoni, P.P., Pizzi, A., Ripepe, M., Scisciani, V., Turco, E., 2000, Quaternary Faults and Seismicity in the Umbro-Marchean Apennines (Central Italy): Evidence from the 1997 Colfiorito Earthquake: *Journal of Geodynamics*, v. 29, p. 245–264.
- Canora, C., Martínez-Díaz, J.J., Villamor, P., Staller, A., Berryman, K., Álvarez-Gómez, J.A., Capote, R., Diaz, M., 2014, Structural evolution of the El Salvador Fault Zone: an evolving fault system within a volcanic arc: *Journal of Iberian Geology*, v. 40, doi:10.5209/rev_JIGE.2014.v40.n3.43559
- Carranza, E.J.M., Wibowo, H., Barritt, S.D., Sumintadireja, P., 2008, Spatial data analysis and integration for regional-scale geothermal potential mapping, West Java, Indonesia: *Geothermics*, v. 37, p. 267–299, doi:10.1016/j.geothermics.2008.03.003
- Carrasco-Núñez, G., Arzate, J., Bernal, J.P., Jaime, C., Cedillo, F., Dávila-Harris, P., Hernández, J., Levresse, G., Lopéz, P., Manea, V., Norini, G., Santoyo, E., Willcox, C., 2015, A New Geothermal Exploration Program at Los Humeros Volcanic and Geothermal Field (Eastern Mexican Volcanic Belt), *Proceedings World Geothermal Congress*: 1–10.
- Cataldi, R., Stefani, G., Tongiorgi, M., 1963, Geology of Larderello Region (Tuscany): Contribution to the Study of the Geothermal Basin: *Nuclear Geology on Geothermal Areas*, p. 235–265.
- Cecchi, E., van Wyk de Vries, B., Lavest, J.-M., 2004, Flank spreading and collapse of weak-cored volcanoes: *Bulletin of Volcanology* v. 67, p. 72–91, doi:10.1007/s00445-004-0369-3

- Cembrano, J., Herve, F., 1993, The Liquiñe Ofqui Fault Zone: A major Cenozoic Strike Slip Duplex in the Southern Andes: Second ISAG, p. 175–178.
- Cembrano, J., Hervé, F., Lavenu, A., 1996, The Liquiñe Ofqui Fault Zone: a Long-Lived Intra-Arc Fault System in Southern Chile: *Tectonophysics*, v. 259, p. 55–66.
- Cembrano, J., Lara, L., 2009, The link between volcanism and tectonics in the southern volcanic zone of the Chilean Andes: A review: *Tectonophysics*, v. 471, p. 96–113, doi:10.1016/j.tecto.2009.02.038
- Cembrano, J., Schermer, E., Lavenu, A., Sanhueza, A., 2000, Contrasting Nature of Deformation Along an Intra-Arc Shear Zone, the Liquiñe-Ofqui Fault Zone, Southern Chilean Andes: *Tectonophysics*, v. 319, p. 129–149.
- Ceroti, M., Fiordelisi, A., Fulignati, P., Marianelli, P., Sbrana, A., Scazzola, S., 2015, Integrated Approach for a Successful Geothermal Wells Location in the Mt. Amiata Area (Southern Tuscany): *Proceedings World Geothermal Congress*, p. 1–9.
- Chavarría, L., Mora, O., Hakanson, E., Galves, M., Rojas, M., Molina, F., Murillo, A., 2010, Geologic Model of the Pailas Geothermal Field, Guanacaste, Costa Rica: *Proceedings World Geothermal Congress*, p. 1–4.
- Chavarría, L., Rodríguez, A., 2015, Geothermal Reconnaissance of the Caribbean Flank of the Rincón de la Vieja Volcano, Costa Rica: *Proceedings World Geothermal Congress*, p. 1–7.
- Chernicoff, C.J., Richards, J.P., Zappenttini, E.O., 2002, Crustal Lineament Control on Magmatism and Mineralization in Northwestern Argentina: Geological, Geophysical, and Remote Sensing Evidence: *Ore Geology Reviews*, v. 21, p. 127–155.
- Chynne, M.A., Muffler, L.J.P., 2010, Geologic Map of Lassen Volcanic National Park and Vicinity, California: USGS Scientific Investigations Map 2899.
- Cladouhos, T.T., Allmendinger, R.W., Coira, B., Farrar, E., 1994, Late Cenozoic Deformation in the Central Andes: Fault Kinematics from the Northern Puna Northwestern Argentina and Southwestern Bolivia: *Journal of South American Earth Sciences*, v. 7, p. 209–228.
- Clausen, S., Nemčok, M., Moore, J., Hulen, J., Bartley, J., 2006, Mapping Fractures in the Medicine Lake Geothermal System: *GRC Transactions*, v. 30, p. 383–386.
- Clynne, M.A., Janik, C.J., Muffler, L.J.P., 2003, “Hot Water” in Lassen Volcanic National Park -- Fumaroles, Steaming Ground, and Boiling Mudpots; USGS Fact Sheet 101-02.
- Cole, J.W., Deering, C.D., Burt, R.M., Sewell, S., Shane, P.A.R., Matthews, N.E., 2014, Okataina Volcanic Centre, Taupo Volcanic Zone, New Zealand: A review of volcanism and synchronous pluton development in an active, dominantly silicic caldera system: *Earth-Science Reviews*, v. 128, p. 1–17. doi:10.1016/j.earscirev.2013.10.008
- Coolbaugh, M., Shevenell, L., Hinz, N.H., Stelling, P., Melosh, G., Cumming, W., Kreemer, C., Wilmarth, M., 2015, Preliminary ranking of geothermal potential in the Cascade and Aleutian volcanic arcs, Part III: Regional data review and modeling: *Geothermal Resources Council Transactions*, v. 39 (this volume).
- Corti, G., Carminati, E., Mazzarini, F., Garcia, M.O., 2005, Active Strike-Slip Faulting in El Salvador, Central America: *Geology*, v. 33, p. 989–992.
- County, C., 1987, *Oil and Gas News: Oregon Geology*, v. 49.
- Cowan, H., Machette, M.N., Amador, X., Morgan, K.S., Dart, R.L., Bradley, L.-A., 2000, Map and Database of Quaternary Faults in the Vicinity of Managua, Nicaragua (Open-File No. 00-437): U.S. Geological Survey.
- Cowan, H., Prentice, C., Pantosti, D., de Martini, P., Strauch, W., 2002, Late Holocene Earthquakes on the Aeropuerto Fault, Managua, Nicaragua: *Bulletin of the Seismological Society of America*, v. 92, p. 1694–1707.
- Curewitz, D. and Karson, J.A., 1997, Structural settings of hydrothermal outflow: fracture permeability maintained by fault propagation and interaction: *Journal of Volcanology and Geothermal Research*, v. 79, p. 149-168.

- Daud, Y., Sudarman, S., Ushijima, K., August 26-29, 2001, Sibayak Geothermal Field (Indonesia): Structure Assessed From Gravity and Hydrogeological Considerations: GRC Transactions, v. 25, p. 395–399.
- Davatzes, N.C., Hickman, S.H., 2011, Preliminary Analysis of Stress in the Newberry EGS Well NWG 55-29: GRC Transactions, v. 35, p. 323–332.
- Decker, P.L., Reifensuhl, A.E., Gillis, R.J., 2008, Structural linkage of major tectonic elements in the Ugashik-Becharof Lakes region, northeastern Alaska Peninsula: Bristol Bay-Alaska Peninsula region, overview of 2004-2007, p. 85–103.
- Denig-Chakroff, D., Reeder, J.W., Economides, M.J., 1985, Development Potential of the Makushin Geothermal Reservoir of Unalaska Island, Alaska: GRC Transactions, v. 9, p. 177–182.
- Detterman, R.L., Case, J.E., Wilson, F.H., Yount, M.E., 1987, Geologic Map of the Ugashik, Bristol Bay, and Western Part of Karluk Quadrangles, Alaska: Miscellaneous Investigations Series.
- Dewey, J.F., 1988, Extensional collapse of orogens: Tectonics, v. 7, no. 6, p. 1123-1139.
- Dewey, J.F., and Lamb, S.H., 1992, Active tectonics of the Andes: Tectonophysics, v. 205, nos. 79-95, p. 79 – 94.
- Distribution of Active Faults and Trenches in the Philippines, 2000.
- Donnelly-Nolan, J.M., 1990, Geology of Medicine Lake Volcano, Northern California Cascade Range: GRC Transactions, v. 14, p. 1395–1396.
- Dougherty, S.L., Clayton, R.W., 2014, Seismicity and structure in central Mexico: Evidence for a possible slab tear in the South Cocos plate: Journal of Geophysical Research: Solid Earth v. 119, p. 3424–3447. doi:10.1002/2013JB010883
- Drewes, H., 1961, Geology of Unalaska Island and adjacent insular shelf, Aleutian Islands, Alaska: US Government Printing Office.
- Dzierma, Y., Thorwart, M., Rabbell, W., Siegmund, C., Comte, D., Bataille, K., Iglesia, P., Prezzi, C., 2012, Seismicity near the slip maximum of the 1960 Mw 9.5 Valdivia earthquake (Chile): Plate interface lock and reactivation of the subducted Valdivia Fracture Zone: Journal of Geophysical Research, v. 117. doi:10.1029/2011JB008914
- Economides, M.J., Morris, C.W., Campbell, D.A., 1985, Evaluation of the Makushin Geothermal Reservoir, Unalaska Island: 10th Workshop on Geothermal Reservoir Engineering, p. 227–232.
- Ego, F., Ansan, V., 2002, Why is the Central Trans-Mexican Volcanic Belt (102°-99°W) in Transtensive Deformation?: Tectonophysics, v. 359, p. 198–208.
- Elizondo, D.B., 2015, Resistivity Imaging of the Santa Maria Sector and the Northern Zone of Las Pailas Geothermal Area, Costa Rica, Using Joint 1D Inversion of Tdem and Mt Data: Proceedings World Geothermal Congress, p. 1–11.
- Engdahl, E.R., van der Hilst, R., Buland, R., 1998, Global Teleseismic Earthquake Relocation with Improved Travel Times and Procedures for Depth Determination: Bulletin of the Seismological Society of America, v. 88, p. 722–743.
- Erdmer, P., Cui, Y., Massey, N.W.D., MacIntyre, D.G., Desjardins, P.J., Cooney, R.T., 2005, Geologic Map of British Columbia.
- Espinosa, A.F., 1984, Seismicity of Alaska and the Aleutian Islands, 1960-1983, Scale 1:2,500,000, 1 Sheet
- Espinosa, A.F., Rukstales, K.S., 1988, Geometry of the Benioff Zone and Mode of Subduction Beneath Southwestern Alaska and the Aleutian Islands: USGS, Miscellaneous Investigations Series, p. 1–4.
- Esquivias, H.P., Vásquez, J.L.M., Monroy, V.H.G., Saldaña, L.A., Tenorio, F.G., Govea, R.C., Layer, P., Girón, R.S., Martínez, C., Haro, A.J., Valdés, G., Meriggi, L., Hernández, R., 2010, Structural and Volcanologic Study on the Stratigraphic Sequence at Mil Cumbres and the Los Azufres Geothermal Field, Mich.: Geothermia, v. 23, p. 51–63.
- Faulds, J.E., Bouchot, V., Moeck, I., and Oğuz, K., 2009, Structural controls of geothermal systems in western Turkey: A preliminary report: Geothermal Resources Council Transactions, v. 33, p. 375-383.

- Faulds, J.E., Hinz, N.H., Coolbaugh, M.F., Cashman, P.H., Kratt, C., Dering, G., Edwards, J., Mayhew, B., and McLachlan, H., 2011, Assessment of favorable structural settings of geothermal systems in the Great Basin, Western USA: Geothermal Resources Council Transactions, v. 35, p. 777-784.
- Faulds, J.E., Hinz, N.H., Kreemer, C., and Coolbaugh, M., 2012, Regional patterns of geothermal activity in the Great Basin region, western USA: Correlation with strain rates: Geothermal Resources Council Transactions, v. 36, p. 897-902.
- Faulds, N.H., and Hinz, N.H., 2015, Favorable tectonic and structural settings of geothermal settings in the Great Basin Region, western USA: Proxies for discovering blind geothermal systems: Proceedings, World Geothermal Congress 2015, Melbourne, Australia.
- Fauzi, A., Permana, H., Indarto, S., Gaffar, E.Z., 2015, Regional Structure Control on Geothermal Systems in West Java, Indonesia: Proceedings World Geothermal Congress, p. 1–14.
- Feather, B.M., Malate, R.C., 2013, Numerical Modeling of the Mita Geothermal Field, Cerro Blanco, Guatemala: 38th Workshop on Geothermal Reservoir Engineering.
- Fernandez, M., 2013, Seismotectonic and the Hypothetical Strike – Slip Tectonic Boundary of Central Costa Rica, in: DAmico, S. (Ed.): Earthquake Research and Analysis - New Advances in Seismology.
- Ferrari, L., Conticelli, S., Vaggelli, G., Petrone, C.M., Manetti, P., 2000, Late Miocene Volcanism and Intra-Arc Tectonics During the Early Development of the Trans-Mexican Volcanic Belt: Tectonophysics, v. 318, p. 161–185.
- Ferrari, L., Orozco-Esquivel, T., Manea, V., Manea, M., 2012, The dynamic history of the Trans-Mexican Volcanic Belt and the Mexico subduction zone: Tectonophysics, v. 522-523, p. 122–149, doi:10.1016/j.tecto.2011.09.018
- Fliedner, M.M., Klemperer, S.L., 2000, Crustal structure transition from oceanic arc to continental arc, eastern Aleutian Islands and Alaska Peninsula: Earth and Planetary Science Letters, v. 179, p. 567–579.
- Folguera, A., Ramos, V.A., Hermanns, R.L., Naranjo, J., 2004, Neotectonics in the foothills of the southernmost central Andes (37°-38°S): Evidence of strike-slip displacement along the Antifñir-Copahue fault zone: NEUQUÉN ANDES NEOTECTONICS, Tectonics: v. 23, doi:10.1029/2003TC001533
- Franco, A., Lasserre, C., Lyon-Caen, H., Kostoglodov, V., Molina, E., Guzman-Speziale, M., Monterosso, D., Robles, V., Figueroa, C., Amaya, W., Barrier, E., Chiquin, L., Moran, S., Flores, O., Romero, J., Santiago, J.A., Manea, M., Manea, V.C., 2012, Fault kinematics in northern Central America and coupling along the subduction interface of the Cocos Plate, from GPS data in Chiapas (Mexico), Guatemala and El Salvador: Kinematics in northern Central America: Geophysical Journal International, v. 189, p. 1223–1236, doi:10.1111/j.1365-246X.2012.05390.x
- Frey, H.M., Lange, R.A., Hall, C.M., Nelson, S.A., Granados, H.D., 2004, Eruptive History of Volcán Tepetitlic, Mexico: Evidence for Remelting of Silicic Ashflows Revealed by $^{40}\text{Ar}/^{39}\text{Ar}$ Geochronology, in: AGU Fall Meeting Abstracts, p. 0606.
- Friele, P., Jakob, M., and Clague, J., 2008, Hazard and risk from large landslides from Mount Meager volcano, British Columbia, Canada: Georisk, v. 2, no. 1, p. 48-64.
- Fulignati, P., Marianelli, P., Sbrana, A., Ciani, V., 2014, 3D Geothermal Modeling of the Mount Amiata Hydrothermal System in Italy: Energies, v. 7, p. 7434–7453, doi:10.3390/en7117434
- Funk, J., Mann, P., McIntosh, K., Stephens, J., 2009, Cenozoic Tectonics of the Nicaraguan Depression, Nicaragua, and Median Trough, El Salvador, Based on Seismic-Reflection Profiling and Remote-Sensing Data: Geological Society of America Bulletin, v. 121, p. 1491–1521.
- Gaedicke, C., Baranov, B., Seliverstov, N., Alexeiev, D., Tsukanov, N., Freitag, R., 2000, Structure of an active arc-continent collision area: the Aleutian–Kamchatka junction: Tectonophysics, v. 325, p. 63–85.

- Galgana, G., Hamburger, M., McCaffrey, R., Corpuz, E., and Chen, Q.-Z., 2007, Analysis of crustal deformation of Luzon Island, Philippines, using geodetic observations and earthquake focal mechanisms: *Tectonophysics*, v. 432, p. 63–87, doi: 10.1016/j.tecto.2006.12.001.
- Ganda, S., Sunaryo, D., Tampubolon, T., 1992, Exploration Progress of High Enthalpy Geothermal Prospect in Indonesia: *GRC Transactions*, v. 16, p. 83–88.
- Garchar, L., Wendlandt, R., 2012, Geochemistry of a volcanic hydrothermal system at Mount Spurr, Alaska, in: *Masters Abstracts International*.
- Gardner, T.W., Verdonck, D., Pinter, N.M., Slingerland, R., Furlong, K.P., Bullard, T.F., Wells, S.G., 1992, Quaternary Uplift Astride the Aseismic Cocos Ridge, Pacific Coast, Costa Rica: *Geological Society of America Bulletin*, v. 104, p. 219–232.
- Miller, T.P., Riehle, J.R., Yount, M.E., 1987, *Geologic Map of Yantarni Volcano, Alaska Peninsula, Alaska: U.S. Geologic Survey, Scale 1:63,360*
- Ghomshei, M.M., 2010, Canadian Geothermal Power Prospects: *Proceedings World Geothermal Congress*, p. 1–5.
- Ghomshei, M., Sanyal, S., MacLeod, K., Henneberger, R., Ryder, A., Meech, J., Fainbank, B., 2004, Status of the South Meager Geothermal Project British Columbia, Canada: *Resource Evaluation and Plans for Development: GRC Transactions*, v. 28, p. 339–344.
- Gioncada, A., Vezzoli, L., Mazzuoli, R., Omarini, R., Nonnotte, P., Guillou, H., 2010, Pliocene intraplate-type volcanism in the Andean foreland at 26 10'S, 64 40'W (NW Argentina): Implications for magmatic and structural evolution of the Central Andes: *Lithosphere*, v. 2, p. 153–171, doi:10.1130/L81.1
- Girard, G., van Wyk de Vries, B., 2005, The Managua Graben and Las Sierras-Masaya volcanic complex (Nicaragua); pull-apart localization by an intrusive complex: results from analogue modeling: *Journal of Volcanology and Geothermal Research*, v. 144, p. 37–57, doi:10.1016/j.jvolgeores.2004.11.016
- Goldsmith, L.H., 1980, Regional and Local Geologic Structure of the Momotombo Field, Nicaragua: *GRC Transactions*, v. 4, p. 125–128.
- Gonzalez Partida, E., Rodriguez, V.T., Birkle, P., Gomez, V.A., Romero, A.C., 1995, *Geology of the Ahuachapan-Chipilapa, El Salvador C.A. Geothermal Zone: World Geothermal Congress*.
- Gordon, M.B., 1997, Neogene Tectonics of the Chortís Block: A Wide Zone of Deformation Responding to Interaction Between the North America and Caribbean Plates, in: *Strike-Slip Faulting and Basin Formation at the Guayape Fault--Valle de Catacasmás Intersection, Honduras, Central America*.
- Gregory, E.C.H., Salazar, R.R., Protti, O.M., Orellana, M.G., 2015, Update of the Geologic Model at the Las Pailas Geothermal Field to the East of Unit 1: *Proceedings World Geothermal Congress*, p. 1–10.
- Gunderson, R., Ganefianto, N., Riedel, K., Sirad-Azwar, L., Syafei, S., 2000, Exploration Results in the Sarulla Block, North Sumatra, Indonesia: *Proceedings World Geothermal Congress*, p. 1–6.
- Gunderson, R.P., Dobson, P.F., Sharp, W.D., Pudjianto, R., Hasibuan, A., 2000, Geology and Thermal Features of the Sarulla Contract Area, North Sumatra, Indonesia: *Proceedings World Geothermal Congress*, p. 687–692.
- Gutiérrez-Negrín, L.C.A., 2015, Mexican Geothermal Plays: *Proceedings World Geothermal Congress*, p. 1–9.
- Guzmán-Speziale, M., 2001, Active Seismic Deformation in the Grabens of Northern Central America and Its Relationship to the Relative Motion of the North America-Caribbean Plate Boundary: *Tectonophysics*, v. 337, p. 39–51.
- Hantono, D., Mulyono, A., Hasibuan, A., 1996, Structural Control is a Strategy for Exploitation Well at Kamojang Geothermal Field, West Java, Indonesia: *21st Workshop on Geothermal Reservoir Engineering*, p. 79–84.
- Harijoko, A., Uruma, R., Wibowo, H.E., Setijadji, L.D., Imai, A., Koichiro, W., 2010, Long-Term Volcanic Evolution Surrounding Dieng Geothermal Area, Indonesia: *Proceedings World Geothermal Congress*, p. 1–6.

- Heidbach, O., Tingay, M., Barth, A., Reinecker, J., Kurfe, D. and Müller, B., 2008, The World Stress Map database release 2008 doi:10.1594/GFZ WSM Rel2008.
- Heit, B., Koulakov, I., Asch, G., Yuan, X., Kind, R., Alcocer-Rodriguez, I., Tawackoli, S., Wilke, H., 2008, More constraints to determine the seismic structure beneath the Central Andes at 21°S using teleseismic tomography analysis: *Journal of South American Earth Sciences*, v. 25, p. 22–36, doi:10.1016/j.jsames.2007.08.009
- Hernandez-Moreno, C., Speranza, F., Di Chiara, A., 2014, Understanding kinematics of intra-arc transcurrent deformation: Paleomagnetic evidence from the Liquiñe-Ofqui fault zone (Chile, 38-41°S): Rotation along the Liquiñe-Ofqui fault: *Tectonics*, v. 33, p. 1964–1988, doi:10.1002/2014TC003622
- Hickman, R.G., Dobson, P.F., Gerven, M. va., Sagala, B.D., Gunderson, R.P., 2004, Tectonic and stratigraphic evolution of the Sarulla graben geothermal area, North Sumatra, Indonesia: *Journal of Asian Earth Sciences*: v. 23, p. 435–448, doi:10.1016/S1367-9120(03)00155-X
- Hiess, J., Cole, J.W., Spinks, K.D., 2007, Influence of the crust and crustal structure on the location and composition of high-alumina basalts of the Taupo Volcanic Zone, New Zealand: *New Zealand Journal of Geology and Geophysics*, v. 50, p. 327–342, doi:10.1080/00288300709509840
- Holbrook, W.S., Lizarralde, D., McGeary, S., Bangs, N., Diebold, J., 1999, Structure and composition of the Aleutian island arc and implications for continental crustal growth: *Geology*, v. 27, p. 31–34.
- Houghton, B.F., Wilson, C.J.N., McWilliams, M.O., Lanphere, M.A., Weaver, S.D., Briggs, R.M., Pringle, M.S., 1995, Chronology and Dynamics of a Large Silicic Magmatic System: Central Taupo Volcanic Zone, New Zealand: *Geology*, v. 23, p. 13–16.
- Hurst, A.W., Bibby, H.M., Robinson, R.R., 2002, Earthquake focal mechanisms in the central Taupo Volcanic Zone and their relation to faulting and deformation: *New Zealand Journal of Geology and Geophysics*, v. 45, p. 527–536, doi:10.1080/00288306.2002.9514989
- Ingebritsen, S.E., Sherrod, D.R., Mariner, R.H., 1989, Heat Flow and Hydrothermal Circulation in the Cascade Range, North-Central Oregon: *Science*, v. 243, p. 1458–1462.
- Isselhardt, C.F., Matlick, J.S., Parmentier, P.P., Bamford, R.W., 1983, Temperature Gradient Hole Results from Makushin Geothermal Area, Unalaska Island, Alaska: *GRC Transactions*, v. 7, p. 95–98.
- Itoh, Y., Kusumoto, S., Takemura VI, K., 2013, Characteristic Basin Formation at Terminations of a Large Transcurrent Fault — Basin Configuration Based on Gravity and Geomagnetic Data, in: Itoh, Y. (Ed.), *Mechanism of Sedimentary Basin Formation - Multidisciplinary Approach on Active Plate Margins*.
- Jensen, E., Cembrano, J., Faulkner, D., Veloso, E., Arancibia, G., 2011, Development of a self-similar strike-slip duplex system in the Atacama Fault system, Chile: *Journal of Structural Geology*, v. 33, p. 1611–1626, doi:10.1016/j.jsg.2011.09.002
- Jicha, B.R., Singer, B.S., 2006, Volcanic history and magmatic evolution of Seguam Island, Aleutian Island arc, Alaska: *Geological Society of America Bulletin*, v. 118, p. 805–822.
- Kalacheva, E.G., Kotenko, T.A., 2015, Hydrothermal Systems of the Shiashkotan Island (Kurile Islands, Russia): *Proceedings World Geothermal Congress*, p. 1–10.
- Kanamori, H., 1970, The Alaska earthquake of 1964: Radiation of long-period surface waves and source mechanism: *Journal of Geophysical Research*, v. 75, p. 5029–5040.
- Kawakami, G., 2013: Foreland Basins at the Miocene Arc-Arc Junction, Central Hokkaido, Northern Japan, in: Itoh, Y. (Ed.), *Mechanism of Sedimentary Basin Formation - Multidisciplinary Approach on Active Plate Margins*. InTech.
- Koehler, R.D., Farrell, R.-E., Burns, P.A., Combellick, R.A., 2012, Alaska's Quaternary Faults, Scale 1:370000
- Koseki, T., Nakashima, K., 2006, Geothermal Structure and Feature of Sulfide Minerals of the Mataloko Geothermal Field, Flores Island, Indonesia: 7th Asian Geothermal Symposium, p. 105–109.
- Kusumoto, S., Itoh, Y., Takano, O., Tamaki, M., 2013, Numerical Modeling of Sedimentary Basin Formation at the Termination of Lateral Faults in a Tectonic Region where Fault Propagation has Occurred, in:

- Itoh, Y. (Ed.), Mechanism of Sedimentary Basin Formation - Multidisciplinary Approach on Active Plate Margins. InTech.
- Kutterolf, S., Freundt, A., Pérez, W., Wehrmann, H., Schmincke, H.-U., 2007, Late Pleistocene to Holocene temporal succession and magnitudes of highly-explosive volcanic eruptions in west-central Nicaragua: *Journal of Volcanology and Geothermal Research*, v. 163, p. 55–82, doi:10.1016/j.jvolgeores.2007.02.006
- La Femina, P.C., Dixon, T.H., Strauch, W., 2002, Bookshelf Faulting in Nicaragua: *Geology*, v. 30, p. 751–754.
- Lagmay, A.M.F., van Wyk de Vries, B., Kerle, N., Pyle, D.M., 2000, Volcano instability induced by strike-slip faulting: *Bulletin of Volcanology*, v. 62, p. 331–346, doi:10.1007/s004450000103
- Lallemant, H.G.A., Oldow, J.S., 2000, Active displacement partitioning and arc-parallel extension of the Aleutian volcanic arc based on Global Positioning System geodesy and kinematic analysis: *Geology*, v. 28, p. 739–742.
- Lange, D., Cembrano, J., Rietbrock, A., Haberland, C., Dahm, T., Bataille, K., 2008, First seismic record for intra-arc strike-slip tectonics along the Liquiñe-Ofqui fault zone at the obliquely convergent plate margin of the southern Andes: *Tectonophysics*, v. 455, p. 14–24, doi:10.1016/j.tecto.2008.04.014
- Lanza, F., Tibaldi, A., Bonali, F.L., Corazzato, C., 2013, Space–time variations of stresses in the Miocene–Quaternary along the Calama–Olacapato–El Toro Fault Zone, Central Andes: *Tectonophysics*, v. 593, p. 33–56, doi:10.1016/j.tecto.2013.02.029
- Layman, E.B., Agus, I., Warsa, S., 2002, The Dieng Geothermal Resource, Central Java, Indonesia: *GRC Transactions*, v. 26, p. 573–579.
- Lewis, J., 2015, Northern Exposure: *Whitman Magazine* Winter, p. 24–29.
- Lobato, E.M.L., Fujino, T., Ayala, J.C.P., 2000, Geothermal Field Exploration in Guatemala: *Geothermal Development*, p. 215–220.
- López, D.L., Padrón, E., Gomez, L., Barrios, L.A., Pérez, N.M., Hernández, P., 2004, Structural Control on Thermal Anomalies and Diffuse Surficial Degassing at Berlín Geothermal Field, El Salvador: *GRC Transactions*, v. 28, p. 477–484.
- Lopez, S., Bouchot, V., Lakhssassi, M., Calcagno, P., Grappe, B., 2010, Modeling of Bouillante Geothermal Field (Guadeloupe, French Lesser Antilles): 35th Workshop on Geothermal Reservoir Engineering.
- Lowenstern, J.B., Donnelly-Nolan, J., Wooden, J.L., Charlier, B.L.A., 2003, Volcanism, Plutonism, and Hydrothermal Alteration at Medicine Lake Volcano, California: 28th Workshop on Geothermal Reservoir Engineering, p. 1–8.
- Lu, Z., Moran, S. C., Thatcher, W., Wicks, C. J., Dzurisin, D., and Power, J. A., 2002, Magmatic inflation at a dormant stratovolcano: 1996–1998 activity at Mount Peulik volcano, revealed by satellite radar interferometry, *Journal of Geophysical Research*, v. 107, p. 4–13.
- Lutz, S.J., Hulen, J.B., Schriener Jr., A., 2000, Alteration, Geothermometry, and Gravitoid Intrusions in Well GMF 31-17, Medicine Lake Volcano Geothermal System, California: 25th Workshop on Geothermal Reservoir Engineering.
- Mahon, T., Modjo, S., Radja, V.T., 1992, The Results of a Joint Scientific Study of the Flores Ulumbu Geothermal Area: *GRC Transactions*, v. 16, p. 97–104.
- Mahony, S.H., Wallace, L.M., Miyoshi, M., Villamor, P., Sparks, R.S.J., and Hasenaka, T., 2011, Volcano-tectonic interactions during rapid plate-boundary evolution in the Kyushu region, SW Japan: *Geological Society of America Bulletin*, v. 123, no. 11/12, p. 2201–2223.
- Manzo, A.R., 2005, Geothermal power development in Guatemala 2000–2005, in: *Proceedings*.
- Marrett, R.A., Allmendinger, R.W., Alonso, R.N., Drake, R.E., 1994, Late Cenozoic Tectonic Evolution of Puna Plateau and Adjacent Foreland, Northwestern Argentine Andes: *Journal of South American Earth Sciences*, v. 7, p. 179–207.

- Martin, B.S., Petcovic, H.L., Reidel, S.P., 2005, Goldschmidt Conference 2005: Field Trip Guide to the Columbia River Basalt Group: Pacific Northwest National Laboratory.
- Martini, B.A., Lide, C., Owens, L., Walsh, P., Delwiche, B., Payne, A., 2011, Geothermal Resource Definition at Mt. Spurr, Alaska: GRC Transactions, v. 35, p. 897–904.
- Mas, G.R., Mas, L.C., Bengochea, L., 1996, Hydrothermal, surface alteration in the Copahue geothermal field (Argentina), in: Proceedings Twenty-Fifth Workshop on Geothermal Reservoir Engineering, Stanford University. Stanford, California. p. 22–24.
- Mas, L.C., Bengochea, L., Mas, G., López, N., 2010, Recent Changes in the Copahue Geothermal Field, Neuquén Province, Argentina: Proceedings World Geothermal Congress, p. 1–6.
- Mas, L., Mas, G., Bengochea, L., 2000, Heatflow of Copahue geothermal field, its relation with tectonic scheme, in: Proceedings of World Geothermal Congress, Tohoku, Japan, p. 1419–1424.
- Mathieu, L., van Wyk de Vries, B., 2011, The impact of strike-slip, transtensional and transpressional fault zones on volcanoes. Part 1: Scaled experiments: *Journal of Structural Geology*, v. 33, p. 907–917, doi:10.1016/j.jsg.2011.03.002
- Mathieu, L., van Wyk de Vries, B., Pilato, M., Troll, V.R., 2011, The interaction between volcanoes and strike-slip, transtensional and transpressional fault zones: Analogue models and natural examples: *Journal of Structural Geology*, v. 33, p. 898–906, doi:10.1016/j.jsg.2011.03.003
- Matteini, M., Mazzuoli, R., Omarini, R., Cas, R., Maas, R., 2002, Geodynamical Evolution of Central Andes at 24°S as Inferred by Magma Composition along the Calama-Olacapato-El Toro Transversal Volcanic Belt: *Journal of Volcanology and Geothermal Research*, v. 118, p. 205–228.
- Matteini, M., Mazzuoli, R., Omarini, R., Cas, R., Maas, R., 2002, The geochemical variations of the upper Cenozoic volcanism along the Calama–Olacapato–El Toro transversal fault system in central Andes (~ 24 S): petrogenetic and geodynamic implications: *Tectonophysics*, v. 345, p. 211–227.
- McCaffrey, R., King, R.W., Payne, S.J., Lancaster, M., 2013, Active tectonics of northwestern U.S. inferred from GPS-derived surface velocities: *Pacific Northwest: Journal of Geophysical Research: Solid Earth*, v. 118, p. 709–723, doi:10.1029/2012JB009473
- McCloughry, J.D., Wiley, T.J., Conrey, R.M., Jones, C.B., Lite Jr., K.E., 2013, The Hood River Graben: A Late Pliocene and Quaternary Intra-Arc Half Graben in the Northern Oregon Cascade Range: *Geologic Society of America Abstracts with Programs*, Paper No. 9-7 45, 14.
- McDowell, J., White, P., 2011, Updated resource assessment and 3-D geological model of the Mita Geothermal System, Guatemala: *Geothermal Resources Council Transactions*, v. 35, p. 99–107.
- McNamara, D.D., Massiot, C., Lewis, B., 2013, A Structural Review of the Wairakei-Tauhara Geothermal Field: *GNS Science Report*, p. 1–20.
- Melosh, G., Cumming, W., Benoit, D., Wilmarth, M., Colvin, A., Winick, J., Soto-Neira, E., Sussman, D., Urzúa-Monsalve, L., Powell, T., others, 2010, Exploration results and resource conceptual model of the Tolhuaca Geothermal Field, Chile.
- Melosh, G., Cumming, W., Sussman, D., Benoit, D., Soto, E., Colvin, A., Wilmarth, M., Winick, J., Fredes, L., 2009, Rapid Exploration of the Tolhuaca Prospect, Southern Chile: *Geothermal Resources Council*, Reno, Nevada.
- Melosh, G., Moore, J., Stacey, R., 2012, Natural reservoir evolution in the Tolhuaca geothermal field, southern Chile: 36th Workshop on Geothermal Reservoir Engineering
- Micklethwaite, S., and Cox, S.F., 2004, Fault-segment rupture, aftershock-zone fluid flow, and mineralization: *Geology*, v. 32, p. 813–816. doi:10.1130/G20559.1.
- Molina, F., Martí, J., Aguirre, G., Vega, E., Chavarría, L., 2014, Stratigraphy and structure of the Cañas Dulces caldera (Costa Rica): *Geological Society of America Bulletin*, v. 126, p. 1465–1480.
- Molnar, P. and Dayem, K.E., 2010, Major intracontinental strike-slip faults and contrasts in lithospheric strength: *Geosphere*, v. 6, no. 6, p. 444–467.

- Moore, D.E., Hickman, S., Lockner, D.A., Dobson, P.F., 2001, Hydrothermal minerals and microstructures in the Silangkitang geothermal field along the Great Sumatran fault zone, Sumatra, Indonesia: Geological Society of America Bulletin, v. 113, p. 1179–1192. doi:10.1130/0016-7606(2001)113<1179:HMAMIT>2.0.CO;2
- Moore, J.L., Osburn, E., Storm, P.V., 1981, Geology and temperature distribution of Momotombo geothermal field, Nicaragua.
- Morell, K.D., Fisher, D.M., Gardner, T.W., 2008, Inner forearc response to subduction of the Panama Fracture Zone, southern Central America: Earth and Planetary Science Letters, v. 265, p. 82–95. doi:10.1016/j.epsl.2007.09.039
- Motyka, R.J., Liss, S.A., Nye, C.J., Moorman, M.A., 1993, Geothermal Resources of the Aleutian Arc, Alaska: Alaska Department of Natural Resources, Division of Geological and Geophysical Surveys: Professional Report 114, 1–4.
- Motyka, R.J., Moorman, M.A., Liss, S.A., 1983, Geothermal Resources of Alaska: Alaska Department of Natural Resources, Division of Geological and Geophysical Surveys, Miscellaneous Publication MP8, Scale 1:2,500,000
- Motyka, R.J., Moorman, M.A., Poreda, R., 1983, Alaska Department of Natural Resources, Division of Geological and Geophysical Surveys: Report of Investigations, v. 83, p. 15.
- Motyka, R.J., Queen, L.D., Janik, C.J., Sheppard, D.S., Poreda, R.J., Liss, S.A., 1988, Fluid Geochemistry and Fluid-Mineral-Equilibria in Test Wells and Thermal Gradient Hole at the Makushin Geothermal Area, Unalaska Island, Alaska: Report of Investigations, v. 88, no. 14, p. 1–90.
- Motyka, R.J., Queen, L.D., Janik, C.J., Sheppard, D.S., Poreda, R.J., Liss, S.A., 1986, Fluid Geochemistry and Fluid-Mineral Equilibria in Test Wells and Thermal-Gradient Holes at the Makushin Geothermal Area, Unalaska Island, Alaska: Alaska Department of Natural Resources, Division of Geological and Geophysical Surveys: Public-data File 86-59, p. 1–155.
- Mouslopoulou, V., Hristopulos, D.T., 2011, Patterns of tectonic fault interactions captured through geostatistical analysis of microearthquakes: Journal of Geophysical Research, v. 116, doi:10.1029/2010JB007804
- Mouslopoulou, V., Hristopulos, D.T., Nicol, A., Walsh, J.J., Bannister, S., 2013, The importance of microearthquakes in crustal extension of an active rift: A case study from New Zealand: Extension Due to Microearthquakes: Journal of Geophysical Research: Solid Earth, v. 118, p. 1556–1568. doi:10.1002/jgrb.50062
- Moya, P., Nietzen, F., Castro, S., Taylor, W., 2011, Behavior of the Geothermal Reservoir at The Miravalles Geothermal Field During 1994-2010, in: Proceedings.
- Moya, P., Taylor, W., 2010, Micro-seismicity at the Miravalles Geothermal Field, Costa Rica (1994-2009): A Tool to Confirm the Real Extent of the Reservoir, in: 2010 :World Geothermal Congress, Bali, Indonesia, p. 25–30.
- Moya, P., Yock, A., 2005, First Eleven Years of Exploitation at the Miravalles Geothermal Field: 13th Workshop on Geothermal Reservoir Engineering.
- Muraoka, H., Nasution, A., Simanjuntak, J., Dwipa, S., Takahashi, M., Takahashi, H., Matsuda, K., Sueyoshi, Y., 2005, Geology and Geothermal Systems in the Bajawa Volcanic Rift Zone, Flores, Eastern Indonesia, in: Proceedings.
- Nakajima, T., 2013, Late Cenozoic Tectonic Events and Intra-Arc Basin Development in Northeast Japan, in: Itoh, Y. (Ed.), Mechanism of Sedimentary Basin Formation - Multidisciplinary Approach on Active Plate Margins. InTech.
- Nanlohy, F., Kusnadi, D., Sulaeman, B., 2001, Geology and geochemistry of Mataloko geothermal field, central Flores, East Nusa Tenggara: Proceeding of The 5th INAGA Scientific Conference & Exhibitions, Yogyakarta.

- Nasution, A., Muraoka, H., Takashima, I., Okubo, Y., Takahashi, H., Takahashi, M., Uchida, T., Andan, A., Matsuda, K., Nanlohi, F., Kusnadi, D., Sulaiman, B., Zulkarnain, N., 1999, Preliminary Survey of Bejawa Geothermal Area, Ngada District, Flores, East Nusa Tenggara, Indonesia: GRC Transactions, v. 23, p. 467–472.
- Nasution, A., Takashima, I., Muraoka, H., Takahashi, H., Matsuda, K., Akasako, H., Futagoishi, M., Kusnadi, D., Nanlohi, F., 2000, The geology and geochemistry of Mataloko-Nage-Bobo geothermal areas, central Flores, Indonesia, in: Proceedings of World Geothermal Congress 2000, Beppu and Morioka, Japan, p. 2165–2170.
- Neal, C., McGimsey, R.G., Diggles, M.F., 2001, Volcanoes of the Wrangell Mountains and Cook Inlet region, Alaska: selected photographs: US Geological Survey.
- Nemčok, M., Moore, J.N., Christensen, C., Allis, R., Powell, T., Murray, B., Nash, G., 2007, Controls on the Karaha–Telaga Bodas geothermal reservoir, Indonesia: Geothermics, v. 36, p. 9–46. doi:10.1016/j.geothermics.2006.09.005
- Nicol, A., Walsh, J.J., Berryman, K., Villamor, P., 2006, Interdependence of fault displacement rates and paleoearthquakes in an active rift: Geology, v. 34, p. 865–868.
- Noda, A., 2013, Strike-Slip Basin – Its Configuration and Sedimentary Facies, in: Itoh, Y. (Ed.), Mechanism of Sedimentary Basin Formation - Multidisciplinary Approach on Active Plate Margins. InTech.
- Nordquist, G.A., Acuna, J., Stimac, J., 2010, Precision Gravity Modeling and Interpretation at the Salak Geothermal Field, Indonesia, in: World Geothermal Congress, Bali, Indonesia, by International Geothermal Association.
- Nye, C.J., McConnell, V.S., Beget, J.E., Roach, A.L., Bean, K.W., 1986, Location of Samples from the Makushin Volcanic Field: Alaska Department of Natural Resources, Division of Geological & Geophysical Surveys, Public Data File 86-80, Scale 1: 50,000.
- Nye, C.J., Motyka, R.J., Turner, D.L., Liss, 1992, Geologic Map and Cross Sections of Geyser Creek Valley and Vicinity Umnak Island, Alaska: Alaska Department of Natural Resources, Division of Geological & Geophysical Surveys, Scale 1:24,000
- Oncken, O., Hindle, D., Kley, J., Elger, K., Victor, P., Schemmann, K., 2006, Deformation of the central Andean upper plate system—Facts, fiction, and constraints for plateau models, in: The Andes. Springer, p. 3–27.
- Padrón, E., López, D.L., Magaña, M.I., Marrero, R., Pérez, N.M., 2003, Diffuse Degassing and Relation to Structural Flow Paths at Ahuachapan Geothermal Field, El Salvador: GRC Transactions, v. 27, p. 325–330.
- Pardo, N., Macias, J.L., Giordano, G., Cianfarra, P., Avellán, D.R., Bellatreccia, F., 2009, The ~1245 yr BP Asososca maar eruption: The youngest event along the Nejapa–Miraflores volcanic fault, Western Managua, Nicaragua: Journal of Volcanology and Geothermal Research, v. 184, p. 292–312. doi:10.1016/j.jvolgeores.2009.04.006
- Partida, E.G., Rodríguez, V.T., Birkle, P., 1997, Plio-Pleistocene Volcanic History of the Ahuachapán Geothermal System, El Salvador: The Concepcion de Ataco Caldera: Geothermics, v. 26, p. 555–575.
- Pérez Esquivias, H., Macías Vázquez, J.L., Garduño Monroy, V.H., Arce Saldaña, J.L., García Tenorio, F., Castro Govea, R., Layer, P., Saucedo Girón, R., Martínez, C., Jiménez Haro, A., others, 2010, Estudio vulcanológico y estructural de la secuencia estratigráfica Mil Cumbres y del campo geotérmico de Los Azufres, Mich.: Geotermia, v. 23, p. 51–63.
- Petersen, S., Herzig, P.M., Hannington, M.D., Jonasson, I.R., Arribas, A., 2002, Submarine gold mineralization near Lihir Island, New Ireland fore-arc, Papua New Guinea: Economic Geology, v. 97, p. 1795–1813.
- Petracchini, L., Scrocca, D., Spagnesi, S., Minelli, F., 2015, 3D Geological Modeling to Support the Assessment of Conventional and Unconventional Geothermal Resources in the Latium Region (Central Italy): Proceedings World Geothermal Congress

- Petrinovic, I.A., Colombo Piñol, F., 2006, Phreatomagmatic and phreatic eruptions in locally extensive settings of Southern Central Andes: The Tocomar Volcanic Centre (24°10'S–66°34'W), Argentina: *Journal of Volcanology and Geothermal Research*, v. 158, p. 37–50. doi:10.1016/j.jvolgeores.2006.04.013
- Petrinovic, I.A., Hongn, F.D., del Papa, C.E., Caffè, P.J., 2009, Comments on “Kinematic variations across Eastern Cordillera at 24°S (Central Andes): Tectonic and magmatic implications” by Accolla, et al. [*Tectonophysics* 434 (2007) 81–92]: *Tectonophysics*, v. 469, p. 150–154. doi:10.1016/j.tecto.2008.02.006
- Petrinovic, I.A., Martí, J., Aguirre-Díaz, G.J., Guzmán, S., Geyer, A., Paz, N.S., 2010, The Cerro Aguas Calientes caldera, NW Argentina: An example of a tectonically controlled, polygenetic collapse caldera, and its regional significance: *Journal of Volcanology and Geothermal Research*, v. 194, p. 15–26. doi:10.1016/j.jvolgeores.2010.04.012
- Petrinovic, I.A., Riller, U., Brod, J.A., Alvarado, G., Arnasio, M., 2006, Bimodal volcanism in a tectonic transfer zone: Evidence for tectonically controlled magmatism in the southern Central Andes, NW Argentina, *Journal of Volcanology and Geothermal Research*: v. 152, p. 240–252. doi:10.1016/j.jvolgeores.2005.10.008
- Phipps Morgan, J., Ranero, C.R., Vannucchi, P., 2008, Intra-arc extension in Central America: Links between plate motions, tectonics, volcanism, and geochemistry: *Earth and Planetary Science Letters*, v. 272, p. 365–371. doi:10.1016/j.epsl.2008.05.004
- Pizzi, A., Calamita, F., Coltorti, M., Pieruccini, P., 2002, Quaternary normal faults, intramontane basins and seismicity in the Umbria-Marche-Abruzzi Apennine Ridge (Italy): contribution of neotectonic analysis to seismic hazard assessment: *Boll. Soc. Geol. It., Spec. Publ* 1, p. 923–929.
- Porrás, E.A., Itoi, R., 2006, The Momotombo Geothermal System and its Conceptual Model: *GRC Transactions*, v. 30, p. 33–38.
- Portnyagin, M., Hoernle, K., Avdeiko, G., Hauff, F., Werner, R., Bindeman, I., Uspensky, V., Garbe-Schönberg, D., 2005, Transition from arc to oceanic magmatism at the Kamchatka-Aleutian junction: *Geology*, v. 33, p. 25–28.
- Priest, George R., Black, Gerald L., Woller, Neil M., Taylor, Edward M., 1988, *Geologic Map of the McKenzie Bridge Quadrangle, Lane County, Oregon: State of Oregon Department of Geology and Mineral Industries, Scale 1:62,500*
- Quintanar, L., Rodríguez-González, M., Campos-Enríquez, O., 2004, A Shallow Crustal Earthquake Doublet from the Trans-Mexican Volcanic Belt (Central Mexico): *Bulletin of the Seismological Society of America*, v. 94, p. 845–855.
- Rae, A.J., Bignall, G., Scott, B.J., Kilgour, G., Rosenberg, M., Sepulveda, F., 2015, *Powerful Landscapes: WGC Post Congress Field Trip Powerful Landscapes*, 1–78.
- Raharjo, I.B., Allis, R.G., Chapman, D.S., 2012, Why Are the Only Volcano-Hosted Vapor-Dominated Geothermal Systems in West Java, Indonesia?: *GRC Transactions*, v. 36.
- Ramos, S.G., Santos, B.N.E.A., Center, O.C., 2012, Updated hydrogeological model of the Bacon-Manito Geothermal Field, Philippines, in: *Proceedings Thirty-Seventh Workshop on Geothermal Reservoir Engineering Stanford University, Stanford, California*. p. 1–4.
- Read, P.B., 1978, *Meager Creek Geothermal Area: Geologic Survey of Canada, British Columbia, Scale 1:20,000*
- Reeder, J.W., Denig-Chakroff, D., Economides, M.J., 1985, *The Geology and Geothermal Resource of the Makushin Volcano Region of Unalaska Island, Alaska: GRC Transactions*, v. 9, p. 479–484.
- Rejeki, S., Rohrs, D., Nordquist, G., Fitriyanto, A., 2010, Geologic conceptual model update of the Darajat geothermal field, Indonesia, in: *Proc. World Geothermal Congress 2010, Bali, Indonesia*, 25–30 April.
- Riedel, M., Dutsch, C., Alexandrakis, C., Buske, S., Dini, I., Ciuffi, S., 2015, *Seismic Investigations of a Geothermal Field in Southern Tuscany, Italy: Proceedings World Geothermal Congress*

- Riehle, J.R., Yount, M.E., Miller, T.P., 1987, Petrography, Chemistry, and Geologic History of Yantarni Volcano, Aleutian Volcanic Arc, Alaska: U.S. Geological Survey Bulletin.
- Riller, U., Oncken, O., 2003, Growth of the Central Andean Plateau by Tectonic Segmentation Is Controlled by the Gradient in Crustal Shortening: *The Journal of Geology*, v. 111, p. 367–384. doi:10.1086/373974
- Rossetti, F., Aldega, L., Tecce, F., Balsamo, F., Billi, A., Brilli, M., 2011, Fluid flow within the damage zone of the Boccheggiano extensional fault (Larderello–Travale geothermal field, central Italy): structures, alteration and implications for hydrothermal mineralization in extensional settings: *Geological Magazine*, v. 148, p. 558–579. doi:10.1017/S001675681000097X
- Rowland, J.V., and Sibson, R.H., 2004, Structural controls on hydrothermal flow in a segmented rift system, Taupo Volcanic Zone, New Zealand: *Geofluids*, v. 4, p. 259–283.
- Rowland, J.V., Simmons, S.F., 2012, Hydrologic, magmatic, and tectonic controls on hydrothermal flow, Taupo Volcanic Zone, New Zealand: implications for the formation of epithermal vein deposits: *Economic Geology*, v. 107, p. 427–457.
- Russo, R.M., Gallego, A., Comte, D., Mocanu, V.I., Murdie, R.E., Mora, C., VanDecar, J.C., 2011, Triggered seismic activity in the Liquiñe–Ofqui fault zone, southern Chile, during the 2007 Aysen seismic swarm: Triggered seismic activity in the LOFZ: *Geophysical Journal International*, v. 184, p. 1317–1326. doi:10.1111/j.1365-246X.2010.04908.x
- Sakai, T., Saneyoshi, M., Sawada, Y., Nakatsukasa, M., Kunimatsu, Y., Mbu, E., 2013, Early Continental Rift Basin Stratigraphy, Depositional Facies and Tectonics in Volcaniclastic System: Examples from the Miocene Successions Along the Japan Sea and in the East African Rift Valley (Kenya), in: Itoh, Y. (Ed.), *Mechanism of Sedimentary Basin Formation - Multidisciplinary Approach on Active Plate Margins*. InTech.
- Sánchez–Rivera, E., Vallejos–Ruíz, O., 2015, Costa Rica Country Update Report, in: *Proceedings World Geothermal Congress 2015*, p. 19–24.
- Sathar, S., Reeves, H.J., Cuss, R.J., Harrington, J.F., 2012, The role of stress history on the flow of fluids through fractures: *Mineralogical Magazine*, v. 76, p. 3165–3177. doi:10.1180/minmag.2012.076.8.30
- Schaefer, J.R., Gallagher, P.E., 2014, *Historically Active Volcanoes of Alaska*: Alaska Department of Natural Resources, Division of Geological Geophysical Surveys, Miscellaneous Publication 133, Scale 1:3,000,000
- Schoenbohm, L.M., Strecker, M.R., 2009, Normal faulting along the southern margin of the Puna Plateau, northwest Argentina: Reactivated Normal Faults, Puna Plateau: *Tectonics*, v. 28. doi:10.1029/2008TC002341
- Schreiber, U., Schwab, K., 1991, Geochemistry of Quaternary shoshonitic lavas related to the Calama–Olacapato–El Toro Lineament, NW Argentina: *Journal of South American Earth Sciences*, v. 4, p. 73–85.
- Schurr, B., 2004, Deep seismic structure of the Atacama basin, northern Chile: *Geophysical Research Letters*, v. 31. doi:10.1029/2004GL019796
- Schurr, B., Asch, G., Rietbrock, A., Kind, R., Pardo, M., Heit, B., Monfret, T., 1999, Seismicity and Average Velocities beneath the Argentine Puna Plateau: *Geophysical Research Letters*, v. 26, p. 3025–3028.
- Selverstone, J., 1988, Evidence for east-west crustal extension in the Eastern Alps: Implications for the unroofing history of the Tauern window: *Tectonics*, v. 7, p. 87–105.
- Sewell, S.M., Cumming, W.B., Azwar, L., Bardsley, C., 2012, Integrated MT and natural state temperature interpretation for a conceptual model supporting reservoir numerical modeling and well targeting at the Rotokawa Geothermal Field, New Zealand, in: *Proceedings of the Thirty-Seventh Workshop on Geothermal Reservoir Engineering*. Stanford University, Stanford California.
- Sherrod, D.R., and Smith, J.G., 2000, Geologic map of upper Eocene to Holocene volcanic and related rocks of the Cascade Range, Oregon: U.S. Geological Survey Miscellaneous Investigations Map I-2569, 1 sheet, scale 1:500,000, 17 p.

- Shevenell, L., Coolbaugh, M., Hinz, N.H., Stelling, P., Melosh, G., Cumming, W., and Kreemer, C., 2015, Preliminary ranking of geothermal potential in the Aleutian and Cascade volcanic arcs, Part I: Geothermal Resources Council Transactions, v. 39 (this volume).
- Sibson, R.H., 1987, Earthquake rupturing as a mineralizing agent in hydrothermal systems: *Geology*, v. 15, p. 701–704.
- Sibson, R.H., 1994, Crustal stress, faulting and fluid flow: Geological Society, London Special Publication, v. 78, p. 69-84.
- Sieh, K., and Natawidjaja, D., 2000, Neotectonics of the Sumatran fault, Indonesia: *Journal of Geophysical Research*, v. 105, p. 28,295–28,326, doi:10.1029/2000JB900120.
- Siler, D.L., Faulds, J.E., and Hinz, N.H., 2015a, Regional and local geothermal potential evaluation: Examples from the Great Basin, USA, Iceland and East Africa: Proceedings, World Geothermal Congress 2015, Melbourne, Australia.
- Siler, D.L., Faulds, J.E., and Hinz, N.H., 2015b, Earthquake-related stress concentration in fault zones and permeability generation in geothermal systems: *Geothermal Resources Council Transactions*, v. 39 (this volume).
- Smith, J.G., 1993, Geologic map of upper Eocene to Holocene volcanic and related rocks in the Cascade Range, Washington: U.S. Geological Survey Miscellaneous Investigations Map I-2005, 1 sheet, scale 1:500,000, 19 p.
- Sorey, M.L., Ingsbritsen, S.E., 1995, Heat and Mass Flow from Thermal Areas in and Adjacent to Lassen Volcanic National Park, California, USA: World Geothermal Congress, p. 751–755.
- Spielman, P., Rickard, W., and Teplow, W., 2006, Puna Geothermal Venture, Hawaii—2005 Drilling Program: *Geothermal Resources Council Transactions*, v. 30, p. 309-313.
- Spinks, K.D., Acocella, V., Cole, J.W., Bassett, K.N., 2005, Structural control of volcanism and caldera development in the transtensional Taupo Volcanic Zone, New Zealand: *Journal of Volcanology and Geothermal Research*, v. 144, p. 7–22. doi:10.1016/j.jvolgeores.2004.11.014
- Stelling, P., Hinz, N.H., and Kolker, A., 2015, Exploration of the Hot Springs Bay Valley (HSBV) Geothermal Resource Area, Akutan, Alaska: *Geothermics*, v. 57, p. 127-144.
- Stimac, J., Nordquist, G., Suminar, A., Sirad-Azwar, L., 2008, An overview of the Awibengkok geothermal system, Indonesia: *Geothermics*, v. 37, p. 300–331. doi:10.1016/j.geothermics.2008.04.004
- Stoiber, R., Carr, M., 1973, Quaternary volcanic and tectonic segmentation of Central America: *Bulletin Volcanologique*, v. 37, p. 304–325.
- Sudarman, S., Boedihardi, M., Pudyastuti, K., Bardan, 1995, Kamojang Geothermal Field 10 Year Operation Experience: World Geothermal Congress, p. 1773–1777.
- Suter, M., Martínez, M.L., Legorreta, O.Q., Martínez, M.C., 2001, Quaternary intra-arc extension in the central Trans-Mexican volcanic belt: *Geological Society of America Bulletin*, v. 113, p. 693–703.
- Tabor, R.W., Fizzell Jr., V.A., Booth, D., Waitt, R.B., 2000, Geologic Map of the Snoqualmie Pass 30x60 Minute Quadrangle, Washington: U.S. Geological Survey, Geologic Investigation Series, Scale 1:100,000
- Takahashi, H., Otake, M., Tagomori, K., Sueyoshi, Y., Futagoishi, M., Nasution, A., 2000, Geothermal geology of the Mataloko area, central Flores, Nusa Tenggara, Timur, Indonesia, in: Proc. World Geothermal Congress 2000.
- Takano, O., Itoh, Y., Kusumoto, S., 2013, Variation in Forearc Basin Configuration and Basin-filling Depositional Systems as a Function of Trench Slope Break Development and Strike-Slip Movement: Examples from the Cenozoic Ishikari–Sanriku–Oki and Tokai–Oki–Kumano–Nada Forearc Basins, Japan, in: Itoh, Y. (Ed.), Mechanism of Sedimentary Basin Formation - Multidisciplinary Approach on Active Plate Margins. InTech.

- Takeuchi, A., 2013, Tectonic Process of the Sedimentary Basin Formation and Evolution in the Late Cenozoic Arc-Arc Collision Zone, Central Japan, in: Itoh, Y. (Ed.), Mechanism of Sedimentary Basin Formation - Multidisciplinary Approach on Active Plate Margins. InTech.
- Talens, M.A., Herras, E.B., Ogena, M.S., 1997, Keys to Successful Drilling in Mahanagdong, in: Proceedings 18th PNOC-EDC Geothermal Conference, p. 325–328.
- Thomson, S.N., 2002, Late Cenozoic geomorphic and tectonic evolution of the Patagonian Andes between latitudes 42°S and 46°S: An appraisal based on fission-track results from the transpressional intra-arc Liquiñe-Ofqui fault zone: Geological Society of America Bulletin, v. 114, p. 1159–1173.
- Townend, J., and Zoback, M.D., 2000, How faulting keeps the crust strong: Geology, v. 28, no. 5, p. 399-402.
- Umeda, K., Ban, M., Hayashi, S., and Kusano, T., 2013, Tectonic shortening and coeval volcanism during the Quaternary, Northeast Japan arc: Journal of Earth System Science, v. 122, no. 1, p. 137-147.
- Traineau, H., Lasne, E., Coppo, N., Baltassat, J.-M., 2015, Recent Geological, Geochemical and Geophysical Surveys of the Roseau Valley, High- Temperature Geothermal Field in Dominica, West Indies: Proceedings World Geothermal Congress 1–11.
- Tripp, A., Moore, J., Ussher, G., McCulloch, J., 2002, Gravity modeling of the Karaha-Telaga Bodas geothermal system, Indonesia, in: Proceedings of the 27th Workshop on Geothermal Reservoir Engineering, Stanford University. p. 444–452.
- Tsutsumi, H., 2007. Active Faults Map: Kyoto University and the Philippine Institute of Volcanology, Sheet No. 7179 III; 7179 II; 7178 IV.
- Turner, H.L., LaFemina, P., Saballos, A., Mattioli, G.S., Jansma, P.E., Dixon, T., 2007, Kinematics of the Nicaraguan forearc from GPS geodesy: Geophysical Research Letters, v. 34. doi:10.1029/2006GL027586
- Umeda, K., Ban, M., 2012, Quaternary Volcanism Along the Volcanic Front in Northeast Japan. INTECH Open Access Publisher.
- Umeda, K., Ban, M., Hayashi, S., Kusano, T., 2013, Tectonic shortening and coeval volcanism during the Quaternary, Northeast Japan arc: Journal of Earth System Science, v. 122, p. 137–147.
- Urban, E., Lermo, J.F., 2012, Relationship Of Local Seismic Activity, Injection Wells And Active Faults In The Geothermal Fields Of Mexico, in: Proceedings of Thirty-Seventh Workshop on Geothermal Reservoir Engineering, Stanford University, Stanford, CA, SGP-TR-194.
- USGS, 2010, United States Geological Survey Quaternary Fault and Fold Database of the United States: <http://earthquake.usgs.gov/hazards/qfaults/>, retrieved 2013.
- Vallejos-Ruiz, O., Sánchez-Rivera, E., González-Vargas, C., 2005, Reservoir Management at the Miravalles Geothermal Field, Costa Rica, in: Proceedings Geothermal World Congress, p. 1–8.
- Vallier, T.L., Scholl, D.W., Fisher, M.A., Burns, T.R., 1994, Geologic Framework of the Aleutian Arc, Alaska: The Geology of North America G-1, p. 367–388.
- Verma, M.P., Martinez, E., Sanchez, M., Miranda, K., Gerardo, J.Y., Araguas, L., 1996: Hydrothermal model of the Momotombo geothermal system, Nicaragua, in: Proceedings of the Twenty-First Workshop on Geothermal Reservoir Engineering, Stanford University, p. 29–34.
- Vicedo, R.O., Stimac, J.A., Capuno, V.T., Lowenstern, J.B., 2008, Establishing Major Permeability controls in the Mak-ban Geothermal Field, Philippines: GRC Transactions, v. 32, p. 309–314.
- Vignaroli, G., Pinton, A., De Benedetti, A.A., Giordano, G., Rossetti, F., Soligo, M., Berardi, G., 2013, Structural compartmentalization of a geothermal system, the Torre Alfina field (central Italy): Tectonophysics, v. 608, p. 482–498. doi:10.1016/j.tecto.2013.08.040
- Villamor, P., Berryman, K., 2001, A late Quaternary extension rate in the Taupo Volcanic Zone, New Zealand, derived from fault slip data: New Zealand Journal of Geology and Geophysics, v. 44, p. 243-269.

- Villamor, P., Berryman, K.R., Nairn, I.A., Wilson, K., Litchfield, N., Ries, W., 2011, Associations between volcanic eruptions from Okataina volcanic center and surface rupture of nearby active faults, Taupo rift, New Zealand: Insights into the nature of volcano-tectonic interactions: *Geological Society of America Bulletin*, v. 123, p. 1383–1405.
- Wallace, L.M., Ellis, S., Miyao, K., Miura, S., Beavan, J., and Goto, J., 2009, Enigmatic, highly active left lateral shear zone in southwest Japan explained by aseismic ridge collision: *Geology*, v. 37, p. 143–146, doi:10.1130/G25221A.1.
- Walker, G.W., MacLeod, N.S., 1991, *Geologic Map of Oregon*: U.S. Geological Survey, Scale 1:500,000
- Wang, K., Hu, Y., Bevis, M., Kendrick, E., Smalley, R., Vargas, R.B., Lauría, E., 2007, Crustal motion in the zone of the 1960 Chile earthquake: Detangling earthquake-cycle deformation and forearc-slover translation: *Chile Earthquake Crustal Motion: Geochemistry, Geophysics, Geosystems*, v. 8.. doi:10.1029/2007GC001721
- Waythomas, C.F., 1999, Stratigraphic framework of Holocene volcanoclastic deposits, Akutan volcano, east-central Aleutian Islands, Alaska: *Bulletin of Volcanology*, v. 61, p. 141–161.
- Weinberg, R.F., 1992, Neotectonic Development of Western Nicaragua: *Tectonics*, v. 11, p. 1010–1017.
- Weller, O., Lange, D., Tilmann, F., Natawidjaja, D., Rietbrock, A., Collings, R., Gregory, L., 2012, The structure of the Sumatran Fault revealed by local seismicity: *The Structure of the Sumatran Fault: Geophysical Research Letters*, v. 39. doi:10.1029/2011GL050440
- Wells, R.E., and McCaffrey, R., 2013, Steady rotation of the Cascade arc: *Geology*, v. 41, no. 9, p. 1027–1030.
- Wells, S.G., Bullard, T.F., Menges, C.M., Drake, P.G., Karas, P.A., Kelson, K.I., Ritter, J.B., Wesling, J.R., 1988, Regional Variations in Tectonic Geomorphology Along a Segmented Convergent Plate Boundary, Pacific Coast of Costa Rica: *Geomorphology*, v. 1, p. 239–265.
- Wescott, E.M., Turner, D.L., Nye, C.J., Motyka, R.J., Moore, P., October, 1988, Exploration for Geothermal Energy Resources at Mt. Spurr, Alaska: *GRC Transactions*, 1988, v. 12, p. 203–210.
- White, P., Lawless, J., Ussher, G., Smith, A., 2008, Recent results from the San Jacinto-Tizate geothermal field, Nicaragua: *New Zealand Geothermal Workshop*.
- White, P., Ussher, G., Hermoso, D., 2010a, Evolution of the Ladolam Geothermal System on Lihir Island, Papua New Guinea, in: *Proceedings World Geothermal Congress 2010*.
- White, P., Ussher, G., Lovelock, B., Charroy, J., Alexander, K., Clotworthy, A., 2010b, Mita, a Newly Discovered Geothermal System in Guatemala, in: *Proceedings World Geothermal Congress*.
- Wilmarth, M., Melosh, G., Sussman, D., Swanson, R., Cumming, W., Colvin, A., Iriarte, S., Lohmar, S., Soto, E., 2010, Tolhuaca Update: *GRC Transactions*, v. 34, p. 237.
- Wilson, C.J., Houghton, B.F., McWilliams, M.O., Lanphere, M.A., Weaver, S.D., Briggs, R.M., 1995, Volcanic and structural evolution of Taupo Volcanic Zone, New Zealand: a review: *Journal of Volcanology and Geothermal Research*, v. 68, p. 1–28.
- Wilson, F.H., Mohadjer, S., Grey, D., 2006, *Reconnaissance Geologic Map of the Western Aleutian Islands, Alaska*: USGS Open-File Report 2006-1302, p. 1–26.
- Wohletz, K., Heiken, G., 1992, *Geothermal Systems in Maturing Composite Cones*, in: *Volcanology and Geothermal Energy*, Berkeley: University of California Press
- Yeats, R., Sieh, K., and Allen, C., 1997, *The geology of earthquakes*: Oxford University Press, New York, 568 p.
- Yin, A., 2000, Mode of Cenozoic east-west extension in Tibet suggesting a common origin of rifts in Asia during the Indo-Asian collision, *Journal of Geophysical Research*, v. 105, no. 21, p.745–721, 759.
- Zoback, M.D., 1999, *Fracture Permeability and in Situ Stress in the Dixie Valley, Nevada, Geothermal Reservoir*: Department of Energy Final Technical Report, p. 1–15.
- Zúñiga, E.V., Rojas, L.C., Viquez, M.B., Zúñiga, F.M., Hakanson, E.C., Protti, O.M., 2010: *Geologic Model of The Miravalles Geothermal Field, Costa Rica*, in: *Proceedings*.

APPENDIX II

Basic information of volcanic centers (VC) evaluated in this work (13 pages).

VC_Num	Volcano Name	Linked_Centers	Most Recent		Crustal Thickness	Primary Volcano Type	Dominant Rock Type	Latitude	Longitude
			Eruption	Under_Plate					
Argentina									
7001	Aracar		1993	Nazca	South America	>25 km	Stratovolcano	Andesite / Basaltic Andesite	-24.2900 -67.7830
7002	Lava domes			Nazca	South America	>25 km	Lava dome(s)		-24.5650 -67.8718
7003	Peinado			Nazca	South America	>25 km	Stratovolcano	Andesite / Basaltic Andesite	-26.6230 -68.1160
7004	Condor, El			Nazca	South America	>25 km	Stratovolcano	No Data (checked)	-26.6320 -68.3610
7005	Blanco, Cerro		-2300	Nazca	South America	>25 km	Caldera	Rhyolite	-26.7890 -67.7650
7006	Tipas			Nazca	South America	>25 km	Complex	No Data (checked)	-27.1960 -68.5610
8001	Atuel, Caldera del			Nazca	South America	>25 km	Caldera	Andesite / Basaltic Andesite	-34.6500 -70.0500
8002	Risco Plateado			Nazca	South America	>25 km	Stratovolcano	Andesite / Basaltic Andesite	-34.9170 -69.9810
8003	Trolon			Nazca	South America	>25 km	Lava dome(s)	Dacite	-37.7380 -70.9060
8005	Huanquihue Group		1750	Nazca	South America	>25 km	Stratovolcano(es)	Basalt / Picro-Basalt	-39.8870 -71.5800
8006	Viedma, Volcan		1988	Antarctica	South America	>25 km	Subglacial	Dacite	-49.3580 -73.2800
Bolivia									
7007	Tambo Quemado			Nazca	South America	>25 km	Pyroclastic shield	Rhyolite	-18.6200 -68.7500
7008	Tata Sabaya			Nazca	South America	>25 km	Stratovolcano	Andesite / Basaltic Andesite	-19.1300 -68.5300
7009	NE 16 km of Irruputuncu			Nazca	South America	>25 km	Stratovolcano		-20.6241 -68.4478
7010	Laguna Qara			Nazca	South America	>25 km	Lava dome(s)		-21.8792 -67.9052
7011	Uturuncu			Nazca	South America	>25 km	Stratovolcano		-22.2700 -67.1800
Canada									
2001	Silverthron			Juan de Fuca	North America	>25 km	Caldera	Andesite / Basaltic Andesite	51.4302 -126.3000
2002	Meager		-410	Juan de Fuca	North America	>25 km	Complex	Dacite	50.6317 -123.5042
2003	Cayley Volcanic Field			Juan de Fuca	North America	>25 km	Volcanic field	Andesite / Basaltic Andesite	50.1200 -123.2800
2004	Garibaldi	Garibaldi Lake	-8060	Juan de Fuca	North America	>25 km	Stratovolcano	Dacite	49.8501 -123.0000
Chile									
7012	Taapaca		-320	Nazca	South America	>25 km	Complex	Dacite	-18.1000 -69.5000
7013	Guallatiri		1985	Nazca	South America	>25 km	Stratovolcano	Andesite / Basaltic Andesite	-18.4200 -69.0920
7014	Isluga		1960	Nazca	South America	>25 km	Stratovolcano	Andesite / Basaltic Andesite	-19.1500 -68.8300
7015	Aucanquilcha			Nazca	South America	>25 km	Stratovolcano		-21.2200 -68.4700
7016	Azufre-Pabellon			Nazca	South America	>25 km	Lava dome(s)		-21.7992 -68.2081
7017	San Pedro		1960	Nazca	South America	>25 km	Stratovolcano(es)	Andesite / Basaltic Andesite	-21.8800 -68.4000
7018	Paniri dome complex			Nazca	South America	>25 km	Lava dome(s)		-22.1060 -68.1551
7019	East of Cerro del Leon			Nazca	South America	>25 km	Lava dome(s)		-22.1607 -68.0313
7020	La Torta-Cerros Tocorpuri			Nazca	South America	>25 km	Lava dome(s)		-22.4335 -67.9156
7021	Putana		1972	Nazca	South America	>25 km	Stratovolcano	Dacite	-22.5500 -67.8500
7022	Purico Complex			Nazca	South America	>25 km	Pyroclastic shield	Dacite	-23.0000 -67.7500
7023	Acamarachi	Colachi		Nazca	South America	>25 km	Stratovolcano	Dacite	-23.3000 -67.6200
7024	Láscar		2013	Nazca	South America	>25 km	Stratovolcano(es)	Andesite / Basaltic Andesite	-23.3700 -67.7300
7025	Chiliques			Nazca	South America	>25 km	Stratovolcano	Andesite / Basaltic Andesite	-23.5800 -67.7000
7026	Cerro Miscanti			Nazca	South America	>25 km	Stratovolcano		-23.6738 -67.7162
7027	Cordon de Puntas Negras			Nazca	South America	>25 km	Stratovolcano(es)	Andesite / Basaltic Andesite	-23.7430 -67.5340
7028	Miniques			Nazca	South America	>25 km	Stratovolcano(es)	Andesite / Basaltic Andesite	-23.8200 -67.7700
7029	Cerro Tuyajto			Nazca	South America	>25 km	Stratovolcano(es)		-23.8421 -67.6246
7030	Caichinque			Nazca	South America	>25 km	Stratovolcano(es)	Andesite / Basaltic Andesite	-23.9500 -67.7300
7031	Tilocalar			Nazca	South America	>25 km	Stratovolcano(es)	Andesite / Basaltic Andesite	-23.9700 -68.1300
7032	Pular		1990	Nazca	South America	>25 km	Stratovolcano(es)	Andesite / Basaltic Andesite	-24.1880 -68.0540
7033	Copiapu			Nazca	South America	>25 km	Stratovolcano	Dacite	-27.3000 -69.1300
8007	Palomo			Nazca	South America	>25 km	Stratovolcano	Andesite / Basaltic Andesite	-34.6080 -70.2950
8008	Tinguiririca		1994	Nazca	South America	>25 km	Stratovolcano	Andesite / Basaltic Andesite	-34.8140 -70.3520
8009	Planchon-Peteroa		2011	Nazca	South America	>25 km	Stratovolcano(es)	Andesite / Basaltic Andesite	-35.2230 -70.5680
8010	Calabozos			Nazca	South America	>25 km	Caldera	Dacite	-35.5580 -70.4960
8011	Descabezado Grande	Cerro Azul	1932	Nazca	South America	>25 km	Stratovolcano(es)	Andesite / Basaltic Andesite	-35.5800 -70.7500
8012	San Pedro-Pellado			Nazca	South America	>25 km	Stratovolcano(es)	Andesite / Basaltic Andesite	-35.9890 -70.8490
8013	Maule, Laguna del			Nazca	South America	>25 km	Caldera	Andesite / Basaltic Andesite	-36.0200 -70.5800
8014	Longavi, Nevado de		-4890	Nazca	South America	>25 km	Stratovolcano	Andesite / Basaltic Andesite	-36.1930 -71.1610
8015	Blancas, Lomas			Nazca	South America	>25 km	Stratovolcano	Basalt / Picro-Basalt	-36.2860 -71.0090
8016	Chillán, Nevados de		2009	Nazca	South America	>25 km	Stratovolcano	Andesite / Basaltic Andesite	-36.8630 -71.3770
8017	Antuco		1972	Nazca	South America	>25 km	Stratovolcano	Basalt / Picro-Basalt	-37.4060 -71.3490
8018	Callaqui		2012	Nazca	South America	>25 km	Stratovolcano	Andesite / Basaltic Andesite	-37.9200 -71.4500
8019	Tolguaca			Nazca	South America	>25 km	Stratovolcano	Andesite / Basaltic Andesite	-38.3100 -71.6450
8020	Lonquimay		1988	Nazca	South America	>25 km	Stratovolcano	Andesite / Basaltic Andesite	-38.3770 -71.5800

VC_Num	Volcano Name	Linked_Centers	Most Recent		Under_Plate	Over_Plate	Crustal Thickness	Primary Volcano Type	Dominant Rock Type	Latitude	Longitude
			Eruption								
8021	Llaima		2008		Nazca	South America	>25 km	Stratovolcano	Basalt / Picro-Basalt	-38.6920	-71.7290
8022	Sollipulli		1240		Nazca	South America	>25 km	Caldera	Andesite / Basaltic Andesite	-38.9700	-71.5200
8023	Villarrica		2013		Nazca	South America	>25 km	Stratovolcano	Basalt / Picro-Basalt	-39.4200	-71.9300
8024	Quetrupillan		1872		Nazca	South America	>25 km	Stratovolcano	Andesite / Basaltic Andesite	-39.5000	-71.7000
8025	Mocho-Choshuencho		1937		Nazca	South America	>25 km	Stratovolcano(es)	Andesite / Basaltic Andesite	-39.9270	-72.0270
8026	Carrán-Los Venados		1979		Nazca	South America	>25 km	Pyroclastic cone(s)	Basalt / Picro-Basalt	-40.3500	-72.0700
8027	Puyehue-Cordón Caulle		2011		Nazca	South America	>25 km	Stratovolcano	Andesite / Basaltic Andesite	-40.5900	-72.1170
8028	Antillanca Group		-230		Nazca	South America	>25 km	Stratovolcano(es)	Basalt / Picro-Basalt	-40.7710	-72.1530
8029	Puntiagudo-Cordon Cenizos		1930		Nazca	South America	>25 km	Stratovolcano	Andesite / Basaltic Andesite	-40.9690	-72.2640
8030	Osorno		1869		Nazca	South America	>25 km	Stratovolcano	Basalt / Picro-Basalt	-41.1000	-72.4930
8031	Calbuco		1972		Nazca	South America	>25 km	Stratovolcano	Andesite / Basaltic Andesite	-41.3260	-72.6140
8032	Cuernos del Diablo				Nazca	South America	>25 km	Stratovolcano	Basalt / Picro-Basalt	-41.4000	-72.0000
8033	Yate		1090		Nazca	South America	>25 km	Stratovolcano	Andesite / Basaltic Andesite	-41.7550	-72.3960
8034	Hornopiren		1835		Nazca	South America	>25 km	Stratovolcano	Andesite / Basaltic Andesite	-41.8740	-72.4310
8035	Huequi		1920		Nazca	South America	>25 km	Lava dome(s)	Andesite / Basaltic Andesite	-42.3770	-72.5780
8036	Minchinmavida		1835		Nazca	South America	>25 km	Stratovolcano	Andesite / Basaltic Andesite	-42.7930	-72.4390
8037	Chaiten		2008		Nazca	South America	>25 km	Caldera	Rhyolite	-42.8330	-72.6460
8038	Corcovado		1835		Nazca	South America	>25 km	Stratovolcano	Andesite / Basaltic Andesite	-43.1890	-72.7940
8039	Yanteles		1835		Nazca	South America	>25 km	Stratovolcano(es)	Andesite / Basaltic Andesite	-43.4970	-72.8100
8040	Melimoyu		200		Nazca	South America	>25 km	Stratovolcano	Andesite / Basaltic Andesite	-44.0800	-72.8800
8041	Mentolat		1710		Nazca	South America	>25 km	Stratovolcano	Andesite / Basaltic Andesite	-44.7000	-73.0800
8042	Cay				Nazca	South America	>25 km	Stratovolcano	Andesite / Basaltic Andesite	-45.0590	-72.9840
8043	Maca		1560		Nazca	South America	>25 km	Stratovolcano	Basalt / Picro-Basalt	-45.1000	-73.1700
8044	Hudson, Cerro		2011		Nazca	South America	>25 km	Stratovolcano	Basalt / Picro-Basalt	-45.9000	-72.9700
8045	Arenales		1979		Antarctica	South America	>25 km	Stratovolcano	No Data (checked)	-47.2000	-73.4800
8046	Lautaro		1979		Antarctica	South America	>25 km	Stratovolcano	Dacite	-49.0200	-73.5500
8047	Aguilera		-1250		Antarctica	South America	>25 km	Stratovolcano	Dacite	-50.3300	-73.7500
8048	Reclus		1908		Antarctica	South America	>25 km	Pyroclastic cone	Dacite	-50.9640	-73.5850
8049	Burney, Monte		1910		Antarctica	South America	>25 km	Stratovolcano	Andesite / Basaltic Andesite	-52.3300	-73.4000
8050	Fuegoينو		1820		Antarctica	Scotia	>25 km	Lava dome(s)	Andesite / Basaltic Andesite	-54.9500	-70.2500
Chile-Argentina											
7034	Socompa		-5250		Nazca	South America	>25 km	Stratovolcano	Dacite	-24.3960	-68.2460
7035	Llullaillaco		1877		Nazca	South America	>25 km	Stratovolcano	Dacite	-24.7200	-68.5300
7036	Escorial				Nazca	South America	>25 km	Stratovolcano	Andesite / Basaltic Andesite	-25.0830	-68.3670
7037	Lastarria				Nazca	South America	>25 km	Stratovolcano	Andesite / Basaltic Andesite	-25.1680	-68.5070
7038	Cordon del Azufre				Nazca	South America	>25 km	Complex	Andesite / Basaltic Andesite	-25.3360	-68.5210
7039	Bayo Gorbea, Cerro				Nazca	South America	>25 km	Complex	Andesite / Basaltic Andesite	-25.4140	-68.5880
7040	Nevada, Sierra				Nazca	South America	>25 km	Complex	No Data (checked)	-26.4800	-68.5800
7041	Falso Azufre				Nazca	South America	>25 km	Complex	No Data (checked)	-26.8000	-68.3700
7042	Incahuasi, Nevado de				Nazca	South America	>25 km	Stratovolcano(es)	Dacite	-27.0330	-68.2960
7043	Las Tres Cruces	El Solo			Nazca	South America	>25 km	Stratovolcano	Dacite	-27.0682	-68.7857
7044	Ojos del Salado, Nevados		1993		Nazca	South America	>25 km	Stratovolcano	Dacite	-27.1090	-68.5410
8056	Cerro Pantojo				Nazca	South America	>25 km	Stratovolcano	Basalt / Picro-Basalt	-40.7680	-71.9430
8057	Tronador				Nazca	South America	>25 km	Stratovolcano	Andesite / Basaltic Andesite	-41.1570	-71.8850
8051	Tupungatito		1987		Nazca	South America	>25 km	Stratovolcano	Andesite / Basaltic Andesite	-33.4250	-69.7970
8052	San Jose		1960		Nazca	South America	>25 km	Stratovolcano	Andesite / Basaltic Andesite	-33.7890	-69.8950
8053	Maipo		1912		Nazca	South America	>25 km	Caldera	Trachyandesite / Basaltic trachy	-34.1640	-69.8320
8054	Copahue		2014		Nazca	South America	>25 km	Stratovolcano	Trachybasalt / Tephrite Basanite	-37.8560	-71.1830
8055	Lanin		560		Nazca	South America	>25 km	Stratovolcano	Trachyandesite / Basaltic trachy	-39.6370	-71.5020
Chile-Bolivia											
7045	Parinacota		290		Nazca	South America	>25 km	Stratovolcano	Andesite / Basaltic Andesite	-18.1700	-69.1500
7046	Irruputuncu		1995		Nazca	South America	>25 km	Stratovolcano	Andesite / Basaltic Andesite	-20.7300	-68.5500
7047	Olca-Paruma		1865		Nazca	South America	>25 km	Stratovolcano(es)	Andesite / Basaltic Andesite	-20.9300	-68.4800
7048	Ollague				Nazca	South America	>25 km	Stratovolcano	Andesite / Basaltic Andesite	-21.3000	-68.1800
7049	Sairecabur				Nazca	South America	>25 km	Stratovolcano(es)	Andesite / Basaltic Andesite	-22.7200	-67.8920
7050	Licancabur				Nazca	South America	>25 km	Stratovolcano	Andesite / Basaltic Andesite	-22.8300	-67.8800
7051	Guayaques				Nazca	South America	>25 km	Lava dome(s)	Dacite	-22.8950	-67.5660
Chile-Peru											
7052	Tacora		1937		Nazca	South America	>25 km	Stratovolcano	Andesite / Basaltic Andesite	-17.7200	-69.7700
Colombia											

VC_Num	Volcano Name	Linked_Centers	Most Recent		Under_Plate	Over_Plate	Crustal Thickness	Primary Volcano Type	Dominant Rock Type	Latitude	Longitude
			Eruption								
6001	Romeral		-5950		Nazca	South America	>25 km	Stratovolcano	Andesite / Basaltic Andesite	5.2060	-75.3640
6002	Bravo, Cerro		1720		Nazca	South America	>25 km	Stratovolcano	Dacite	5.0920	-75.3000
6003	Ruiz, Nevado del	Santa Isabel	2012		Nazca	South America	>25 km	Stratovolcano	Andesite / Basaltic Andesite	4.8950	-75.3220
6004	Tolimá, Nevado del		1943		Nazca	South America	>25 km	Stratovolcano	Andesite / Basaltic Andesite	4.6700	-75.3300
6005	Machin		1180		Nazca	South America	>25 km	Stratovolcano	Dacite	4.4800	-75.3920
6006	Huila, Nevado del		2008		Nazca	South America	>25 km	Stratovolcano	Andesite / Basaltic Andesite	2.9300	-76.0300
6007	Purace		1977		Nazca	South America	>25 km	Stratovolcano(es)	Andesite / Basaltic Andesite	2.3200	-76.4000
6008	Sotara				Nazca	South America	>25 km	Stratovolcano	Andesite / Basaltic Andesite	2.1080	-76.5920
6009	Petacas				Nazca	South America	>25 km	Lava dome	No Data (checked)	1.5670	-76.8577
6010	Dona Juana		1897		Nazca	South America	>25 km	Stratovolcano	Andesite / Basaltic Andesite	1.5010	-76.9330
6011	Galeras		2012		Nazca	South America	>25 km	Complex	Andesite / Basaltic Andesite	1.2200	-77.3700
6012	Azufral		-930		Nazca	South America	>25 km	Stratovolcano	Dacite	1.0853	-77.7179
6013	Cumbal		1926		Nazca	South America	>25 km	Stratovolcano	Andesite / Basaltic Andesite	0.9500	-77.8700
6014	Negro de Mayasquer, Cerro		1936		Nazca	South America	>25 km	Stratovolcano	Dacite	0.8280	-77.9640
Costa Rica											
4001	Orosi				Cocos	Caribbean	>25 km	Stratovolcano(es)	Andesite / Basaltic Andesite	10.9800	-85.4730
4002	Rincon de la Vieja		2014		Cocos	Caribbean	>25 km	Complex	Andesite / Basaltic Andesite	10.8300	-85.3240
4003	Miravalles		1946		Cocos	Caribbean	>25 km	Stratovolcano	Andesite / Basaltic Andesite	10.7480	-85.1530
4004	Tenorio				Cocos	Caribbean	>25 km	Stratovolcano(es)	Andesite / Basaltic Andesite	10.6730	-85.0150
4005	Arenal		1968		Cocos	Caribbean	>25 km	Stratovolcano	Andesite / Basaltic Andesite	10.4630	-84.7030
4006	Platanar				Cocos	Caribbean	>25 km	Stratovolcano(es)	Andesite / Basaltic Andesite	10.3000	-84.3660
4007	Poas		2009		Cocos	Caribbean	>25 km	Stratovolcano	Andesite / Basaltic Andesite	10.2000	-84.2330
4008	Barva		1867		Cocos	Caribbean	>25 km	Complex	Andesite / Basaltic Andesite	10.1350	-84.1000
4009	Irazu-Turrialba	Turrialba	1994		Cocos	Caribbean	>25 km	Stratovolcano	Andesite / Basaltic Andesite	9.9790	-83.8520
Dominica											
5001	Diablos, Morne aux				North America	Caribbean	Oceanic < 15 km	Lava dome(s)	Andesite / Basaltic Andesite	15.6120	-61.4300
5002	Diablotins, Morne				North America	Caribbean	Oceanic < 15 km	Stratovolcano	Andesite / Basaltic Andesite	15.5030	-61.3970
5003	Watt, Morne	Morne Trois Pitons, Morne Plat Pays	1997		North America	Caribbean	Oceanic < 15 km	Stratovolcano(es)	Andesite / Basaltic Andesite	15.3070	-61.3050
Ecuador											
6015	Soche		-6650		Nazca	South America	>25 km	Stratovolcano	Dacite	0.5525	-77.6137
6016	Chachimbiro		-3740		Nazca	South America	>25 km	Stratovolcano	Dacite	0.4749	-78.3279
6017	Cuicocha		650		Nazca	South America	>25 km	Caldera	Dacite	0.3080	-78.3640
6018	Imbabura		-5500		Nazca	South America	>25 km	Compound	Andesite / Basaltic Andesite	0.2580	-78.1830
6019	Mojanda				Nazca	South America	>25 km	Stratovolcano(es)	Andesite / Basaltic Andesite	0.1300	-78.2700
6020	Pululagua		290		Nazca	South America	>25 km	Caldera	Dacite	0.0467	-78.4946
6021	Cayambe		1785		Nazca	South America	>25 km	Compound	Andesite / Basaltic Andesite	0.0290	-77.9860
6022	Reventador		2008		Nazca	South America	>25 km	Stratovolcano	Andesite / Basaltic Andesite	-0.0770	-77.6560
6023	Guagua Pichincha		2009		Nazca	South America	>25 km	Stratovolcano	Andesite / Basaltic Andesite	-0.1710	-78.5980
6024	Atacazo		-320		Nazca	South America	>25 km	Stratovolcano	Andesite / Basaltic Andesite	-0.3530	-78.6170
6025	Chacana		1773		Nazca	South America	>25 km	Caldera	Rhyolite	-0.3750	-78.2500
6026	Antisana		1801		Nazca	South America	>25 km	Stratovolcano	Andesite / Basaltic Andesite	-0.4810	-78.1410
6027	Aliso		-2450		Nazca	South America	>25 km	Stratovolcano	Andesite / Basaltic Andesite	-0.5300	-78.0000
6028	Sumaco		1933		Nazca	South America	>25 km	Stratovolcano	Trachybasalt / Tephrite Basanite	-0.5380	-77.6260
6029	Illiniza				Nazca	South America	>25 km	Stratovolcano	Andesite / Basaltic Andesite	-0.6590	-78.7140
6030	Cotopaxi		1942		Nazca	South America	>25 km	Stratovolcano	Andesite / Basaltic Andesite	-0.6770	-78.4360
6031	Quilotoa		1797		Nazca	South America	>25 km	Caldera	Dacite	-0.8500	-78.9000
6032	Chimborazo		550		Nazca	South America	>25 km	Stratovolcano	Andesite / Basaltic Andesite	-1.4640	-78.8150
6033	Tungurahua		2010		Nazca	South America	>25 km	Stratovolcano	Andesite / Basaltic Andesite	-1.4670	-78.4420
6034	Sangay		1934		Nazca	South America	>25 km	Stratovolcano	Andesite / Basaltic Andesite	-2.0050	-78.3410
El Salvador											
4010	Guazapa				Cocos	Caribbean	>25 km	Stratovolcano	Basalt / Picro-Basalt	13.9000	-89.1200
4011	Apaneca Range		1990		Cocos	Caribbean	>25 km	Stratovolcano(es)	Basalt / Picro-Basalt	13.8910	-89.7860
4012	Coatepeque Caldera				Cocos	Caribbean	>25 km	Caldera	Rhyolite	13.8700	-89.5500
4013	Santa Ana	Izalco	2005		Cocos	Caribbean	>25 km	Stratovolcano	Andesite / Basaltic Andesite	13.8530	-89.6300
4014	San Salvador		1917		Cocos	Caribbean	>25 km	Stratovolcano	Andesite / Basaltic Andesite	13.7340	-89.2940
4015	Ilopango		1879		Cocos	Caribbean	>25 km	Caldera	Dacite	13.6720	-89.0530
4016	San Vicente				Cocos	Caribbean	>25 km	Stratovolcano	Andesite / Basaltic Andesite	13.5950	-88.8370
4017	Tecapa-El Tigre	El Tigre, Taburete, Usulután	1878		Cocos	Caribbean	>25 km	Stratovolcano	Andesite / Basaltic Andesite	13.4940	-88.5020

VC_Num	Volcano Name	Linked_Centers	Most Recent		Under_Plate	Over_Plate	Crustal Thickness	Primary Volcano Type	Dominant Rock Type	Latitude	Longitude
			Eruption								
4018	San Miguel	Chinameca	2013		Cocos	Caribbean	>25 km	Stratovolcano	Andesite / Basaltic Andesite	13.4340	-88.2690
4019	Conchagua	Conchaguita			Cocos	Caribbean	>25 km	Stratovolcano	Basalt / Picro-Basalt	13.2750	-87.8450
Fiji											
17001	Taveuni		1550		Australia	Pacific	Unknown	Shield	Basalt / Picro-Basalt	-16.8200	-179.9700
17002	Koro				Australia	Pacific	Unknown	Pyroclastic cone(s)	Basalt / Picro-Basalt	-17.3200	179.4000
17003	Nabukelevu		1660		Australia	Pacific	Unknown	Lava dome(s)	Andesite / Basaltic Andesite	-19.1200	177.9800
France											
5004	Soufriere Guadeloupe	Bouillante Chain	1976		North America	Caribbean	Oceanic < 15 km	Stratovolcano	Andesite / Basaltic Andesite	16.0440	-61.6640
5005	Pelee		1929		South America	Caribbean	Oceanic < 15 km	Stratovolcano	Andesite / Basaltic Andesite	14.8090	-61.1650
Greece											
20001	Methana		1922		Africa	Aegean Sea	>25 km	Lava dome(s)	Andesite / Basaltic Andesite	37.6150	23.3360
20002	Milos		140		Africa	Aegean Sea	>25 km	Stratovolcano(es)	Rhyolite	36.6990	24.4390
20003	Nisyros	Yali	1888		Africa	Aegean Sea	>25 km	Stratovolcano	Dacite	36.5860	27.1600
20004	Santorini		1950		Africa	Aegean Sea	>25 km	Shield(s)	Dacite	36.4040	25.3960
Grenada											
5006	St. Catherine				South America	Caribbean	Oceanic < 15 km	Stratovolcano	Andesite / Basaltic Andesite	12.1500	-61.6700
Guatemala											
4020	Tajumulco		1863		Cocos	North America	>25 km	Stratovolcano	Dacite	15.0340	-91.9030
4021	Santa Maria	Almolonga	1922		Cocos	North America	>25 km	Stratovolcano	Dacite	14.7560	-91.5520
4022	Zunil-Santo Tomas		-1170		Cocos	North America	>25 km	Stratovolcano(es)		14.7401	-91.4497
4023	Atitlan	Toliman	1856		Cocos	North America	>25 km	Stratovolcano/caldera	Andesite / Basaltic Andesite	14.5830	-91.1860
4024	Ipala				Cocos	Caribbean	>25 km	Stratovolcano	Basalt / Picro-Basalt	14.5500	-89.6300
4025	Fuego	Acatenango	2002		Cocos	North America	>25 km	Stratovolcano	Basalt / Picro-Basalt	14.4730	-90.8800
4026	Agua		1541		Cocos	North America	>25 km	Stratovolcano	Andesite / Basaltic Andesite	14.4650	-90.7430
4027	Tahual				Cocos	Caribbean	>25 km	Stratovolcano	Basalt / Picro-Basalt	14.4300	-89.9000
4028	Ixtepeque				Cocos	Caribbean	>25 km	Lava dome(s)	Rhyolite	14.4200	-89.6800
4029	Suchitan		1469		Cocos	Caribbean	>25 km	Stratovolcano(es)	Andesite / Basaltic Andesite	14.4000	-89.7800
4030	Pacaya		2013		Cocos	Caribbean	>25 km	Complex	Basalt / Picro-Basalt	14.3810	-90.6010
4031	Jumaytepeque				Cocos	Caribbean	>25 km	Stratovolcano	Basalt / Picro-Basalt	14.3360	-90.2690
4032	Santiago, Cerro				Cocos	Caribbean	>25 km	Volcanic field	Basalt / Picro-Basalt	14.3300	-89.8700
4033	Flores		-950		Cocos	Caribbean	>25 km	Volcanic field	Basalt / Picro-Basalt	14.3080	-89.9920
4034	Tecuamburro		-960		Cocos	Caribbean	>25 km	Stratovolcano	Andesite / Basaltic Andesite	14.1560	-90.4070
4035	Moyuta				Cocos	Caribbean	>25 km	Stratovolcano	Andesite / Basaltic Andesite	14.0300	-90.1000
4036	Chingo				Cocos	Caribbean	>25 km	Stratovolcano	Andesite / Basaltic Andesite	14.1200	-89.7300
Honduras											
4037	Tigre, Isla el	Isla Zacate Grande			Cocos	Caribbean	>25 km	Stratovolcano	Basalt / Picro-Basalt	13.2720	-87.6410
Indonesia											
14005	Tongkoko		1880		Molucca Sea?	Celebes Sea?	>25 km	Stratovolcano	Andesite / Basaltic Andesite	1.5200	125.2000
14007	Klabat				Molucca Sea?	Celebes Sea?	>25 km	Stratovolcano	Andesite / Basaltic Andesite	1.4700	125.0300
14009	Lokon-Empung-Mahawu	Mahawu	2012		Molucca Sea?	Celebes Sea?	>25 km	Stratovolcano	Basalt / Picro-Basalt	1.3580	124.7920
14011	Tondano Caldera				Molucca Sea?	Celebes Sea?	>25 km	Caldera	Andesite / Basaltic Andesite	1.2300	124.8300
14012	Soputan-Sempu	Sempu	2012		Molucca Sea?	Celebes Sea?	>25 km	Stratovolcano	Andesite / Basaltic Andesite	1.1150	124.7367
14015	Ambang		2005		Molucca Sea?	Celebes Sea?	>25 km	Complex	Andesite / Basaltic Andesite	0.7500	124.4200
15001	Pulau Weh				Capricorn	Sunda	>25 km	Stratovolcano		5.8200	95.2800
15002	Seulawah Agam		1839		Capricorn	Sunda	>25 km	Stratovolcano	Andesite / Basaltic Andesite	5.4480	95.6580
15003	Peuet Sague		2000		Capricorn	Sunda	>25 km	Complex	Andesite / Basaltic Andesite	4.9140	96.3290
15004	Geureudong-Telong, Bur ni	Bur ni Telong			Capricorn	Sunda	>25 km	Stratovolcano		4.8130	96.8200
15005	Kembar				Capricorn	Sunda	>25 km	Shield		3.8500	97.6640
15006	Sibayak		-2240		Capricorn	Sunda	>25 km	Stratovolcano(es)	Andesite / Basaltic Andesite	3.2476	98.5005
15007	Sinabung		2013		Capricorn	Sunda	>25 km	Stratovolcano	Andesite / Basaltic Andesite	3.1700	98.3920
15008	Toba				Capricorn	Sunda	>25 km	Caldera	Dacite	2.5800	98.8300
15009	Imun				Capricorn	Sunda	>25 km	Lava cone	Dacite	2.1580	98.9300
15010	Sibualbuali				Capricorn	Sunda	>25 km	Stratovolcano	Dacite	1.5560	99.2550
15011	Lubukraya				Capricorn	Sunda	>25 km	Stratovolcano	Andesite / Basaltic Andesite	1.4780	99.2090
15012	Sorikmarapi		1996		Capricorn	Sunda	>25 km	Stratovolcano	Andesite / Basaltic Andesite	0.6860	99.5390
15013	Malintang				Capricorn	Sunda	>25 km	Stratovolcano	Andesite / Basaltic Andesite	0.4700	99.6700
15014	Talakmau		1937		Capricorn	Sunda	>25 km	Complex	Andesite / Basaltic Andesite	0.0790	99.9800
15015	Marapi		2014		Capricorn	Sunda	>25 km	Complex	Andesite / Basaltic Andesite	-0.3810	100.4730
15016	Tandikat		1924		Capricorn	Sunda	>25 km	Stratovolcano(es)	Andesite / Basaltic Andesite	-0.4330	100.3170
15017	Talang		2007		Capricorn	Sunda	>25 km	Stratovolcano	Andesite / Basaltic Andesite	-0.9780	100.6790

VC_Num	Volcano Name	Linked_Centers	Most Recent		Crustal Thickness	Primary Volcano Type	Dominant Rock Type	Latitude	Longitude	
			Eruption	Under_Plate						Over_Plate
15018	Kerinci		2009	Capricorn	Sunda	>25 km	Stratovolcano	Andesite / Basaltic Andesite	-1.6970	101.2640
15019	Kunyit			Capricorn	Sunda	>25 km	Stratovolcano	Dacite	-2.2740	101.4830
15020	Hutapanjang			Capricorn	Sunda	>25 km	Stratovolcano	No Data (checked)	-2.3300	101.6000
15021	Sumbing		1921	Capricorn	Sunda	>25 km	Stratovolcano	Andesite / Basaltic Andesite	-2.4140	101.7280
15022	Pendan			Capricorn	Sunda	>25 km	Unknown	No Data (checked)	-2.8200	102.0200
15023	Belirang-Beriti			Capricorn	Sunda	>25 km	Compound	Basalt / Picro-Basalt	-2.8791	102.1520
15024	Daun, Bukit			Capricorn	Sunda	>25 km	Stratovolcano(es)	Basalt / Picro-Basalt	-3.3800	102.3700
15025	Kaba		2000	Capricorn	Sunda	>25 km	Stratovolcano	Andesite / Basaltic Andesite	-3.5200	102.6200
15026	Dempo		2009	Capricorn	Sunda	>25 km	Stratovolcano(es)	Andesite / Basaltic Andesite	-4.0300	103.1300
15027	Lumut Balai, Bukit			Capricorn	Sunda	>25 km	Stratovolcano?	Andesite / Basaltic Andesite	-4.2200	103.6200
15028	Patah			Capricorn	Sunda	>25 km	Stratovolcano?	No Data (checked)	-4.2700	103.3000
15029	Besar		1940	Capricorn	Sunda	>25 km	Stratovolcano?	Andesite / Basaltic Andesite	-4.4300	103.6700
15030	Ranau-Gunung Semuning volcano		1903	Capricorn	Sunda	>25 km	Caldera	Dacite	-4.9119	103.9607
15031	Sekincau Belirang			Capricorn	Sunda	>25 km	Caldera(s)	Andesite / Basaltic Andesite	-5.1072	104.3164
15032	Suoh		1933	Capricorn	Sunda	>25 km	Caldera(s)	No Data (checked)	-5.2500	104.2700
15033	Hulubelu			Capricorn	Sunda	>25 km	Caldera	Andesite / Basaltic Andesite	-5.3333	104.5907
15034	Rajabasa			Australia	Sunda	>25 km	Stratovolcano	Andesite / Basaltic Andesite	-5.7800	105.6250
15035	Karang			Australia	Sunda	>25 km	Stratovolcano	Andesite / Basaltic Andesite	-6.2700	106.0420
15036	Pulosari			Australia	Sunda	>25 km	Stratovolcano	Andesite / Basaltic Andesite	-6.3420	105.9750
15037	Muria		-160	Australia	Sunda	>25 km	Stratovolcano	Trachybasalt / Tephrite Basanite	-6.6200	110.8800
15038	Salak	Perbakti-Gagak	1938	Australia	Sunda	>25 km	Stratovolcano	Andesite / Basaltic Andesite	-6.7200	106.7300
15040	Tangkubanparahu		2013	Australia	Sunda	>25 km	Stratovolcano	Andesite / Basaltic Andesite	-6.7700	107.6000
15041	Tampomas			Australia	Sunda	>25 km	Stratovolcano	Andesite / Basaltic Andesite	-6.7700	107.9500
15042	Gede		1957	Australia	Sunda	>25 km	Stratovolcano	Andesite / Basaltic Andesite	-6.7800	106.9800
15043	Cereme		1951	Australia	Sunda	>25 km	Stratovolcano	Andesite / Basaltic Andesite	-6.8920	108.4000
15045	Malabar			Australia	Sunda	>25 km	Stratovolcano	Andesite / Basaltic Andesite	-7.1350	107.6301
15046	Guntur	Kawah Kamojang	1887	Australia	Sunda	>25 km	Complex	Andesite / Basaltic Andesite	-7.1430	107.8400
15047	Patuha			Australia	Sunda	>25 km	Stratovolcano	Andesite / Basaltic Andesite	-7.1600	107.4000
15048	Ungaran			Australia	Sunda	>25 km	Stratovolcano	Trachyandesite / Basaltic trachy	-7.1800	110.3300
15049	Wayang-Windu			Australia	Sunda	>25 km	Lava dome	Andesite / Basaltic Andesite	-7.2080	107.6300
15050	Dieng Volcanic Complex		2009	Australia	Sunda	>25 km	Complex	Andesite / Basaltic Andesite	-7.2189	109.9072
15051	Slamet		2014	Australia	Sunda	>25 km	Stratovolcano	Basalt / Picro-Basalt	-7.2420	109.2080
15052	Galunggung-Talagabodas	Talagabodas	1984	Australia	Sunda	>25 km	Stratovolcano	Basalt / Picro-Basalt	-7.2500	108.0580
15053	Sundoro		1971	Australia	Sunda	>25 km	Stratovolcano	Andesite / Basaltic Andesite	-7.3000	109.9920
15054	Papandayan-Kendang	Kendang	2002	Australia	Sunda	>25 km	Stratovolcano(es)	Andesite / Basaltic Andesite	-7.3200	107.7300
15055	Telomoyo			Australia	Sunda	>25 km	Stratovolcano	Andesite / Basaltic Andesite	-7.3700	110.4000
15056	Sumbing		1730	Australia	Sunda	>25 km	Stratovolcano	Andesite / Basaltic Andesite	-7.3840	110.0700
15057	Merbabu		1797	Australia	Sunda	>25 km	Stratovolcano	Basalt / Picro-Basalt	-7.4500	110.4300
15058	Merapi		2014	Australia	Sunda	>25 km	Stratovolcano	Andesite / Basaltic Andesite	-7.5420	110.4420
15059	Penanggungan		200	Australia	Sunda	>25 km	Stratovolcano	Andesite / Basaltic Andesite	-7.6200	112.6300
15060	Lawu		1885	Australia	Sunda	>25 km	Stratovolcano	Andesite / Basaltic Andesite	-7.6250	111.1920
15061	Arjuno-Welirang		1991	Australia	Sunda	>25 km	Stratovolcano	Andesite / Basaltic Andesite	-7.7250	112.5800
15062	Lurus			Australia	Sunda	>25 km	Complex	Andesite / Basaltic Andesite	-7.7300	113.5800
15063	Wilis		1641	Australia	Sunda	>25 km	Stratovolcano	Andesite / Basaltic Andesite	-7.8080	111.7580
15064	Baluran			Australia	Sunda	>25 km	Stratovolcano	Andesite / Basaltic Andesite	-7.8500	114.3700
15065	Kawi-Butak			Australia	Sunda	>25 km	Stratovolcano(es)	No Data (checked)	-7.9200	112.4500
15066	Kelut		2014	Australia	Sunda	>25 km	Stratovolcano	Andesite / Basaltic Andesite	-7.9300	112.3080
15067	Tengger Caldera	Semeru	2010	Australia	Sunda	>25 km	Stratovolcano(es)	Trachyandesite / Basaltic trachy	-7.9420	112.9500
15068	Iyang-Argapura		1597	Australia	Sunda	>25 km	Complex	Andesite / Basaltic Andesite	-7.9700	113.5700
15069	Lamongan		1953	Australia	Sunda	>25 km	Stratovolcano	Basalt / Picro-Basalt	-7.9790	113.3420
15070	Ijen		2002	Australia	Sunda	>25 km	Stratovolcano(es)	Andesite / Basaltic Andesite	-8.0580	114.2420
15071	Raung		2008	Australia	Sunda	>25 km	Stratovolcano	Andesite / Basaltic Andesite	-8.1250	114.0420
15072	Sangeang Api		2014	Australia	Sunda	>25 km	Complex	Trachybasalt / Tephrite Basanite	-8.2000	119.0700
15073	Batur		1999	Australia	Sunda	>25 km	Caldera	Andesite / Basaltic Andesite	-8.2420	115.3750
15074	Tambora		1967	Australia	Sunda	>25 km	Stratovolcano	Trachybasalt / Tephrite Basanite	-8.2500	118.0000
15076	Bratan			Australia	Sunda	>25 km	Caldera	Andesite / Basaltic Andesite	-8.2800	115.1300
15079	Agung		1963	Australia	Sunda	>25 km	Stratovolcano	Andesite / Basaltic Andesite	-8.3420	115.5080
15082	Rinjani		2009	Australia	Sunda	>25 km	Stratovolcano	Andesite / Basaltic Andesite	-8.4200	116.4700
15090	Sano, Wai			Australia	Sunda	>25 km	Caldera	Dacite	-8.7105	119.9898
15075	Lewotolo		2012	Australia	Banda Sea?	Unknown	Stratovolcano	Andesite / Basaltic Andesite	-8.2720	123.5050

VC_Num	Volcano Name	Linked_Centers	Most Recent		Under_Plate	Over_Plate	Crustal Thickness	Primary Volcano Type	Dominant Rock Type	Latitude	Longitude
			Eruption								
15077	Ilikedeka				Australia	Banda Sea?	Unknown	Stratovolcano		-8.3010	122.9070
15078	Paluweh		2012		Australia	Banda Sea?	Unknown	Stratovolcano	Andesite / Basaltic Andesite	-8.3200	121.7080
15080	Iliboleng		1993		Australia	Banda Sea?	Unknown	Stratovolcano	Basalt / Picro-Basalt	-8.3420	123.2580
15081	Leroboleng		2003		Australia	Banda Sea?	Unknown	Complex	Andesite / Basaltic Andesite	-8.3580	122.8420
15083	Ilimuda				Australia	Banda Sea?	Unknown	Stratovolcano	Andesite / Basaltic Andesite	-8.4880	122.6856
15084	Sirung		2012		Australia	Banda Sea?	Unknown	Complex	Andesite / Basaltic Andesite	-8.5080	124.1300
15085	Iliwerung		2013		Australia	Banda Sea?	Unknown	Complex	Basalt / Picro-Basalt	-8.5300	123.5700
15086	Lewotobi		2003		Australia	Banda Sea?	Unknown	Stratovolcano(es)	Andesite / Basaltic Andesite	-8.5420	122.7750
15087	Ilibalekan				Australia	Banda Sea?	Unknown	Stratovolcano	Basalt / Picro-Basalt	-8.5500	123.3800
15088	Egon		2008		Australia	Banda Sea?	Unknown	Stratovolcano	Andesite / Basaltic Andesite	-8.6700	122.4500
15089	Poco Leok	Ranakah			Australia	Sunda	Unknown	Stratovolcano	Andesite / Basaltic Andesite	-8.6587	120.4849
15091	Inielika		2001		Australia	Sunda	Unknown	Complex	Andesite / Basaltic Andesite	-8.7300	120.9800
15092	Kelimutu	Sukaria Caldera	1968		Australia	Banda Sea?	Unknown	Complex	Andesite / Basaltic Andesite	-8.7700	121.8200
15093	Ebulobo		1969		Australia	Sunda	Unknown	Stratovolcano	Andesite / Basaltic Andesite	-8.8162	121.1914
15094	Inierie		-8050		Australia	Sunda	Unknown	Stratovolcano	Andesite / Basaltic Andesite	-8.8750	120.9500
15095	Iya		1971		Australia	Banda Sea?	Unknown	Stratovolcano	Basalt / Picro-Basalt	-8.8970	121.6450
14001	Awu		2004		Molucca Sea?	Celebes Sea?	Oceanic < 15 km	Stratovolcano	Andesite / Basaltic Andesite	3.6700	125.5000
14002	Karangatang [Api Siau]		2014		Molucca Sea?	Celebes Sea?	Oceanic < 15 km	Stratovolcano	Andesite / Basaltic Andesite	2.7800	125.4000
14003	Dukono		1933		Molucca Sea?	Halmahera Sea?	Oceanic < 15 km	Complex	Andesite / Basaltic Andesite	1.6997	127.8791
14004	Tobaru				Molucca Sea?	Halmahera Sea?	Oceanic < 15 km	Unknown	Andesite / Basaltic Andesite	1.6300	127.6700
14006	Ibu		2008		Molucca Sea?	Halmahera Sea?	Oceanic < 15 km	Stratovolcano	Andesite / Basaltic Andesite	1.4880	127.6300
14008	Gamkonora		2013		Molucca Sea?	Halmahera Sea?	Oceanic < 15 km	Stratovolcano	Andesite / Basaltic Andesite	1.3800	127.5300
14010	Todoko-Ranu				Molucca Sea?	Halmahera Sea?	Oceanic < 15 km	Caldera(s)	Andesite / Basaltic Andesite	1.2500	127.4700
14013	Jailolo				Molucca Sea?	Halmahera Sea?	Oceanic < 15 km	Stratovolcano	Andesite / Basaltic Andesite	1.0800	127.4200
14014	Gamalama		2012		Molucca Sea?	Halmahera Sea?	Oceanic < 15 km	Stratovolcano(es)	Andesite / Basaltic Andesite	0.8000	127.3300
14016	Tidore				Molucca Sea?	Halmahera Sea?	Oceanic < 15 km	Stratovolcano	Andesite / Basaltic Andesite	0.6580	127.4000
14017	Moti		1774		Molucca Sea?	Halmahera Sea?	Oceanic < 15 km	Stratovolcano	Andesite / Basaltic Andesite	0.4500	127.4000
14018	Makian		1988		Molucca Sea?	Halmahera Sea?	Oceanic < 15 km	Stratovolcano	Andesite / Basaltic Andesite	0.3200	127.4000
14019	Tigalalu				Molucca Sea?	Halmahera Sea?	Oceanic < 15 km	Stratovolcano	Andesite / Basaltic Andesite	0.0700	127.4200
14020	Amasing				Molucca Sea?	Halmahera Sea?	Oceanic < 15 km	Stratovolcano(es)	Andesite / Basaltic Andesite	-0.5300	127.4800
14021	Bibinoi				Molucca Sea?	Halmahera Sea?	Oceanic < 15 km	Stratovolcano(es)	Andesite / Basaltic Andesite	-0.7700	127.7200
15039	Nila		1968		Australia	Banda Sea?	Oceanic < 15 km	Stratovolcano	Andesite / Basaltic Andesite	-6.7300	129.5000
15044	Wurlali		1892		Australia	Banda Sea?	Oceanic < 15 km	Stratovolcano	Andesite / Basaltic Andesite	-7.1250	128.6750
Italy											
21001	Larderello		1282		Adria	Eurasia	>25 km	Explosion crater(s)	No Data (checked)	43.2500	10.8700
21002	Amiata				Adria	Eurasia	>25 km	Lava dome(s)		42.9000	11.6300
21003	Vulsini		-104		Adria	Eurasia	>25 km	Caldera	Trachyte / Trachyandesite	42.6000	11.9300
21004	Alban Hills				Adria	Eurasia	>25 km	Caldera	Foidite	41.7300	12.7000
21005	Campi Flegrei		1538		Adria	Eurasia	>25 km	Caldera	Trachyte / Trachyandesite	40.8270	14.1390
21006	Vesuvius		1913		Africa	Eurasia	>25 km	Somma	Phono-tephrite / Tephri-phonol	40.8210	14.4260
21007	Ischia		1302		Africa	Eurasia	>25 km	Complex	Trachyte / Trachyandesite	40.7300	13.8970
21008	Vulcano	Lipari	1968		Africa	Eurasia	>25 km	Stratovolcano(es)	Trachybasalt / Tephrite Basanite	38.4040	14.9620
21009	Etna		2013		Africa	Eurasia	>25 km	Stratovolcano(es)	Trachybasalt / Tephrite Basanite	37.7340	15.0040
Japan											
10001	Shiretoko-Iozan	Rausudake, Tenchozan	1935		Pacific	Okhotsk	>25 km	Stratovolcano	Andesite / Basaltic Andesite	44.1330	145.1610
10002	Taisetsuzan		1739		Pacific	Okhotsk	>25 km	Stratovolcano(es)	Andesite / Basaltic Andesite	43.6640	142.8540
10003	Kussharo	Mashu	1320		Pacific	Okhotsk	>25 km	Caldera	Dacite	43.6080	144.4430
10004	Maruyama		1898		Pacific	Okhotsk	>25 km	Stratovolcano(es)	Andesite / Basaltic Andesite	43.4530	143.0360
10005	Tokachidake		2004		Pacific	Okhotsk	>25 km	Stratovolcano(es)	Andesite / Basaltic Andesite	43.4180	142.6860
10006	Akan		2008		Pacific	Okhotsk	>25 km	Caldera	Andesite / Basaltic Andesite	43.3840	144.0130
10007	Shikaribetsu Group				Pacific	Okhotsk	>25 km	Lava dome(s)	Andesite / Basaltic Andesite	43.3120	143.0960
10008	Niseko		-4900		Pacific	Amur	>25 km	Stratovolcano(es)	Andesite / Basaltic Andesite	42.8800	140.6300
10009	Yoteizan		-1050		Pacific	Amur	>25 km	Stratovolcano	Andesite / Basaltic Andesite	42.8270	140.8110
10010	Shiribetsu				Pacific	Amur	>25 km	Stratovolcano	Andesite	42.7670	140.9160
10011	Shikotsu		1981		Pacific	Amur	>25 km	Caldera	Andesite / Basaltic Andesite	42.6880	141.3800
10012	Toya		2000		Pacific	Amur	>25 km	Stratovolcano	Basalt / Picro-Basalt	42.5440	140.8390
10013	Kuttara		1820		Pacific	Amur	>25 km	Stratovolcano(es)	Basalt / Picro-Basalt	42.4910	141.1600
10014	Nigorikawa				Pacific	Amur	>25 km	Caldera		42.1200	140.4500
10015	Hokkaido-Komagatake		2000		Pacific	Amur	>25 km	Stratovolcano	Andesite / Basaltic Andesite	42.0630	140.6770
10016	Esan		1874		Pacific	Amur	>25 km	Lava dome(s)	Andesite / Basaltic Andesite	41.8050	141.1660

VC_Num	Volcano Name	Linked_Centers	Most Recent		Under_Plate	Over_Plate	Crustal Thickness	Primary Volcano Type	Dominant Rock Type	Latitude	Longitude
			Eruption								
10017	Mutsu-Hiuchi-dake				Pacific	Amur	>25 km	Stratovolcano		41.4360	141.0560
10018	Osorezan		1787		Pacific	Amur	>25 km	Stratovolcano	Andesite / Basaltic Andesite	41.2760	141.1240
10019	Hakkodasan		1550		Pacific	Amur	>25 km	Stratovolcano(es)	Andesite / Basaltic Andesite	40.6590	140.8770
10020	Iwakisan		1863		Pacific	Amur	>25 km	Stratovolcano	Andesite / Basaltic Andesite	40.6560	140.3030
10021	Towada		915		Pacific	Amur	>25 km	Caldera	Andesite / Basaltic Andesite	40.5100	140.8800
10022	Akita-Yakeyama		1997		Pacific	Amur	>25 km	Stratovolcano	Andesite / Basaltic Andesite	39.9640	140.7570
10023	Hachimantai		-5350		Pacific	Amur	>25 km	Stratovolcano	Andesite / Basaltic Andesite	39.9580	140.8540
10024	Kanpu				Pacific	Amur	>25 km			39.9310	139.8790
10025	Iwatesan		1934		Pacific	Amur	>25 km	Complex	Basalt / Picro-Basalt	39.8530	141.0010
10026	Akita-Komagatake		1970		Pacific	Amur	>25 km	Stratovolcano(es)	Basalt / Picro-Basalt	39.7610	140.7990
10027	Chokaisan		1974		Pacific	Amur	>25 km	Stratovolcano(es)	Andesite / Basaltic Andesite	39.0990	140.0490
10028	Kurikomayama		1950		Pacific	Amur	>25 km	Stratovolcano	Andesite / Basaltic Andesite	38.9610	140.7880
10029	Onikobe				Pacific	Amur	>25 km	Caldera		38.8300	140.6950
10056	Naruko				Pacific	Amur	>25 km	Caldera	Rhyolite	38.7337	140.7249
10030	Hijiori				Pacific	Amur	>25 km	Caldera	Dacite	38.6060	140.1780
10031	Zaozan		1940		Pacific	Amur	>25 km	Complex	Andesite / Basaltic Andesite	38.1440	140.4400
10032	Azumayama		1977		Pacific	Amur	>25 km	Stratovolcano(es)	Andesite / Basaltic Andesite	37.7350	140.2440
10033	Adatarayama		1992		Pacific	Amur	>25 km	Stratovolcano(es)	Andesite / Basaltic Andesite	37.6470	140.2810
10034	Bandaisan		1888		Pacific	Amur	>25 km	Stratovolcano	Andesite / Basaltic Andesite	37.6010	140.0720
10035	Numazawa				Pacific	Amur	>25 km	Shield	Dacite	37.4440	139.5660
10036	Nasudake		1963		Pacific	Amur	>25 km	Stratovolcano(es)	Andesite / Basaltic Andesite	37.1250	139.9630
10037	Hiuchigatake		1544		Pacific	Amur	>25 km	Stratovolcano	Andesite / Basaltic Andesite	36.9550	139.2850
10038	Takaharayama		-4570		Pacific	Amur	>25 km	Stratovolcano	Andesite / Basaltic Andesite	36.9000	139.7770
10039	Myokosan	Niigata-Yakeyama	-750		Pacific	Amur	>25 km	Stratovolcano	Andesite / Basaltic Andesite	36.8910	138.1140
10040	Nikko-Shiranesan		1952		Pacific	Amur	>25 km	Shield	Andesite / Basaltic Andesite	36.7990	139.3760
10041	Nantai	Omanago Group	-9540		Pacific	Amur	>25 km	Stratovolcano	Andesite / Basaltic Andesite	36.7620	139.4940
10042	Kusatsu-Shiranesan	Shiga	1989		Pacific	Amur	>25 km	Stratovolcano(es)	Andesite / Basaltic Andesite	36.6180	138.5280
10043	Midagahara		1858		Pacific	Amur	>25 km	Stratovolcano	Andesite / Basaltic Andesite	36.5710	137.5900
10044	Akagisan		1938		Pacific	Amur	>25 km	Stratovolcano	Andesite / Basaltic Andesite	36.5600	139.1930
10045	Harunasan		550		Pacific	Amur	>25 km	Stratovolcano	Andesite / Basaltic Andesite	36.4770	138.8510
10046	Washiba-Kumonotaira				Pacific	Amur	>25 km	Shield(s)	Andesite / Basaltic Andesite	36.4080	137.5940
10047	Asamayama		2009		Pacific	Amur	>25 km	Complex	Andesite / Basaltic Andesite	36.4060	138.5230
10048	Yakedake		1995		Pacific	Amur	>25 km	Stratovolcano(es)	Andesite / Basaltic Andesite	36.2270	137.5870
10049	Hakusan		1659		Pacific	Amur	>25 km	Stratovolcano	Andesite / Basaltic Andesite	36.1550	136.7710
10050	Norikuradake		-50		Pacific	Amur	>25 km	Stratovolcano(es)	Andesite / Basaltic Andesite	36.1060	137.5540
10051	Yokodake		1200		Pacific	Amur	>25 km	Stratovolcano(es)	Andesite / Basaltic Andesite	36.0870	138.3200
10052	Ontakesan		2014		Pacific	Amur	>25 km	Complex	Andesite / Basaltic Andesite	35.8930	137.4800
10053	Fujisan		1854		Pacific	Amur	>25 km	Stratovolcano	Basalt / Picro-Basalt	35.3610	138.7280
10054	Hakoneyama		1170		Pacific	Amur	>25 km	Complex	Andesite / Basaltic Andesite	35.2330	139.0210
10055	Izu-Tobu		1989		Pacific	Amur	>25 km	Pyroclastic cone(s)	Basalt / Picro-Basalt	34.9000	139.0980
12001	Sanbesan		650		Philippine Sea	Amur	>25 km	Stratovolcano	Dacite	35.1390	132.6210
12002	Abu		-6850		Philippine Sea	Amur	>25 km	Shield(s)	Andesite / Basaltic Andesite	34.5000	131.6000
12003	Yufu-Tsurumi		867		Philippine Sea	Amur	>25 km	Lava dome(s)	Andesite / Basaltic Andesite	33.2820	131.3900
12004	Kujusan		1995		Philippine Sea	Amur	>25 km	Stratovolcano(es)	Andesite / Basaltic Andesite	33.0860	131.2490
12005	Asosan		2014		Philippine Sea	Amur	>25 km	Caldera	Andesite / Basaltic Andesite	32.8840	131.1040
12006	Unzendake		1996		Philippine Sea	Yangtze	>25 km	Complex	Andesite / Basaltic Andesite	32.7610	130.2990
12007	Kirishimayama		2011		Philippine Sea	Satunam	>25 km	Shield	Andesite / Basaltic Andesite	31.9340	130.8620
12008	Aira		1955		Philippine Sea	Satunam	>25 km	Caldera	Andesite / Basaltic Andesite	31.5930	130.6570
12009	Ibusuki Volcanic Field		1615		Philippine Sea	Satunam	>25 km	Caldera(s)	Andesite / Basaltic Andesite	31.2200	130.5700
11006	Ioto		2012		Pacific	Philippine Sea	Unknown	Caldera	Trachyandesite / Basaltic trachy	24.7510	141.2890
11001	Izu-Oshima		1990		Pacific	Philippine Sea	Oceanic < 15 km	Stratovolcano	Basalt / Picro-Basalt	34.7240	139.3940
11002	Niijima		886		Pacific	Philippine Sea	Oceanic < 15 km	Lava dome(s)	Rhyolite	34.3970	139.2700
11003	Miyakejima		2010		Pacific	Philippine Sea	Oceanic < 15 km	Stratovolcano	Basalt / Picro-Basalt	34.0940	139.5260
11004	Mikurajima		-4100		Pacific	Philippine Sea	Oceanic < 15 km	Stratovolcano	Basalt / Picro-Basalt	33.8740	139.6020
11005	Hachijojima		1707		Pacific	Philippine Sea	Oceanic < 15 km	Stratovolcano(es)	Basalt / Picro-Basalt	33.1370	139.7660
12010	Kuchinoerabujima		2014		Philippine Sea	Satunam	Oceanic < 15 km	Stratovolcano(es)	Andesite / Basaltic Andesite	30.4430	130.2170
12011	Nakanoshima		1949		Philippine Sea	Satunam	Oceanic < 15 km	Stratovolcano(es)	Andesite / Basaltic Andesite	29.8590	129.8570
12012	Suwanosijima		2004		Philippine Sea	Satunam	Oceanic < 15 km	Stratovolcano(es)	Andesite / Basaltic Andesite	29.6380	129.7140
9001	Rakkibetsudake [Demon]				Pacific	Okhotsk	15-25 km	Stratovolcano	No Data (checked)	45.5000	148.8500
9002	Moyorodake [Medvezhia]		1999		Pacific	Okhotsk	15-25 km	Somma	Andesite / Basaltic Andesite	45.3890	148.8380

VC_Num	Volcano Name	Linked_Centers	Most Recent		Crustal Thickness	Primary Volcano Type	Dominant Rock Type	Latitude	Longitude	
			Eruption	Under_Plate						Over_Plate
9003	Chirippusan [Chirip]		1860	Pacific	Okhotsk	15-25 km	Stratovolcano(es)	Basalt / Picro-Basalt	45.3380	147.9200
9004	Sashiusudake [Baransky]		1951	Pacific	Okhotsk	15-25 km	Stratovolcano	Andesite / Basaltic Andesite	45.1000	148.0190
9005	Odamoisan [Tebenkov]	Etorofu-Yakeyama		Pacific	Okhotsk	15-25 km	Stratovolcano		45.0260	147.9220
9006	Nishihitokappuyama [Bogatyr Ridge]			Pacific	Okhotsk	15-25 km	Stratovolcano	Andesite / Basaltic Andesite	44.8330	147.3420
9007	Etorofu-Atosanupuri [Atosanupuri]		2013	Pacific	Okhotsk	15-25 km	Stratovolcano	Andesite / Basaltic Andesite	44.8080	147.1310
9008	Moekeshiwan [Lvinaya Past]		-7480	Pacific	Okhotsk	15-25 km	Stratovolcano	Andesite / Basaltic Andesite	44.6080	146.9940
9009	Berutarubesan [Berutarube]		1812	Pacific	Okhotsk	15-25 km	Stratovolcano	Andesite / Basaltic Andesite	44.4620	146.9320
9010	Ruruidake [Smirnov]			Pacific	Okhotsk	15-25 km	Stratovolcano	Andesite / Basaltic Andesite	44.4540	146.1390
9011	Chachadake [Tiatia]		1982	Pacific	Okhotsk	15-25 km	Stratovolcano	Basalt / Picro-Basalt	44.3530	146.2520
9012	Raususan [Mendeleev]		1900	Pacific	Okhotsk	15-25 km	Stratovolcano	Andesite / Basaltic Andesite	43.9790	145.7330
9013	Tomariyama [Golovnin]		1848	Pacific	Okhotsk	15-25 km	Caldera	Andesite / Basaltic Andesite	43.8440	145.5040
Malaysia										
14022	Bombalai			Celebes Sea?	Sunda?	>25 km	Pyroclastic cone	Basalt / Picro-Basalt	4.4000	117.8800
Mexico										
3001	Sanguaney		1742	Rivera	North America	>25 km	Stratovolcano	Andesite / Basaltic Andesite	21.4500	-104.7300
3002	Ceboruco		1870	Rivera	North America	>25 km	Stratovolcano	Andesite / Basaltic Andesite	21.1250	-104.5080
3003	Mascota Volcanic Field			Rivera	North America	>25 km	Pyroclastic cone(s)	Andesite / Basaltic Andesite	20.6200	-104.8300
3004	Primavera, Sierra la			Rivera	North America	>25 km	Caldera		20.6200	-103.5200
3005	Azufres, Los			Cocos	North America	>25 km	Caldera		19.8500	-100.6300
3006	Atlixcos, Los			Cocos	North America	>25 km	Shield	Basalt / Picro-Basalt	19.8090	-96.5260
3007	Jocotitlan		1270	Cocos	North America	>25 km	Stratovolcano	Dacite	19.7300	-99.7580
3008	Humeros, Los			Cocos	North America	>25 km	Caldera(s)	Rhyolite	19.6800	-97.4500
3009	Colima		2013	Rivera	North America	>25 km	Stratovolcano(es)	Andesite / Basaltic Andesite	19.5140	-103.6200
3010	Cofre de Perote		1150	Cocos	North America	>25 km	Shield(s)	Andesite / Basaltic Andesite	19.4920	-97.1500
3011	Zitacuaro-Valle de Bravo		-3050	Cocos	North America	>25 km	Caldera	Dacite	19.4000	-100.2500
3012	Serdan-Oriental			Cocos	North America	>25 km	Tuff cone(s)	Rhyolite	19.2700	-97.4700
3013	Malinche, La		-1170	Cocos	North America	>25 km	Stratovolcano	Andesite / Basaltic Andesite	19.2310	-98.0320
3014	Ajusco			Cocos	North America	>25 km	Volcanic field	Andesite / Basaltic Andesite	19.2076	-99.2579
3015	Iztaccihuatl-Popocatepetl	Popocatepetl, Papayo		Cocos	North America	>25 km	Stratovolcano	Andesite / Basaltic Andesite	19.1790	-98.6420
3016	Toluca, Nevado de		-1350	Cocos	North America	>25 km	Stratovolcano	Andesite / Basaltic Andesite	19.1080	-99.7580
3017	Chichinautzin		400	Cocos	North America	>25 km	Volcanic field	Andesite / Basaltic Andesite	19.0890	-99.1388
3018	Tlaloc			Cocos	North America	>25 km	Volcanic field	Andesite / Basaltic Andesite	19.1096	-99.0325
3019	Orizaba, Pico de	Las Cumbres	1846	Cocos	North America	>25 km	Stratovolcano	Andesite / Basaltic Andesite	19.0300	-97.2680
3020	San Martin		1932	Cocos	North America	>25 km	Shield	Trachybasalt / Tephrite Basanite	18.5700	-95.2000
3021	Chichon, El		1982	Cocos	North America	>25 km	Lava dome(s)	Trachyandesite / Basaltic trachy	17.3600	-93.2280
4038	Tacana		1986	Cocos	North America	>25 km	Stratovolcano	Andesite / Basaltic Andesite	15.1300	-92.1120
Netherlands										
5007	Saba		1640	North America	Caribbean	Oceanic < 15 km	Stratovolcano	Andesite / Basaltic Andesite	17.6300	-63.2300
5008	Quill, The		250	North America	Caribbean	Oceanic < 15 km	Stratovolcano	Andesite / Basaltic Andesite	17.4780	-62.9600
New Zealand										
19001	Rotorua			Pacific	Australia	>25 km	Caldera		-38.0800	176.2700
19002	Okataina		1981	Pacific	Australia	>25 km	Lava dome(s)	Rhyolite	-38.1200	176.5000
19003	Reporoa		1180	Pacific	Australia	>25 km	Caldera	Rhyolite	-38.4200	176.3300
19004	Maroa		180	Pacific	Australia	>25 km	Caldera(s)	Rhyolite	-38.4200	176.0800
19005	Taupo		260	Pacific	Australia	>25 km	Caldera	Rhyolite	-38.8200	176.0000
19006	Tongariro		2012	Pacific	Australia	>25 km	Stratovolcano(es)	Andesite / Basaltic Andesite	-39.1570	175.6320
19007	Ruapehu		2007	Pacific	Australia	>25 km	Stratovolcano	Andesite / Basaltic Andesite	-39.2800	175.5700
19008	Taranaki [Egmont]		1854	Pacific	Australia	>25 km	Stratovolcano	Andesite / Basaltic Andesite	-39.3000	174.0700
18001	Raoul Island		2006	Pacific	Australia	Oceanic < 15 km	Stratovolcano	Andesite / Basaltic Andesite	-29.2700	-177.9200
Nicaragua										
4039	Cosiguina		1859	Cocos	Caribbean	>25 km	Stratovolcano	Andesite / Basaltic Andesite	12.9800	-87.5700
4040	San Cristobal		2014	Cocos	Caribbean	>25 km	Stratovolcano	Basalt / Picro-Basalt	12.7020	-87.0040
4041	Telica		2011	Cocos	Caribbean	>25 km	Stratovolcano(es)	Basalt / Picro-Basalt	12.6020	-86.8450
4042	Rota			Cocos	Caribbean	>25 km	Stratovolcano	Andesite / Basaltic Andesite	12.5500	-86.7500
4043	Pilas, Las	Cerro Negro	1954	Cocos	Caribbean	>25 km	Complex	Andesite / Basaltic Andesite	12.4950	-86.6880
4044	Momotombo		1918	Cocos	Caribbean	>25 km	Stratovolcano	Basalt / Picro-Basalt	12.4220	-86.5400
4045	Apoyeque		-50	Cocos	Caribbean	>25 km	Pyroclastic shield	Dacite	12.2420	-86.3420
4046	Masaya		2008	Cocos	Caribbean	>25 km	Caldera	Basalt / Picro-Basalt	11.9840	-86.1610
4047	Mombacho		1850	Cocos	Caribbean	>25 km	Stratovolcano	Andesite / Basaltic Andesite	11.8260	-85.9680
4048	Zapatera			Cocos	Caribbean	>25 km	Shield	Andesite / Basaltic Andesite	11.7300	-85.8200

VC_Num	Volcano Name	Linked_Centers	Most Recent		Crustal Thickness	Primary Volcano Type	Dominant Rock Type	Latitude	Longitude	
			Eruption	Under_Plate						Over_Plate
4049	Concepcion		2009	Cocos	Caribbean	>25 km	Stratovolcano	Andesite / Basaltic Andesite	11.5380	-85.6220
4050	Maderas			Cocos	Caribbean	>25 km	Stratovolcano	Basalt/Dacite	11.4468	-85.5152
Panama										
4051	Baru		1550	Nazca	Caribbean	>25 km	Stratovolcano	Andesite / Basaltic Andesite	8.8080	-82.5430
4052	Valle, El			Nazca	Caribbean	>25 km	Stratovolcano	Dacite	8.6047	-80.1300
4053	Yeguada, La			Nazca	Caribbean	>25 km	Stratovolcano		8.4700	-80.8200
Papua New Guinea										
16004	Rabaul-Tavurvur		2014	Woodlark	South Bismarck	>25 km	Pyroclastic shield	Dacite	-4.2390	152.2100
16006	Lolobau		1911	Woodlark	South Bismarck	>25 km	Caldera	Basalt / Picro-Basalt	-4.9200	151.1580
16007	Ulawun		2013	Woodlark	South Bismarck	>25 km	Stratovolcano	Basalt / Picro-Basalt	-5.0500	151.3300
16008	Dakataua		1895	Woodlark	South Bismarck	>25 km	Caldera	Andesite / Basaltic Andesite	-5.0560	150.1080
16009	Bola			Woodlark	South Bismarck	>25 km	Stratovolcano	Andesite / Basaltic Andesite	-5.1500	150.0300
16010	Bamus		1886	Woodlark	South Bismarck	>25 km	Stratovolcano	Andesite / Basaltic Andesite	-5.2000	151.2300
16011	Garua Harbour			Woodlark	South Bismarck	>25 km	Volcanic field	Rhyolite	-5.3000	150.0700
16012	Hargy		950	Woodlark	South Bismarck	>25 km	Stratovolcano	Dacite	-5.3300	151.1000
16013	Sakar			Woodlark	South Bismarck	>25 km	Stratovolcano	Basalt / Picro-Basalt	-5.4140	148.0940
16014	Garbuna Group		2008	Woodlark	South Bismarck	>25 km	Stratovolcano(es)	Andesite / Basaltic Andesite	-5.4500	150.0300
16015	Lolo			Woodlark	South Bismarck	>25 km	Stratovolcano	Andesite / Basaltic Andesite	-5.4680	150.5070
16016	Sulu Range			Woodlark	South Bismarck	>25 km	Stratovolcano(es)	Andesite / Basaltic Andesite	-5.5000	150.9420
16017	Langila		2012	Woodlark	South Bismarck	>25 km	Complex	Basalt / Picro-Basalt	-5.5250	148.4200
16018	Witori		2012	Woodlark	South Bismarck	>25 km	Caldera	Dacite	-5.5800	150.5200
16019	Umboi			Woodlark	South Bismarck	>25 km	Complex	Basalt / Picro-Basalt	-5.5890	147.8750
16001	Lihir			Pacific	North Bismarck	Unknown	Compound	Trachybasalt / Tephrite Basanite	-3.1250	152.6420
16002	Tanga			Pacific	North Bismarck	Unknown	Stratovolcano		-3.5000	153.2200
16003	Ambittle		-350	Pacific	North Bismarck	Unknown	Stratovolcano	Phono-tephrite / Tephri-phonol	-4.0800	153.6500
16020	Balbi	Tore	1825	Woodlark	North Bismarck	Unknown	Stratovolcano	Andesite / Basaltic Andesite	-5.9200	154.9800
16021	Bagana-Billy Mitchell	Billy Mitchell	2000	Woodlark	North Bismarck	Unknown	Lava cone	Andesite / Basaltic Andesite	-6.1370	155.1960
16022	Takuan Group	Loloru		Woodlark	North Bismarck	Unknown	Compound	Andesite / Basaltic Andesite	-6.4420	155.6080
16005	Garove			Woodlark	South Bismarck	Oceanic < 15 km	Stratovolcano	Andesite / Basaltic Andesite	-4.6920	149.5000
Peru										
7053	Sara Sara			Nazca	South America	>25 km	Stratovolcano	Andesite / Basaltic Andesite	-15.3300	-73.4500
7054	Coropuna			Nazca	South America	>25 km	Stratovolcano	Andesite / Basaltic Andesite	-15.5200	-72.6500
7055	Sabancaya		2014	Nazca	South America	>25 km	Stratovolcano(es)	Andesite / Basaltic Andesite	-15.7800	-71.8500
7056	Chachani, Nevado			Nazca	South America	>25 km	Stratovolcano	Andesite / Basaltic Andesite	-16.1910	-71.5300
7057	Misti, El		1985	Nazca	South America	>25 km	Stratovolcano	Andesite / Basaltic Andesite	-16.2940	-71.4090
7058	Ubinas		2013	Nazca	South America	>25 km	Stratovolcano	Andesite / Basaltic Andesite	-16.3550	-70.9030
7059	Huaynaputina		1600	Nazca	South America	>25 km	Stratovolcano	Dacite	-16.6080	-70.8500
7060	Ticsani		1800	Nazca	South America	>25 km	Lava dome(s)	Dacite	-16.7550	-70.5950
7061	Tutupaca			Nazca	South America	>25 km	Stratovolcano	Andesite / Basaltic Andesite	-17.0250	-70.3580
7062	Yucamane		1902	Nazca	South America	>25 km	Stratovolcano(es)	Andesite / Basaltic Andesite	-17.1800	-70.2000
7063	Francisco-Chajina			Nazca	South America	>25 km	Lava dome(s)		-17.2404	-70.0542
7064	Purupuruni			Nazca	South America	>25 km	Lava dome(s)		-17.2747	-69.8892
7065	Casiri, Nevados			Nazca	South America	>25 km	Stratovolcano(es)	Trachyte / Trachyandesite	-17.4700	-69.8130
Philippines										
13004	Cagua		1860	Sunda	Philippine Sea	>25 km	Stratovolcano	Andesite / Basaltic Andesite	18.2220	122.1230
13005	Ambalatangan Group		1952	Sunda	Philippine Sea	>25 km	Compound	Dacite	17.3200	121.1000
13006	Patoc			Sunda	Philippine Sea	>25 km	Stratovolcano	Andesite / Basaltic Andesite	17.1470	120.9800
13007	Santo Tomas			Sunda	Philippine Sea	>25 km	Stratovolcano	Andesite / Basaltic Andesite	16.3300	120.5500
13008	Arayat			Sunda	Philippine Sea	>25 km	Stratovolcano	Basalt / Picro-Basalt	15.2000	120.7420
13009	Pinatubo		1993	Sunda	Philippine Sea	>25 km	Stratovolcano	Dacite	15.1300	120.3500
13010	Natib			Sunda	Philippine Sea	>25 km	Stratovolcano	Andesite / Basaltic Andesite	14.7200	120.4000
13011	Mariveles		-2050	Sunda	Philippine Sea	>25 km	Stratovolcano	Andesite / Basaltic Andesite	14.5200	120.4700
13012	Laguna Caldera			Sunda	Philippine Sea	>25 km	Caldera	Andesite / Basaltic Andesite	14.4200	121.2700
13013	San Pablo Volcanic Field - Makiling		1350	Sunda	Philippine Sea	>25 km	Stratovolcano	Trachyandesite / Basaltic trachy	14.1312	121.1907
13014	Banahaw		1909	Sunda	Philippine Sea	>25 km	Complex	Andesite / Basaltic Andesite	14.0700	121.4800
13015	Labo			Philippine Sea	Sunda	>25 km	Compound		14.0200	122.7920
13016	Taal		1977	Sunda	Philippine Sea	>25 km	Caldera	Andesite / Basaltic Andesite	14.0020	120.9930
13017	Panay			Sunda	Philippine Sea	>25 km	Stratovolcano		13.7230	120.8930
13018	Isarog			Philippine Sea	Sunda	>25 km	Stratovolcano	Andesite / Basaltic Andesite	13.6580	123.3800
13019	Iriga			Philippine Sea	Sunda	>25 km	Stratovolcano	Andesite / Basaltic Andesite	13.4570	123.4570

VC_Num	Volcano Name	Linked_Centers	Most Recent		Crustal Thickness	Primary Volcano Type	Dominant Rock Type	Latitude	Longitude
			Eruption	Under_Plate					
13020	Malinao			Philippine Sea	Sunda	>25 km	Stratovolcano		13.4160 123.6080
13021	Masaraga			Philippine Sea	Sunda	>25 km	Stratovolcano	Andesite / Basaltic Andesite	13.3200 123.6000
13022	Mayon		2014	Philippine Sea	Sunda	>25 km	Stratovolcano	Andesite / Basaltic Andesite	13.2570 123.6850
13023	Malindig			Sunda	Philippine Sea	>25 km	Stratovolcano	Andesite / Basaltic Andesite	13.2400 122.0180
13024	Pocdol Mountains			Philippine Sea	Sunda	>25 km	Compound	Andesite / Basaltic Andesite	13.0500 123.9580
13025	Bulusan		2010	Philippine Sea	Sunda	>25 km	Stratovolcano(es)	Andesite / Basaltic Andesite	12.7700 124.0500
13026	Biliran		1939	Philippine Sea	Sunda	>25 km	Compound	Andesite / Basaltic Andesite	11.5230 124.5350
13027	Mahagnaos		1895	Philippine Sea	Sunda	>25 km	Stratovolcano	Andesite / Basaltic Andesite	10.8960 124.8700
13045	Silay			Philippine Sea	Sunda	>25 km	Stratovolcano	Andesite / Basaltic Andesite	10.7672 123.2196
13028	Mandalagan			Philippine Sea	Sunda	>25 km	Complex	Andesite / Basaltic Andesite	10.6500 123.2500
13029	Kanlaon		2006	Philippine Sea	Sunda	>25 km	Stratovolcano	Andesite / Basaltic Andesite	10.4120 123.1320
13030	Cabalán		1820	Philippine Sea	Sunda	>25 km	Stratovolcano	Andesite / Basaltic Andesite	10.2870 125.2210
13031	Paco			Philippine Sea	Sunda	>25 km	Stratovolcano	Andesite / Basaltic Andesite	9.5930 125.5200
13032	Cuernos de Negros			Philippine Sea	Sunda	>25 km	Complex	Andesite / Basaltic Andesite	9.2500 123.1700
13033	Camiguin		1948	Philippine Sea	Sunda	>25 km	Stratovolcano(es)	Andesite / Basaltic Andesite	9.2030 124.6730
13034	Balatukan			Philippine Sea	Sunda	>25 km	Compound	Basalt / Picro-Basalt	8.7700 124.9800
13035	Malindang			Philippine Sea	Sunda	>25 km	Stratovolcano	Basalt / Picro-Basalt	8.2200 123.6300
13036	Kalatungan			Philippine Sea	Sunda	>25 km	Stratovolcano	Basalt / Picro-Basalt	7.9500 124.8000
13037	Musuan		1886	Philippine Sea	Sunda	>25 km	Lava dome	Andesite / Basaltic Andesite	7.8770 125.0680
13038	Ragang	Latukan, Makaturing	1916	Philippine Sea	Sunda	>25 km	Stratovolcano	Basalt / Picro-Basalt	7.6878 124.5072
13039	Leonard Range		120	Philippine Sea	Sunda	>25 km	Stratovolcano	Andesite / Basaltic Andesite	7.3947 126.0636
13040	Apo			Philippine Sea	Sunda	>25 km	Stratovolcano	Andesite / Basaltic Andesite	6.9890 125.2690
13041	Matutum		1911	Philippine Sea	Sunda	>25 km	Stratovolcano	Andesite / Basaltic Andesite	6.3700 125.0700
13042	Parker		1640	Philippine Sea	Sunda	>25 km	Stratovolcano	Andesite / Basaltic Andesite	6.1130 124.8920
13044	Balut			Philippine Sea	Sunda	>25 km	Stratovolcano	Andesite / Basaltic Andesite	5.4000 125.3750
13001	Iraya		1454	Sunda	Philippine Sea	Unknown	Stratovolcano	Andesite / Basaltic Andesite	20.4690 122.0100
13002	Babuyan Claro		1924	Sunda	Philippine Sea	Unknown	Stratovolcano(es)	Andesite / Basaltic Andesite	19.5230 121.9400
13003	Camiguin de Babuyan		1857	Sunda	Philippine Sea	Unknown	Stratovolcano	Andesite / Basaltic Andesite	18.8300 121.8600
13043	Jolo		1897	Celebes Sea?	Sunda?	Unknown	Pyroclastic cone(s)	Basalt / Picro-Basalt	6.0130 121.0570
Russia									
9014	Sheveluch		1999	Pacific	Okhotsk	>25 km	Stratovolcano	Andesite / Basaltic Andesite	56.6530 161.3600
9015	Ushkovsky		1890	Pacific	Okhotsk	>25 km	Compound	Basalt / Picro-Basalt	56.1130 160.5090
9016	Kamen	Klyuchevskoy,Bezmianny		Pacific	Okhotsk	>25 km	Stratovolcano	Basalt / Picro-Basalt	56.0200 160.5930
9017	Zimina			Pacific	Okhotsk	>25 km	Stratovolcano(es)	Andesite / Basaltic Andesite	55.8620 160.6030
9018	Tolbachik		2012	Pacific	Okhotsk	>25 km	Shield	Basalt / Picro-Basalt	55.8320 160.3260
9019	Udina			Pacific	Okhotsk	>25 km	Stratovolcano(es)	Andesite / Basaltic Andesite	55.7550 160.5270
9020	Kizimen		2010	Pacific	Okhotsk	>25 km	Stratovolcano	Andesite / Basaltic Andesite	55.1310 160.3200
9021	Komarov	Schmidt, Gamchen, Vysok	950	Pacific	Okhotsk	>25 km	Stratovolcano	Basalt / Picro-Basalt	55.0324 160.7258
9022	Kronotsky		1923	Pacific	Okhotsk	>25 km	Stratovolcano	Basalt / Picro-Basalt	54.7530 160.5330
9023	Krashenninikov		1550	Pacific	Okhotsk	>25 km	Caldera	Basalt / Picro-Basalt	54.5960 160.2700
9024	Taunshits		-550	Pacific	Okhotsk	>25 km	Stratovolcano	Andesite / Basaltic Andesite	54.5280 159.8040
9025	Uzon		200	Pacific	Okhotsk	>25 km	Caldera(s)	Andesite / Basaltic Andesite	54.5000 159.9700
9026	Kikhpinych		1550	Pacific	Okhotsk	>25 km	Stratovolcano(es)	Basalt / Picro-Basalt	54.4890 160.2510
9027	Bolshoi Semiachik		-4450	Pacific	Okhotsk	>25 km	Stratovolcano(es)	Basalt / Picro-Basalt	54.3200 160.0200
9028	Maly Semyachik		1952	Pacific	Okhotsk	>25 km	Caldera	Basalt / Picro-Basalt	54.1350 159.6740
9029	Akademia Nauk	Karymsky	1996	Pacific	Okhotsk	>25 km	Stratovolcano(es)	Andesite / Basaltic Andesite	53.9800 159.4500
9030	Bakening		-550	Pacific	Okhotsk	>25 km	Stratovolcano	Andesite / Basaltic Andesite	53.9050 158.0700
9031	Zhupanovsky	Dzensursky	2014	Pacific	Okhotsk	>25 km	Compound	Andesite / Basaltic Andesite	53.5890 159.1500
9032	Koryaksky		2008	Pacific	Okhotsk	>25 km	Stratovolcano	Andesite / Basaltic Andesite	53.3210 158.7120
9033	Avachinsky		2001	Pacific	Okhotsk	>25 km	Stratovolcano	Andesite / Basaltic Andesite	53.2560 158.8360
9034	Unnamed			Pacific	Okhotsk	>25 km	Shield(s)	Basalt / Picro-Basalt	52.9200 158.5200
9035	Bolshe-Bannaya			Pacific	Okhotsk	>25 km	Lava dome(s)	Basalt / Picro-Basalt	52.9000 157.7800
9036	Barkhatnaya Sopka	300086		Pacific	Okhotsk	>25 km	Lava dome(s)	Basalt / Picro-Basalt	52.8230 158.2700
9037	Vilyuchik		-8050	Pacific	Okhotsk	>25 km	Stratovolcano	Andesite / Basaltic Andesite	52.7000 158.2800
9038	Tolmachev Dol		300	Pacific	Okhotsk	>25 km	Pyroclastic cone(s)	Basalt / Picro-Basalt	52.6300 157.5800
9039	Gorely		2010	Pacific	Okhotsk	>25 km	Caldera	Basalt / Picro-Basalt	52.5590 158.0300
9040	Opala		1894	Pacific	Okhotsk	>25 km	Caldera	Basalt / Picro-Basalt	52.5430 157.3390
9041	Mutnovsky		2000	Pacific	Okhotsk	>25 km	Complex	Basalt / Picro-Basalt	52.4490 158.1960
9042	Visokiy			Pacific	Okhotsk	>25 km	Stratovolcano	Basalt / Picro-Basalt	52.4300 157.9300
9043	Asacha			Pacific	Okhotsk	>25 km	Complex	Basalt / Picro-Basalt	52.3550 157.8270

VC_Num	Volcano Name	Linked_Centers	Most Recent		Crustal Thickness	Primary Volcano Type	Dominant Rock Type	Latitude	Longitude	
			Eruption	Under_Plate						Over_Plate
9044	Otdelniy			Pacific	Okhotsk	>25 km	Shield(s)	Basalt / Picro-Basalt	52.2200	157.4280
9045	Ostanets			Pacific	Okhotsk	>25 km	Shield(s)	Basalt / Picro-Basalt	52.1460	157.3220
9046	Piratkovsky			Pacific	Okhotsk	>25 km	Stratovolcano	No Data (checked)	52.1130	157.8490
9047	Khodutka		-300	Pacific	Okhotsk	>25 km	Stratovolcano(es)	Andesite / Basaltic Andesite	52.0620	157.7110
9048	Olkoviy Volcanic Group			Pacific	Okhotsk	>25 km	Volcanic field	Basalt / Picro-Basalt	52.0200	157.5300
9049	Ozernoy			Pacific	Okhotsk	>25 km	Shield	Basalt / Picro-Basalt	51.8800	157.3800
9050	Ksudach		1907	Pacific	Okhotsk	>25 km	Stratovolcano	Andesite / Basaltic Andesite	51.8440	157.5720
9051	Belenkaya			Pacific	Okhotsk	>25 km	Stratovolcano	Basalt / Picro-Basalt	51.7500	157.2700
9052	Kell			Pacific	Okhotsk	>25 km	Stratovolcano(es)	Basalt / Picro-Basalt	51.6500	157.3500
9053	Zhel'tovsky		1972	Pacific	Okhotsk	>25 km	Stratovolcano	Basalt / Picro-Basalt	51.5770	157.3280
9054	Yavinsky		-4050	Pacific	Okhotsk	>25 km	Stratovolcano	Basalt / Picro-Basalt	51.5700	156.6000
9055	Iliinsky		1901	Pacific	Okhotsk	>25 km	Stratovolcano	Andesite / Basaltic Andesite	51.4980	157.2030
9056	Diky Greben		350	Pacific	Okhotsk	>25 km	Lava dome(s)	Dacite	51.4520	156.9780
9057	Kurile Lake		-6440	Pacific	Okhotsk	>25 km	Caldera	Dacite	51.4500	157.1200
9058	Koshelev		1741	Pacific	Okhotsk	>25 km	Stratovolcano	Basalt / Picro-Basalt	51.3560	156.7530
9059	Kambalny		1350	Pacific	Okhotsk	>25 km	Stratovolcano	Basalt / Picro-Basalt	51.3060	156.8750
9060	Mashkovtsev			Pacific	Okhotsk	>25 km	Stratovolcano	Basalt / Picro-Basalt	51.1000	156.7200
9061	Alaid		2012	Pacific	Okhotsk	>25 km	Stratovolcano	Basalt / Picro-Basalt	50.8610	155.5650
9062	Ebeko-Vernadskii Ridge	Vernadskii Ridge	2010	Pacific	Okhotsk	>25 km	Somma	Andesite / Basaltic Andesite	50.6860	156.0140
9063	Chikurachki		2008	Pacific	Okhotsk	>25 km	Stratovolcano(es)	Basalt / Picro-Basalt	50.3240	155.4610
9064	Fuss Peak		1933	Pacific	Okhotsk	>25 km	Stratovolcano	Andesite / Basaltic Andesite	50.2670	155.2460
9065	Karpinsky Group			Pacific	Okhotsk	>25 km	Cone(s)	Andesite / Basaltic Andesite	50.1480	155.3730
9066	Nemo Peak		1938	Pacific	Okhotsk	15-25 km	Caldera	Andesite / Basaltic Andesite	49.5700	154.8080
9067	Tao-Rusyr Caldera		1952	Pacific	Okhotsk	15-25 km	Stratovolcano	Andesite / Basaltic Andesite	49.3500	154.7000
9068	Kharimkotan		1933	Pacific	Okhotsk	15-25 km	Stratovolcano	Andesite / Basaltic Andesite	49.1200	154.5080
9069	Ekarma		2010	Pacific	Okhotsk	15-25 km	Stratovolcano	Andesite / Basaltic Andesite	48.9580	153.9300
9070	Sinarka		1872	Pacific	Okhotsk	15-25 km	Stratovolcano	Andesite / Basaltic Andesite	48.8750	154.1750
9071	Kuntomintar		1872	Pacific	Okhotsk	15-25 km	Stratovolcano		48.7500	154.0200
9072	Sarychev Peak		2010	Pacific	Okhotsk	15-25 km	Stratovolcano	Andesite / Basaltic Andesite	48.0920	153.2000
9080	Kolokol Group		2009	Pacific	Okhotsk	15-25 km	Somma(es)	Andesite / Basaltic Andesite	46.0420	150.0500
9081	Tri Sestry			Pacific	Okhotsk	15-25 km	Stratovolcano	Andesite / Basaltic Andesite	45.9300	149.9200
9082	Rudakov			Pacific	Okhotsk	15-25 km	Stratovolcano	Andesite / Basaltic Andesite	45.8800	149.8300
9083	Ivao Group			Pacific	Okhotsk	15-25 km	Pyroclastic cone(s)	No Data (checked)	45.7700	149.6800
9073	Rasshua		1957	Pacific	Okhotsk	Oceanic < 15 km	Stratovolcano	Andesite / Basaltic Andesite	47.7700	153.0200
9074	Ketoi		2013	Pacific	Okhotsk	Oceanic < 15 km	Stratovolcano	Andesite / Basaltic Andesite	47.3500	152.4750
9075	Urataman			Pacific	Okhotsk	Oceanic < 15 km	Somma	Andesite / Basaltic Andesite	47.1200	152.2500
9076	Prevo Peak		1825	Pacific	Okhotsk	Oceanic < 15 km	Stratovolcano	Basalt / Picro-Basalt	47.0200	152.1200
9077	Zavaritzki Caldera		1957	Pacific	Okhotsk	Oceanic < 15 km	Caldera	Andesite / Basaltic Andesite	46.9250	151.9500
9078	Goriaschaia Sopka	Milne	1944	Pacific	Okhotsk	Oceanic < 15 km	Stratovolcano	Andesite / Basaltic Andesite	46.8300	151.7500
9079	Chirpoi		2012	Pacific	Okhotsk	Oceanic < 15 km	Caldera	Andesite / Basaltic Andesite	46.5250	150.8750
Saint Kitts and Nevis										
5009	Liamuiga		1843	North America	Caribbean	Oceanic < 15 km	Stratovolcano	Andesite / Basaltic Andesite	17.3700	-62.8000
5010	Nevis Peak			North America	Caribbean	Oceanic < 15 km	Stratovolcano	Andesite / Basaltic Andesite	17.1500	-62.5800
Saint Lucia										
5011	Qualibou		1766	South America	Caribbean	Oceanic < 15 km	Caldera	Andesite / Basaltic Andesite	13.8300	-61.0500
Saint Vincent and the Grenadines										
5012	Soufrière St. Vincent		1979	South America	Caribbean	Oceanic < 15 km	Stratovolcano	Andesite / Basaltic Andesite	13.3300	-61.1800
Solomon Islands										
16023	Nonda			Woodlark	Solomon Islands	Unknown	Stratovolcano		-7.6700	156.6000
16024	Savo		1865	Australia	Pacific	Unknown	Stratovolcano	Andesite / Basaltic Andesite	-9.1300	159.8200
16025	Gallego			Australia	Pacific	Unknown	Volcanic field	Andesite / Basaltic Andesite	-9.3500	159.7300
Taiwan										
12013	Kueishantao		1785	Philippine Sea	Yangtze	>25 km	Stratovolcano	Andesite / Basaltic Andesite	24.8500	121.9200
Tonga										
18002	Niuafu'ou		1985	Pacific	Tonga	Oceanic < 15 km	Shield	Basalt / Picro-Basalt	-15.6000	-175.6300
18003	Tofua	Kao	2004	Pacific	Tonga	Oceanic < 15 km	Caldera	Andesite / Basaltic Andesite	-19.7500	-175.0700
United Kingdom										
5013	Soufrière Hills		2005	North America	Caribbean	Oceanic < 15 km	Stratovolcano	Andesite / Basaltic Andesite	16.7200	-62.1800
United States										
1001	Spurr		1992	Pacific	North America	>25 km	Stratovolcano	Andesite / Basaltic Andesite	61.2992	-152.2514

VC_Num	Volcano Name	Linked_Centers	Most Recent		Under_Plate	Over_Plate	Crustal Thickness	Primary Volcano Type	Dominant Rock Type	Latitude	Longitude
			Eruption								
1002	Hayes		1200		Pacific	North America	>25 km	Stratovolcano	Dacite	61.6400	-152.4111
1003	Redoubt		2009		Pacific	North America	>25 km	Stratovolcano	Andesite / Basaltic Andesite	60.4851	-152.7423
1004	Iliamna		1953		Pacific	North America	>25 km	Stratovolcano	Andesite / Basaltic Andesite	60.0321	-153.0902
1005	Augustine		2005		Pacific	North America	>25 km	Lava dome(s)	Andesite / Basaltic Andesite	59.3632	-153.4304
1006	Fourpeaked	Douglas	2006		Pacific	North America	>25 km	Stratovolcano	Andesite / Basaltic Andesite	58.7701	-153.6722
1007	Kaguyak		-3850		Pacific	North America	>25 km	Lava dome(s)	Dacite	58.6085	-154.0288
1008	Kukak	Denison, Steller			Pacific	North America	>25 km	Stratovolcano	Andesite / Basaltic Andesite	58.4531	-154.3552
1009	Snowy Mountain		1710		Pacific	North America	>25 km	Stratovolcano(es)	Andesite / Basaltic Andesite	58.3365	-154.6827
1010	Katmai	Trident, Novarupta	1912		Pacific	North America	>25 km	Stratovolcano	Andesite / Basaltic Andesite	58.2811	-154.9644
1011	Griggs		-1790		Pacific	North America	>25 km	Stratovolcano	Andesite / Basaltic Andesite	58.3547	-155.0928
1012	Mageik	Martin	1953		Pacific	North America	>25 km	Stratovolcano	Andesite / Basaltic Andesite	58.1951	-155.2532
1013	Unnamed				Pacific	North America	>25 km	Lava dome	No Data (checked)	57.8700	-155.4132
1014	Ugashik-Peulik		1852		Pacific	North America	>25 km	Stratovolcano	Andesite / Basaltic Andesite	57.7512	-156.3687
1015	Chiginagak		1998		Pacific	Bering Sea	>25 km	Stratovolcano	Andesite / Basaltic Andesite	57.1350	-156.9899
1016	Yantarni		-800		Pacific	Bering Sea	>25 km	Stratovolcano	Andesite / Basaltic Andesite	57.0178	-157.1861
1017	Aniakchak		1942		Pacific	Bering Sea	>25 km	Caldera	Andesite / Basaltic Andesite	56.8796	-158.1706
1018	Black Peak		-1900		Pacific	Bering Sea	>25 km	Stratovolcano	Andesite / Basaltic Andesite	56.5523	-158.7852
1019	Veniaminof		2013		Pacific	Bering Sea	>25 km	Stratovolcano	Andesite / Basaltic Andesite	56.1702	-159.3800
1020	Stepovak Bay 4	Stepovak Bay 2,3, Kupreai	1987		Pacific	Bering Sea	>25 km	Stratovolcano	No Data (checked)	55.9548	-159.9547
1021	Dana		-1890		Pacific	Bering Sea	>25 km	Stratovolcano	Andesite / Basaltic Andesite	55.6412	-161.2140
1022	Pavlof	Pavlof Sister	2014		Pacific	Bering Sea	>25 km	Stratovolcano	Andesite / Basaltic Andesite	55.4172	-161.8940
1023	Emmons Lake				Pacific	Bering Sea	>25 km	Caldera	Andesite / Basaltic Andesite	55.3417	-162.0792
1024	Dutton				Pacific	Bering Sea	>25 km	Stratovolcano	Andesite / Basaltic Andesite	55.1841	-162.2766
1025	Frosty				Pacific	Bering Sea	>25 km	Stratovolcano(es)	Andesite / Basaltic Andesite	55.0825	-162.8141
1026	Roundtop	Isanotski	1845		Pacific	Bering Sea	>25 km	Stratovolcano	Rhyolite	54.8012	-163.5893
1027	Shishaldin		2014		Pacific	Bering Sea	>25 km	Stratovolcano	Basalt / Picro-Basalt	54.7568	-163.9705
1028	Fisher		1830		Pacific	Bering Sea	>25 km	Stratovolcano	Andesite / Basaltic Andesite	54.6515	-164.4304
1029	Westdahl		1991		Pacific	Bering Sea	>25 km	Stratovolcano?	Basalt / Picro-Basalt	54.5191	-164.6503
1044	Korovin	Atka	2006		Pacific	Bering Sea	>25 km	Stratovolcano(es)	Basalt / Picro-Basalt	52.3817	-174.1549
2005	Baker		1884		Juan de Fuca	North America	>25 km	Stratovolcano(es)	Andesite / Basaltic Andesite	48.7781	-121.8155
2006	Glacier Peak		1700		Juan de Fuca	North America	>25 km	Stratovolcano	Dacite	48.1121	-121.1130
2007	Rainier		1894		Juan de Fuca	North America	>25 km	Stratovolcano	Andesite / Basaltic Andesite	46.8534	-121.7627
2008	Adams		950		Juan de Fuca	North America	>25 km	Stratovolcano	Andesite / Basaltic Andesite	46.2062	-121.4901
2009	St. Helens		2004		Juan de Fuca	North America	>25 km	Stratovolcano	Dacite	46.1958	-122.1899
2010	Indian Heaven/Lemei Rock		-6250		Juan de Fuca	North America	>25 km	Shield(s)	Basalt / Picro-Basalt	46.0185	-121.7598
2011	West Crater	Bare Mtn, Trout Ck Hill	-5750		Juan de Fuca	North America	>25 km	Volcanic field	Andesite / Basaltic Andesite	45.8802	-122.0800
2012	Hood		1907		Juan de Fuca	North America	>25 km	Stratovolcano	Andesite / Basaltic Andesite	45.3740	-121.6950
2013	Jefferson		950		Juan de Fuca	North America	>25 km	Stratovolcano	Andesite / Basaltic Andesite	44.6741	-121.8001
2014	Belknap	Mt. Washington	480		Juan de Fuca	North America	>25 km	Shield(s)	Andesite / Basaltic Andesite	44.2857	-121.8415
		North & Middle Sisters,									
		Broken Top			Juan de Fuca	North America	>25 km	Stratovolcano	Basalt / Basaltic Andesite	44.1024	-121.7707
2016	Bachelor	Tumalo	-5800		Juan de Fuca	North America	>25 km	Stratovolcano	Andesite / Basaltic Andesite	43.9791	-121.6877
2017	Newberry		690		Juan de Fuca	North America	>25 km	Shield	Andesite / Basaltic Andesite	43.7221	-121.2290
2018	Davis Lake		-2790		Juan de Fuca	North America	>25 km	Volcanic field	Andesite / Basaltic Andesite	43.5601	-121.8120
2019	Crater Lake		-2850		Juan de Fuca	North America	>25 km	Caldera	Dacite	42.9297	-122.1207
2020	McLoughlin				Juan de Fuca	North America	>25 km	Stratovolcano	Basaltic Andesite	42.4446	-122.3152
2021	Medicine Lake		1910		Juan de Fuca	North America	>25 km	Shield	Basalt / Picro-Basalt	41.6112	-121.5533
2022	Shasta		1786		Juan de Fuca	North America	>25 km	Stratovolcano	Andesite / Basaltic Andesite	41.4102	-122.1952
2023	Burney Mtn				Juan de Fuca	North America	>25 km			40.8092	-121.6284
2024	Harvey Mtn	Ashhurst Mtn			Juan de Fuca	North America	>25 km	Shield		40.7412	-121.0354
2025	Magee Peak				Juan de Fuca	North America	>25 km		Basaltic Andesite	40.6929	-121.6169
2026	Crater Mtn	Bogard Buttes			Juan de Fuca	North America	>25 km	Shield		40.6266	-121.0415
2027	Antelope Mtn	Logan Mtn			Juan de Fuca	North America	>25 km	Shield		40.5923	-120.9105
2028	Prospect Peak	West Prospect Pk			Juan de Fuca	North America	>25 km	Shield	Andesite / Basaltic Andesite	40.5724	-121.3453
2029	Red Cinder Chain				Juan de Fuca	North America	>25 km		Basalt / Basaltic Andesite / Ande	40.4960	-121.2472
2030	Lassen Volcanic Center		1914		Juan de Fuca	North America	>25 km	Stratovolcano	Andesite / Basaltic Andesite	40.4896	-121.5091
11007	Agrigan		1917		Pacific	Mariana	Unknown	Stratovolcano	Basalt / Picro-Basalt	18.7700	145.6700
11008	Pagan		2012		Pacific	Mariana	Unknown	Stratovolcano(es)	Basalt / Picro-Basalt	18.1300	145.8000
11009	Anatahan		2007		Pacific	Mariana	Unknown	Stratovolcano	Andesite / Basaltic Andesite	16.3500	145.6700
1031	Akutan		1992		Pacific	Bering Sea	15-25 km	Stratovolcano	Basalt / Picro-Basalt	54.1341	-165.9862

VC_Num	Volcano Name	Linked_Centers	Most Recent		Under_Plate	Over_Plate	Crustal Thickness	Primary Volcano Type	Dominant Rock Type	Latitude	Longitude
			Eruption								
1033	Makushin		1995		Pacific	Bering Sea	15-25 km	Stratovolcano	Andesite / Basaltic Andesite	53.8913	-166.9232
1034	Okmok		2008		Pacific	Bering Sea	15-25 km	Shield	Basalt / Picro-Basalt	53.4305	-168.1305
1035	Recheshnoi	Vsevidof	1957		Pacific	Bering Sea	15-25 km	Stratovolcano	Andesite / Basaltic Andesite	53.1547	-168.5380
1036	Kagamil	Uliaga	1929		Pacific	Bering Sea	15-25 km	Stratovolcano	No Data (checked)	52.9723	-169.7221
1037	Tana				Pacific	Bering Sea	15-25 km	Stratovolcano(es)	Rhyolite	52.8303	-169.7701
1038	Cleveland		2013		Pacific	Bering Sea	15-25 km	Stratovolcano	Andesite / Basaltic Andesite	52.8224	-169.9469
1039	Carlisle		1987		Pacific	Bering Sea	15-25 km	Stratovolcano	Andesite / Basaltic Andesite	52.8915	-170.0584
1040	Herbert				Pacific	Bering Sea	15-25 km	Stratovolcano	Andesite / Basaltic Andesite	52.7420	-170.1110
1041	Yunaska		1937		Pacific	Bering Sea	15-25 km	Shield	Andesite / Basaltic Andesite	52.6431	-170.6291
1042	Amukta	Chagulak	1997		Pacific	Bering Sea	15-25 km	Stratovolcano	Andesite / Basaltic Andesite	52.5002	-171.2521
1043	Seguam		1993		Pacific	Bering Sea	15-25 km	Stratovolcano(es)	Andesite / Basaltic Andesite	52.3152	-172.5102
1045	Great Sitkin		1987		Pacific	Bering Sea	15-25 km	Stratovolcano	Andesite / Basaltic Andesite	52.0765	-176.1300
1046	Adagdak				Pacific	Bering Sea	15-25 km	Stratovolcano		51.9897	-176.5860
1047	Moffett		-1600		Pacific	Bering Sea	15-25 km	Stratovolcano	Andesite / Basaltic Andesite	51.9369	-176.7417
1048	Kanaga		2012		Pacific	Bering Sea	15-25 km	Stratovolcano	Andesite / Basaltic Andesite	51.9241	-177.1647
1049	Tanaga	Takawangha	1914		Pacific	Bering Sea	15-25 km	Stratovolcano(es)	Basalt / Picro-Basalt	51.8841	-178.1428
1050	Gareloi		1996		Pacific	Bering Sea	15-25 km	Stratovolcano	Basalt / Picro-Basalt	51.7906	-178.7942
1051	Semisopchnoi		1987		Pacific	Bering Sea	15-25 km	Stratovolcano	Basalt / Picro-Basalt	51.9300	179.5798
1052	Little Sitkin		1828		Pacific	Bering Sea	15-25 km	Stratovolcano	Andesite / Basaltic Andesite	51.9501	178.5429
1053	Segula				Pacific	Bering Sea	15-25 km	Stratovolcano	Andesite / Basaltic Andesite	52.0155	178.1364
1054	Kiska		1990		Pacific	Bering Sea	15-25 km	Stratovolcano	Andesite / Basaltic Andesite	52.1030	177.6019
2031	Goat Rocks				Juan de Fuca	North America		Complex		46.4907	-121.4218
2032	Lakeview Mountain				Juan de Fuca	North America		Shield		46.3867	-121.4053
2034	Olallie Butte				Juan de Fuca	North America		Shield		44.8166	-121.7665
2035	Three-fingered Jack				Juan de Fuca	North America		Stratovolcano		44.4760	-121.8446
2036	Maiden Peak				Juan de Fuca	North America		Shield		43.6238	-121.9672
2037	Diamond Peak				Juan de Fuca	North America		Shield		43.5167	-122.1499
2038	Mt. Theilson	Howlock Mtn			Juan de Fuca	North America		Shield		43.1483	-122.0679
2039	Mt. Bailey				Juan de Fuca	North America		Shield		43.1497	-122.2216
2040	Yamsay Mountain				Juan de Fuca	North America		Shield		42.9256	-121.3639
2041	Sugarloaf				Juan de Fuca	North America		Stratocone		40.6939	-121.4600
Vanuatu											
17004	Motlav				Australia	Pacific	15-25 km	Stratovolcano	Basalt / Picro-Basalt	-13.6700	167.6700
17005	Suretatai		1965		Australia	Pacific	15-25 km	Complex	Andesite / Basaltic Andesite	-13.8000	167.4700
17006	Gaua		2011		Australia	Pacific	15-25 km	Stratovolcano	Andesite / Basaltic Andesite	-14.2700	167.5000
17007	Aoba		2011		Australia	Pacific	15-25 km	Shield	Basalt / Picro-Basalt	-15.4000	167.8300
17008	Ambrym		2008		Australia	Pacific	15-25 km	Pyroclastic shield	Basalt / Picro-Basalt	-16.2500	168.1200
17009	Lopevi		2008		Australia	Pacific	15-25 km	Stratovolcano	Basalt / Picro-Basalt	-16.5070	168.3460
17010	North Vate				Australia	Pacific	15-25 km	Stratovolcano(es)	Basalt / Picro-Basalt	-17.4700	168.3530
17011	Traitor's Head		1959		Australia	Pacific	15-25 km	Stratovolcano	Basalt / Picro-Basalt	-18.7500	169.2300
17012	Yasur		1774		Australia	Pacific	15-25 km	Stratovolcano	Andesite / Basaltic Andesite	-19.5300	169.4420
17013	Aneityum				Australia	Pacific	15-25 km	Stratovolcano(es)	Basalt / Picro-Basalt	-20.2000	169.7800

APPENDIX III

Listing of international VC with power plants that are used as the training set (benchmarks) in this work (5 pages).

Volcano Name	Plant Name	Country	Commission	Installed	
			Year	MW	Res Temp (°C)
Meager	Meager	Canada	x	4.8	
Isluga	Puchildiza	Chile	x	10.0	190
Azufre-Pabellon	Pabellon (Apacheta)	Chile	x	20.0	240
La Torta-Cerros Tocorpuri	El Tatio	Chile	x	25.0	
La Torta-Cerros Tocorpuri	Laguna Colorada	Chile	x	30.0	250
Chillán, Nevados de	Chillan	Chile	x	5.0	190
Tolguaca	Tolhuaca	Chile	x	12.0	
Copahue	Copehue	Chile-Argentina	1988	0.7	
Rincon de la Vieja	Las Pailas	Costa Rica	2011	42.0	
Miravalles	Miravalles	Costa Rica	1994	165.5	235
Watt, Morne	Roseau Valley	Dominica	x	11.0	
Apaneca Range	Ahuachapan	El Salvador	1975	95.0	250
Tecapa-El Tigre	Berlin	El Salvador	1999	109.4	290
Soufriere Guadeloupe	La Bouillante	France	1986	15.0	250
Santa Maria	Orzunil	Guatemala	1999	28.0	290
Ixtepeque	Cerro Blanco	Guatemala	x	5.0	
Pacaya	Amatitlan	Guatemala	2007	24.0	285
Tondano Caldera	Lahendong	Indonesia	2002	62.5	300
Sibayak	Sibayak	Indonesia	1996	13.2	
Sibualbuali	Namora-i-Langgit	Indonesia	x	105.0	
Sibualbuali	Sibualbuali	Indonesia	x	9.0	
Sibualbuali	Silangkitang	Indonesia	x	65.0	
Kerinci	Muara Laboh	Indonesia	x	110.0	
Kunyit	Lempur Kerinci	Indonesia	x	10.0	
Lumut Balai, Bukit	Lumut Balai	Indonesia	x	55.0	230
Patah	Rantau Dedap	Indonesia	x	110.0	
Hulubelu	Ulubelu	Indonesia	2012	110.0	250
Salak	Salak (Awibengkok)	Indonesia	1994	377.0	260
Guntur	Kamojang	Indonesia	1983	200.0	245
Patuha	Patuha-Cibuni	Indonesia	x	60.0	
Wayang-Windu	Wayang Windu	Indonesia	2000	227.0	260
Dieng Volcanic Complex	Dieng	Indonesia	1998	60.0	270
Galunggung-Talagabodas	Karaja-Telaga Bodas	Indonesia	x	13.0	
Papandayan-Kendang	Darajat	Indonesia	1994	260.0	245
Poco Leok	Ulumbu	Indonesia	2014	5.0	
Inierie	Mataloko	Indonesia	2013	2.5	
Larderello	Larderello	Italy	1913	795.0	235
Amiata	Amiata Piancastagnaio	Italy	1969	60.0	328
Amiata	Bagnore	Italy	1998	60.0	317
Nigorikawa	Mori	Japan	1982	25.0	235
Hachimantai	Sumikawa-Ohnuma	Japan	1974	59.5	250
Iwatesan	Matsukawa	Japan	1966	23.5	255
Akita-Komagatake	Kakkonda	Japan	1978	80.0	275
Kurikomayama	Uenotai	Japan	1994	28.8	310
Onikobe	Onikobe	Japan	1975	12.5	250
Numazawa	Yanaizu-Nishiyama	Japan	1995	65.0	290

Volcano Name	Plant Name	Country	Commission	Installed	Res Temp (°C)
			Year	MW	
Hachijojima	Hachijojima	Japan	1999	3.3	275
Yufu-Tsurumi	Suginoi Hotel	Japan	1980	3.0	
Kujusan	Hatchobaru-Otake	Japan	1967	124.5	270
Kujusan	Takigami	Japan	1996	25.0	245
Kirishimayama	Ogiri	Japan	1996	30.0	230
Ibusuki Volcanic Field	Yamakawa (Fushime)	Japan	1995	30.0	320
Sashiusudake [Baransky]	Okeanskaya	Japan	2007	3.6	
Raususan [Mendeleev]	Mendeleevskaya	Japan	2007	1.8	
Ceboruco	Domo de San Pedro	Mexico	x	25.0	
Primavera, Sierra la	Cerritos Colorados	Mexico	x	10.0	
Azufres, Los	Los Azufres	Mexico	1982	195.0	275
Humeros, Los	Los Humeros	Mexico	1990	40.0	341
Rotorua	Rotorua	New Zealand	x	50.0	
Okataina	Kawerau	New Zealand	1966	122.2	280
Reporoa	Reporoa-Waiotapu	New Zealand	x	50.0	
Reporoa	Ohaaki-Broadlands	New Zealand	1989	103.0	275
Maroa	Wairakei-Tauhara	New Zealand	1958	364.0	250
Maroa	Rotokawa	New Zealand	1997	175.0	300
Maroa	Ngatamariki	New Zealand	2013	82.0	273
Maroa	Mokai	New Zealand	1999	111.0	295
Maroa	Orakeikorako	New Zealand	x	25.0	
Telica	San Jacinto-Tizate	Nicaragua	2005	72.0	275
Momotombo	Momotombo	Nicaragua	1983	77.5	220
Lihir	Lihir	Papua NG	2001	56.0	275
San Pablo Volcanic Field - Makilin ₁ Mak-Ban (Bulalo)		Philippines	1979	442.8	285
San Pablo Volcanic Field - Makilin ₁ Maribarara		Philippines	2014	20.0	
Malinao	Tiwi	Philippines	1979	330.0	280
Pocdol Mountains	Bacman (Bacon-Manito)	Philippines	1993	150.0	270
Mahagnao	Leyte	Philippines	1983	700.0	278
Kanlaon	NNGP (Mambucal)	Philippines	2007	49.0	
Cuernos de Negros	Palinpinon	Philippines	1993	232.5	300
Apo	Mindanao	Philippines	1995	106.0	280
Uzon	Dolina Geizerov	Russia	x	25.0	
Barkhatnaya Sopka	Paratunskaya	Russia	1967	0.7	
Mutnovsky	Mutnovskaya-Verkhne	Russia	1998	62.0	255
Diky Greben	Pauzhetskaya	Russia	1966	14.5	195
Kueishantao	Chingshui	Taiwan	1981	3.0	
Medicine Lake	Medicine Lake	United States	x	25.0	

APPENDIX IV

Known flank fumarole occurrences, with noted surface area of disturbance if available, for the Cascade, Aleutian and international benchmark VC (4 pages).

Volcano Name	Installed		Subregion	Fumarole Area (m ²)	Flank/Summit
	MW	Region			
Adagdak		Aleutians	Alaska		None
Akutan		Aleutians	Alaska	5,000	Flank
Amukta		Aleutians	Alaska		Unknown
Aniakchak		Aleutians	Alaska		Unknown
Augustine		Aleutians	Alaska		Summit
Black Peak		Aleutians	Alaska		None
Carlisle		Aleutians	Alaska		None
Chiginagak		Aleutians	Alaska		Summit
Cleveland		Aleutians	Alaska		Summit
Dana		Aleutians	Alaska		None
Douglas		Aleutians	Alaska		Summit
Dutton		Aleutians	Alaska		Unknown
Emmons Lake		Aleutians	Alaska		Unknown
Fisher		Aleutians	Alaska		Unknown
Fourpeaked		Aleutians	Alaska		Unknown
Frosty		Aleutians	Alaska		None
Gareloi		Aleutians	Alaska		Unknown
Gilbert		Aleutians	Alaska		Unknown
Great Sitkin		Aleutians	Alaska		Flank
Griggs		Aleutians	Alaska		Summit
Hayes		Aleutians	Alaska		None
Herbert		Aleutians	Alaska		Unknown
Iliamna		Aleutians	Alaska		Summit
Isanotski		Aleutians	Alaska		None
Kagamil		Aleutians	Alaska	75,744	Flank
Kaguyak		Aleutians	Alaska	5,832	Flank
Kanaga		Aleutians	Alaska		Summit
Katmai		Aleutians	Alaska		Flank
Kialagvik		Aleutians	Alaska		None
Kiska		Aleutians	Alaska		Unknown
Korovin		Aleutians	Alaska		Flank
Kukak		Aleutians	Alaska		Summit
Kupreanof		Aleutians	Alaska		Both
Little Sitkin		Aleutians	Alaska		Flank
Mageik		Aleutians	Alaska		Both
Makushin		Aleutians	Alaska		Flank
Martin		Aleutians	Alaska		Summit
Moffett		Aleutians	Alaska		None
Okmok		Aleutians	Alaska		Summit
Pavlof		Aleutians	Alaska		Summit
Pogromni		Aleutians	Alaska		Unknown
Recheschnoi		Aleutians	Alaska		Flank
Redoubt		Aleutians	Alaska		Summit
Roundtop		Aleutians	Alaska		None
Seguam		Aleutians	Alaska		Unknown

Volcano Name	Installed		Subregion	Fumarole Area (m ²)	Flank/Summit
	MW	Region			
Segula		Aleutians	Alaska		Unknown
Semisopochnoi		Aleutians	Alaska	2,068	Flank
Shishaldin		Aleutians	Alaska		Summit
Snowy Mountain		Aleutians	Alaska		Summit, transient
Spurr		Aleutians	Alaska		Summit
Stepovak Bay 4		Aleutians	Alaska		Unknown
Table Top		Aleutians	Alaska		None
Tana		Aleutians	Alaska		Unknown
Tanaga		Aleutians	Alaska		Unknown
Trident		Aleutians	Alaska		Summit
Ugashik-Peulik		Aleutians	Alaska		None
Unnamed		Aleutians	Alaska		None
Unnamed		Aleutians	Alaska		None
Veniaminof		Aleutians	Alaska		None
Vsididov		Aleutians	Alaska		Unknown
Westdahl		Aleutians	Alaska		Unknown
Yantarni		Aleutians	Alaska		None
Yunaska		Aleutians	Alaska		Unknown
Silverthron		Cascades	Canada		Unknown
Meager	4.8	Cascades	Canada	473	Flank
Cayley Volcanic Field		Cascades	Canada		Unknown
Garibaldi		Cascades	Canada		Unknown
Medicine Lake	25.0	Cascades	California		Flank
Shasta		Cascades	California		Summit
Burney Mtn		Cascades	California		Unknown
Harvey Mtn		Cascades	California		Unknown
Magee Peak		Cascades	California		Unknown
Crater Mtn		Cascades	California		Unknown
Antelope Mtn		Cascades	California		Unknown
Prospect Peak		Cascades	California		Unknown
Red Cinder Chain		Cascades	California		Unknown
Lassen Volcanic Center		Cascades	California	25,411	Flank
Sugarloaf		Cascades	California		Unknown
Hood		Cascades	Oregon		Summit
Jefferson		Cascades	Oregon		Unknown
Belknap		Cascades	Oregon		Unknown
South Sister		Cascades	Oregon		None
Bachelor		Cascades	Oregon		Summit
Newberry		Cascades	Oregon		Unknown
Davis Lake		Cascades	Oregon		Unknown
Crater Lake		Cascades	Oregon		None
McLoughlin		Cascades	Oregon		Unknown
Olallie Butte		Cascades	Oregon		Unknown
Three-fingered Jack		Cascades	Oregon		Unknown
Maiden Peak		Cascades	Oregon		Unknown

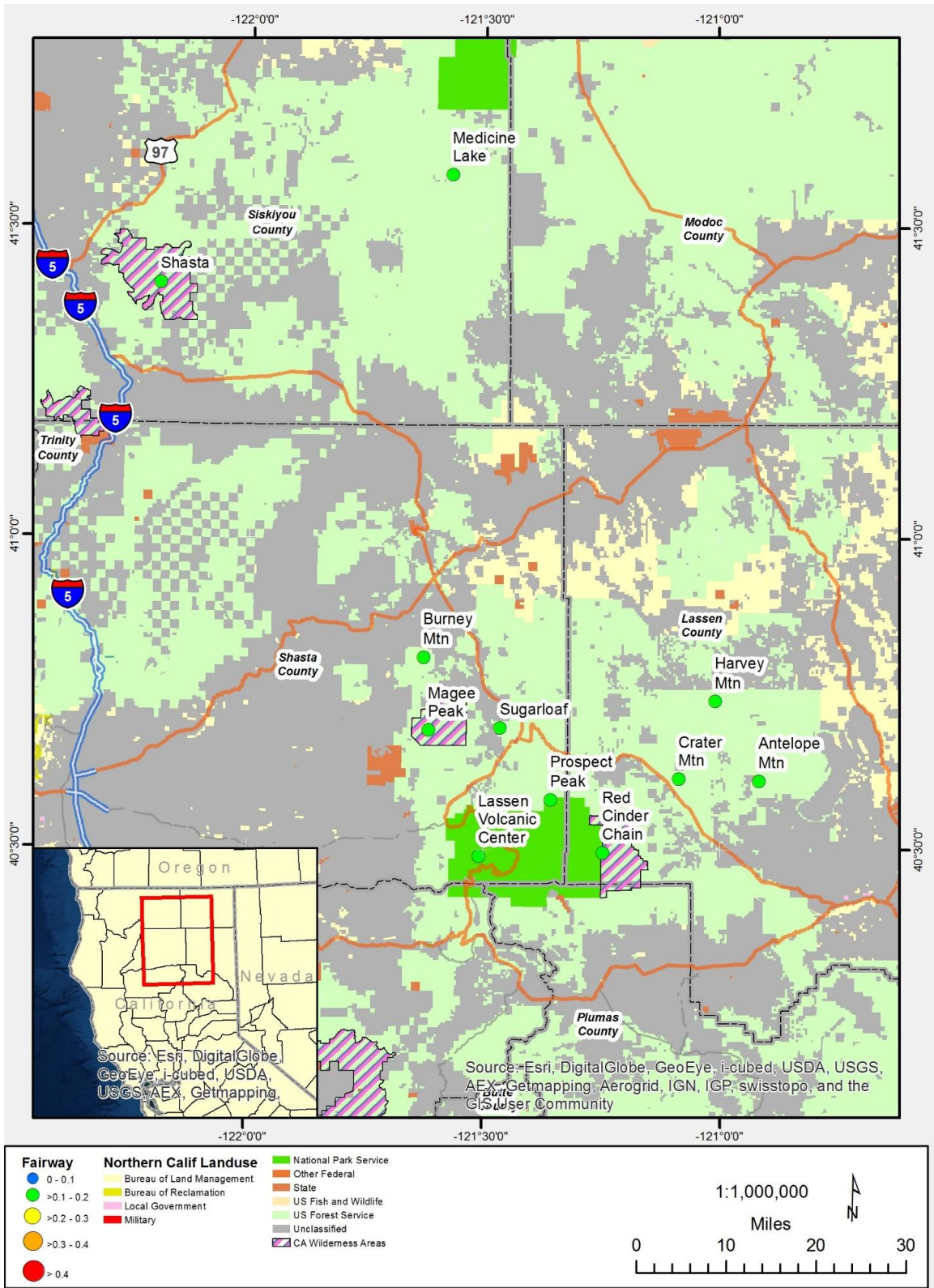
Volcano Name	Installed		Subregion	Fumarole Area (m ²)	Flank/Summit
	MW	Region			
Diamond Peak		Cascades	Oregon		Unknown
Mt. Theilson		Cascades	Oregon		Unknown
Mt. Bailey		Cascades	Oregon		Unknown
Yamsay Mountain		Cascades	Oregon		Unknown
Baker		Cascades	Washington		Summit
Glacier Peak		Cascades	Washington		None
Rainier		Cascades	Washington		Summit
Adams		Cascades	Washington		Unknown
St. Helens		Cascades	Washington		Summit
Indian Heaven/Lemei Rock		Cascades	Washington		Unknown
West Crater		Cascades	Washington		Unknown
Goat Rocks		Cascades	Washington		Unknown
Lakeview Mountain		Cascades	Washington		Unknown
Marble Mountain (just S. of MSH)		Cascades	Washington		Unknown
Rincon de la Vieja	42.0	Central America	Costa Rica	52,562	Flank
Miravalles	165.5	Central America	Costa Rica	4,618	Flank
Tecapa-El Tigre	109.4	Central America	El Salvador	6,762	Flank
Apaneca Range	95.0	Central America	El Salvador	25,136	Flank
Ixtepeque	5.0	Central America	Guatemala		Unknown
Pacaya	24.0	Central America	Guatemala	2,525	Flank
Santa Maria	28.0	Central America	Guatemala	10,019	Flank
Primavera, Sierra la	10.0	Central America	Mexico		Unknown
Ceboruco	25.0	Central America	Mexico		Unknown
Humeros, Los	40.0	Central America	Mexico		Unknown
Azufres, Los	195.0	Central America	Mexico		Unknown
Telica	72.0	Central America	Nicaragua	43,530	Flank
Momotombo	77.5	Central America	Nicaragua	20,512	Flank
Galunggung-Talagaboda:	13.0	Indonesia	Java	29,214	Flank
Patuha	60.0	Indonesia	Java	120,045	Flank
Dieng Volcanic Complex	60.0	Indonesia	Java	42,492	Flank
Guntur	200.0	Indonesia	Java	52,561	Flank
Wayang-Windu	227.0	Indonesia	Java	30,611	Flank
Papandayan-Kendang	260.0	Indonesia	Java	17,421	Flank
Salak	377.0	Indonesia	Java	130,867	Flank
Inerie	2.5	Indonesia	Lesser Sunda Islands	4,280	Flank
Poco Leok	5.0	Indonesia	Lesser Sunda Islands	66,282	Flank
Tondano Caldera	62.5	Indonesia	Sulawesi	21,628	Flank
Kunyit	10.0	Indonesia	Sumatra		Flank
Sibayak	13.2	Indonesia	Sumatra	17,542	Both
Lumut Balai, Bukit	55.0	Indonesia	Sumatra	13,429	Flank
Kerinci	110.0	Indonesia	Sumatra	26,595	Flank
Patah	110.0	Indonesia	Sumatra	78,342	Flank
Hulubelu	110.0	Indonesia	Sumatra	41,003	Flank
Sibualbuali	179.0	Indonesia	Sumatra	53,310	Flank
Amiata	120.0	Italy	Italy		Unknown

Volcano Name	Installed		Subregion	Fumarole	Flank/Summit
	MW	Region		Area (m ²)	
Larderello	795.0	Italy	Italy	85,087	Flank
Nigorikawa	25.0	Japan	Hokkaido		Unknown
Onikobe	12.5	Japan	Honshu	40,477	Flank
Iwatesan	23.5	Japan	Honshu		Unknown
Kurikomayama	28.8	Japan	Honshu	134,469	Flank
Hachimantai	59.5	Japan	Honshu		Unknown
Numazawa	65.0	Japan	Honshu		Unknown
Akita-Komagatake	80.0	Japan	Honshu		Unknown
Hachijojima	3.3	Japan	Izu & Mariana Islands		Unknown
Yufu-Tsurumi	3.0	Japan	Ryukyu Islands and Kyushu		Unknown
Kirishimayama	30.0	Japan	Ryukyu Islands and Kyushu	3,412	Flank
Ibusuki Volcanic Field	30.0	Japan	Ryukyu Islands and Kyushu		Unknown
Kujusan	149.5	Japan	Ryukyu Islands and Kyushu		Unknown
Rotorua	50.0	New Zealand	New Zealand		Unknown
Okataina	122.2	New Zealand	New Zealand		Unknown
Reporoa	153.0	New Zealand	New Zealand	1,641	Flank
Whakamaru	757.0	New Zealand	New Zealand	361,101	Flank
Lihir	56.0	Papua New Guinea	New Ireland	4,679,468	Flank
Kanlaon	49.0	Philippines	Central Philippines	19,193	Flank
Cuernos de Negros	232.5	Philippines	Central Philippines	220,530	Flank
Mahagnao	700.0	Philippines	Central Philippines	106,767	Flank
Pocdol Mountains	150.0	Philippines	Luzon	26,853	Flank
Malinao	330.0	Philippines	Luzon	6,479	Flank
San Pablo Volcanic Field	462.8	Philippines	Luzon	804	Flank
Apo	106.0	Philippines	Mindanao	43,971	Flank
Barkhatnaya Sopka	0.7	Russia	Kamchatka Peninsula		Unknown
Diky Greben	14.5	Russia	Kamchatka Peninsula	52,940	Flank
Uzon	25.0	Russia	Kamchatka Peninsula	9,824	Flank
Mutnovsky	62.0	Russia	Kamchatka Peninsula	18,989	Flank
Raususan [Mendeleev]	1.8	Russia	Kuril Islands	115,663	Flank
Sashiusudake [Baransky]	3.6	Russia	Kuril Islands		Unknown
Copahue	0.7	South America	Chile-Argentina	74,692	Flank
Chillán, Nevados de	5.0	South America	Chile	213,364	Flank
Tolguaca	12.0	South America	Chile	2,817	Flank
Puchildiza	10.0	South America	Chile		Unknown
Azufre-Pabellon	20.0	South America	Chile	2,157	Flank
El Tatio	25.0	South America	Chile	112,099	Flank
La Torta-Cerros Tocorpu	30.0	South America	Chile	51,697	Flank
Kueishantao	3.0	Taiwan	Taiwan		Unknown
Watt, Morne	11.0	West Indies	West Indies	54,891	Flank
Soufriere Guadeloupe	15.0	West Indies	West Indies		Unknown

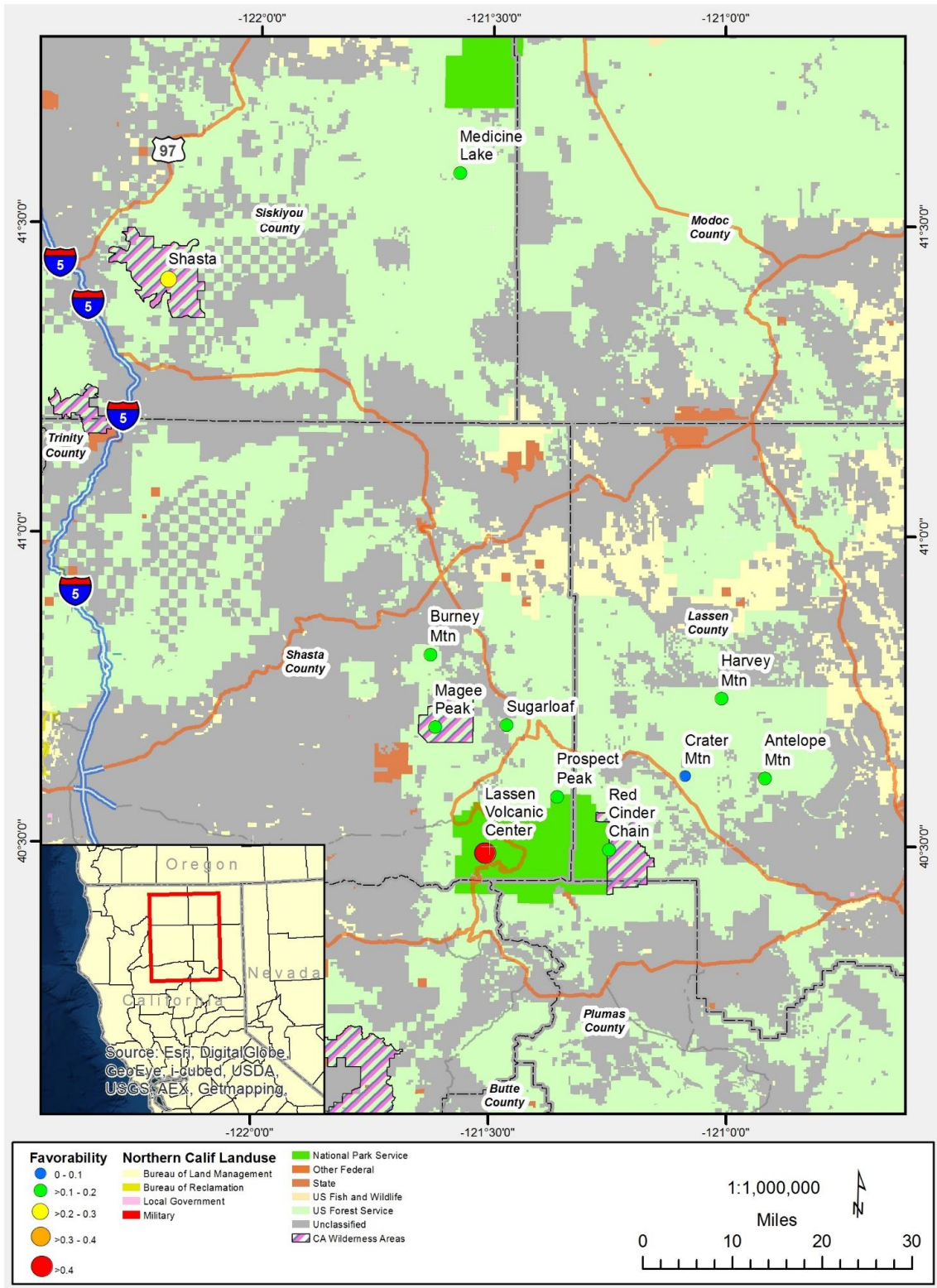
APPENDIX V

Play Fairway and Favorability Maps for the Cascades showing land use designations and major transmission corridors (8 pages)

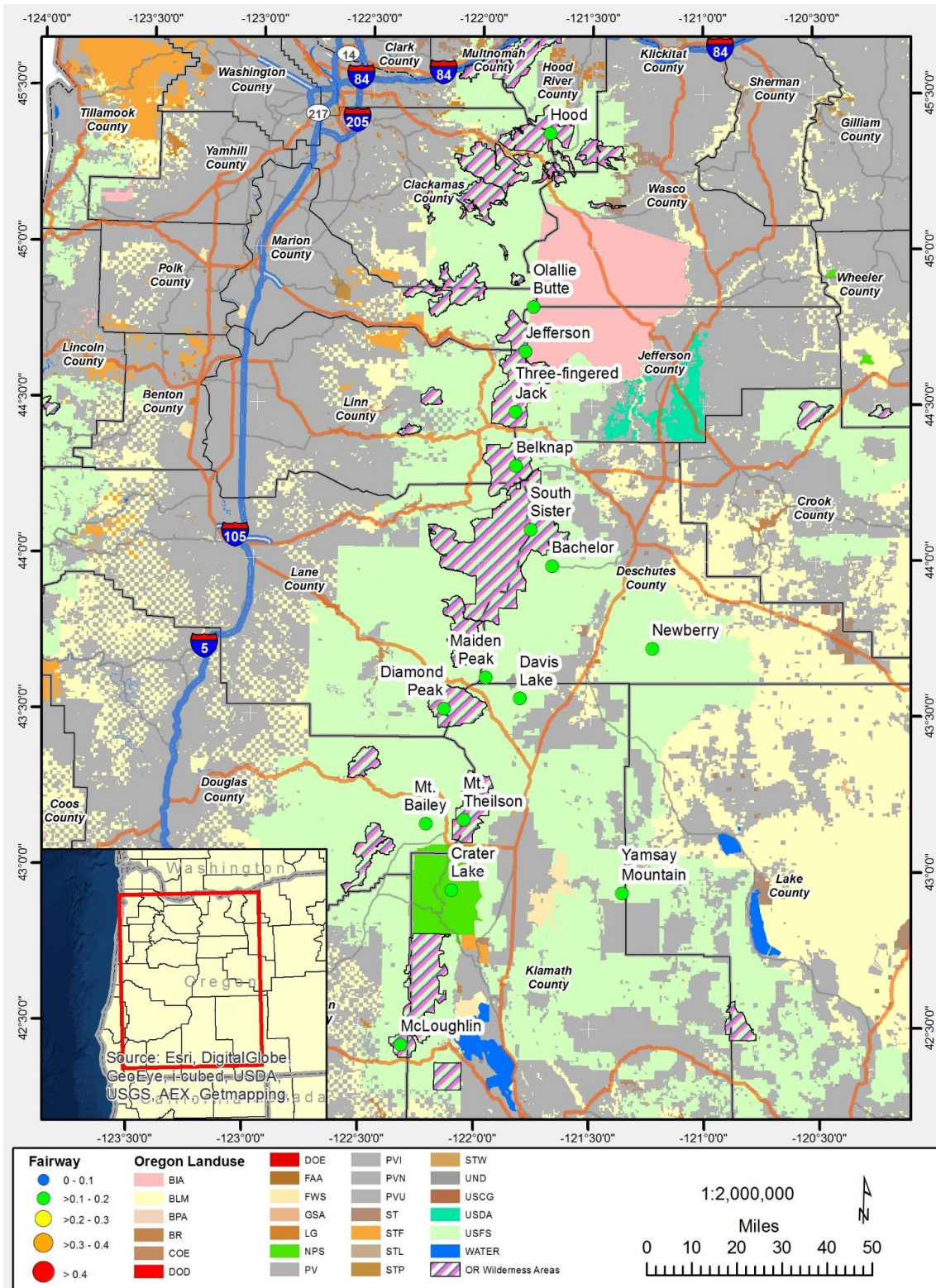
Play Fairway model results for Northern California with land use designations.



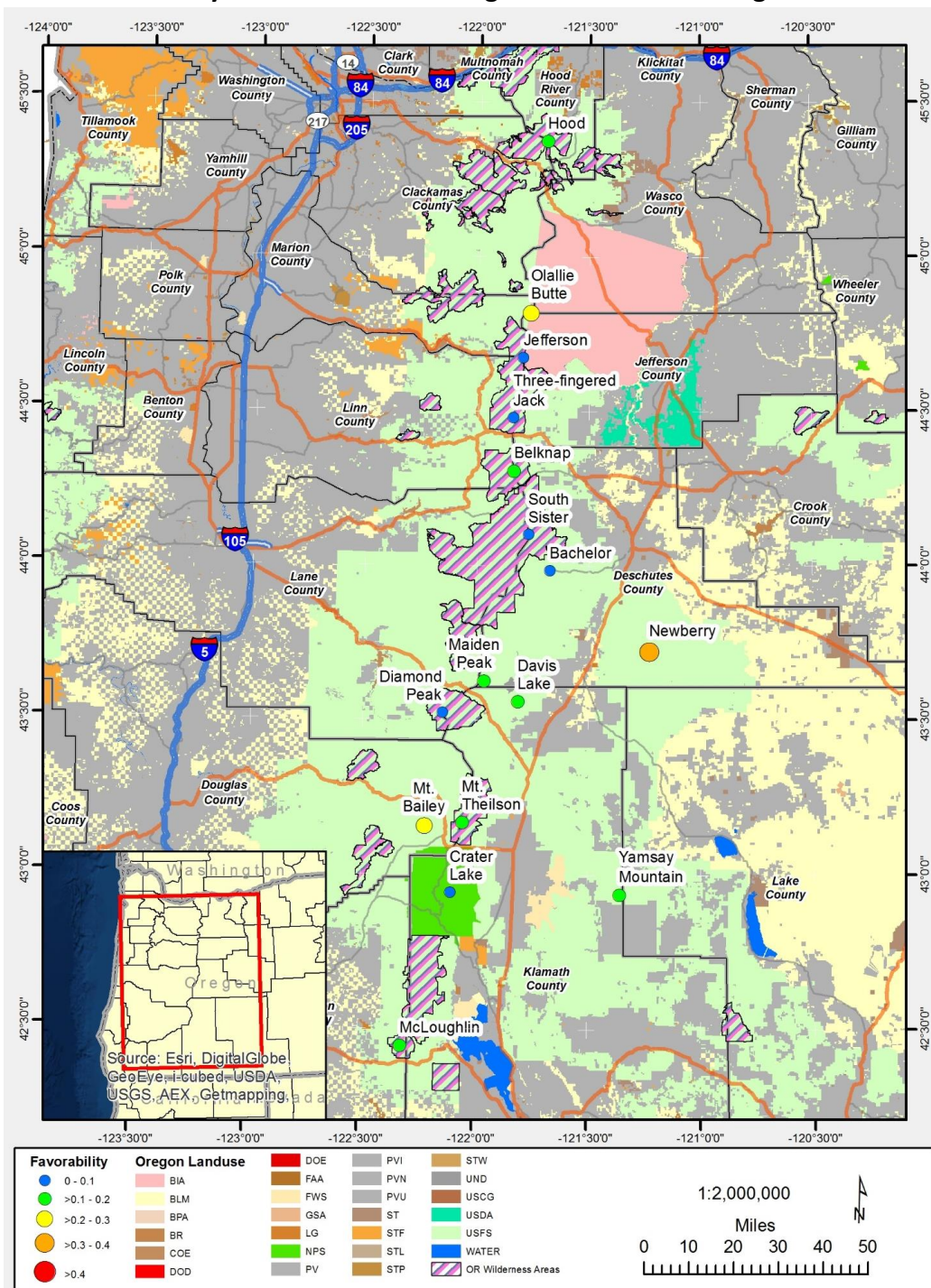
Favorability model results for Northern California with land use designations.



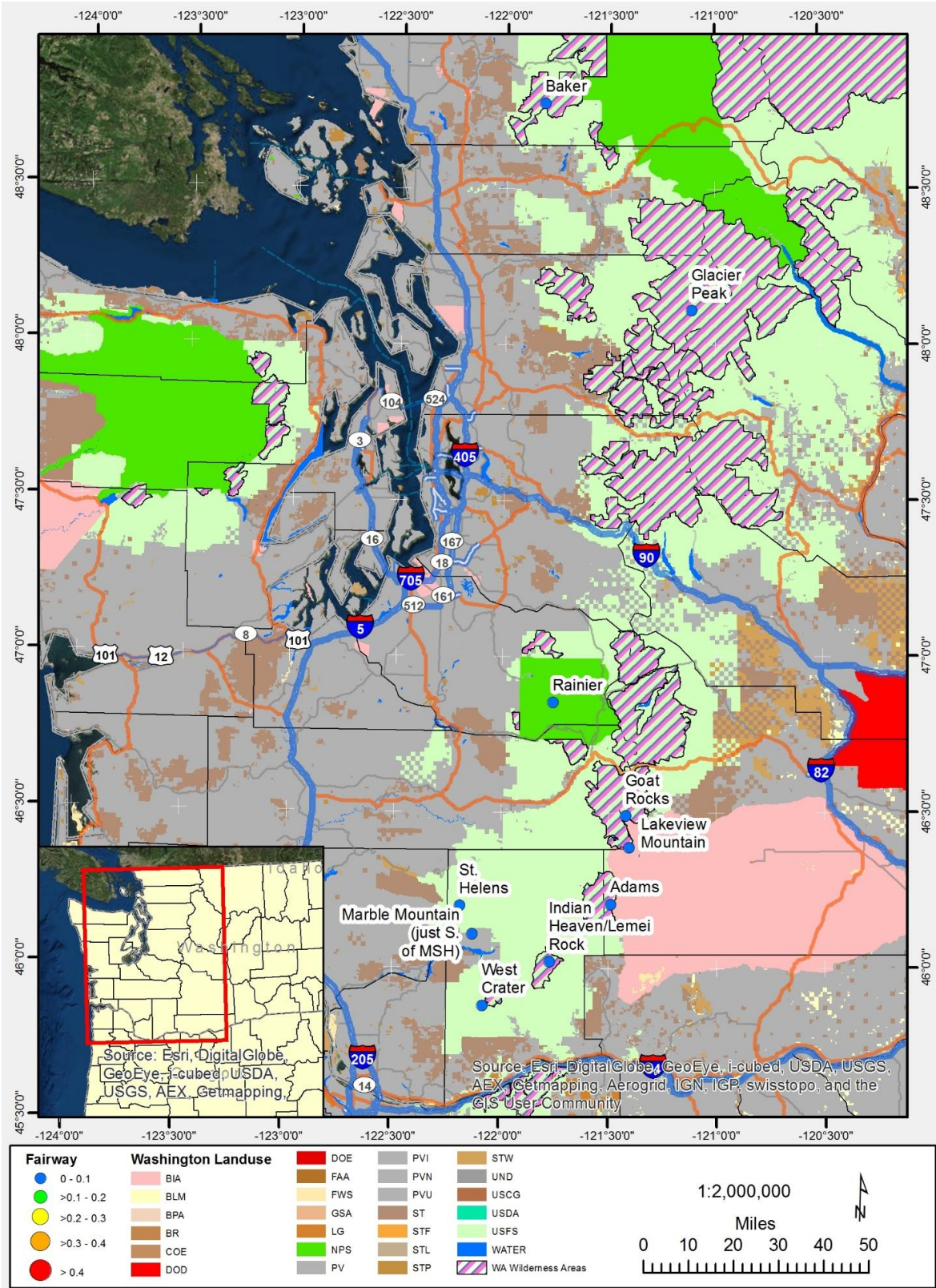
Play Fairway model results for Oregon with land use designations.



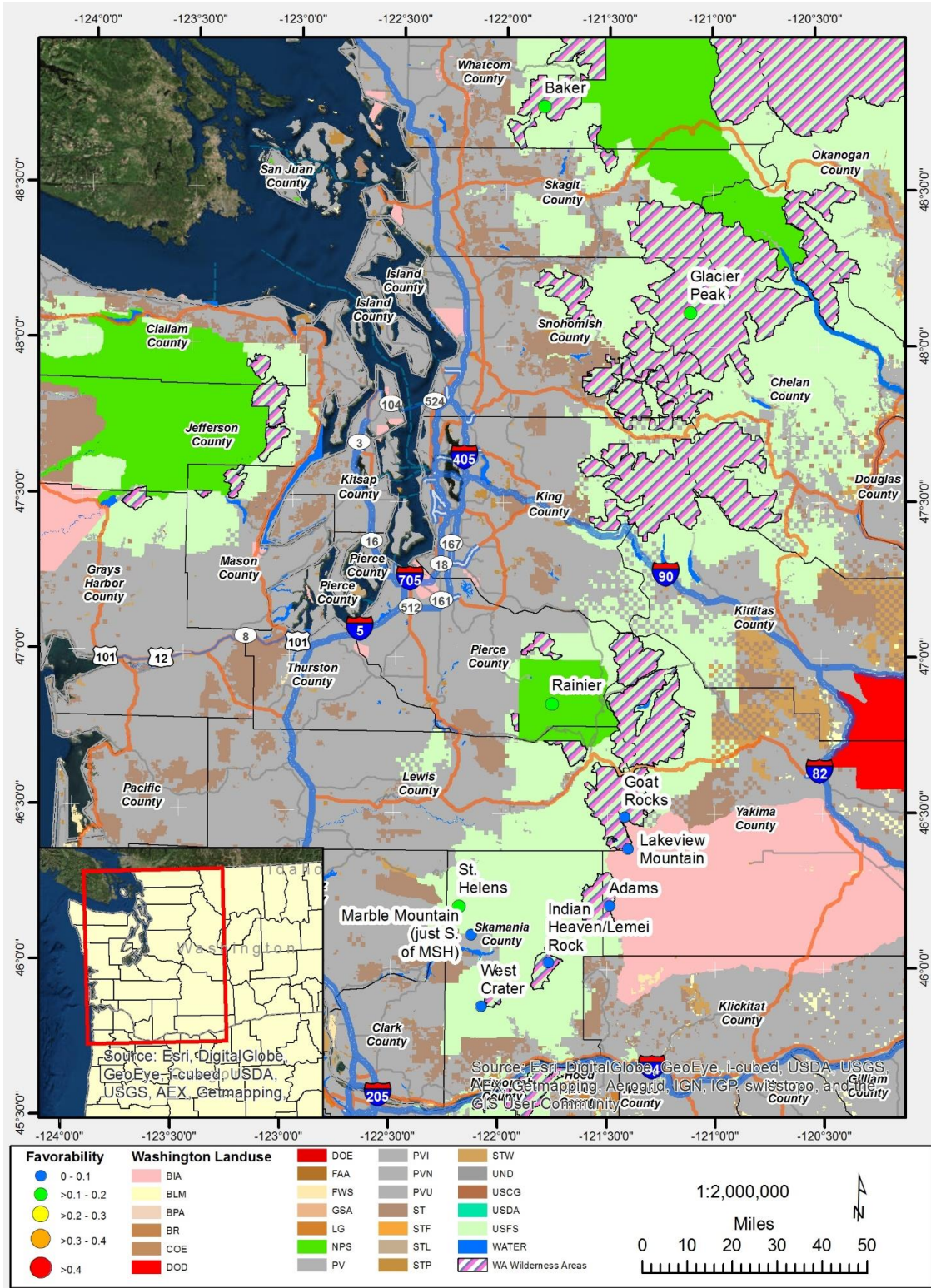
Favorability model results for Oregon with land use designations.



Play Fairway model results for Washington with land use designations.



Favorability model results for Washington with land use designations.



Play Fairway model results for the Cascades showing major power line corridors.

